Universidad de Málaga

Escuela Técnica Superior de Ingeniería de Telecomunicación

TESIS DOCTORAL

Analysis of Gaussian Quadratic Forms with Application to Statistical Channel Modeling

Autor:

Pablo Ramírez Espinosa

Doctorado en Ingeniería de Telecomunicación

Ph.D. in Telecommunication Engineering

Directores:

Eduardo Martos Naya
José Antonio Cortés Arrabal

Año 2020

AUTORIZACIÓN PARA LA LECTURA DE LA TESIS

D. Eduardo Martos Naya y D. José Antonio Cortés Arrabal, profesores doctores del Departamento de Ingeniería de Comunicaciones de la Universidad de Málaga

CERTIFICAN

Que D. Pablo Ramírez Espinosa, Ingeniero de Telecomunicación, ha realizado en el Departamento de Ingeniería de Comunicaciones de la Universidad de Málaga, bajo su dirección el trabajo de investigación correspondiente a su TESIS DOCTORAL titulada:

"**Analysis of Gaussian Quadratic Forms with Application to Statistical Channel Modeling**"

En dicho trabajo, se han propuesto aportaciones originales en el problema de análisis estadístico de formas cuadráticas gaussianas, así como la introducción de un nuevo método de análisis de variables aleatorias. Igualmente, basándose en dichas aportaciones, se han introducido nuevos modelos generalizados de desvanecimientos. Esto ha dado lugar a varias publicaciones científicas, superando el requisito de 1 punto ANECA del programa de doctorado regulado por el Real Decreto 99/2011.

Por todo ello, y dada la unidad temática de las distintas contribuciones y la metodología común seguida en todas ellas, los directores consideran que esta tesis es apta para su presentación al Tribunal que ha de juzgarla y AUTORIZAN la presentación de la tesis por COMPENDIO DE PUBLICACIONES en la Universidad de Málaga. Igualmente, certifican que las publicaciones que avalan la tesis no han sido empleadas en trabajos anteriores a la misma.

Málaga, 26 de septiembre de 2019

Los directores:

Fdo.: Eduardo Martos Naya

Fdo.: José Antonio Cortés Arrabal

UNIVERSIDAD DE MÁLAGA

ESCUELA TÉCNICA SUPERIOR DE INGENIERÍA DE TELECOMUNICACIÓN

Reunido el tribunal examinador en el día de la fecha, constituido por:

Presidente: Dr. D. _____

Secretario: Dr. D. _____

Vocal: Dr. D. _____

para juzgar la Tesis Doctoral titulada "*Analysis of Gaussian Quadratic Forms with Application to Statistical Channel Modeling*", realizada por D. Pablo Ramírez Espinosa y dirigida por los Dres. D. Eduardo Martos Naya y D. José Antonio Cortés Arrabal,

acordó por _____ otorgar la calificación de

_____

y, para que conste, se extiende firmada por los componentes del tribunal la presente diligencia.

Málaga, a _____ de _____ del _____

El presidente: El secretario: El vocal:

Fdo.: _____ Fdo.: _____ Fdo.: _____

"I have no special talent. I am only passionately curious."

Albert Einstein

Agradecimientos

Me gustaría dar las gracias, en primer lugar, a mis directores de tesis, Eduardo y José Antonio, por guiarme a lo largo de estos años. Mucho de lo que he aprendido a lo largo de mi doctorado se lo debo a ellos, desde esas charlas aparentemente infinitas sobre variables aleatorias hasta profundas lecciones acerca de cómo redactar y preparar documentos científicos. Me siento afortunado de haber contado con ellos como directores, pues son ejemplo no sólo de profesores, sino de personas.

No podría olvidarme tampoco de otras personas que me han aportado tanto en este tiempo. En especial, querría agradecer a Javier y a José Paris todo lo que se han implicado conmigo; pues sin ser mis directores han actuado como tal, enseñándome y guiándome a lo largo del proceso. Igualmente, quisiera agradecer a Laureano todo su apoyo, tanto como compañero en la Universidad de Málaga como desde la distancia en su aventura investigadora en Hong Kong.

Gracias también a David, por haber sido mi apoyo profesional y personal durante mi estancia en Queen's University. Siempre es un placer trabajar junto a investigadores de su calibre.

Y por último, pero quizás lo más importante de todo, gracias a mi familia, en especial a mis padres, por el incondicional apoyo ya no sólo durante el doctorado sino durante toda mi vida. Gracias por creer en mí.

Abstract

This thesis provides novel and tight approximations to the distribution of both real and complex non-central Gaussian quadratic forms (GQFs). To that end, a new method to analyze random variables is proposed, which is based on the analysis of a suitably defined sequence of auxiliary random variables that converges in distribution to the target one. Consequently, the major advantage of this proposal is that the resulting expressions always represent a valid distribution, in contrast to classical approximation methods based on series expansions.

By leveraging such convergence, simple and recursive approximations for the probability density function (PDF) and the cumulative distribution function (CDF) of positive definite real GQFs are given. In the context of indefinite complex GQFs, the application of the proposed technique leads to very tractable approximants for their first order statistics in terms of elementary functions, i.e., exponentials and powers. Thus, the obtained expressions are more useful for further analytical purposes than other solutions available in the literature. This tractability is exemplified through the performance analysis of maximal ratio combining systems over correlated Rice channels, providing closed-form approximations for the outage probability and the bit error.

Moreover, in the context of channel modeling, the proposed methodology of analysis of variables gives raise to two generalizations of the well-know κ-μ shadowed fading model. These new models, namely the fluctuating Beckmann and the correlated κ-μ shadowed models, include as particular cases the vast majority of fading distributions, ranging from the classical ones such as Rayleigh and Rice models to more refined extensions as the Beckmann distribution or the η-μ model. The statistical characterization of both distributions is provided, giving closed-form expressions for their moment generating function (MGF), PDF and CDF; along with the formulation of the second order statistics of the fluctuating Beckmann model.

Resumen

En esta tesis se presenta una nueva aproximación a la distribución de formas cuadráticas gaussianas (FCGs) no centrales tanto en variables reales como complejas. Para ello, se propone un nuevo método de análisis de variables aleatorias que, en lugar de centrarse en el estudio de la variable en cuestión, se basa en la caracterización estadística de una secuencia de variables aleatorias auxiliares convenientemente definida. Como consecuencia, las expresiones obtenidas, con independencia del grado de precisión adquirido, siempre representan una distribución válida, siendo ésta su principal ventaja frente a otros métodos de aproximación clásicos basados en expansiones en series.

Aplicando este método, se obtienen simples expresiones recursivas para la función densidad de probabilidad (PDF) y la función de distribución (CDF) de las FCGs reales definidas positivas. En el caso de las formas complejas, esta nueva forma de análisis conduce a aproximaciones para los estadísticos de primer orden en términos de funciones elementales (exponenciales y potencias), siendo más convenientes para cálculos posteriores que otras soluciones disponibles en la literatura. La tratabilidad matemática de estos resultados se ejemplifica mediante el análisis de sistemas de combinación por razón máxima (MRC) sobre canales Rice correlados, proporcionando aproximaciones cerradas para la probabilidad de *outage* y la probabilidad de error de bit.

Finalmente, en el contexto de modelado de canal, la metodología de análisis de variables propuesta permite obtener dos nuevas generalizaciones del conocido modelo de desvanecimiento κ-μ *shadowed*. Estas dos nuevas distribuciones, nombradas Beckmann fluctuante y κ-μ *shadowed* correlado, incluyen como casos particulares a la gran mayoría de distribuciones de desvanecimientos usadas en la literatura, abarcando desde los modelos clásicos de Rayleigh y Rice hasta otros más generales y complejos como el Beckmann y el η-μ. Para ambas distribuciones, se presenta su caracterización estadística de primer orden, i.e., función generadora de momentos (MGF), PDF y CDF; así como los estadísticos de segundo orden del modelo Beckmann fluctuante.

Contents

List of Figures

List of Acronyms

AFD	**A**verage **F**ade **D**uration
AWGN	**A**dditive **W**hite **G**aussian **N**oise
BER	**B**it **E**rror **R**ate
CDF	**C**umulative **D**istribution **F**unction
CF	**C**haracteristic **F**unction
CGF	**C**umulant **G**enerating **F**unction
FB	**F**luctuating **B**eckmann
GQF	**G**aussian **Q**uadratic **F**orm
i.i.d.	**I**ndependent and **I**dentically **D**istributed
LCR	**L**evel **C**rossing **R**ate
LoS	**L**ine-of-**S**ight
MGF	**M**oment **G**enerating **F**unction
MIMO	**M**ultiple-**I**nput **M**ultiple-**O**utput
ML	**M**aximum **L**ikelihood
MRC	**M**aximal **R**atio **C**ombining
MSE	**M**ean **S**quared **E**rror
NLoS	**N**on **L**ine-of-**S**ight
OSTBC	**O**rthogonal **S**pace **T**ime **B**lock **C**oding
PDF	**P**robability **D**ensity **F**unction
QAM	**Q**uadrature **A**mplitude **M**odulation
SNR	**S**ignal-to-**N**oise **R**atio

Chapter 1

Introduction

Gaussian random variables — both real and complex — are massively used in communications and signal processing mostly as a consequence of the central limit theorem, which states that the sum of independent random variables is asymptotically Gaussian distributed [1]. However, this interest does not only lie in the widespread use of the Gaussian distribution as a limiting case, but also in the analysis of random variables arising from normal ones.

Among these variables, linear combinations of squares of Gaussian variables, known as Gaussian quadratic forms (GQFs), have a remarkable relevance. Their importance is due to their wide number of applications, not only in the communication and signal processing fields, but also in statistics. For instance, they naturally arise in problems related to the detection of signals in Gaussian noise [2][3, sec. 13.5], the spectral detection of normally distributed stationary processes, χ^2 tests [4, sec. 7], analysis of variance [5], performance analysis of adaptive filter algorithms [6], energy detection [7] or performance analysis of maximum likelihood (ML) estimators [8]. In general, any statistical test based on Euclidean distances or any application of the method of least squares when the involved variables are Gaussian will automatically bring a GQF [4, chap. 7].

In communications, GQFs play an important role when analyzing differential modulation schemes [9], non-coherent modulations [10], diversity techniques [11]–[14], orthogonal space time block coding (OSTBC) [15] or relay systems [16], since the signal-to-noise ratio (SNR) at the output of these systems is given in terms of a GQF when the channel gains are assumed to be Gaussian distributed.

Moreover, GQFs have also a considerable importance in channel modeling, although little attention has traditionally been paid to them in this context. Classically, in wireless channels, it has been assumed that the number of reflections arriving to the receiver is sufficiently large so that the central limit theorem can be applied, modeling the received complex baseband signal as Gaussian [17]–[19]. Depending on the choice of the parameters of this underlying Gaussian variable (mean and variance of its real and imaginary parts), different fading models arose in the related literature, e.g., Rayleigh, Rice and Hoyt. All these classical distributions, including some generalizations introduced tens of

years ago such as Nakagami-m model (with integer m) [20], can be seen as very particular cases of a GQF.

In the last years, with the increased interest on channel modeling due to the emergence of new scenarios and technologies, as the use of millimeter waves [21]–[24], large intelligent surfaces [25], [26] and underwater communications [27], several novel distributions have been proposed [28]–[31]. Many of them, which aim to improve the fitting to measured data in these emerging scenarios and to provide more flexibility than classical fading models, can also be regarded as particular cases of a more general GQF. Therefore, the analysis of GQFs would unify the vast majority of fading models nowadays available in the literature, sometimes with slight differences between them.

Unfortunately, despite their large number of applications, no closed-form expressions are known for the distribution of arbitrary GQFs, and only a few particular cases admit a closed formulation. Therefore, inherent to GQFs is the classical problem of approximating the distribution of random variables, for which several approaches have been given in the literature over the years. These proposed methods include, among others, the saddle-point technique [32]–[35], Edgeworth series [35]–[38], series expansions in terms of orthogonal polynomials [39] or approximations in terms of other random variables [40]–[45].

Although many of these classical techniques have been applied to the analysis of GQFs, all the derived results suffer from the same common drawback: the resulting expressions *do not* represent a proper distribution, i.e., the approximated probability density functions (PDFs) may not have unit area and probabilities greater than one (or even negative) can be obtained [39, p. 731][38, sec. 2]. In addition, the accuracy of these techniques typically depends on the parametrization of the target variable, leading in some cases to poor approximations or rendering convergence issues.

Motivated by the aforementioned importance of GQFs in communications and signal processing, and taking into account that deriving exact expressions for the distribution of such an intricate variables may pose a challenge from an analytic point of view, this thesis revisits the problem of analyzing non-central GQFs. Along this line, a new method to characterize these variables is proposed, aiming to circumvent the major drawbacks of classical approaches and seeking simple and tractable approximations for the PDF and cumulative density function (CDF) of both real and complex GQFs. The proposed approach is later leveraged to be applied to arbitrary positive random variables, showing the potential of the method and highlighting its main advantage: it ensures, for any level of accuracy, that the resulting expressions represent a *valid distribution*.

Finally, exploiting the connection between GQFs and the distinct fading models, part of this thesis is also devoted to the analysis of fading distributions, providing very general and versatile — albeit tractable — models that unify the majority of the existing distributions emerging from the application of the central limit theorem.

1.1 Objectives

This thesis has two clearly defined objectives: *i)* proposing a new method to approximate the distribution of both real and complex non-central GQFs, and *ii)* unifying most of the fading distributions available in the literature under the umbrella of very general models. Although these objectives seem apparently unconnected, it will be later shown that in fact they are considerably related, and both are achieved by applying the same underlying methodology. More specifically, the main objectives in the context of the analysis of GQFs are as follows:

- Derivation of novel general approximations for both the PDF and CDF of positive random variables which guarantee that the resulting expressions represent a valid distribution.
- Application of the proposed method to positive definite real GQFs in order to provide new simple expressions that outperform the alternative results given in the literature.
- Providing a new approximation to the distribution of complex GQFs that are tractable enough to be useful for analytical purposes and its application to the performance analysis of maximal ratio combining (MRC) systems with correlated branches over line-of-sight (LoS) channels.

Regarding the second aforementioned objective, this thesis aim to propose new fading models that generalizes the majority of fading distributions arising from the central limit theorem. To this end, the versatile and popular κ-μ shadowed distribution will be used as starting point due to its tractability and empirical validation, and more general (yet tractable) expansions will be sought.

1.2 Organization

This is a compilation thesis composed by several publications and some chapters that provide coherence to the whole document. Therefore, the organization varies with respect to the more classical structure of a monograph thesis. Specifically, it is organized in four main chapters and the appendix section as follows:

1. Chapter 1. The current chapter, which contains the introduction and motivation of the thesis, along with the objectives and organization of the rest of the document.
2. Chapter 2 provides the necessary background to understand the main contributions of the thesis. It includes some basic concepts of probability, an overview of the techniques classically employed to approximate the distribution of random variables, an introduction to GQFs and a review of their state of the art and finally a brief summary of both the classical and some of the generalized fading models available in the literature.

3. Chapter 3 summarizes the distinct publications gathered in this thesis, presenting their main contributions and discussing their results.

4. Chapter 4. The last chapter, containing the conclusions and some future research lines arisen from this thesis.

Finally, the publications included in the compilation are attached in Appendix A.

1.3 Publications

The following is a list of publications in refereed journals and conference proceedings included as part of the compilation of this thesis:

- [46] P. Ramírez-Espinosa, D. Morales-Jimenez, J. A. Cortés, J. F. París, and E. Martos-Naya, "New approximation to distribution of positive RVs applied to Gaussian quadratic forms", *IEEE Signal Process. Lett.*, vol. 26, no. 6, pp. 923–927, Jun. 2019. DOI: 10.1109/LSP.2019.2912295.

- [47] P. Ramírez-Espinosa, L. Moreno-Pozas, J. F. París, J. A. Cortés, and E. Martos-Naya, "A new approach to the statistical analysis of non-central complex Gaussian quadratic forms with applications", *IEEE Trans. Veh. Technol.*, vol. 68, no. 7, pp. 6734–6746, Jul. 2019. DOI: 10.1109/TVT.2019.2916725.

- [48] P. Ramírez-Espinosa, F. J. López-Martínez, J. F. París, M. D. Yacoub, and E. Martos-Naya, "An extension of the κ-μ shadowed fading model: Statistical characterization and applications", *IEEE Trans. Veh. Technol.*, vol. 67, no. 5, pp. 3826–3837, May 2018. DOI: 10.1109/TVT.2017.2787204.

- [49] P. Ramírez-Espinosa, J. F. París, J. A. Cortés, and E. Martos-Naya, "The κ-μ shadowed fading model with arbitrary intercluster correlation", in *2018 15th Int. Symp. Wireless Commun. Syst. (ISWCS)*, Aug. 2018, pp. 1–5. DOI: 10.1109/ISWCS.2018.8491099.

Publications [46] and [47] gather the results referring to the approximation to the distribution of random variables and the analysis of GQFs, while papers [48] and [49] present the new general fading models.

Chapter 2

Background

The purpose of this chapter is to introduce several preliminary results and definitions, providing the necessary background to understand the results that will be later presented.

It is organized as follows. Section 2.1 introduces the general notation, while in Section 2.2 some well-known results on random variables are introduced along with a couple of relevant statistical distributions that will be used throughout this thesis. In addition, some of the most classical approaches that are used to approximate the distribution of random variables are summarized. Section 2.3 deals with Gaussian quadratic forms, considering both the real and complex cases and providing an overview of the different approaches given in the literature to approximate their distribution. Finally, Section 2.4 revisits several models that have been traditionally used to characterize fading in wireless environments, along with new distributions recently proposed to that end.

2.1 General notation

Notation for common sets

j	imaginary unit, $\sqrt{-1}$.
$\mathrm{Re}\{\cdot\}, \mathrm{Im}\{\cdot\}$	Real and imaginary parts.
$\mathbb{C}, \mathbb{R}, \mathbb{N}$	Complex, reals and natural numbers.
$\mathbb{R}^+$, $\mathbb{N}^+$	Positive real and integers numbers excluding 0.

Notation for used functions

$\ln$	Natural logarithm.
$\max, \min$	Maximum and minimum.
$\lim$	Limit.
$\forall$	For all.
$\triangleq$	Defined as.
$\lvert\cdot\rvert$	Absolute value.
$\lVert\cdot\rVert$	Modulus.
$I_\nu(\cdot)$	Modified Bessel function of first kind [50, eq. (9.6.18)].
$\Gamma(\cdot)$	Gamma function [50, eq. (6.1.1)].
$\gamma(\cdot,\cdot)$	Lower incomplete gamma function [50, eq. (6.5.2)].
${}_1F_1(\cdot;\cdot;\cdot)$	Kummer's hypergeometric function [51, eq. (9.210 1)].
$\mathcal{L}\{\cdot\}, \mathcal{L}^{-1}\{\cdot\}$	Laplace transform and inverse Laplace transform.

Notation for probability and asymptotics

$P\{\cdot\}$	Probability.
$\mathbb{E}[\cdot]$	Expectation operator.
$\sim$	Statistically distributed as.
$f_X(x)$	PDF of X.
$F_X(x)$	CDF of X.
$M_X(s)$	MGF of X.

Matrix-vector notation

$\mathbf{x}, \mathbf{X}$	Vectors and matrices are denoted with bold lower and upper case, respectively.
$\mathbb{R}^{m\times n}, \mathbb{C}^{m\times n}$	Real and complex $m \times n$ matrices.
$(\mathbf{X})_{i,j}$	(i,j)-th element of the matrix $\mathbf{X}$.
$\mathbf{I}_n$	$n \times n$ identity matrix.
$\mathbf{0}_{n\times m}$	$n \times m$ matrix of all zeroes.
$(\cdot)^T, (\cdot)^\dagger$	Transpose, conjugate-transpose.

2.2 Some results on random variables

This section defines some types of convergence of random variables, focusing on the relationships between them. Moreover, the Gaussian, the χ^2 and the gamma distribution are revisited, not only providing their first order statistics but also presenting the connection between them as well as some properties that will be used later. Finally,

this section briefly summarizes some of the most widely used techniques to approximate the distribution of random variables, i.e., the saddle-point technique, Gram-Charlier and Edgeworth series and expansions in terms of orthogonal polynomials and other density functions.

2.2.1 Convergence between sequences of random variables

Many of the most relevant results in probability, e.g., the central limit theorem [1, sec. 27] or Lévy's continuity theorem (also known as Lévy's convergence theorem) [52, chap. 18], are related to the asymptotic behavior of distributions of random variables. The work presented in this thesis is also partially based on the limit behavior of sequences of random variables and the concept of convergence. Thus, different types of convergence are defined next, as well as the relationships between them.

Weak convergence

Let $\{X_n : n \in \mathbb{N}^+\}$ be a sequence of real random variables. Then, $\{X_n\}$[1] converges weakly, or converges in distribution, to the random variable $X \in \mathbb{R}$ if

$$\lim_{n\to\infty} F_{X_n}(x) = F_X(x) \tag{2.1}$$

at every continuity point x, with $F_{X_n}(x)$ and $F_X(x)$ denoting the CDF of X_n and X, respectively [1, sec. 25]. This is expressed as $\{X_n\} \Rightarrow X$.

Note that weak convergence ensures that the sequence $\{F_{X_n}(x)\}$ has a limit $F_X(x)$, but it does not guarantee the convergence of the respective PDFs. The conditions under which weak convergence also implies that of PDFs are given in [53]. Specifically, let $f_{X_n}(x)$ and $f_X(x)$ denote the PDFs of X_n and X, respectively. Therefore, if $\{X_n\} \Rightarrow X$ and

i $f_{X_n}(x)$ and $f_X(x)$ are continuous functions,

ii $f_{X_n}(x)$ is bounded, i.e., $\sup_n f_{X_n}(x) \leq a < \infty$ for all x with a any number,

iii $\{f_{X_n}(x)\}$ is equicontinuous, i.e., for each point x and y, there exists $g(x,\epsilon)$ and $h(x,\epsilon)$ with $\epsilon > 0$ such that $|x - y| < g(x,\epsilon)$ implies that $|f_{X_n}(x) - f_{X_n}(y)| < \epsilon$ for all $n \geq h(x,\epsilon)$,

then $\lim_{n\to\infty} f_{X_n}(x) = f_X(x)$. In turn, convergence of PDFs always implies that of CDFs by virtue of Scheffe's theorem [54].

[1] For simplicity, the notation for sequences of random variables is simplified when no confusion may arise.

Moreover, consider $\{X_n\} \Rightarrow X$ and let $g : \mathbb{R} \to \mathbb{R}$ be any continuous and bounded function. Therefore, from Helly-Bray theorem [55, sec. 1.3], we have that

$$\lim_{m\to\infty} \mathbb{E}[g(X_n)] = \mathbb{E}[g(X)]. \tag{2.2}$$

Convergence in probability

Consider again a sequence of real random variables defined as $\{X_n : n \in \mathbb{N}^+\}$. Then, $\{X_n\}$ converges in probability to another random variable $X \in \mathbb{R}$ if

$$\lim_{n\to\infty} P\{|X_n - X| > \epsilon\} = 0 \tag{2.3}$$

for $\epsilon > 0$ [56, sec. 6.2]. It is denoted by $\{X_n\} \xrightarrow{p} X$.

It can be proved that condition in (2.3) is more restrictive than that in (2.1). In fact, if $\{X_n\} \xrightarrow{p} X$ then $\{X_n\} \Rightarrow X$, although the converse does not hold in general [1, thm. 25.2]. Convergence in distribution implies convergence in probability when the limit random variable is a constant, i.e., $X = c$. Under this condition, $\{X_n\} \Rightarrow c$ also implies $\{X_n\} \xrightarrow{p} c$ [1, thm. 25.3].

L_p convergence

The last type of convergence here presented is the L_p convergence. It is said that a sequence of real random variables $\{X_n : n \in \mathbb{N}^+\}$ converges in L_p to a limit random variable $X \in \mathbb{R}$ if

$$\lim_{n\to\infty} \mathbb{E}\left[|X_n - X|^p\right] = 0 \tag{2.4}$$

for $p \in \mathbb{N}^+$ [56, sec. 6.5], and it is expressed as $\{X_n\} \xrightarrow{L_p} X$.

The most common types of L_p convergence are for $p = 1, 2$. If $\{X_n\} \xrightarrow{L_p} X$ for $p = 1$, then it is said that $\{X_n\}$ converges in mean to X, and if it does for $p = 2$ then $\{X_n\}$ converges in mean square to X. Moreover, L_p convergence for a certain value of p ensures that (2.4) holds for any p' such that $p > p' \geq 1$.

An important remark is that L_p convergence for $p \geq 1$ implies convergence in probability and, consequently, convergence in distribution. This can be straightforwardly proved by applying Markov's inequality [52, sec. 6.4] to (2.3):

$$\lim_{n\to\infty} P\{|X_n - X| > \epsilon\} \leq \lim_{n\to\infty} \frac{\mathbb{E}[|X_n - X|^p]}{\epsilon^p} \overset{(a)}{=} 0, \tag{2.5}$$

where L_p convergence is assumed in (a).

2.2.2 The Gaussian distribution

Gaussian random variables (both real and complex) appear in a multitude of applications in communications and signal processing, mainly as a limit distribution due to the central limit theorem. Hence, the Gaussian distribution is used, e.g., to characterize random noise [57] and channel gains in wireless communications [17], [18], to mention but a couple of relevant examples. Its importance in this thesis is also relevant, since most of the random variables here considered are based on the Gaussian distribution.

The real case

A real random variable X follows a Gaussian distribution with mean μ and variance σ^2, i.e., $X \sim \mathcal{N}(\mu, \sigma^2)$, if its PDF is expressed as [19, eq. (2.3-8)]

$$f_X(x) = \frac{1}{\sqrt{2\pi\sigma^2}} e^{-(x-\mu)^2/(2\sigma^2)}. \tag{2.6}$$

Its CDF is calculated by integrating (2.6) as

$$F_X(x) = \int_{-\infty}^{x} \frac{1}{\sqrt{2\pi\sigma^2}} e^{-(x-\mu)^2/(2\sigma^2)} dx = 1 - Q\left(\frac{x-\mu}{\sigma}\right) \tag{2.7}$$

where $Q(\cdot)$ is the Gaussian Q-function [18, eq. (4.1)].

The complex case

Consider now two independent real Gaussian random variables X_1 and X_2 such that $X_1 \sim \mathcal{N}(\mu_1, \sigma_1^2)$ and $X_2 \sim \mathcal{N}(\mu_2, \sigma_2^2)$. Then, the random variable $X = X_1 + jX_2$ follows a complex Gaussian distribution with mean $\mu = \mu_1 + j\mu_2$, variance $\sigma^2 = \sigma_1^2 + \sigma_2^2$ and pseudovariance $c^2 = \sigma_1^2 - \sigma_2^2$, i.e., $X \sim \mathcal{CN}(\mu, \sigma^2, c^2)$. The PDF of X is readily obtained due to the independence between X_1 and X_2 as

$$f_X(x) = \frac{1}{\pi\sqrt{\sigma^4 - c^4}} \exp\left(-\frac{\sigma^2\|x-\mu\|^2}{\sigma^4 - c^4} + \mathrm{Re}\left\{\frac{c^2(x-\mu)^2}{\sigma^4 - c^4}\right\}\right). \tag{2.8}$$

If $\sigma_1^2 = \sigma_2^2 = \sigma^2/2$, then (2.8) simplifies to [58, eq. (2)]

$$f_X(x) = \frac{1}{\pi\sigma^2} e^{\|x-\mu\|^2/\sigma^2} \tag{2.9}$$

and the shorthand notation $X \sim \mathcal{CN}(\mu, \sigma^2)$ is used.

Of special interest in many cases is the analysis of circularly symmetric Gaussian variables. A complex random variable X is said to be circularly symmetric if $f_X(x) = f_Y(y)$ with $Y = e^{j\phi}X$ for all $\phi \in \mathbb{R}$, requiring thus that $\mu = c^2 = 0$ [59]. However, in

some applications (e.g., channel modeling), non-circularly symmetric Gaussian variables are also relevant.

2.2.3 The χ^2 distribution

The χ^2 distribution plays an important role in many statistics applications, specially in hypothesis and goodness-of-fit testing [60, chap. 30]. Closely related to the Gaussian distribution, the χ^2 distribution describes the statistical behavior of the sum of n independent squared Gaussian random variables. Thus, consider

$$X = \sum_{i=1}^{n} Z_i^2 \tag{2.10}$$

where Z_i are independent and real Gaussian random variables. Then X follows a χ^2 distribution with n degrees of freedom [19, sec. 2.3]. Depending on whether Z_i have zero mean or not, we differentiate between the central and the non-central case.

The central χ^2 distribution

If Z_i in (2.10) have zero mean and equal variance σ^2 for all i, i.e., $Z_i \sim \mathcal{N}(0, \sigma^2)\ \forall\ i$, then X follows a central χ^2 distribution with PDF [19, eq. (2.3-21)]

$$f_X(x) = \frac{1}{2^{n/2}\Gamma(n/2)\sigma^n} x^{n/2-1} e^{-x/(2\sigma^2)} \tag{2.11}$$

where $\Gamma(\cdot)$ is the gamma function [50, eq. (6.1.1)], and it is denoted by $X \sim \chi_n^2(\sigma^2)$. Its CDF can be directly obtained by integrating (2.11) as

$$F_X(x) = \frac{2^{-n/2}}{\sigma^n \Gamma\left(\frac{n}{2}\right)} \int_0^x y^{n/2-1} e^{-y/(2\sigma^2)} dy = \frac{1}{\Gamma\left(\frac{n}{2}\right)} \int_0^{\frac{x}{2\sigma^2}} u^{n/2-1} e^{-u} du = \frac{1}{\Gamma\left(\frac{n}{2}\right)} \gamma\left(\frac{n}{2}, \frac{x}{2\sigma^2}\right) \tag{2.12}$$

where $\gamma(\cdot,\cdot)$ is the lower incomplete gamma function [50, eq. (6.5.2)].

Finally, the moment generating function (MGF) of X is calculated using [51, eq. (3.381 4)] as

$$M_X(s) = \int_0^\infty f_X(x) e^{sx} dx = \left(1 - 2\sigma^2 s\right)^{-n/2}, \tag{2.13}$$

which is valid for all $s \in \mathbb{C}$ such that $\mathrm{Re}\{s\} < 1/(2\sigma^2)$.

The non-central χ^2 distribution

In case Z_i in (2.10) have non-zero mean but equal variances, i.e., $Z_i \sim \mathcal{N}(\mu_i, \sigma^2)\ \forall\ i$, then the PDF of X is given by [19, eq. (2.3-29)]

$$f_X(x) = \frac{1}{2\sigma^2}\left(\frac{x}{\delta^2}\right)^{(n-2)/4} \exp\left(-\frac{x+\delta^2}{2\sigma^2}\right) I_{n/2-1}\left(\delta/\sigma^2\sqrt{x}\right) \tag{2.14}$$

where $I_\nu(\cdot)$ is the modified Bessel function of the first kind [50, eq. (9.6.18)] and $\delta^2 = \sum_{i=1}^{n} \mu_i^2$ is the non-centrality parameter. We denote that by $X \sim \chi_n^2(\sigma^2, \delta^2)$.

The MGF of X in this case can be obtained from (2.14) by using [51, eqs. (6.643 2), (9.220 2) and (9.215 1)] as

$$M_X(s) = \int_0^\infty f_X(x)e^{sx}dx = \frac{\exp\left(\frac{\delta^2 s}{1-2\sigma^2 s}\right)}{(1-2\sigma^2 s)^{n/2}}, \quad \mathrm{Re}\{s\} < 1/(2\sigma^2). \tag{2.15}$$

2.2.4 The gamma distribution

Due to its mathematical tractability and its connection to the exponential and Gaussian distribution, the gamma distribution is extensively used in a wide variety of applications in physics, statistics and communications, e.g., waiting times in queues [61], electromigration for submicron interconnects [62] and wireless channel modeling [18], to mention but some relevant examples. The gamma distribution is also of special interest to the main results derived in this thesis.

Definition and first order statistics

A random variable X follows a gamma distribution with shape parameter $m \in \mathbb{R}^+$ and scale parameter $\theta \in \mathbb{R}^+$, i.e., $X \sim \Gamma(m, \theta)$, if its PDF is expressed as [63, eq. (17.23)]

$$f_X(x) = \frac{1}{\Gamma(m)\theta^m} x^{m-1} e^{-x/\theta}. \tag{2.16}$$

Comparing (2.11) and (2.16), it can be observed that the gamma distribution generalizes the central χ^2 distribution by letting the m parameter (equivalent to the degrees of freedom in the χ^2 distribution) take any positive real value instead of only natural numbers.

As with the χ^2 distribution, the CDF of X is directly obtained by integrating (2.16) as

$$F_X(x) = \frac{1}{\Gamma(m)\theta^m}\int_0^x t^{m-1}e^{-t/\theta}dt = \frac{1}{\Gamma(m)}\int_0^{x/\theta} y^{m-1}e^{-y}dy = \frac{1}{\Gamma(m)}\gamma(m, x/\theta). \tag{2.17}$$

Moreover, the MGF of gamma distribution is readily calculated from (2.16) as

$$M_X(s) = \int_0^\infty f_X(x) e^{sx} dx, \tag{2.18}$$

where the application of [51, eq. (3.381 4)] leads to

$$M_X(s) = (1 - \theta s)^{-m}, \quad \mathrm{Re}\{s\} < 1/\theta, \tag{2.19}$$

obtaining an expression very similar to (2.13). Finally, from (2.19), the n-th moment of the distribution are derived as

$$\mathbb{E}[X^n] = \frac{d^n}{ds^n} M_X(s)\bigg|_{s=0} = \frac{\Gamma(m+n)}{\Gamma(m)} \theta^n. \tag{2.20}$$

The gamma distribution is alternatively formulated in terms of the shape parameter m and the rate parameter $\beta = 1/\theta$, or in terms of m and $\Omega = \mathbb{E}[X] = m\theta$. Expressions for the MGF, PDF and CDF of the gamma distribution with the distinct formulations are straightforwardly obtained from (2.16), (2.17) and (2.19) just by applying the equivalences between the different parameters.

Gamma distribution with integer parameters

An interesting particular case of the gamma distribution is that in which the shape parameter m is a positive integer, i.e., $m \in \mathbb{N}^+$. If so, then the gamma random variable X can be generated from independent and identically distributed (i.i.d.) real Gaussian random variables as

$$X = \sum_{i=1}^{2m} Z_i^2, \tag{2.21}$$

where $Z_i \in \mathbb{R}$ follow a Gaussian distribution with zero mean and variance $\theta/2$, i.e., $Z \sim \mathcal{N}(0, \theta/2)$. As stated before, this case corresponds to the central χ^2 distribution with $n = 2m$ degrees of freedom and $\sigma^2 = \theta/2$.

Remarkably, the CDF of gamma distribution (and that of the central χ^2 distribution when n is even) can be simplified under the assumption of $m \in \mathbb{N}^+$ by applying [51, eq. (3.351 1)] to the integral in (2.17), obtaining

$$F_X(x) = 1 - e^{-x/\theta} \sum_{k=0}^{m-1} \frac{x^k}{k! \theta^k} \tag{2.22}$$

and considerably improving the mathematical tractability of the distribution.

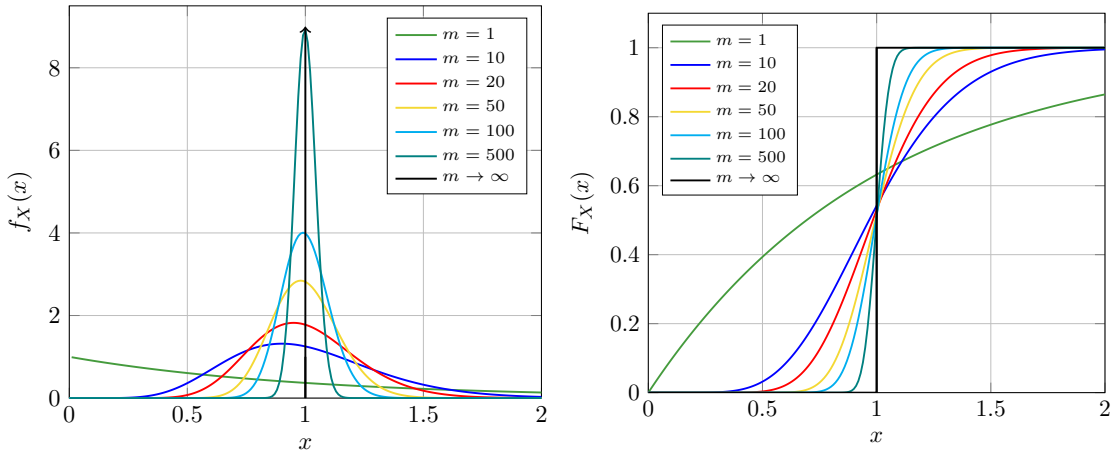

FIGURE 2.1: PDF and CDF of gamma distribution for different values of m and $\Omega = 1$

Degeneration of the gamma distribution

Of special interest to this thesis is the property of the gamma distribution of becoming a degenerate distribution. It is said that a distribution is degenerate if its corresponding random variable $X \in \mathbb{R}$ has only one possible value x_0 with probability $P(X = x_0) = 1$ [64, sec. 3.1] [2]. Consequently, the PDF of X is a delta function at x_0.

That can be achieved in the case of the gamma distribution by letting $m \to \infty$. To prove that, consider first the sequence $\{X_m : m \in \mathbb{N}^+\}$ where X_m is gamma distributed with shape parameter m and $\mathbb{E}[X_m] = \Omega$ and whose characteristic function (CF) is given by

$$\phi_{X_m}(jt) = \mathbb{E}\left[e^{jtX_m}\right] = M_{X_m}(jt) = \left(1 - \frac{j\Omega t}{m}\right)^{-m} \tag{2.23}$$

where j denotes the imaginary number $j = \sqrt{-1}$. Taking the limit in (2.23) leads to

$$\lim_{m\to\infty} \phi_{X_m}(jt) = e^{j\Omega t}, \tag{2.24}$$

which correspond to the CF of the constant variable $C = \Omega$. Therefore, by virtue of Levy's convergence theorem [52, chap. 18], we have that $\{X_m\} \Rightarrow C$. That is, increasing the value of m leads to a reduction in the variance of the gamma distribution and, in the limit, it becomes a constant variable whose PDF is a delta function at $x = \Omega$ (equivalently, its CDF tends to the step function). This behavior is shown in Fig. 2.1, where both the PDF and CDF of a gamma distribution is depicted for distinct m.

2.2.5 Classical approximations to the distribution of random variables

As introduced in Chapter 1, approximating the distribution of a random variable is a classical problem in applied statistics, mainly because of the difficulty of deriving exact

[2] Note that this definition only applies for 1-dimensional distributions.

and tractable expressions for the PDF and CDF of many random variables, e.g., GQFs [4]. Therefore, several efforts have been devoted to providing general methods that allow to approximate the distribution of such intricate variables. Most of these techniques are based on the knowledge of either the moments or the CF (or, equivalently, the MGF) of the target variable. This subsection aims to present a brief overview of the most classical methods to obtain approximations to distributions, highlighting their main flaws.

The saddle-point technique

The saddle-point technique (or method of steepest descent) is a generalization of Laplace's method to approximate integrals of the form

$$I = \int_{\mathcal{C}} f(t) e^{\alpha g(t)} dt \tag{2.25}$$

where $\mathcal{C}$ is a contour on the complex plane and α is a large number. It is extensively used in statistics to approximate the distribution of random variables from its MGF or its characteristic function by means of the inversion theorem [1, sec. 26]. Therefore, since the MGF can be seen as the Laplace transform of the PDF, the latter is calculated by performing the inverse transform as

$$f_X(x) = \frac{1}{j2\pi} \int_{\tau - j\infty}^{\tau + j\infty} e^{-sx} M_X(s) ds \tag{2.26}$$

with $\tau \in \mathbb{R}$. The above integral is rewritten as

$$f_X(x) = \frac{1}{j2\pi} \int_{\tau - j\infty}^{\tau + j\infty} \exp\left(K_X(s) - sx\right) ds \tag{2.27}$$

where $K_X(s) = \ln M_X(s)$ is the cumulant generating function (CGF). Expanding $K_X(s) - sx$ in Taylor series around a point $s = t_0(x)$ such that $K'_X(t_0(x)) = x$, we have

$$f_X(x) \approx \frac{1}{j2\pi} \exp\left(K_X(t_0(x)) - t_0(x)x\right) \int_{\tau - j\infty}^{\tau + j\infty} \exp\left(\frac{1}{2}(s - t_0(x))^2 K''_X(t_0(x))\right) ds. \tag{2.28}$$

The point $s = t_0(x)$ is a saddle-point of $K_X(s) - sx$, where the function is constant in the imaginary direction and has an extreme in the real one [32]. Hence, choosing $\tau = t_0(x)$, the integral in (2.28) is dominated by the value of the integrand at this point, and the approximation is tight. Solving the integral we obtain the saddle-point approximation for $f_X(x)$ as [32, eq. (21)]

$$f_X(x) \approx \exp\left(K_X(t_0(x)) - t_0(t)x\right) \sqrt{\frac{1}{2\pi K''_X(t_0(x))}}. \tag{2.29}$$

Similarly, the saddle-point technique can also be used to derive approximations for the CDF of X (see [32]–[35] for a more detailed explanation of this technique).

Despite it is widely used in statistics, the above approximation has two main drawbacks. First, there is no guarantee that (2.29) represents a valid distribution (generally it does not), i.e., the approximated PDF may not have unit area and probabilities greater than one might be obtained. Second, increasing the accuracy of the approximation is not trivial since it implies considering higher terms in the Taylor series, considerably complicating the calculation of the integral in (2.28).

Gram-Charlier and Edgeworth series

Gram-Charlier and Edgeworth series are used to approximate the PDF and CDF of a random variable, whose moments or cumulants are known, from another baseline distribution. We here present the formulation given in [35, chap. 3][36, chap. 5], although alternative formulations can be found in other works (see e.g. [37], [38]).

Consider two random variables X and Y with PDFs $f_X(x)$ and $f_Y(y)$ and MGFs $M_X(s)$ and $M_Y(t)$, respectively. The MGF of X can be expressed in terms of a power series as [35, p. 32]

$$M_X(s) = M_Y(s) \sum_{i=0}^{\infty} \mu_i \frac{s^i}{i!}, \tag{2.30}$$

where μ_i are the moments of the distribution whose cumulants are given by the difference of those of X and Y. Hence, defining κ_j^x and κ_j^y as the cumulants of X and Y respectively, μ_i are calculated as [65]

$$\mu_i = \sum_{j=0}^{i-1} \binom{i-1}{j} \mu_j (\kappa_{i-j}^x - \kappa_{i-j}^y) \tag{2.31}$$

for $i > 1$ with $\mu_0 = 1$ and $\mu_1 = \kappa_1^x - \kappa_1^y$. Formally, μ_i are not true moments of a distribution, since $\kappa_j^x - \kappa_j^y$ do not necessarily represent the cumulants of any random variable [36, p. 153].

To obtain the approximation to $f_X(x)$ is necessary to invert (2.30) term by term, taking into account that from the definition of the MGF the first term is $f_Y(x)$. For the other terms, it can be proved that, if $f_Y(x)$ is uniformly continuous, then [36, eq. (38)]

$$\int_{-\infty}^{\infty} e^{sx} f_Y^{(n)}(x) dx = s^n (-1)^n M_Y(s) \tag{2.32}$$

and, therefore, the PDF of X is expanded as

$$f_X(x) = \sum_{i=0}^{\infty} f_Y^{(i)}(x) \frac{(-1)^i \mu_i}{i!} = f_Y(x) \sum_{i=0}^{\infty} g_i(x) \frac{\mu_i}{i!}, \tag{2.33}$$

where $g_i(x) = (-1)^i f_Y^{(i)}(x)/f_Y(x)$. The complexity of the series expansions is thus determined by the computation of the derivatives of the baseline PDF, $f_Y(x)$. If Y is chosen to follow a standard Gaussian distribution, i.e., $Y \sim \mathcal{N}(0,1)$, then the expansion in (2.33) is known as Gram-Charlier series and $g_i(x)$ is given by

$$g_i(x) = 2^{-i/2} H_i(x/\sqrt{2}), \tag{2.34}$$

with $H_i(\cdot)$ the i-th order Hermite polynomial [51, eq. (8.950 1)]. Similarly, the CDF of X can be expanded in the same way just by dividing by s both terms in (2.30).

Although useful in some cases (e.g., the sum of independent and identically distributed random variables), Edgeworths series have important flaws. First, as with the saddle-point method, the approximated functions are not guaranteed to be proper PDFs (in fact negative probabilities may be obtained), and the accuracy is typically low in the tails of the distribution (the method ensures an absolute error but not a relative one) [35, chap. 3]. Therefore, if we are interested in estimating low probabilities (as in performance analysis in communications and signal detection), this type of approximations may lead to large errors. Moreover, under certain conditions, increasing the number of terms that are computed does not necessary increase the accuracy of the approximation [38, p. 14].

Orthogonal polynomials series

Another classical way of approximating the distribution of a random variable $X \in \mathbb{R}$ is expressing its PDF as a series of the form

$$f_X(x) = g(x) \sum_{i=0}^{\infty} \omega_i h_i(x) \tag{2.35}$$

where $g(x)$ is a known function, ω_i are constants and $h_i(x)$ is a sequence of orthogonal polynomials. Gram-Charlier series in (2.33) belongs to these type of expansions, for which $g(x)$ is the standard Gaussian PDF and $h_i(x)$ are the Hermite polynomials.

Expansions of the form (2.35) in terms of Lagrange and Laguerre polynomials are derived in [66, chap. 7][39] under some conditions. As with Edgeworth series, the moments of X (or its cumulants, since they are related as proved in [65]) are needed to build these approximations.

Specifically, consider a random variable X whose PDF has finite domain $[-1, 1]$ and whose n-th moment is given by μ_n^x. Therefore, $f_X(x)$ admits the following expansion [39, eq. (1)]

$$f_X(x) = \sum_{i=0}^{\infty} \lambda_i P_i(x), \tag{2.36}$$

with $P_i(x)$ the i-th order Legrendre polynomial [51, eq. (8.911 1)] and

$$\lambda_i = \frac{2i+1}{2^{i+1}} \sum_{j=0}^{\lceil i/2 \rceil} (-1)^j \frac{(2i-2j)!}{j!(i-j)!(i-2j)!} \mu_{i-2j}^x, \tag{2.37}$$

where $\lceil \cdot \rceil$ is the ceiling function, i.e., for any real number α it gives the least integer greater than or equal to α.

The approximant in (2.36) can be generalized to any random variable Y defined in a closed interval $[a, b]$ with moments μ_j^y by performing the change of variables

$$\widehat{X} = \frac{2Y - (a+b)}{b-a} \tag{2.38}$$

such that $\widehat{X} \in [-1, 1]$. Using now (2.36) and reverting the change of variables the PDF of Y is expressed as

$$f_Y(y) = \frac{2}{b-a} \sum_{i=0}^{\infty} \widehat{\lambda}_i P_i \left(\frac{2y - (a+b)}{b-a} \right), \tag{2.39}$$

where $\widehat{\lambda}_i$ are calculated as in (2.37) but replacing μ_j^x by the moments of $\widehat{X}$, which are obtained from those of Y as

$$\mu_j^{\widehat{x}} = \frac{1}{(b-a)^j} \sum_{k=0}^{j} \binom{j}{k} 2^k \mu_k^y (-1)^{j-k} (a+b)^{j-k}. \tag{2.40}$$

Moreover, for positive random variables $X \in \mathbb{R}^+$ with moments μ_n^x and whose PDF has domain $[0, \infty)$, a similar expansion can be obtained for $f_X(x)$ based on Laguerre polynomials, which is given by [39, eq. (27)]

$$f_X(x) = \frac{(x-a)^v e^{-y/c}}{c^{v+1}} \sum_{i=0}^{\infty} \delta_i L_i^{\alpha}(y/c) \tag{2.41}$$

with $c = (\mu_2^x - (\mu_1^x)^2)/\mu_1^x$, $v = \mu_1^x/c - 1$, $L_i^{\alpha}(\cdot)$ the i-th order Laguerre polynomial [51, eq. (8.970 1)] and

$$\delta_i = \sum_{k=0}^{i} (-1)^k \frac{i! \mu_{i-k}^x}{c^{i-k} k! (i-k)! \Gamma(v+i-k+1)}. \tag{2.42}$$

Expansions (2.39) and (2.41) are in general more tractable than other approximations arising, e.g., from the application of saddle-point technique, being therefore useful for further analytical purposes. However, once again, these series need to be truncated in order to be computed, rendering expressions which do not represent a proper distribution. In addition, the accuracy of the approximation strongly depends on the random variable under analysis. Thus, expansions of the type (2.41) are only recommended when the tail behavior of the target distribution is similar to that of the gamma distribution [66, p. 301].

Series expansions as mixtures of other densities

As already stated, the main drawback of the aforementioned techniques is that the resulting expressions do not represent proper distributions [40]. Aiming to overcome this issue, several efforts have been devoted in the related literature to seeking alternative approximants that fulfill the condition of being valid PDFs themselves. In this context, approximations based on mixture of density functions have been proposed [40]–[45], specially to fit the distribution of empirical data, providing approximants to a target PDF $f_X(x)$ of the form [41, eq. (1.4)]

$$f_X(x) \approx \sum_{i=1}^{n} w_i g(x; \boldsymbol{\theta}_i) \tag{2.43}$$

where $g(x; \boldsymbol{\theta}_i)$ is the PDF of the baseline distribution depending on a set of parameters $\boldsymbol{\theta}_i$ and w_i are constants such that $\sum_{i=1}^{n} w_i = 1$. The issue is now the choice of the baseline density function and the calculation of the mixture parameters, namely n, w_i and $\boldsymbol{\theta}_i$. Unfortunately, due to the generality of the problem, it is remarkably difficult to provide a general method to approximate an arbitrary distribution by (2.43).

Due to its mathematical properties and its practical importance, one of the most common choices for $g(\cdot)$ is the Gaussian distribution. In fact, it can be proved that any random variable can be obtained as the limit of a linear combination of Gaussian variables [43], [44]. However, other distributions such as gamma [42] or exponential [41, chap. 3] have also been proposed to approximate positive variables.

Similarly, several techniques have been classically used to estimate the mixture parameters. The method of moments is perhaps the most widely-extended preference, imposing that the first p moments of the mixture must be equal to those of the target distribution. Hence, a system of equations given by

$$\mu_j = \sum_{i=1}^{n} w_i \widehat{\mu}_j(\boldsymbol{\theta_i}),\ j = 1, \ldots, p \tag{2.44}$$

arise, where μ_j and $\widehat{\mu}_j$ denote the exact and mixture moments, respectively. This system can be solved to determine w_i and $\boldsymbol{\theta_i}$ for a given n, although for relatively large n it may be extremely tedious.

When the mixture model is used to approximate the distribution of empirical data, the distinct parameters can be estimated by solving the optimization problem that minimizes the L^p distance between the empirical and the mixture PDFs, defined as

$$L^p = \mathbb{E}\left[\left|\widehat{f}_X(\boldsymbol{x}) - \sum_{i=1}^{n} w_i g(\boldsymbol{x}; \boldsymbol{\theta}_i)\right|^p\right] \tag{2.45}$$

where $\boldsymbol{x}$ is the observed data. Another alternative is using the ML estimation [41, chap. 1]. Bayesian estimation has also been proposed to seek the mixture parameters when

characterizing stochastic non-linear systems [45] and linear systems with non-Gaussian noise [40].

On the whole, although approximants based on mixtures of density functions are a good alternative to the other techniques, the lack of a general methodology and the difficulty in estimating the mixture parameters ultimately limit their usefulness.

2.3 Gaussian quadratic forms

Due to their vast number of applications, and because one of the main purposes of this thesis is the analysis of GQFs, this section summarizes some of their most relevant properties, as well as the distinct methods that have been proposed to their statistical characterization.

2.3.1 Definition

The real case

Let $\overline{\mathbf{x}} \in \mathbb{R}^{n\times 1}$ be a constant vector, $\mathbf{A} \in \mathbb{R}^{n\times n}$ be a symmetric matrix and $\mathbf{x} \in \mathbb{R}^{n\times 1}$ be a random vector following a multivariate normal distribution with zero mean and covariance matrix $\mathbf{\Sigma} \in \mathbb{R}^{n\times n}$, i.e., $\mathbf{x} \sim \mathcal{N}_n(\mathbf{0}_{n\times 1}, \mathbf{\Sigma})$. Then, the real random variable

$$Q_R = (\mathbf{x} + \overline{\mathbf{x}})^T \mathbf{A} (\mathbf{x} + \overline{\mathbf{x}}) \tag{2.46}$$

is a real GQF [4, eq. (3.1.1)]. If all the entries of $\overline{\mathbf{x}}$ are zero, i.e., $\overline{\mathbf{x}} = \mathbf{0}_{n\times 1}$, then Q_R is a central quadratic form. In turn, if $\overline{\mathbf{x}} \neq \mathbf{0}_{n\times 1}$, it is non-central. Moreover, Q_R is said to be definite or indefinite depending on whether $\mathbf{A}$ is definite or not, respectively.

The quadratic form Q_R admits an alternative formulation in terms of independent standard Gaussian variables, which can be derived by applying simple algebraic transformations to (2.46). Thus, consider any decomposition of the form $\mathbf{\Sigma} = \mathbf{C}\mathbf{C}^T$, e.g., $\mathbf{C} = \mathbf{\Sigma}^{1/2}$, and the vector $\mathbf{s} = \mathbf{C}\mathbf{z}$ where $\mathbf{z} \sim \mathcal{N}_n(\mathbf{0}_{n\times 1}, \mathbf{I}_n)$. It can be easily proved that $\mathbf{s}$ is Gaussian distributed with

$$\mathbb{E}[\mathbf{s}] = \mathbf{C}\mathbb{E}[\mathbf{z}] = \mathbf{0}_{n\times 1} = \mathbb{E}[\mathbf{x}], \tag{2.47}$$

$$\mathbb{E}[\mathbf{s}\mathbf{s}^T] = \mathbf{C}\mathbb{E}[\mathbf{z}\mathbf{z}^T]\mathbf{C}^T = \mathbf{\Sigma} = \mathbb{E}[\mathbf{x}\mathbf{x}^T] \tag{2.48}$$

and, therefore, Q_R can be expressed as

$$Q_R = \left(\mathbf{z} + \mathbf{C}^{-1}\overline{\mathbf{x}}\right)^T \mathbf{C}^T\mathbf{A}\mathbf{C} \left(\mathbf{z} + \mathbf{C}^{-1}\overline{\mathbf{x}}\right). \tag{2.49}$$

Since $\mathbf{C}^T\mathbf{A}\mathbf{C}$ is symmetric, it can be diagonalized as $\mathbf{C}^T\mathbf{A}\mathbf{C} = \mathbf{U}\mathbf{\Lambda}\mathbf{U}^T$, where $\mathbf{U}$ is an orthogonal matrix and $\mathbf{\Lambda}$ is a diagonal matrix whose entries, λ_i for $i = 1, \ldots, n$ are

the eigenvalues of $\mathbf{C}^T\mathbf{A}\mathbf{C}$ (or, equivalently, those of $\mathbf{\Sigma}\mathbf{A}$) [67, chap. 2]. Hence, relabeling $\mathbf{y} = \mathbf{U}^T\mathbf{z}$ and $\mathbf{b} = \mathbf{U}^T\mathbf{C}^{-1}\overline{\mathbf{x}}$, we finally have

$$Q_R = (\mathbf{y} + \mathbf{b})^T\mathbf{\Lambda}(\mathbf{y} + \mathbf{b}) = \sum_{i=1}^{n} \lambda_i (y_i + b_i)^2 \tag{2.50}$$

where y_i and b_i are the entries of $\mathbf{y}$ and $\mathbf{b}$ respectively. Note that, since $\mathbf{U}$ is orthogonal, the distribution of $\mathbf{y}$ is the same as that of $\mathbf{z}$, i.e., $\mathbf{y} \sim \mathcal{N}_n(\mathbf{0}_{n\times 1}, \mathbf{I}_n)$. Therefore, Q_R is expressed as a linear combination of independent squared Gaussian random variables with means b_i, or equivalently, as a linear combination of independent noncentral χ^2 distributions of the form

$$Q_R = \sum_{i=1}^{n} \lambda_i Y_i, \quad Y_i \sim \chi_1^2(1, b_i^2). \tag{2.51}$$

Also, regarding (2.50), it can be observed that if $\lambda_i = 0$ for some i, then Q_R is equivalent to another quadratic form of less order. That corresponds to the case in which either or both $\mathbf{A}$ and $\mathbf{\Sigma}$ are rank deficient, and consequently the rank of $\mathbf{C}^T\mathbf{A}\mathbf{C}$ is $r < n$ and $\lambda_i = 0$ for $i = r+1, \ldots, n$. For simplicity, and without any loss of generality, hereinafter we will assume that both $\mathbf{A}$ and $\mathbf{\Sigma}$ are full-rank. Moreover, if $\mathbf{A}$ is positive or negative definite then $\lambda_i > 0$ and $\lambda_i < 0$ for all i, respectively, and equivalently λ_i can take both positive and negative values if $\mathbf{A}$ is indefinite.

The complex case

Analogously to the real case, GQFs in complex variables are defined as

$$Q_C = (\mathbf{v} + \overline{\mathbf{v}})^\dagger \mathbf{A}(\mathbf{v} + \overline{\mathbf{v}}) \tag{2.52}$$

where, in this case, $\overline{\mathbf{v}} \in \mathbb{C}^{n\times 1}$ is a constant vector representing the mean of $\mathbf{v}$, $\mathbf{A} \in \mathbb{C}^{n\times n}$ is an Hermitian matrix and $\mathbf{v} \in \mathbb{C}^{n\times 1}$ is complex multivariate Gaussian vector with zero mean and covariance matrix $\mathbf{\Sigma} \in \mathbb{C}^{n\times n}$, i.e. $\mathbf{v} \sim \mathcal{CN}_n(\mathbf{0}_{n\times 1}, \mathbf{\Sigma})$.

By following similar steps as in the real case, Q_C can also be written in terms of independent Gaussian variables. To that end, consider again any decomposition of $\mathbf{\Sigma}$ such that $\mathbf{\Sigma} = \mathbf{C}\mathbf{C}^\dagger$, e.g., the Cholesky factorization [68, p. 441], and diagonalize $\mathbf{C}^\dagger\mathbf{A}\mathbf{C}$ as $\mathbf{C}^\dagger\mathbf{A}\mathbf{C} = \mathbf{U}\mathbf{\Lambda}\mathbf{U}^\dagger$, where $\mathbf{U}$ is an unitary matrix and $\mathbf{\Lambda}$ is a diagonal matrix whose entries are the eigenvalues of $\mathbf{C}^\dagger\mathbf{A}\mathbf{C}$. Note that since $\mathbf{C}^\dagger\mathbf{A}\mathbf{C}$ is Hermitian, all its eigenvalues are real [67, p. 42]. By doing so and naming $\overline{\mathbf{h}} = \mathbf{U}^\dagger\mathbf{C}^{-1}\overline{\mathbf{v}}$, we obtain

$$Q_C = (\mathbf{s} + \overline{\mathbf{h}})^\dagger \mathbf{\Lambda}(\mathbf{s} + \overline{\mathbf{h}}) \tag{2.53}$$

where $\mathbf{s}$ is a complex multivariate standard Gaussian vector, i.e., $\mathbf{s} \sim \mathcal{CN}_n(\mathbf{0}_{n\times 1}, \mathbf{I}_n)$. Furthermore, denoting by $s_i = x_i + jy_i$ and $h_i = p_i + jq_i$ the entries of $\mathbf{s}$ and $\overline{\mathbf{h}}$ respectively,

with $x_i, y_i \sim \mathcal{N}(0, 1/2)\ \forall\ i$, Q_C can be finally expressed as

$$Q_C = \sum_{i=1}^{n} \lambda_i \left\| s_i + h_i \right\|^2 = \sum_{i=1}^{n} \lambda_i \left[(x_i + p_i)^2 + (y_i + q_i)^2 \right]. \tag{2.54}$$

Comparing (2.54) and (2.50), it is clear that a complex quadratic form is equivalent to a real one of double order n for which the eigenvalues λ_i are equal in pairs. As with Q_R, Q_C can also be expressed as a linear combination of independent non-central χ^2 distributions as

$$Q_C = \sum_{i=1}^{n} \lambda_i Y_i, \quad Y_i \sim \chi^2_2(1/2, \|h_i\|^2). \tag{2.55}$$

Moreover, if $p_i = q_i = 0\ \forall\ i$, then (2.54) corresponds to the gamma distribution with integer parameters in (2.21) by mapping $n = m$ and $\lambda_i = \theta\ \forall\ i$. Lastly, note that as in the real case, if $\mathbf{C}^\dagger\mathbf{A}\mathbf{C}$ is rank deficient then some λ_i are zero, and Q_C is equivalent to another quadratic form of order $r < n$.

2.3.2 Statistical characterization of non-central Gaussian quadratic forms

Although the MGF of both real and complex GQFs can be straightforwardly obtain from that of the χ^2 distribution, closed-form expressions for their PDF and CDF remain unknown for the general case. In the real case, exact closed-form expressions can only be obtained under certain conditions (e.g., $\mathbf{A} = \mathbf{\Sigma} = \mathbf{I}$, the identity matrix), remaining in complicated integral form for the general case, even when the involved random variables have zero mean. Quadratic forms in complex Gaussian variables are slightly more tractable, allowing a simple formulation for the main statistics in the central case. However, only approximated solutions have been given in the non-central one.

Due to the vast number of applications of both real an complex GQFs and the challenge that poses their statistical characterization, considerable efforts have been devoted in the last decades to their study [4], [5], [11], [69]–[79]. This section aims to provide a brief overview of the distinct approximations given in the literature to the distribution of these type of variables, focusing on the non-central case due to its generality. The real and complex cases are reviewed separately, although as stated before, any complex GQF can be considered as a real one with the eigenvalues given in pairs, so the analysis for real variables actually includes both cases.

The real case

Since any real GQF can be expressed as a linear combination of independent non-central χ^2 distributions as in (2.51), the MGF of Q_R is readily calculated as the product of

the individual MGFs of the χ^2 random variables. Thus, from (2.15) we obtain

$$M_{Q_R}(s) = \prod_{i=1}^{n} \exp\left(\frac{b_i^2 \lambda_i s}{1-2\lambda_i s}\right)(1-2\lambda_i s)^{-1/2}, \quad \lambda_i \mathrm{Re}\{s\} < 1/2 \; \forall \; i. \tag{2.56}$$

Note that in the central case, i.e., $b_i = 0 \; \forall \; i$, then the exponential term vanishes.

As for the PDF and the CDF, their analysis can be traced back to the work by Robbins and Pitman [69], where the distribution of positive definite central quadratic forms was expressed as a mixture of central χ^2 densities. A similar expansion was proposed and extended to the ratio of central GQFs in [5] in the context of the analysis of variances. Ruben [80] generalized the analysis by presenting another approximation in terms of non-central χ^2 variables which is also valid in the non-central case, although the restriction of positive definiteness still holds.

Other types of series expansions were proposed, e.g., by Gurland [74], who proposed an approximant of the form (2.36) in terms of Laguerre polynomials in the positive definite central case and in terms of more complicated polynomials in the non-central case. In [72], Shah extended the work by Gurland, considering by first time the most general case, i.e., indefinite non-central GQFs, giving expressions for the PDF and CDF in terms of intricate orthogonal polynomials. Unfortunately, the challenging computation of such polynomials and the complexity of the derived expressions considerably limit the usefulness of the proposed results. Imhof also considered the indefinite non-central case [73], proposing the inversion of the CF by numerical integration.

All the above series expansions were unified (although restricted to the positive definite case) by Kotz et al. for both the central [70] and non-central case [71], and revisited several years later in [4], providing a general method to seek approximations for positive definite real GQFs in terms of powers, orthogonal polynomials and χ^2 densities. This general method aims to find a series expansion for the PDF of the form [71, eq. (106)]

$$f_{Q_R}(x) = \sum_{k=0}^{\infty} c_k h_k(x) \tag{2.57}$$

where c_k are constants and $\{h_k(x) : k \in \mathbb{N}\}$ is a sequence of known functions. Therefore, if

$$\sum_{k=0}^{\infty} c_k h_k(x) \leq \sum_{k=0}^{\infty} |c_k||h_k(x)| \leq \beta e^{\alpha x} \tag{2.58}$$

for all $x \in \mathbb{R}^+$ with α and β real constants, then the Laplace transform of $f_{Q_R}(x)$ is calculated as [4, lem. 4.2a.1]

$$\mathcal{L}\{f_{Q_R}(x)\} \triangleq \widehat{f}(s) \triangleq \sum_{k=0}^{\infty} c_k \widehat{h}_k(s), \quad \mathrm{Re}\{s\} > \alpha \tag{2.59}$$

where $\widehat{h}_k(s)$ denotes the Laplace transform of $h_k(x)$.

The method is then based on choosing $h_k(s)$ such that (2.58) holds and

$$\widehat{h}_k(s) = g(s)\eta^k(s) \tag{2.60}$$

with $g(s)$ an analytic, non-vanishing function and $\eta(s)$ is analytic for $\mathrm{Re}\{s\} > \alpha$ and has inverse function $\phi(s)$, i.e. $\eta(\phi(s_0)) = s_0$.

Once the baseline sequence of functions $\{h_k(x)\}$ is chosen, the coefficients c_k are obtained from equating (2.59) with (2.56). Moreover, the CDF can be obtained by integrating term by term (2.57). At this point, different series arise depending on this choice:

- **Power series**. In this case $h_k(s)$ is given by

$$h_k(x) = (-1)^k \frac{x^{n/2+k-1}}{\Gamma(n/2+k)} \tag{2.61}$$

  and, therefore, $g(s) = s^{-n/2}$ and $\eta(s) = (-s)^{-1}$. With this choice, the CDF of real non-central Gaussian quadratic forms is expressed as [4, eq. (4.2b.13)]

$$F_{Q_R}(x) = \sum_{i=0}^{\infty} c_k (-1)^k \frac{x^{n/2+k-1}}{\Gamma(n/2+k)} \tag{2.62}$$

  where c_k are calculated as in [4, eqs. (4.2b.5), (4.2b.8) and (4.2b.10)]. The major limitation of (2.62) is the calculation of c_k, since numerical issues could be significantly relevant. The problem is that, although c_k usually take small values for all k, they are calculated as the difference of large numbers, which is a challenging task due to the limited floating-point precision in calculation software [71, p. 840].

- **Laguerre series**. This particular case arises when choosing

$$h_k(x) = \frac{k!}{2\beta_L \Gamma(n/2+k)} \left(\frac{x}{2\beta_L}\right)^{n/2-1} e^{-x/2} L_k^{n/2-1}\left(\frac{x}{2\beta_L}\right) \tag{2.63}$$

  with $L_k^{\alpha}(\cdot)$ the k-th order Laguerre polynomial [51, eq. (8.970 1)] and β a real constant such that $\beta_L > \lambda_{\max}/2$, where $\lambda_{\max} = \max_i\{\lambda_i\}$. With that, and using [70, eq. (47)], we can straightforwardly identify $g(s) = (1+2s\beta_L)^{-n/2}$ and $\eta(s) = 2s\beta_L/(1+2s\beta_L)$, obtaining an expansion for the CDF of Q_R of the form [71, eq. (132)]

$$F_Q(x) = F\left(n, \beta_L, x\right) + \sum_{k=1}^{\infty} c_k \frac{\Gamma(k)}{\Gamma\left(k+\frac{n}{2}\right)} \left(\frac{x}{2\beta_L}\right)^{n/2} e^{-x/(2\beta_L)} L_{k-1}^{n/2}\left(\frac{x}{2\beta_L}\right) \tag{2.64}$$

  where $F\left(n, \beta_L, x\right)$ is given in [4, p. 109] and coefficients c_k are calculated according to [4, eqs. (4.2b.5) and (4.2c.14)].

  An important drawback of this approximation is the choice of β_L, which controls the convergence of the series. In [70], [71], a value of $\beta_L = (\lambda_{\max} + \lambda_{\min})/2$ is recommended. However, this value may render numerical errors depending on

the parameters of the quadratic form, preventing the series convergence. Hence, it is not clear how to find the value of β_L that yields the best approximation in each case.

- **Expansion in χ^2 densities.** The baseline function $h_k(x)$ is now the PDF of the central χ^2 distribution (2.11) with order $n + 2k$ and variance β_χ, where β_χ is a real parameter controlling the series convergence. Thus, from (2.13), it is readily observed that $g(s) = (1 + 2s\beta_\chi)^{-n/2}$ and $\eta(s) = (1 + 2s\beta_\chi)^{-1}$. This choice leads to a series expansion given by

$$F_{Q_R}(x) = \sum_{k=0}^{\infty} c_k \frac{1}{\Gamma(n/2+k)} \gamma\left(\frac{n}{2}+k, \frac{x}{2\beta_\chi}\right), \tag{2.65}$$

  which is valid for $0 < \beta_\chi < \lambda_{\min}$ with c_k given by [4, eqs. (4.2b.8) and (4.2b.9)]. The choice of β_χ in this case seems less problematic than in the Laguerre series, observing that higher values in the given interval accelerate the series convergence in all cases.

The above method also allows another types of approximants based on non-central χ^2 densities or hypergeometric functions, but the mathematical tractability of the resulting expressions is considerably reduced.

An alternative approximation for the distribution of real GQFs was recently given in [11, eq. (46)], where the saddle-point technique is applied to approximate the integral that defines the CDF. However, the results are restricted to the central case. Moreover, it inherits the drawbacks of this type of approximations, i.e., difficulty in increasing the accuracy of the approximation and probability values that may be greater than one.

The complex case

Although they can be seen as a particular case of the real case, complex GQFs have interest by themselves due to their massive number of applications, specially in communications and signal detection, where most of the involved random variables are complex (e.g. the Gaussian noise) [6]–[16]. Therefore, considerable efforts have been also devoted to their study.

The MGF of Q_C can be derived from (2.55) and (2.15) in the same way as in the real case, obtaining [76, eq. (4b)]

$$M_{Q_C}(s) = \prod_{i=1}^{n} \exp\left(\frac{\mu_i \lambda_i s}{1-\lambda_i s}\right)(1-\lambda_i s)^{-1}, \quad \lambda_i \mathrm{Re}\{s\} < 1 \; \forall \, i \tag{2.66}$$

where $\mu_i = \|h_i\|^2$.

Note that, since a complex quadratic form is equivalent to a real one with the eigenvalues given in pairs, as stated in Section 2.3.1, the exponent of the terms $(1 - \lambda_i s)$ is

always an integer number, in contrast to that in (2.56). Consequently, $M_{Q_C}(s)$ is given by a rational function in the central case, where the exponential term vanishes, allowing to obtain exact closed-form expressions for both the PDF and the CDF by directly inverting $M_{Q_C}(s)$. However, in the non-central case, no closed-form expressions are known in the general case and thus it is necessary to rely on approximations to both statistics.

Most of these approximations arise, similarly as those in the real case, by the inversion of the MGF or, equivalently, the CF [77]–[79], rendering different approximated expressions for the PDF and CDF of complex GQFs.

The work by Biyari and Lindsey considers a particular case of non-central quadratic form which is of special interest in communications [77]. Specifically, it analyzes the quadratic form resulting from the sum of L independent and identically distributed quadratic forms of order $n = 2$ and inverts its MGF by solving some convolution integrals. As a result, the PDF and CDF of this specific quadratic form are given in terms of an infinite sum of Laguerre polynomials.

A more general approximation is given by Raphaeli, where the indefinite non-central case is considered [78]. He uses the residue theorem to invert the MGF of Q_C, expressing the residues as infinite series in order to circumvent the essential singularities of $M_{Q_C}(s)$. Therefore, the CDF of Q_C is calculated as [78, eq. (26)]

$$F_{Q_C}(x) = 1 + \frac{1}{2\pi j}\int_{\mathcal{C}} \frac{1}{s} e^{-sx} M_{Q_C}(s) ds \tag{2.67}$$

where $\mathcal{C}$ is a contour circling the right half plane but excluding the imaginary axis if $x > 0$ and circling the left half plane when $x < 0$. Thus, applying the residue theorem we have

$$F_{Q_C}(x) = \begin{cases} 1 + \displaystyle\sum_{\lambda_k > 0} \operatorname{Res}\left\{\widehat{F}_k(0)\right\} & \text{if } \; x > 0 \\ -\displaystyle\sum_{\lambda_k < 0} \operatorname{Res}\left\{\widehat{F}_k(0)\right\} & \text{if } \; x < 0 \end{cases}, \tag{2.68}$$

with [78, eq. (27)]

$$\widehat{F}_k(s) = \frac{1}{s + \lambda_k^{-1}} \exp\left(-x(s + \lambda_k^{-1})\right) M_{Q_C}(s + \lambda_k^{-1}). \tag{2.69}$$

Note that, for each $\widehat{F}_k(s)$, the pole at $s = \lambda_k^{-1}$ is translated to $s = 0$ for convenience. Also, this procedure assumes that all the eigenvalues λ_k are distinct with multiplicities m_k.

The next step is expressing $\widehat{F}_k(s)$ as the product of two functions $\widehat{g}_k(s, x)$ and $f_k(s)$ as in [78, eq. (30)], and then expanding $f_k(s)$ in Laurent series and $\widehat{g}_k(s, x)$ in Taylor series. By doing that, the residues of $\widehat{F}_k(s)$ can therefore be computed recursively, and the CDF

of Q_C is finally expressed as [78, eq. (32)]

$$F_{Q_C}(x) = 1 + \exp\left(\sum_{j=1}^{N} \mu_j\right) \sum_{\lambda_k > 0} \frac{1}{(-\lambda_k/2)^{m_k-1}} e^{-x/\lambda_k} \sum_{i=m_k-1}^{\infty} \widehat{g}_k^{(i)}(0, x/2) \frac{(2\mu_k/\lambda_k)^{i-m_k+1}}{i!(i-m_k+1)!} \tag{2.70}$$

for $x > 0$ with N denoting the number of distinct eigenvalues λ_k. If $x < 0$, then the sum is over all $\lambda_k < 0$ as stated in (2.68). The derivatives of $\widehat{g}_k(s, x)$ are calculated according to [78, eqs. (18-21) and (31)] but taking into account that, due to slight differences in the definitions of λ_k and μ_k, we should replace $\underline{\lambda}_k = \lambda_k/2$ and $\underline{\mu}_k^2 = 2\mu_k$, where the parameters in [78] have been underlined in order to avoid confusion. Note that these equivalences have been already applied in (2.70).

A very similar expansion for the PDF is given in [78, eq. (25)], but due to the recursion that involves the independent variable x the expression is not useful for further analytic purposes, e.g., the calculation of expectations over the quadratic form. Being aware of this issue, Raphaeli proposed an alternative approximation for the PDF [78, eq. (38)] in terms of an infinite sum of modified Bessel functions. In this case, although the recursion does not involve x, the Bessel functions considerably limit the tractability of the series.

Another approximation was given by Tziritas in [79], where he considered the positive definite case and proposed series expansions for the PDF and CDF in terms of other distributions. Specifically, the gamma and the non-central χ^2 distributions are considered in the central and non-central case, respectively. Remarkably, the results are valid for both real and complex quadratic forms (with slight modifications).

Hence, focusing on the non-central case, the proposed baseline density is

$$f(x) = \frac{x^{a/2}}{bc^a} \exp\left(-\frac{x + c^2}{b}\right) I_a(2c\sqrt{x}/b), \tag{2.71}$$

which corresponds to the PDF of $X = bY/2$ with $Y \sim \chi^2_{2(a+1)}(1, 2c^2/b)$. The parameters a, b and c are chosen so that the first three moments of X are equal to those of Q_C. With that, the resulting series expansion for the CDF is given by [79, eq. (40)]

$$F_{Q_C}(x) = \sum_{i=0}^{\infty} c_i \binom{a+i}{i} \sum_{k=0}^{i} \binom{i}{k} \left(\frac{-b}{\beta}\right)^k \left[1 - Q_{a+1}\left(\sqrt{\frac{2}{b}}c, \sqrt{\frac{2x}{b}}\right)\right], \tag{2.72}$$

where $Q_M(\alpha, \delta)$ is the generalized Marcum Q function [18, eq. (4.59)], β is a real constant that controls the series convergence and must satisfies [79, eq. (23)]

$$\beta^{-1} > 2(b^{-1} - \lambda_{\max}^{-1}) \quad \text{in the complex case,} \tag{2.73}$$

$$\beta^{-1} > 2(b^{-1} - (2\lambda_{\max})^{-1}) \quad \text{in the real case,} \tag{2.74}$$

and c_i are constants that are obtained recursively according to [79, eqs. (26-28)]. The main drawback of this approximation is its complexity, i.e., the intricate recursion of constants

c_i that involves infinite sums and the required calculation of several Marcum Q functions undoubtedly limit the usefulness of (2.72). Moreover, when truncated, the series does not represent a valid CDF.

Taking into account the limitations of the direct inversion methods above introduced, since the solutions provided for the PDF and the CDF are difficult to compute and not suitable for any further insightful analysis, very recently, Al-Naffouri et al. presented a different approach [11]. They applied a transformation to the inequality that defines the CDF of Q_C, and approximated the resulting integral by the saddle-point technique.

Hence, the starting point is the integral definition of the CDF, expressed as [11, eq. (9)]

$$F_{Q_C}(x) = \int_{\mathcal{A}} f_{\mathbf{s}}(\mathbf{s}) d\mathbf{s} = \int_{-\infty}^{\infty} f_{\mathbf{s}}(\mathbf{s}) \mathrm{u}\left(x - (\mathbf{s}+\overline{\mathbf{h}})^{\dagger}\mathbf{\Lambda}(\mathbf{s}+\overline{\mathbf{h}})\right) d\mathbf{s} \tag{2.75}$$

where $\mathcal{A}$ is the area in the n-dimensional complex plane defined by the inequality $Q_C < x$, $\mathrm{u}(\cdot)$ is the unit step function whose value is 1 if the argument is non-negative and 0 otherwise, and $\mathbf{s}$, $\overline{\mathbf{h}}$ and $\mathbf{\Lambda}$ are the parameters of the quadratic form defined in (2.53).

Manipulating (2.75) and using [11, eq. (14)] we have

$$F_{Q_C}(x) = \frac{1}{2\pi} \int_{-\infty}^{\infty} \frac{1}{\det\left(\mathbf{I}_n + (j\omega+\beta)\mathbf{\Lambda}\right)} \frac{e^{x(j\omega+\beta)}}{j\omega+\beta} e^{-c(\omega)} d\omega \tag{2.76}$$

where β is a positive real constant and

$$c(\omega) = \overline{\mathbf{h}}^{\dagger}\left(\mathbf{I}_n + \frac{1}{j\omega+\beta}\mathbf{\Lambda}^{-1}\right)^{-1}\overline{\mathbf{h}}. \tag{2.77}$$

Since the above integral cannot be put in closed-form, the authors in [11] applied the saddle-point technique described in Section 2.2.5, obtaining

$$F_{Q_C}(x) \approx \frac{1}{2\pi} \exp\left(s(\omega_0)\right) \sqrt{\frac{2\pi}{\|s''(\omega_0)\|}} \tag{2.78}$$

where

$$s(\omega) = x(j\omega+\beta) - c(\omega) - \ln(j\omega+\beta) - \sum_{i=1}^{n} \ln\left(1+\lambda_i(j\omega+\beta)\right) \tag{2.79}$$

and ω_0 is a complex point such that $s^{'}(\omega_0) = 0$.

Despite the compactness of the expression in (2.78), that approximation has the same drawbacks as the previous ones, i.e., it does not represent a valid CDF. Moreover, it is difficult to increase the accuracy of the approximation and it is not clear how to obtain the PDF of Q_C by using this approach.

Finally, for reader's convenience, a summary of the aforementioned methods to approximate the CDF of non-central complex GQFs is given in Table 2.1.

TABLE 2.1: Summary of the distinct approximations to the CDF, $F_{Q_C}(x)$, of non-central complex GQFs.

Reference	Type of approximation	Main drawbacks
[77]	Infinite sum of Laguerre polynomials	Only valid for a particular complex GQF Not a proper CDF when the series is truncated
[78]	Infinite series of elementary functions	Recursion involving the independent variable x Not a proper CDF when the series is truncated
[79]	Double infinite series of Marcum functions	Coefficients involve intricate recursions Not a proper CDF when the series is truncated Computation of several Marcum functions is required
[11]	Saddle-point approximation	Not a proper CDF Increasing the accuracy is difficult

2.4 Fading models overview

In wireless environments, the radio signal is affected by a number of random phenomena (reflection, diffraction and scattering among others) as it travels from transmitter to receiver. Consequently, the received signal appears as a linear combination of multipath waves, each of which with their own (random) amplitudes and phases. This constructive and destructive addition of the distinct multipath waves renders strong and rapidly-varying fluctuations in the received signal amplitude, known as *fast fading*. Due to the multipath propagation, the complex based-band signal can therefore be written as [81, eq. (1)]

$$\widetilde{V} = \sum_{i=1}^{N} V_i e^{j\phi_i}, \tag{2.80}$$

where N denotes the number of multipath waves, V_i their amplitudes and ϕ_i their phases.

Aiming to analyze and improve the performance of wireless communication systems, considerable efforts have been devoted to the characterization of fading. Consequently, a wide variety of models have been developed in the related literature in order to describe the statistical behavior of the received signal amplitude $R = \|\widetilde{V}\|$, including both the classical fading models along with more general models. In the following, a brief overview of most widely used fading distributions is given. Note that we consider only flat-fading models, i.e., those employed to characterize fading which affects narrowband wireless systems.

2.4.1 Classical fading models

When N is sufficiently large, the baseband voltage $\widetilde{V}$ in (2.80) can be regarded as a complex Gaussian random variable because of the central limit theorem [1, sec. 27]. Depending on the choice of the parameters characterizing this complex Gaussian variable,

namely the mean and variance of the in-phase and quadrature components, different classical fading models emerge. A more detailed review of these classical models can be found in standard reference books, e.g., [17, chap. 2] and [18, chap. 2].

Rayleigh

Rayleigh model assumes that all the multipath components in (2.80) have similar amplitudes and independent phases which are uniformly distributed. Therefore, under the central limit theorem assumption, the received signal envelope R is model as the magnitude of a zero mean circularly-symmetric complex Gaussian random variable, i.e.,

$$R = \|\sigma X + j\sigma Y\| \tag{2.81}$$

where X and Y are independent standard Gaussian random variables, i.e., $X, Y \sim \mathcal{N}(0,1)$ and σ is a positive real constant. The PDF of R is then given by

$$f_R(r) = \frac{2r}{\Omega} \exp\left(-\frac{r^2}{\Omega}\right), \tag{2.82}$$

with $\Omega = \mathbb{E}[R^2] = 2\sigma^2$.

Due to its mathematical simplicity, Rayleigh distribution is massively used to model fading arising from non line of sight (NLoS) scenarios, where all the multipath components are assumed to have the same average power.

Rice

In contrast to Rayleigh model, Rice model (also known as Nakagami-n or Rician) considers that the complex Gaussian random variable arising from the application of the central limit theorem has non-zero mean, i.e.,

$$R = \|\sigma X + j\sigma Y + p + jq\| \tag{2.83}$$

with $X, Y \sim \mathcal{N}(0,1)$ and p, q and σ real constants.

The PDF of R is therefore given by [82, eq. (3.12)]

$$f_R(r) = \frac{2r(1+K)e^{-K}}{\Omega} \exp\left(-\frac{r^2(1+K)}{\Omega}\right) I_0\left(2r\sqrt{\frac{K(1+K)}{\Omega}}\right) \tag{2.84}$$

where $\Omega = \mathbb{E}[R^2] = p^2 + q^2 + 2\sigma^2$ and $K = (p^2+q^2)/(2\sigma^2)$ is the Rice factor, which corresponds to the ratio of the power of the dominant component to the average power of the scattering. Since for $K = 0$ the Rayleigh distribution is obtained, Rice model can be seen as the natural extension of the Rayleigh model to LoS scenarios.

Hoyt

Neither Rayleigh nor Rice models take into account the effect of the power imbalance between the in-phase and the quadrature components of the received signal, i.e., both of them assumes that the real and imaginary part of the complex Gaussian random variable have equal variances. This effect is considered by the Hoyt (Nakagami-q) distribution, according to which the received amplitude is modeled as

$$R = \|\sigma_x X + j\sigma_y Y\| \tag{2.85}$$

where $X, Y \sim \mathcal{N}(0,1)$ and $\sigma_x, \sigma_y \in \mathbb{R}^+$.

The PDF of Hoyt distribution is given by [83, eq. (3.4)]

$$f_R(r) = \frac{(1+\eta)r}{\sqrt{\eta}\Omega} \exp\left(-\frac{(1+\eta)^2 r^2}{4\eta\Omega}\right) I_0\left(\frac{(1-\eta^2)r^2}{4\eta\Omega}\right) \tag{2.86}$$

with $\Omega = \mathbb{E}[R^2]$ and $\eta = \sigma_x^2/\sigma_y^2$ representing the ratio of the powers of X (in-phase component) and Y (quadrature component)[3]. Note that if $\eta = 1$, then (2.86) reduces to (2.82).

Hoyt distribution is one of the distribution employed to model the so-called worse-than-Rayleigh fading conditions, i.e., scenarios where the fading conditions are more severe than those given by Rayleigh distribution [18], [84].

Beckmann

Although not very used due to its mathematical complexity, the Beckmann model [85] is the most general fading model arising from the central limit theorem assumption, taking into account not only the power imbalance between the scattering components but also between the LoS component. Therefore, the received signal amplitude is described as

$$R = \|\sigma_x X + j\sigma_y Y + p + jq\| \tag{2.87}$$

where X, Y are independent random variables such as $X, Y \sim \mathcal{N}(0,1)$ and $\sigma_x, \sigma_y \in \mathbb{R}^+$ and $p, q \in \mathbb{R}$ are constants.

[3]Traditionally, η is also denoted as q^2. However, we here prefer the first notation in order to be coherent with the definition of equivalent parameters in more general fading models.

Due to its generality, the PDF of the Beckmann distribution is only given in terms of double infinite sums of products of Bessel functions or in integral form

$$f_R(r) = \frac{r(1+\eta)(1+K)}{2\pi\Omega\sqrt{\eta}} \times \int_0^{2\pi} \exp\left[-\frac{\left(r\cos\theta - \sqrt{\frac{\varrho^2 K\Omega}{(1+\varrho^2)(1+K)}}\right)^2}{\frac{2\eta\Omega}{(1+\eta)(1+K)}} - \frac{\left(r\sin\theta - \sqrt{\frac{K\Omega}{(1+\varrho^2)(1+K)}}\right)^2}{\frac{2\Omega}{(1+\eta)(1+K)}} \right] d\theta \quad (2.88)$$

with $\Omega = \mathbb{E}[R^2] = \sigma_x^2 + \sigma_y^2 + p^2 + q^2$ and

$$K = \frac{p^2+q^2}{\sigma_x^2+\sigma_y^2}, \qquad \eta = \frac{\sigma_x^2}{\sigma_y^2}, \qquad \varrho^2 = \frac{p^2}{q^2}. \quad (2.89)$$

Parameter K is directly related to the Rice factor, since it corresponds to the ratio of the power of the dominant component to that of the scattering, and parameter η is also equivalent to that in Hoyt distribution. Finally, ϱ determines the power imbalance in the dominant component. Remarkably, if $\eta = 1$ and/or $K = 0$, then it can be proved that ϱ vanishes in (2.88).

Beckmann distribution includes as particular cases the three aforementioned classical models: Rayleigh ($K = 0$, $\eta = 1$, $\forall\varrho$), Rice ($K = K_{\text{Rice}}$, $\eta = 1$, $\forall\varrho$) and Hoyt ($K = 0$, $\eta = \eta_{\text{Hoyt}}$, $\forall\varrho$).

Nakagami-m

Nakagami-m model was introduced in [20] with the aim of generalizing Rayleigh model to improve the fitting to data measurement. Although the model accurately characterize the propagation conditions in many scenarios, no physical justification is given for its use. The PDF of Nakagami-m distribution is given by

$$f_R(r) = \frac{2m^m r^{2m-1}}{\Omega^m \Gamma(m)} e^{-mr^2/\Omega}, \quad (2.90)$$

where $m > 1/2$ is the Nakagami parameter and $\Omega = \mathbb{E}[R^2]$. If $m = 1$, then we obtain the Rayleigh distribution. Also, for $m \in \mathbb{N}^+$, the received signal amplitude can be obtained from the same underlying Gaussian model than the previous distributions as

$$R = \left(\sum_{i=1}^{m} \|\sigma X_i + j\sigma Y_i\|^2 \right)^{1/2} \quad (2.91)$$

where X_i and Y_i $\forall\, i$ are independent standard Gaussian random variables.

Because of its good agreement with empirical data and its mathematical tractability, the Nakagami-m distribution is one of the most employed to characterize fading conditions in a wide variety of scenarios. Moreover, it can approximate both Hoyt and Rice distribution by the mapping given in [18, eqs. (2.25) and (2.26)],.

An important remark is the connection between Nakagami-m and Gamma distributions. Specifically, if X is Nakagami-m distributed, then $Y = X^2$ is Gamma distributed with shape parameter m and scale parameter Ω/m, i.e., $Y \sim \Gamma(m, \Omega/m)$.

2.4.2 Generalized fading models

As introduced before, aiming to provide more flexibility when attempting to characterize fading conditions in more intricate scenarios (e.g. underwater acoustic or millimeter wave propagation) as well as to unify the distinct classical fading distributions under the umbrella of more general models, several distributions have been proposed in the last years.

These general fading models not only increase the accuracy of fittings to data measurement, but they also sometimes improve the mathematical tractability of the classical models. We here revisit some of these general distributions, focusing on their connections to other fading models.

Rician shadowed

The Rician shadowed model was originally proposed in [86] as a generalization of Rice model to describe fading behavior in land mobile satellite link [18, chap. 2]. It considers that the dominant (LoS) component is no longer deterministic but instead lognormally distributed. However, Rician shadowed model inherits the complicated formulation of lognormal distribution, and its PDF is only given in integral form [86, eq. (6)].

Aiming to gain mathematical tractability but maintaining the closeness to measured data, an alternative formulation of Rician shadowed model was given in [87], in which the LoS component is Gamma distributed, describing the received signal amplitude as

$$R = \|\sigma X + j\sigma Y + \xi(p + jq)\| \tag{2.92}$$

with $X, Y \sim \mathcal{N}(0, 1)$, $\xi^2 \sim \Gamma(m, 1/m)$ and σ_x, σ_y, p and q constants as in Rice model. Note that all the involved random variables are independent. The PDF of R is therefore given by

$$f_R(r) = \left(\frac{m}{m+K}\right)^m \frac{2r(1+K)}{\Omega} e^{-r^2(1+K)/\Omega} {}_1F_1\left(m; 1; \frac{r^2K(1+K)}{\Omega(m+K)}\right) \tag{2.93}$$

where $K = (p^2 + q^2)/(2\sigma^2)$, $\Omega = \mathbb{E}[R^2] = p^2 + q^2 + 2\sigma^2$ and ${}_1F_1(\cdot)$ is the Kummer's hypergeometric function [51, eq. (9.210 1)].

The addition of the random variable ξ introduces a random fluctuation in the dominant component that characterizes the shadowing. This fluctuation is controlled by parameter m, reducing its severity as m becomes larger. If $m \to \infty$, then Rice model is obtained, as can be easily proved by taking the limit in (2.93) and applying [50, eq. (13.3.1)].

κ-μ

The κ-μ model [28], [88] was introduced as a generalization of the Rice distribution in the same way as Nakagami-m extends Rayleigh model. In [28], a physical explanation for such generalization is given, according to which the received signal amplitude is built out of the superposition of clusters of waves. The power of the LoS component is distinct within each cluster, but the scattered waves of all clusters are assumed to have the same power. Therefore, the received signal amplitude is given by [28, eq. (6)]

$$R = \left(\sum_{i=1}^{\mu} \left\| \sigma X_i + j\sigma Y_i + p_i + jq_i \right\|^2 \right)^{1/2} \tag{2.94}$$

where $X_i, Y_i \sim \mathcal{N}(0,1)\ \forall\ i$,$\sigma \in \mathbb{R}^+$ and $p_i, q_i \in \mathbb{R}$ are constants and $\mu \in \mathbb{N}^+$ is the parameter that effectively generalizes Rice distribution, being equivalent to m in the Nakagami-m model.

The PDF of R is given in a similar form to that of the Rice distribution as [28, eq. (1)]

$$f_R(r) = \frac{2\mu(1+\kappa)^{\mu/2+1/2}}{\kappa^{\mu/2-1/2} e^{\mu\kappa}} \frac{r^{\mu}}{\Omega^{\mu/2+1/2}} e^{-r^2\mu(1+\kappa)/\Omega} I_{\mu-1}\left(2\mu r \sqrt{\frac{\kappa(1+\kappa)}{\Omega}} \right) \tag{2.95}$$

with

$$\kappa = \frac{\sum_{i=1}^{\mu} p_i^2 + q_i^2}{2\mu\sigma^2}, \qquad \Omega = \mathbb{E}[R^2] = \sum_{i=1}^{\mu} p_i^2 + q_i^2 + 2\mu\sigma^2. \tag{2.96}$$

Note that the meaning of κ is similar to that of the Rice K-factor, corresponding to the ratio of the power of the LoS component to that of the diffuse component.

The physical model in (2.94) forces μ to be a positive integer number. However, (2.95) is valid for $\mu \in \mathbb{R}^+$ although it loses its physical meaning.

Nevertheless, the extra parameter compared to Rice model (which is obtained by setting $\mu = 1$ and $\kappa = K$) provides a better accuracy in fitting data measurements but maintaining the mathematical tractability of the original model. In addition, it also includes Nakagami-m distribution as particular case ($\mu = m$, $\kappa = 0$).

An important remark is that R^2 in (2.94) can be identified as a particular case of the complex Gaussian quadratic form in (2.52) in which $\mathbf{A} = \mathbf{\Sigma} = \mathbf{I}_{\mu}$. Therefore, the κ-μ

model, as well as all the fading distributions derived from it, can be analyzed as part of a more general problem.

η-μ

Similarly as the κ-μ distribution generalizes the Rice model, the η-μ distribution arises as an extension of the Hoyt model under the same physical argument of clustering of waves [28]. Therefore, the received signal envelope is built as

$$R = \left(\sum_{i=1}^{\mu} \|\sigma_x X_i + j\sigma_y Y_i\|^2 \right)^{1/2} \tag{2.97}$$

where μ is the same parameter as in the κ-μ model, $X_i, Y_i \sim \mathcal{N}(0,1)\ \forall\ i$ and $\sigma_x, \sigma_y \in \mathbb{R}^+$ correspond to the variance of the in-phase and quadrature scattering components, respectively. Some details should be pointed out here: *(i)* the author in [28] proposed two different formats for the η-μ distribution, and the physical model in (2.97) corresponds to what he called *format one*; *(ii)* the number of clusters in this format was originally denoted by 2μ, but we here prefer to redefine the parameter μ in order to be coherent with that in κ-μ fading model. Therefore, according to (2.97), the PDF of R is given by

$$f_R(r) = \left(\frac{\mu(1+\eta)}{2\Omega} \right)^{\frac{\mu+1}{2}} \frac{2\sqrt{\pi}(1-\eta)^{\frac{1-\mu}{2}}}{\Gamma(\mu/2)\sqrt{\eta}} r^{\mu} \exp\left(-\frac{r^2\mu(1+\eta)^2}{4\Omega\eta} \right) I_{\frac{\mu-1}{2}}\left(r^2 \frac{\mu(1-\eta^2)}{4\Omega\eta} \right) \tag{2.98}$$

with $\eta = \sigma_x^2/\sigma_y^2$ being consistent with the corresponding parameter in Hoyt model and $\Omega = \mathbb{E}[R^2] = \mu(\sigma_x^2 + \sigma_y^2)$.

As the κ-μ model with Rice, the η-μ distribution generalizes the Hoyt model ($\mu = 1$, $\eta = \eta_{Hoyt}$) without penalizing the mathematical tractability. Moreover, it also includes Nakagami-m model as a particular case ($\mu = m$, $\eta = 1$). However, both κ-μ and η-μ models fail when attempting to characterize the power imbalance of the LoS component as the Beckmann distribution does.

κ-μ shadowed

The κ-μ shadowed was originally proposed in [29] as a natural extension of the κ-μ model in which the deterministic component representing the LoS contribution is allowed to randomly fluctuate, similarly as the Rician shadowed model arises from the Rice distribution. Later, the author in [89] proposed the same distribution in the context of device-to-device communications, although from another physical model that was finally proved to be wrong [90]. According to [29], the received signal amplitude under

TABLE 2.2: Connections between the κ-μ shadowed fading model and others models in the literature. In order to avoid confusion, the parameters corresponding to the κ-μ shadowed distribution are underlined.

Channels	κ-μ shadowed parameters
Rayleigh	$\underline{\kappa} = 0, \quad \underline{\mu} = 1, \quad \forall\, \underline{m}$
Rice	$\underline{\kappa} = K, \quad \underline{\mu} = 1, \quad \underline{m} \to \infty$
Nakagami-m	$\underline{\kappa} = 0, \quad \underline{\mu} = m, \quad \forall\, \underline{m}$
Hoyt	$\underline{\kappa} = (1-\eta)/(2\eta), \quad \underline{\mu} = 1, \quad \underline{m} = 0.5$
κ-μ	$\underline{\kappa} = \kappa, \quad \underline{\mu} = \mu, \quad \underline{m} \to \infty$
η-μ	$\underline{\kappa} = (1-\eta)/(2\eta), \quad \underline{\mu} = 2\mu, \quad \underline{m} = \mu$
Rician shadowed	$\underline{\kappa} = K, \quad \underline{\mu} = 1, \quad \underline{m} = m$

κ-μ shadowed fading is given by

$$R = \left(\sum_{i=1}^{\mu} \left\| \sigma X_i + j\sigma Y_i + \xi(p_i + jq_i) \right\|^2 \right)^{1/2} \tag{2.99}$$

where μ denotes the number of clusters, $X_i, Y_i \sim \mathcal{N}(0,1)\ \forall\ i$, $\sigma \in \mathbb{R}^+$ and $p_i, q_i \in \mathbb{R}$ are constants and ξ is a random variable such that $\xi^2 \sim \Gamma(m, 1/m)$. All the involved random variables are assumed to be independent. Note that, conditioned on ξ, (2.99) corresponds to the physical model of the κ-μ distribution in (2.94). The PDF of R under κ-μ shadowed fading is therefore calculated by averaging (2.95) over all possible states of ξ, obtaining [29, eq. (4)]

$$f_R(r) = \frac{2\mu^\mu m^m (1+\kappa)^\mu}{\Omega^\mu \Gamma(\mu)(\mu\kappa + m)^m} r^{2\mu-1} \exp\left(-\frac{\mu(1+\kappa)r^2}{\Omega} \right) {}_1F_1\left(m; \mu; \frac{\mu^2\kappa(1+\kappa)r^2}{(\mu\kappa+m)\Omega} \right) \tag{2.100}$$

where parameters κ and Ω are defined as in the κ-μ model (2.96). As in the latter, (2.100) is a valid PDF even for $\mu \in \mathbb{R}^+$, although it looses its physical meaning. Moreover, if $m \to \infty$, it easy to proved by taking the limit and using [50, eq. (13.3.1)] that (2.100) reduces to κ-μ PDF (2.95).

Remarkably, the κ-μ shadowed distribution does not only include the underlying fading models derived from the κ-μ model but also, somehow counterintuitively, the η-μ and the Hoyt distributions [91]. Hence, it unifies most of the here presented fading models, providing a large versatility on modeling propagation conditions [29], [89], [92]. The connections between the κ-μ shadowed fading model and the others distributions are summarized in Table 2.2.

Furthermore, it was proved in [30] that κ-μ shadowed distribution, under the assumption of μ and m being positive integers, can be given in terms of a mixture of

Nakagami-m distributions as

$$f_R(r|m, \mu \in \mathbb{N}^+) = \sum_{i=0}^{M} C_i f_{\mathcal{N}}(m_i, \Omega_i m_i; r) \tag{2.101}$$

where $f_{\mathcal{N}}(m_i, \Omega_i m_i; r)$ denotes the Nakagami-m PDF (2.90) with parameter m_i and mean power $\Omega_i m_i$, and M, m_i and Ω_i are constants depending on the κ-μ shadowed parameters as given in [30, Table 1]. Therefore, any result given in the literature for Nakagami-m distribution can straightforwardly leveraged to the κ-μ shadowed.

Chapter 3

Summary of Results

This chapter presents the main results obtained in this thesis. A twofold contribution is provided: *i)* a new method to approximate the distribution of random variables and its application to the statistical analysis of both complex and real non-central GQFs, and *ii)* two generalizations of the already versatile κ-μ shadowed fading model. Although these contributions seem a priori unconnected, it will be later shown that both actually share the same underlying methodology.

The chapter is organized as follows. Section 3.1.1 introduces the proposed method to approximate the distribution of random variables, providing general expressions for the PDF and CDF of arbitrary positive variables. This technique is applied to both real and complex GQFs in sections 3.1.2 and 3.1.3, respectively. Finally, the two proposed fading models are presented in sections 3.2.1 and 3.2.2.

3.1 Analysis of random variables through confluence

Most of the approaches to approximate the distribution of random variables presented in Chapter 2 have the same main drawback: the resulting expressions does not represent a valid distribution, i.e., the approximated PDF does not necessarily integrate to one and the probabilities may be negative [39, p. 731][38, sec. 2]. Moreover, in the case of the saddle-point technique, it is not obvious how to increase the accuracy of the approximation.

The only exception are the approximants arising from mixtures of distributions, which in fact ensure that the resulting function is a valid PDF. However, as pointed out in Section 2.2.5, the calculation of the mixture parameters may be extremely difficult, and the lack of a general method considerably limits its usefulness.

These limitations are also present in the distinct series expansions given for the PDF and CDF of GQFs in Section 2.3, along with other downsides such as the numerical issues in some cases (e.g., power series expansions), the convergence problems associated with the introduction of artificial parameters and the strong dependence between the required number of terms to be computed and the parameters of the quadratic form.

Motivated by all the above-mentioned drawbacks, one of the main goals of this thesis is to provide a new approach that circumvents these limitations, giving as a result alternative and more robust approximations not only for the distribution of GQFs but also for that of any random variable.

3.1.1 Proposed approach

The new method is desired to have the following properties: *i)* the resulting expressions always represent a valid distribution and *ii)* any target level of accuracy can be achieved independently of the parameters of the random variable under analysis. Taking into consideration these requirements, it is clear that we have to disregard any method based on series expansions. Therefore, instead of approximating a certain statistic of a random variable by an infinite series, we analyze a sequence of auxiliary random variables that, in the limit, converges in distribution to the target one. That is, given a random variable $X \in \mathbb{R}$, we aim to find a sequence $\{X_m : m \in \mathbb{N}^+\}$ such that $\{X_m\} \Rightarrow X$.

Once the sequence is suitably defined, we can leverage this convergence and approximate the CDF (and the PDF if the conditions given in Section 2.2.1 hold) by that of the auxiliary variables, ensuring that, for any value of m, the resulting expressions will represent a valid distribution since they are the statistics of another random variable.

The problem is now how to define the auxiliary sequence. Ideally, $\{X_m\}$ should be chosen so that it converges rapidly to X and it is mathematically tractable, i.e., the PDF and CDF of X_m should be easily obtainable for all m. To that end, we propose defining X_m by somehow perturbing X, i.e., introducing an artificial random fluctuation in X so that it simplifies its statistical analysis. In order to achieve the desired convergence, this fluctuation should vanish in the limit.

Due to the mathematical tractability of the gamma distribution and its limit property of converging to a constant, this artificial fluctuation is chosen to be gamma distributed. Specifically, we will generate the sequence $\{X_m\}$ from X by letting its mean or variance to randomly fluctuate according to a gamma distribution. If X is built as a function of other random variables, an alternative way of defining $\{X_m\}$ is introducing the fluctuation in either the mean or variance of such underlying variables.

In this thesis, the above technique is used to provide very general expressions to approximate the distribution of any positive real random variable from its MGF. The approach, which is given below, is presented in

[46] P. Ramírez-Espinosa, D. Morales-Jimenez, J. A. Cortés, J. F. París, and E. Martos-Naya, "New approximation to distribution of positive RVs applied to Gaussian quadratic forms", *IEEE Signal Process. Lett.*, vol. 26, no. 6, pp. 923–927, Jun. 2019,

attached in Appendix A.1.

Consider a random variable $X \in \mathbb{R}^+$ with continuous distribution, and assume that the MGF of X is given by $M_X(s)$. In order to approximate its CDF, and according to the proposed method, we define the auxiliary sequence of random variables $\{X_m : m \in \mathbb{N}^+\}$ with

$$X_m \triangleq X/\xi_m, \tag{3.1}$$

where ξ_m is a random variable, independent of X, which follows a gamma distribution with shape parameter m and scale parameter $1/(m-1)$, i.e., $\xi_m \sim \Gamma(m, 1/(m-1))$. The PDF of ξ_m is therefore given by (2.16)

$$f_{\xi_m}(u) = \frac{(m-1)^m}{\Gamma(m)} u^{m-1} e^{-(m-1)u}. \tag{3.2}$$

That is, we generate X_m by introducing a random fluctuation in X, whose severity decreases as m increases. As proved in Section 2.2.4, the sequence $\{\xi_m : m \in \mathbb{N}^+\}$ converges in distribution to the constant $C = \mathbb{E}[\xi_m]$, which is calculated according to (2.20), obtaining $\mathbb{E}[\xi_m] = 1$. Therefore, we have that $\{\xi_m\} \Rightarrow 1$ and, from Slutsky's theorem [93, sec. 3.6][55, sec. 1.2], that $\{X_m\} \Rightarrow X$.

Hence, the above result allows us to approximate the CDF of X by that of X_m with sufficiently large m, as stated in the following lemma.

Lemma 3.1 *Let X be a positive random variable with continuous distribution and MGF given by $M_X(s)$, and X_m as in* (3.1)*. Then, the CDF of X satisfies*

$$F_X(x) = \lim_{m\to\infty} F_{X_m}(x) = \lim_{m\to\infty} \sum_{k=0}^{m-1} \frac{(m-1)^k}{x^k k!} \frac{d^k}{ds^k} M_X(s)\bigg|_{s=(1-m)/x}. \tag{3.3}$$

The conditions for which convergence in distribution also implies convergence of PDFs are stated in Section 2.2.1. In our case, these conditions are met if the PDF of X, namely $f_X(x)$, is uniformly continuous, i.e., for all $x_1, x_2 \in [0, \infty)$ exits $\delta > 0$ and $\epsilon > 0$ such that $|x_1 - x_2| < \delta$ implies $|f_X(x_1) - f_X(x_2)| < \epsilon$. Therefore, if $f_X(x)$ is uniformly continuous, we can also approximate it by the PDF of X_m. This is stated in the following corollary.

Corollary 3.2 *Let X be a positive random variable with MGF $M_X(s)$ and uniformly continuous PDF, and X_m as in* (3.1)*. Then, the PDF of X satisfies*

$$f_X(x) = \lim_{m\to\infty} f_{X_m}(x) = \lim_{m\to\infty} \frac{(m-1)^m}{x^{m+1}\Gamma(m)} \frac{d^m}{ds^m} M_X(s)\bigg|_{s=(1-m)/x}. \tag{3.4}$$

Lemma 3.1 and Corollary 3.2 provide a general result to approximate the distribution of a positive random variable in terms of the derivatives of its MGF. As already highlighted, the main benefit of this method is that, since we approximate the distribution of

a X by that of another variable X_m, the approximation (for any m) always represents a valid distribution.

We also aimed that any level of accuracy could be reached independently of the target variable under analysis. This is ensured by the weak convergence of $\{X_m\}$ to X, i.e., increasing the value of m always leads to a more accurate approximation. In fact, the normalized mean squared error (MSE) between the target variable and X_m, which is a good indicator of the similarity between both random variables, is a monotonic decreasing function that does not depend on X, as given in the following lemma.

Lemma 3.3 *Let X be a positive random variable, and X_m as in* (3.1)*. For $m > 2$, the normalized MSE admits the following compact expression:*

$$\overline{\epsilon^2} = \mathbb{E}\left[(X - X_m)^2\right] / \mathbb{E}\left[X^2\right] = (m-2)^{-1}. \tag{3.5}$$

From (3.5), it is clear that $\lim_{m\to\infty} \epsilon^2 = 0$, and thus we can achieve any target accuracy in the approximation by choosing m large enough. Note however that, although informative on the closeness between X_m and X, the normalized MSE does not directly translate into the error between the approximated CDF and the true one. An expression for the error in probability is unfortunately difficult to obtain due to the generality of the problem.

We consider appropriate to name this method of approximating the distribution of random variables as *analysis through confluence*, since the target variable is perturbed in order to generate an auxiliary sequence that facilitates the analysis and converge to the original variable in the limit, achieving that confluence. Therefore, for coherence, we denoted the auxiliary variables, X_m, as *confluent variables*.

As with most of the classical series expansions, where the moments are required, the calculation of (3.3) and (3.4) may be challenging if the derivatives of the MGF of X are difficult to compute or not expressible in closed form. Thus, large values of m imply the computation of high-order derivatives of $M_X(s)$, which may be tedious in some cases. For instance, if numerical integration (e.g., Cauchy integrals) are used, the computational cost can grow exponentially and round-off errors can lead to a total amount of error that increases with the order of differentiation [94].

However, there are cases where these derivatives can be readily obtained. That is, for instance, the case of those variables whose MGF is given as a product of elementary functions, since its derivatives can be calculated recursively from the derivatives of the logarithm of the MGF (the CGF).

Specifically, consider an arbitrary function $f(s)$. The k-th order derivative of $f(s)$ can be calculated as [4, eq. (3.2b.3)]

$$\frac{d^k}{ds^k} f(s) = \left(\sum_{r_1=0}^{k-1} \binom{k-1}{r_1} g_{k-1-r_1}(s) \sum_{r_2=0}^{r_1-1} \binom{r_1-1}{r_2} g_{r_1-1-r_2}(s) \dots \right) f(s) \tag{3.6}$$

where

$$g_k(s) = \frac{d^k}{ds^k} g(s) = \frac{d^{k+1}}{ds^{k+1}} \ln f(s). \tag{3.7}$$

From (3.6), the derivatives of $f(s)$ can be calculated recursively as

$$\frac{d^k}{ds^k} f(s) = f(s) D_k(s) \tag{3.8}$$

with $D_0(s) = 1$ and, for $k > 1$,

$$D_k(s) = \sum_{j=0}^{k-1} \frac{(k-1)!}{j!(k-j-1)!} g_{k-1-j}(s) D_j(s). \tag{3.9}$$

Thus, if the MGF of X is given as a product of elementary functions, then $\ln M_X(s)$ is written in terms of a sum of such simple functions, and its derivatives could be easily written in closed form. This allows a straightforward calculation of the derivatives of $M_X(s)$ from (3.7) and (3.9) by replacing $f(s) = M_X(s)$.

With that, we conclude the presentation of our new method to approximate the distribution of random variables. In next sections, we apply the proposed technique to both complex and real GQFs.

3.1.2 Application to non-central real Gaussian quadratic forms

In this section, the proposed approach is used to give a simple and efficient approximation for the distribution of non-central positive definite GQFs, i.e., we aim to provide approximated expressions for both the PDF and CDF of the quadratic form (2.46)

$$Q_R = (\mathbf{x} + \overline{\mathbf{x}})^T \mathbf{A} (\mathbf{x} + \overline{\mathbf{x}}) \tag{3.10}$$

where $\overline{\mathbf{x}} \in \mathbb{R}^{n \times 1}$ is a constant vector, $\mathbf{A} \in \mathbb{R}^{n \times n}$ is a *positive definite* symmetric matrix and $\mathbf{x} \sim \mathcal{N}_n(\mathbf{0}_{n \times 1}, \mathbf{\Sigma})$.

These results, along with the comparison with other classical approaches listed in Section 2.3.2, are given in

[46] P. Ramírez-Espinosa, D. Morales-Jimenez, J. A. Cortés, J. F. París, and E. Martos-Naya, "New approximation to distribution of positive RVs applied to Gaussian quadratic forms", *IEEE Signal Process. Lett.*, vol. 26, no. 6, pp. 923–927, Jun. 2019.

Distribution of $\mathbf{Q_R}$

Since Q_R in (3.10) is a positive random variable, (3.3) and (3.4) can be directly used to approximate its chief statistics, namely PDF and CDF. The only remaining task is

calculating the derivatives of the MGF of Q_R, for which the approach in (3.7)-(3.9) is employed.

Thus, from (2.56), the CGF of Q_R is readily written as

$$\ln M_{Q_R}(s) = \sum_{i=1}^{n} \frac{b_i^2 \lambda_i s}{1 - 2\lambda_i s} - \frac{1}{2}\ln(1 - 2\lambda_i s) \tag{3.11}$$

and, straightforwardly, its derivatives are calculated in closed form as

$$g_k(s) = \frac{d^{k+1}}{ds^{k+1}} \ln M_{Q_R}(s) = 2^k\, k! \sum_{j=1}^{n} \frac{\lambda_j^{k+1}\left[(k+1)b_j^2 + 1 - 2\lambda_j s\right]}{(1 - 2\lambda_j s)^{k+2}}. \tag{3.12}$$

With the above results, approximated expressions for both the PDF and CDF of Q_R are given in the next corollary.

Corollary 3.4 *Consider a positive definite real GQF as in* (3.10)*. Then, its PDF and CDF can be approximated by*

$$f_{Q_R}(x) \approx \frac{(m-1)^m}{x^{m+1}\Gamma(m)} M_{Q_R}\left(\frac{1-m}{x}\right) D_m\left(\frac{1-m}{x}\right), \tag{3.13}$$

$$F_{Q_R}(x) \approx M_{Q_R}\left(\frac{1-m}{x}\right) \sum_{k=0}^{m-1} \frac{(m-1)^k}{x^k k!} D_k\left(\frac{1-m}{x}\right), \tag{3.14}$$

where $M_{Q_R}(s)$ is given in (2.56) *and $D_k(s)$ in* (3.9) *with $g_k(s)$ as in* (3.12)*.*

Numerical results and discussion

We now compare the proposed approximation for real GQFs in Corollary 3.4 with the classical results in Section 2.3.2. Specifically, we consider the power series in (2.62) and the Laguerre and χ^2 expansions in (2.64) and (2.65), respectively. The other approaches proposed in the literature are disregarded due to the drawbacks listed in Section 2.3.2.

For the sake of simplicity, both $\mathbf{A}$ and $\mathbf{\Sigma}$ are considered exponential matrices, i.e., $(\mathbf{A})_{i,j} = \alpha^{|i-j|}$ and $(\mathbf{\Sigma})_{i,j} = \rho^{|i-j|}$ with $0 < \alpha, \rho < 1$. With this assumption, which does not imply any loss of generality in the obtained results, our proposal is compared with the above-mentioned techniques in Figs. 3.1-3.4.

We first consider the comparison with the power series showed in Fig. 3.1. It can be observed that the power series renders a valid approximation only up to a certain point in x, remarkably failing thereafter; the value of x from which the series diverges depends on the parameters of the quadratic form. As illustrated, increasing the number of terms in the series from $N = 100$ to $N = 150$ does not seem to solve the problem. In contrast, our proposed solution shows an excellent agreement with simulations for all parameter choices and all x.

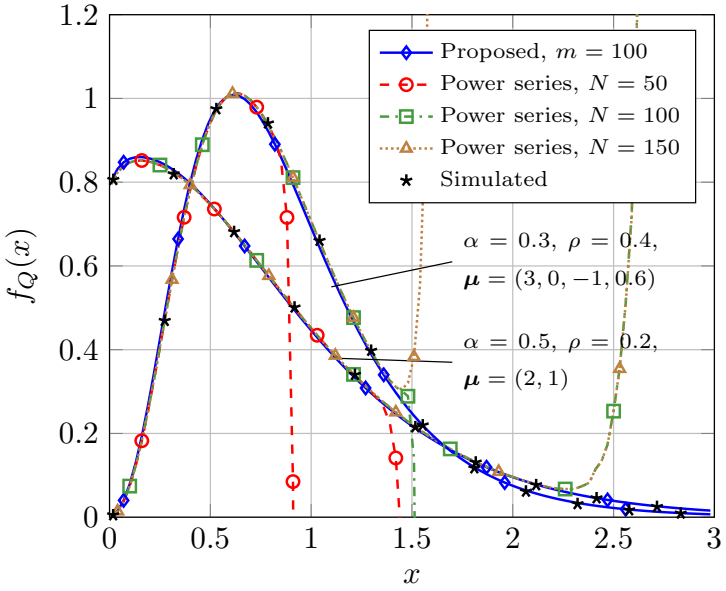

FIGURE 3.1: PDF of Q_R for different values of α, ρ and $\bar{\mathbf{x}}$. The proposed approximation in (3.13) is compared with the power series expansion in and with Monte Carlo simulations. N denotes the number of terms calculated in the power series.

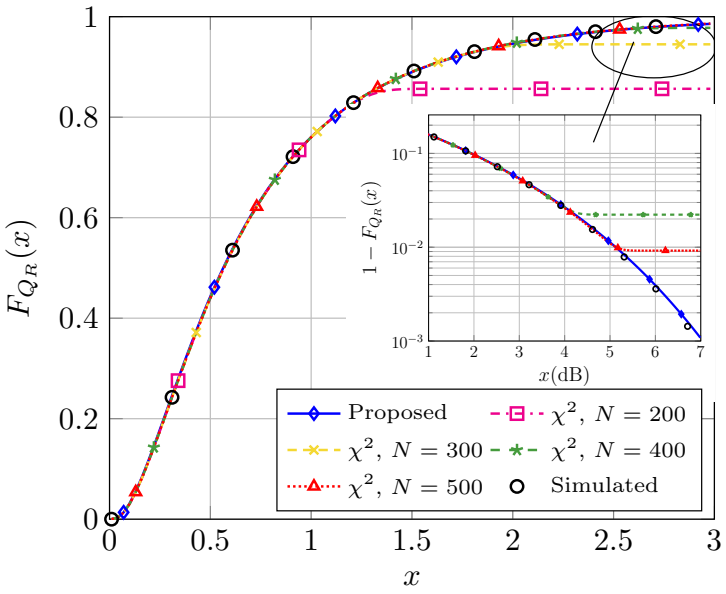

FIGURE 3.2: CDF of Q_R for α=0.7, $\rho = 0.5$ and $\bar{\mathbf{x}} = (2, 1, -1, 0.6, -0.9)$. Our proposed method in (3.14) with $m = 100$ is compared with the χ^2 expansion in (2.65) and with Monte Carlo simulations. N denotes the number of terms calculated in the χ^2 series expansion.

Fig. 3.2 compares our results with the χ^2 densities expansion in (2.65) by plotting in this case the CDF of Q_R (similar trends are observed for the PDF). As pointed out in Section 2.3.2, the χ^2 approximation artificially introduces an additional parameter $0 < \beta_\chi < \min_j\{\lambda_j\}$ that controls the series convergence. Since a higher value of β_χ in this interval seems to accelerate the series convergence, i.e., smaller values of β_χ requires a larger N to achieve the same accuracy, a value $\beta_\chi = 0.9\min_j\{\lambda_j\}$ has been chosen. Regarding Fig. 3.2, it is observed that the number of terms required for the χ^2 expansion, N,

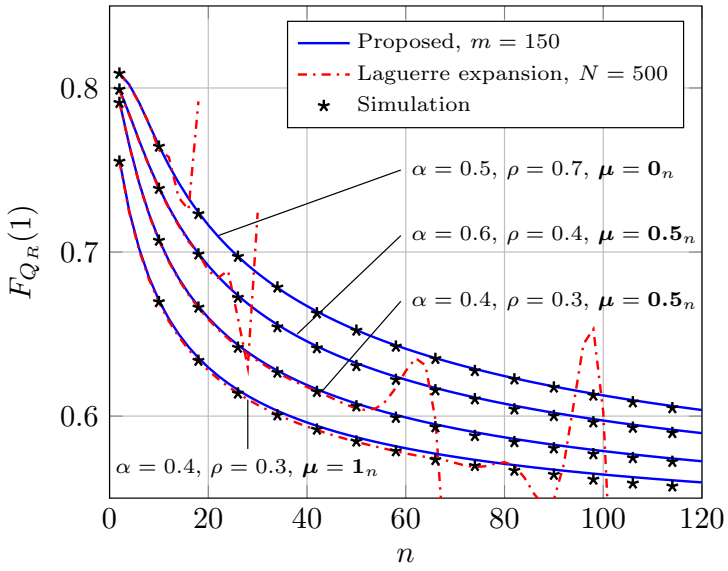

FIGURE 3.3: CDF of Q_R at $x = 1$ for distinct quadratic form order, n. Our proposed expression in (3.14) is compared with the Laplace approximation in (2.64) with $\beta_L = 10$ and with Monte Carlo simulations.

is much larger than in our method (the value of m) to accurately approximate the distribution of the quadratic form. Furthermore, it is important to note that the χ^2 expansion does not yield a valid CDF, as observed in the right-hand tail, where the approximated CDF does not reach to one if N is not sufficiently large.

A comparison between (3.14) and the Laguerre series expansion in (2.64) is shown in Fig. 3.3, where $F_{Q_R}(x)$ at $x = 1$ is depicted for distinct quadratic form orders, n. Although useful in many situations, this approximation has two clear drawbacks. The first one is that, as the previous approximations, the resulting function is not a proper CDF if the number of terms computed, N, is not large enough (in fact, the resulting CDF presents an oscillatory behavior). The second one is the uncertainty in the actual value of the parameter β_L, introduced to control the series convergence, that yields the best approximation. As stated in Section 2.3.2, the convergence is mathematically ensured for all x only if $\beta_l > \max_j\{\lambda_j\}/2$. Specifically, a value of $\beta_l > (\max_j\{\lambda_j\} + \min_j\{\lambda_j\})/2$ is recommended in order to minimize the approximation error. However, we noticed that, in some cases, this choice renders considerable numerical errors that prevent the series convergence. In fact, increasing the value of N in those cases makes the approximation even less accurate, probably due to the total increased amount of error, while maintaining the same N and changing the value of β_L lead to a tight approximation. Hence, finding the value of β_L that yields the best approximation in each case is a difficult task. For the calculation in Fig. 3.3, a value of $\beta_L = 10$ has been chosen, which seems to minimize such numerical issues.

As shown in this figure, the series diverges when the order of Q_R increases, with independence of the quadratic form parameters. Note that the considered values of n are not particularly extreme, but rather moderate, particularly in applications such as signal

detection where large numbers of samples are typically employed.

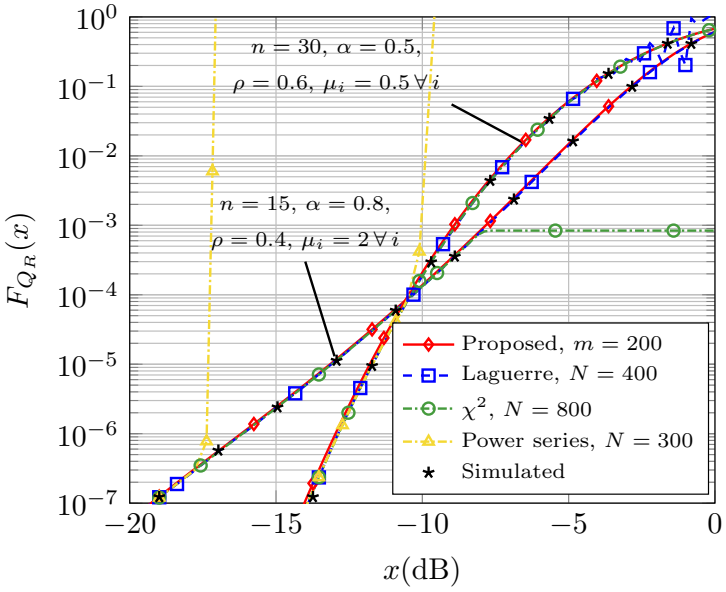

FIGURE 3.4: CDF of Q_R for different values of n, α, ρ and $\overline{\mathbf{x}}$. The proposed method is compared with the power series in (2.62), the Laguerre expansion in (2.64) and the χ^2 expansion in (2.65) and contrasted with Monte Carlo simulations. Parameters: $\beta_L = 9$ for $n = 15$ and $\beta_L = 12$ for $n = 30$.

The last comparison is shown in Fig. 3.4, where the CDF of Q_R is plotted in logarithmic scale in order to analyze the accuracy of the distinct approaches to approximate the left tail of the distribution. As observed, the aforementioned drawbacks of the alternative methods are also relevant when focusing on the left tail of the distribution. In turn, our proposed technique renders again an excellent approximation with independence of the parameters of Q_R.

Overall, obtained results show that the analysis through confluence is a good alternative to classical approaches to approximate not only the left tail, but also the complete range of the distribution. Moreover, it has a distinctive feature over the classical ones: the robustness. Hence, it provides accurate results with independence of the parameters of the quadratic form, also ensuring that the resulting functions properly represent a valid distribution independently of the number of terms (m) that are computed. Furthermore, the goodness of the approximation does not depend on arbitrary constants as in the χ^2 and the Laguerre series expansions.

3.1.3 Application to non-central complex Gaussian quadratic forms

The proposed technique is now employed to characterize non-central complex GQFs, i.e., we seek an approximation for the PDF and CDF of the quadratic form (2.52)

$$Q_C = (\mathbf{v} + \overline{\mathbf{v}})^{\dagger}\mathbf{A}(\mathbf{v} + \overline{\mathbf{v}}) \tag{3.15}$$

where $\mathbf{A} \in \mathbb{C}^{n\times n}$ is an Hermitian matrix and $\mathbf{v} \sim \mathcal{CN}_n(\mathbf{0}_{n\times 1}, \mathbf{\Sigma})$.

Since it has been proved that a complex GQF is equivalent to a real one with the eigenvalues given in pairs (see Section 2.3.1), (3.13) and (3.14) could be directly used to approximate the distribution of Q_C in the positive definite case. However, we can exploit the particularities of the complex case and go one step further, obtaining an alternative approximation with two additional advantages. The first one is that it is valid not only for positive definite complex GQFs but also in the indefinite case, providing more generality. The second one is that the resulting expressions are more suitable for further analytical purposes. The recursion in (3.13) and (3.14) involving the independent variable x may pose a challenge to that end, and therefore circumventing this recursion is an additional value due to the importance of complex GQFs in performance analysis of communications systems and signal processing applications (e.g., signal detection). These alternative approximation is achieved by defining the sequence $\{X_m : m \in \mathbb{N}^+\}$ in a different way as in (3.1).

The analysis of Q_C with the proposed technique, its comparison with other approaches given in 2.3.2 and its application to the analysis of MRC systems is presented in

[47] P. Ramírez-Espinosa, L. Moreno-Pozas, J. F. París, J. A. Cortés, and E. Martos-Naya, "A new approach to the statistical analysis of non-central complex Gaussian quadratic forms with applications", *IEEE Trans. Veh. Technol.*, vol. 68, no. 7, pp. 6734–6746, Jul. 2019,

attached in Appendix A.2, and summarized below.

Distribution of Q_C

As introduced before, in order to characterize Q_C, an alternative auxiliary sequence of variables is used. Thus, instead of defining X_m by directly perturbing the quadratic form as in the real case, we here introduce the random fluctuation in the mean of the underlying Gaussian variables of Q_C. To that end, we consider the formulation in (2.53)

$$Q_C = (\mathbf{s} + \overline{\mathbf{h}})^\dagger \mathbf{\Lambda} (\mathbf{s} + \overline{\mathbf{h}}) \tag{3.16}$$

where the distinct parameters are properly defined in Section 2.3.1. From (3.16), we define the sequence $\{Q_m : m \in \mathbb{N}^+\}$ such that

$$Q_m = (\mathbf{s} + \mathbf{D}_\xi \overline{\mathbf{h}})^\dagger \mathbf{\Lambda} (\mathbf{s} + \mathbf{D}_\xi \overline{\mathbf{h}}), \tag{3.17}$$

with $\mathbf{D}_\xi \in \mathbb{R}^{n\times n}$ a diagonal matrix whose entries, $\xi_{m,i}$ for $i = 1, \ldots, n$, are independent and identically distributed (i.i.d.) random variables such that $\xi_{m,i}^2$ are gamma distributed with shape parameter m and $\mathbb{E}[\xi_{m,i}^2] = 1$, i.e., $\xi_{m,i}^2 \sim \Gamma(m, 1/m)$.

As proved in Section 2.2.4, $\xi_{m,i}^2 \Rightarrow \mathbb{E}[\xi_{m,i}^2] = 1$ for all i and, from the relationship between the CDF of $\xi_{m,i}^2$ and that of $\xi_{m,i}$, it can also be proved that $\xi_{m,i} \Rightarrow 1$. Therefore, $\mathbf{D}_\xi$ becomes the identity matrix when $m \to \infty$ and, intuitively, it can be observed that $\{Q_m\}$ converges to Q_C in the limit. Note also that, in the central case, i.e., $\overline{\mathbf{h}} = \mathbf{0}_{n\times 1}$, $Q_m = Q_C$ for any value of m.

However, this convergence needs to be formally proved before approximating the distribution of Q_C by that of Q_m. In order to do so, we first calculate the MGF of Q_m by conditioning $M_Q(s)$ on $\mathbf{D}_\xi$ and averaging over all its possible values.

Lemma 3.5 *Consider Q_m as in* (3.17)*. Then, its MGF is given by*

$$M_{Q_m}(s) = \prod_{i=1}^{n} \frac{\left(1 - \frac{\lambda_i \mu_i s}{m(1-\lambda_i s)}\right)^{-m}}{1 - \lambda_i s}, \quad \mathrm{Re}\{s\}\lambda_i \left(1 + \mu_i/m\right) < 1 \; \forall \; i, \tag{3.18}$$

where $\mu_i = \|h_i\|^2$.

From (3.18), and taking into account that

$$\lim_{m\to\infty} \left(1 - \frac{\lambda_i \mu_i s}{m(1-\lambda_i s)}\right)^{-m} = \exp\left(\frac{\lambda_i \mu_i s}{1-\lambda_i s}\right), \tag{3.19}$$

it is clear that $\lim_{m\to\infty} M_{Q_m}(s) = M_{Q_C}(s)$ for any $s = jt$ with $t \in \mathbb{R}$. Therefore, from Lévy's continuity theorem, we have that $\{Q_m\} \Rightarrow Q_C$ [52, chap. 18].

An important remark is that $M_{Q_m}(s)$ does not have the exponential term present in (2.66). This considerably eases the mathematical analysis by allowing to write (3.18) as a rational function of the form

$$M_{Q_m}(s) = B \prod_{i=1}^{n} \frac{(s - 1/\lambda_i)^{m-1}}{(s - \beta_i)^m} \tag{3.20}$$

where $\beta_i = [\lambda_i(1 + \mu_i/m)]^{-1}$ and

$$B = \prod_{k=1}^{n} \left[-\lambda_k \left(1 + \frac{\mu_k}{m}\right)^m\right]^{-1}. \tag{3.21}$$

Assuming there can be repeated zeroes ($1/\lambda_i$) and poles (β_i), and taking into consideration that, if $\mu_i = 0$ for a certain i then $\beta_i = 1/\lambda_i$, the rational function in (3.20) can be simplified. Thus, denoting as $\widetilde{\beta}_i$ and $1/\widetilde{\lambda}_j$ for $i = 1, \ldots, n_\beta$ and $j = 1, \ldots, n_\lambda$ the distinct poles and zeroes resulting from this simplification with multiplicities p_i and q_i, respectively, the MGF of Q_m is finally expressed as

$$M_{Q_m}(s) = B \, \frac{\prod_{j=1}^{n_\lambda} \left(s - 1/\widetilde{\lambda}_j\right)^{q_j}}{\prod_{i=1}^{n_\beta} \left(s - \widetilde{\beta}_i\right)^{p_i}}. \tag{3.22}$$

Observe that, in contrast to the MGF of the original quadratic form Q_C in (2.66), the expression of M_{Q_m} in (3.22) allows an straightforward inversion, i.e., we can directly obtain the PDF and CDF of Q_m by performing an inverse Laplace transformation as

$$f_{Q_m}(s) = \mathcal{L}^{-1}\left\{M_{Q_m}(-s)\right\}, \qquad F_{Q_m}(s) = \mathcal{L}^{-1}\left\{\frac{1}{s}M_{Q_m}(-s)\right\} \tag{3.23}$$

and then approximating the PDF and CDF of Q_C by leveraging the convergence between both variables, as stated in the following lemma.

Lemma 3.6 *Consider an indefinite non-central complex GQF as in* (3.16)*. Then, its PDF and CDF can be approximated by those of Q_m as*

$$f_{Q_C}(x) \approx f_{Q_m}(x) = \sum_{i=1}^{n_\beta}\sum_{j=1}^{p_i} \alpha_{i,j} e^{-\widetilde{\beta}_i x} x^{j-1} \mathrm{u}\left(\widetilde{\beta}_i x\right) \mathrm{sgn}(x), \tag{3.24}$$

$$F_{Q_C}(x) \approx F_{Q_m}(x) = \mathrm{u}(x) + \sum_{i=1}^{n_\beta}\sum_{j=1}^{p_i} \omega_{i,j} e^{-\widetilde{\beta}_i x} x^{j-1} \mathrm{u}\left(\widetilde{\beta}_i x\right) \mathrm{sgn}(x), \tag{3.25}$$

where $\mathrm{u}(\cdot)$ *is the unit step function,* $\mathrm{sgn}(\cdot)$ *is the sign function and*

$$\alpha_{i,j} = \frac{(-1)^n}{(j-1)!} B A_{i,j}, \qquad \omega_{i,j} = \frac{(-1)^n}{(j-1)!} B C_{i,j}, \tag{3.26}$$

with $A_{i,j}$ and $C_{i,j}$ the residues arising from performing a partial fraction decomposition in (3.22) *after evaluating $M_{Q_m}(-s)$ and $M_{Q_m}(-s)/s$, respectively.*

Note that, although m does not appear explicitly in (3.24) and (3.25), both the poles $\widetilde{\beta}_i$ and their multiplicities p_i depends on m, as well as zeroes multiplicities q_i. Moreover, in the central case, *exact* expressions for both $f_{Q_C}(x)$ and $F_{Q_C}(x)$ can be obtained from (3.24) and (3.25) for any value of m, e.g., $m = 1$.

As for the calculation of the residues $A_{i,j}$ and $C_{i,j}$, although they admit a closed formulation, their computation is impractical for very large m due to the resulting combinatorial expressions. A more suitable approach is the algorithm proposed in [95], which provides recursive expressions for the partial fraction residues of both proper and improper rational functions. The recursion starts from the higher order residues, i.e., A_{i,p_i} and C_{i,p_i}, which can be directly calculated from the definition in [96, eq. (A.36)], and computes the other residues recursively according to [95, eqs. (11a) and (11b)].

Finally, to complete the statistical analysis of Q_C, we aim to characterize somehow the approximation error. As in the real case, a closed form expression for the error between $F_{Q_m}(x)$ and $F_{Q_C}(x)$ would be desirable. However, it is difficult to obtain an useful expression for such error. Therefore, since we are not truncating any series expansion but instead approximating the distribution of a target variable from that of another, we resort again on the normalized MSE as an informative measurement of the closeness between Q_C and Q_m.

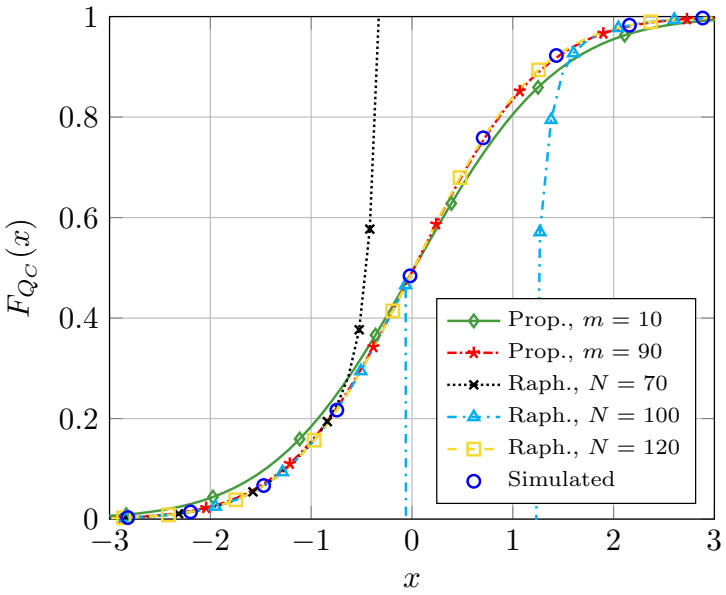

FIGURE 3.5: CDF of Q_C for $n = 6$, $\boldsymbol{\lambda} = (-3, -1.8, -1, 1, 2.1, 3)$ and $\boldsymbol{\mu} = (8.5, 7.4, 4, 5, 6.8, 7.9)$. Exact (simulated) CDF is compared with the proposed approximation in (3.25) and Raphaeli's approach in (2.70) with N terms computed.

Lemma 3.7 *Consider Q and Q_m as in* (3.16) *and* (3.17)*, respectively. Then, the normalized MSE between Q and Q_m is given by*

$$\overline{\epsilon^2} \triangleq \frac{\mathbb{E}\left[(Q_m - Q)^2\right]}{\mathbb{E}\left[Q^2\right]} = \frac{\sum_{i=1}^{n} \lambda_i^2 \mu_i \left[4\left(1 - \frac{\Gamma(m+1/2)}{m^{1/2}\Gamma(m)}\right) + \frac{\mu_i}{m}\right]}{\sum_{j=1}^{n}\left(\lambda_j^2(1+2\mu_j)\right) + \left(\sum_{j=1}^{n}\lambda_i(1+\mu_i)\right)^2}. \tag{3.27}$$

Regarding (3.27) we observe that, when $\mu_i = \|h_i\|^2 = 0$ for $i = 1, \ldots, n$, then $\overline{\epsilon^2} = 0$ for any value of m. This is coherent with the fact that setting $\mu_i = 0 \; \forall \; i$ implies having a central quadratic form and, therefore, $\mathbf{D}_\xi$ vanishes in (3.17). Additionally, it is easy to prove that the error also goes to zero when $m \to \infty$ by taking the limit in (3.27) and using [50, eq. (6.1.39)].

Comparison with other approaches

The proposed results are now compared to other approximations given in the literature. Specifically, Raphaeli's approach in (2.70) and the saddle-point approximation in (2.78) are considered. Compared to these results, our proposed method provides a twofold benefit. The first one is that approximations in (3.4) and (3.25) are useful for further analytic purposes (e.g., calculation of expectations over Q_C) since they are given in terms of elementary functions. The second one is that our approach always renders a valid distribution (for any m), in contrast to the other methods. This is shown in Figs. 3.5 and 3.6, where the CDF of Q_C, calculated using the different techniques, is depicted.

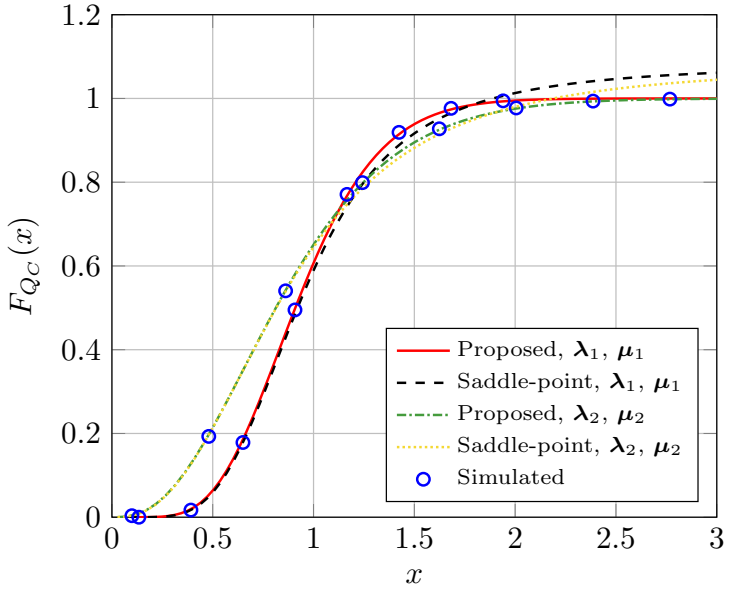

FIGURE 3.6: CDF of Q_C for different parameters. Exact (simulated) CDF is compared with the proposed approximation in (3.25) with $m = 50$ and the saddle-point approach in (2.78). Data: $\boldsymbol{\lambda}_1 = [0.2, 1, 1.4, 3, 5]$, $\boldsymbol{\lambda}_2 = [0.1, 0.6, 1]$, $\boldsymbol{\mu}_1 = [0.6, 7.4, 3, 2.6, 5.5]$ and $\boldsymbol{\mu}_2 = [1, 0.8, 3.4]$.

For simplicity, the vector containing the n eigenvalues λ_i is denoted by $\boldsymbol{\lambda}$ and, analogously, the vector $\boldsymbol{\mu}$ is defined such that $\boldsymbol{\mu} = (\mu_1, \ldots, \mu_n)$. The theoretical calculations are validated through Monte Carlo simulations of Q_C.

Thus, Fig. 3.5 focuses on the comparison with Raphaeli's method in (2.70). It is clear that this approximation produces invalid CDF values for certain x if the number of terms computed, N, is not large enough. Not until a value of $N = 120$ is reached that the CDF converges for all x. Moreover, we have observed that the number of terms required strongly depends on the eigenvalues λ_i. That is, the smaller the difference between the eigenvalues the larger the value of N needed. In turn, our approach renders a valid distribution with independence of m.

On the other hand, Fig. 3.6 compares the proposed method with the saddle-point approach in (2.78). Although the latter arises as a very efficient approximation, it suffers from the same drawbacks as the previous one. As observed, it gives probabilities greater than one in the right tail. In addition, it is not suitable for further analytic purposes.

Practical example: MRC systems over correlated Rice fading channels

The usefulness of the proposed method is now exemplified through the performance analysis of MRC systems over correlated Rice channels. To the best of the authors' knowledge, only asymptotic expressions have been given in the literature for the bit error rate (BER) and the outage probability (P_{out}) for arbitrary number of branches and correlation between them [97], [98] and infinite series representations when the number of

branches is limited to $P = 2$ [99], [100]. Taking advantage of the mathematical tractability of our derived results, we here provide expressions for these metrics.

Considering perfect synchronization and channel estimation, the SNR at the output of the receiver when applying MRC can be written as

$$\gamma = \overline{\gamma}\, \mathbf{g}^{\dagger}\mathbf{g} \tag{3.28}$$

where $\overline{\gamma}$ is the average SNR at each branch and $\mathbf{g} \in \mathbb{C}^{P\times 1}$ is the channel gain vector. Since the fading at each branch is assumed to be Rice distributed with K_i factor for $i = 1, \ldots, P$, $\mathbf{g}$ is a complex Gaussian vector such that $\mathbf{g} \sim \mathcal{CN}_P(\overline{\mathbf{g}}, \mathbf{\Sigma})$, with $\overline{\mathbf{g}} = \mathbb{E}[\mathbf{g}]$ and $\mathbf{\Sigma} = \mathbb{E}[(\mathbf{g} - \overline{\mathbf{g}})(\mathbf{g} - \overline{\mathbf{g}})^{\dagger}]$ the covariance matrix. The entries of both the mean vector and the covariance matrix can be expressed in terms of the Rice factor as[1]

$$\overline{g}_i = \sqrt{\frac{K_i}{K_i + 1}}, \quad (\mathbf{\Sigma})_{i,j} = \sqrt{\frac{1}{(1 + K_i)(1 + K_j)}}(\mathbf{R})_{i,j} \tag{3.29}$$

with $(\mathbf{R})_{i,j}$ for $i, j = 1, \ldots, P$ the entries of the correlation matrix $\mathbf{R}$ of $\mathbf{g}$. Note that each element of $\mathbf{g}$ has unit power, i.e., $\mathbb{E}[\|g_i\|^2] = 1$, so we consider normalized fading channels.

It is observed that γ in (3.28) is a particular case of the quadratic form in (3.15) with $\mathbf{A} = \mathbf{I}_P$, and, therefore, we can use the proposed method to analyze the performance of the system. To that end, the sequence $\{\gamma_m : m \in \mathbb{N}^+\}$ is defined with γ_m directly obtained by particularizing (3.17). Hence, we can approximate both P_{out} and the BER from the statistical analysis of γ_m when m takes appropriate large values:

- **Outage probability**. Defining γ_{th} as the minimum SNR required for a reliable communication, the outage probability is given by [101, eq. (6.46)]

$$P_{\text{out}}(\gamma_{\text{th}}) = \; P(\gamma < \gamma_{\text{th}}) \approx P(\gamma_m < \gamma_{\text{th}}) = \int_0^{\gamma_{\text{th}}} f_{\gamma_m}(\gamma_m)\, d\gamma_m, \tag{3.30}$$

  which corresponds to the CDF of γ_m. Then, from (3.25), we straightforwardly have

$$P_{\text{out}}(\gamma_{\text{th}}) \approx 1 + \sum_{i=1}^{n_\beta}\sum_{j=1}^{p_i} \omega_{i,j} e^{-\widetilde{\beta}_i \gamma_{th}/\overline{\gamma}} \left(\frac{\overline{\gamma}}{\gamma_{\text{th}}}\right)^{-j+1} \tag{3.31}$$

  where $\omega_{i,j}$, $\widetilde{\beta}_k$, n_β and p_i are obtained by identification with (3.25).

- **BER**. Since the BER is a continuous and bounded function, Helly-Bray theorem allows to approximate the BER over the SNR variable γ through the analysis of γ_m, as stated in Section 2.2.1. The probability error for an arbitrary modulation can be obtained by averaging the BER in additive white Gaussian noise (AWGN) channels, which is denoted by $P_0(\cdot)$, over the distribution of the fading, which in our case is

[1] There is a typo in [47, eq. (34)] which has been corrected in this thesis.

represented by γ_m, as [18, eq. (8.102)]

$$P_b\left(\overline{\gamma}\right) \approx \int_0^{\infty} P_0\left(\gamma_m\right) f_{\gamma_m}(\gamma_m)\, d\gamma_m \tag{3.32}$$

where $f_{\gamma_m}(\gamma_m)$ is readily obtained from (3.24).

Assuming a Gray coded constellation, $P_0(\gamma_m)$ for an arbitrary M-ary square quadrature amplitude modulation (QAM) is given by [102], finally obtaining

$$P_b\left(\overline{\gamma}\right) \approx \sqrt{M} \sum_{i=1}^{n_\beta} \sum_{j=1}^{p_i} \sum_{k=1}^{\sqrt{M}-1} \omega(k)\alpha_{i,j} \left[\frac{\Gamma(j)}{2\widetilde{\beta}_i^{j}} - \frac{\delta_k \Gamma\left(j+\frac{1}{2}\right)}{\widetilde{\beta}_i^{j+1/2}} \times \sqrt{\frac{\overline{\gamma}}{2\pi}}\, {}_2F_1\left(\frac{1}{2}, j+\frac{1}{2}; \frac{3}{2}; \frac{-\delta_k^2}{2\widetilde{\beta}_i}\overline{\gamma}\right)\right] \tag{3.33}$$

where $\delta_k = (2k-1)\sqrt{3/(M-1)}$, constants $\omega(k)$ are given in [102, eqs. (6), (14) and (21)] and ${}_2F_1(\cdot)$ is the Gauss hypergeometric function [50, eq. (15.1.1)].

Numerical results

In the following, the influence of the channel parameters and the number of branches of the receiver in the outage probability and the BER is assessed using (3.31) and (3.33) and contrasted through Monte Carlo simulations. For simplicity, the vector containing the P Rice K factors is denoted as $\mathbf{k} = (K_1, \ldots, K_P)$ and the correlation matrix $\mathbf{R}$ is assumed to be exponential, i.e., $(\mathbf{R})_{i,j} = \rho^{|i-j|}$ with $\|\rho\| < 1$ [103], [104]. The results are plotted in Figs. 3.7-3.9, showing a perfect match between the analytic and the simulated values in all cases.

First, the impact of the correlation matrix and the Rice K factors in the outage probability is studied both in the low-SNR and high-SNR regime. Since P_{out} exhibits complementary behaviors in both regimes, a different representation is employed in each case. Thus, Fig. 3.7 depicts the complementary outage probability $(1 - P_{\text{out}})$ for $P = 2$ when the SNR takes low values compared to the threshold, whereas Fig. 3.8 show the values of P_{out} in the high-SNR regime and for a larger number of branches ($P = 4$) in order to enrich the system.

Regarding both Figs. 3.7 and 3.8, we observe that the strength of the LoS has an opposite effect in the low- and high-SNR regimes. Hence, while in the former a weak direct component (low values for K_i) seems to be beneficial, a strong LoS achieves in general a better performance in the latter. This behavior can be justified as follows. A strong LoS component implies less random fluctuation in the received signal, i.e., the scattering is less relevant. In the high SNR regime, where the mean of the instantaneous SNR is large enough, this fluctuation represented by the scattering may occasionally lead to deep fading that makes the instantaneous SNR drops below the threshold. Therefore, increasing

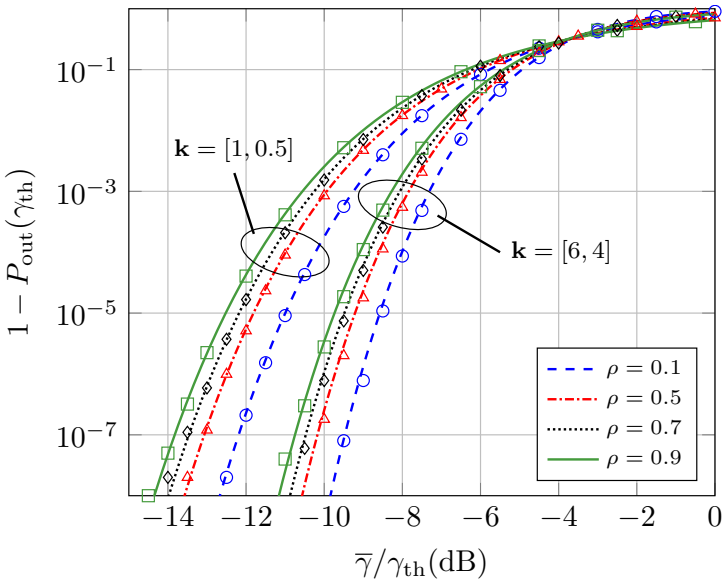

FIGURE 3.7: Complementary P_{out} vs. $\overline{\gamma}/\gamma_{\text{th}}$ for $P = 2$, different values of ρ and different values of K at each path. Solid lines correspond to theoretical calculation with $m = 40$ for $\mathbf{k} = (1, 0.5)$ and $m = 100$ for $\mathbf{k} = (6, 4)$, while markers correspond to Monte Carlo simulations.

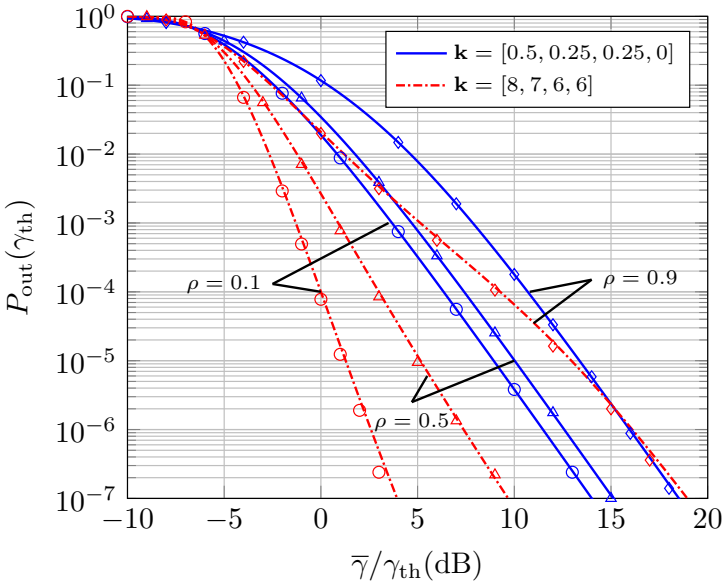

FIGURE 3.8: P_{out} vs. $\overline{\gamma}/\gamma_{\text{th}}$ for $P = 4$, different values of ρ and different values of K at each path. Solid lines correspond to theoretical calculation while markers correspond to Monte Carlo simulations. For theoretical calculation, $m = 40$ for $\mathbf{k} = (0.5, 0.25, 0.25, 0)$ and $m = 200$ for $\mathbf{k} = (8, 7, 6, 6)$.

the K factor (the power of the LoS) when the mean SNR takes large values is beneficial since it reduces such probability. In turn, in the low-SNR regime, the fluctuation in the received signal may have the opposite effect, punctually rendering values for the instantaneous SNR much larger than the mean value. In that case, increasing the K factor will reduce the probability of getting SNR values that are greater than the threshold.

Similarly, a high correlation factor gives a better performance for low values of $\overline{\gamma}$,

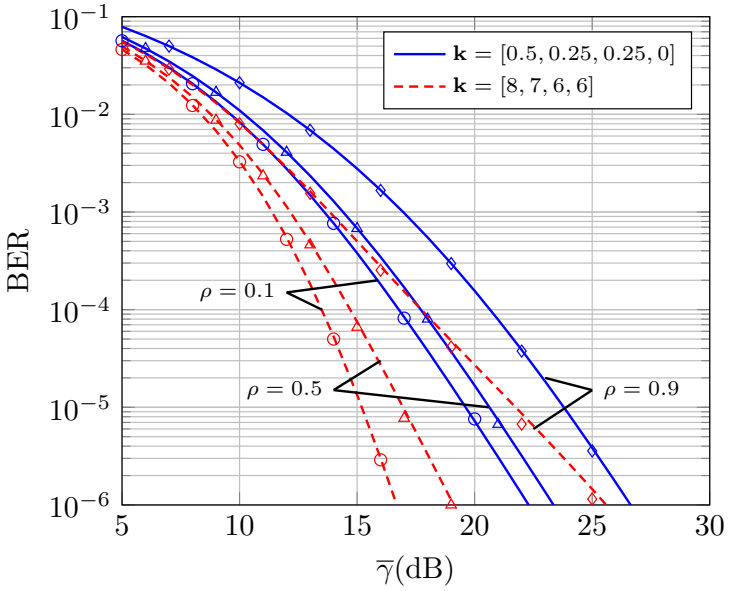

FIGURE 3.9: BER vs. $\overline{\gamma}$ for 16-QAM, $P = 4$ and different values of ρ and $\mathbf{k}$. Solid lines correspond to theoretical calculation with $m = 40$ for $\mathbf{k} = (0.5, 0.25, 0.25, 0)$ and $m = 150$ for $\mathbf{k} = (8, 7, 6, 6)$, while markers correspond to Monte Carlo simulations.

while the opposite behavior is observed in the high-SNR regime. Similar conclusions are drawn in [99], [100] for large $\overline{\gamma}$, but none of these works pay attention to the behavior of P_{out} in the low SNR regime.

An interesting behavior is noticed in the case of strongly correlated branches and large $\overline{\gamma}$. Regarding Fig. 3.8, we can observe that for $\rho = 0.9$ a strong LoS implies a considerable degradation of the system performance, being the outage probability asymptotically higher for large values of K. However, this effect is not observed for lower values of ρ, i.e., less correlated branches. This behavior is deeply analyzed in [105], where it is shown that, in multiple-input multiple-output (MIMO)-MRC systems, increasing the distinct K_i factors have a negative impact on the system performance until a certain value, K_{th}, is reached, from which P_{out} starts to decrease as K_i increase. In fact, expressions for this threshold are provided in [105, sec. IV-B] under the assumption of identically distributed Rice channels, observing that K_{th} depends on the correlation matrix. However, despite this assumption, it is difficult to determine how an arbitrary correlation between branches would impact this turning value of K.

Finally, the impact of the correlation and of the strength of the LoS in the BER is evaluated in Fig. 3.9, where $P_b(\overline{\gamma})$ is depicted for 16-QAM and different values of ρ and $\mathbf{k}$. Same conclusions as with the outage probability can be given: negative effect of correlated branches and better performance in general as Rice K factors increase. However, for values of ρ close to one, we observe again that increasing the LoS power does not always render a clear benefit. Similar results are observed for distinct values of M.

3.2 Generalizations of the κ-μ shadowed distribution

The auxiliary (confluent) random variables defined in the previous section were used just as simple tools to facilitate the analysis of the original random variable from which they emerge, i.e., we were interested only in the limit behavior of their distributions.

However, these auxiliary random variables can also be interesting by themselves. For instance, in channel modeling, the addition of a random fluctuation to a variable representing the fading can be used to characterize shadowing at the same time. In fact, this is the same idea from which some generalized fading model arise, e.g., the Rician shadowed and the κ-μ shadowed models: introducing a random fluctuation in the LoS component in order to better characterize the fluctuations produced by shadowing. To that end, the perturbation is chosen to be gamma distributed because of two main reasons: *i)* its mathematical tractability and *ii)* it has been proved that gamma distribution can be as accurate as lognormal distribution when characterizing shadowing [87], [106].

Although both the Rician shadowed and the κ-μ shadowed models are in fact generalizations of the classical ones (Rayleigh, Rice), in the context of the analysis through confluence, a κ-μ shadowed random variable can be seen as the confluent version of a κ-μ one and the same relationship can be established between the Rician shadowed model and the Rice distribution, though in these cases there is no interest in using the confluence approach since closed-form expressions are known for the distribution of the original variables.

With this idea, two new fading models are proposed in this thesis. The first one, namely the fluctuating Beckmann (FB) distribution, arises as an extension of both the κ-μ shadowed and the Beckmann distributions. From the point of view of the analysis through confluence, the FB distribution can be seen as the auxiliary variable used to characterize the classical Beckmann model, simplifying its analysis and allowing the derivation of closed-form expressions for its PDF and CDF. Compared to the κ-μ shadowed model, the FB distribution is a natural generalization by considering the effect of power imbalance in both LoS and non-line-of-sight (NLoS) components, as the Beckmann model does.

The second model here introduced takes advantage of the partial results obtained through the analysis of complex GQFs, generalizing the κ-μ shadowed distribution by accounting for the impact of the correlation between the contributions of each cluster.

3.2.1 The fluctuating Beckmann fading model

This section introduces the very general FB fading model, providing its first and second order statistics as well as discussing the impact of the distinct model parameters on its distribution. A more detailed analysis of this fading model can be found in

[48] P. Ramírez-Espinosa, F. J. López-Martínez, J. F. París, M. D. Yacoub, and E. Martos-Naya, "An extension of the κ-μ shadowed fading model: Statistical characterization and applications", *IEEE Trans. Veh. Technol.*, vol. 67, no. 5, pp. 3826–3837, May 2018,

attached in Appendix A.3.

Physical model

As stated before, the physical model of the FB distribution arises as a generalization of both the κ-μ shadowed and the Beckmann distribution. Thus, it inherits the clustering structure, i.e., the model is built out of the sum of the square modulus of independent random variables, together with the fluctuating LoS component already present in the physical model of the κ-μ shadowed distribution. In addition, the FB model also takes into account the effect of the in-phase and quadrature power imbalance in the LoS and NLoS components. Therefore, the received signal amplitude is expressed as

$$R = \left(\sum_{i=1}^{\mu} \left\| \sigma_x X_i + j\sigma_y Y_i + \xi(p_i + jq_i) \right\|^2 \right)^{1/2} \tag{3.34}$$

where $\mu \in \mathbb{N}^+$, $\sigma_x, \sigma_y \in \mathbb{R}^+$ and $p_i, q_i \in \mathbb{R}$ are constants; X_i, Y_i for all i are i.i.d. standard Gaussian random variables, i.e., $X_i, Y_i \sim \mathcal{N}(0,1)$, and ξ is a random variable, independent of X_i and Y_i, such that ξ^2 is gamma distributed[2] with shape parameter m and $\mathbb{E}[\xi^2] = 1$, i.e., $\xi^2 \sim \Gamma(m, 1/m)$.

As in other generalized fading models, ξ in (3.34) accounts for the fluctuation of the LoS component, being controlled by the parameter m. Thus, this fluctuation is less severe as m increases. On the other hand, as opposed to the κ-μ shadowed model, the FB model considers that the in-phase and quadrature components (X_i and Y_i) can have different variances, namely σ_x^2 and σ_y^2. This allows to characterize the effect of power imbalance in the diffuse components associated to NLoS propagation. Similarly, it can also be considered that the power of the LoS components can be imbalanced. Hence, the physical model in (3.34) can be also regarded as a generalization of the Beckmann fading model through the consideration of clustering and LoS fluctuation.

Due to its generality, the FB distribution inherits the parametrization from both the Beckmann model and the κ-μ shadowed model, being completely described by parameters m, μ and

$$\kappa = \frac{\sum_{i=1}^{\mu} p_i^2 + q_i^2}{\mu(\sigma_x^2 + \sigma_y^2)}, \qquad \eta = \frac{\sigma_x^2}{\sigma_y^2}, \qquad \varrho^2 = \frac{\sum_{i=1}^{\mu} p_i^2}{\sum_{j=1}^{\mu} q_i^2}. \tag{3.35}$$

[2] or, equivalently, ξ is Nakagami-m distributed with $\mathbb{E}[\xi^2] = 1$.

TABLE 3.1: Connections between the FB fading model and other models in the literature. In order to avoid confusion, FB parameters are underlined. Note that setting $\kappa = 0$ implies that m and ϱ vanish.

Channels	Fluctuating Beckmann Fading Parameters
Rayleigh	$\underline{\kappa} = 0, \quad \underline{\mu} = 1, \quad \underline{\eta} = 1$
Rice	$\underline{\kappa} = K, \quad \underline{\mu} = 1, \quad \underline{m} \to \infty, \quad \underline{\eta} = 1 \quad , \forall \underline{\varrho}$
Nakagami-m	$\underline{\kappa} = 0, \quad \underline{\mu} = m, \quad \underline{\eta} = 1$
Hoyt	$\underline{\kappa} = 0, \quad \underline{\mu} = 1, \quad \underline{\eta} = \eta$
η-μ	$\underline{\kappa} = 0, \quad \underline{\mu} = \mu, \quad \underline{\eta} = \eta$
Beckmann	$\underline{\kappa} = K, \quad \underline{\mu} = 1, \quad \underline{m} \to \infty, \quad \underline{\eta} = \eta, \quad \underline{\varrho} = \varrho$
κ-μ	$\underline{\kappa} = \kappa, \quad \underline{\mu} = \mu, \quad \underline{m} \to \infty, \quad \underline{\eta} = 1, \quad \forall \underline{\varrho}$
Rician Shadowed	$\underline{\kappa} = \kappa, \quad \underline{\mu} = 1, \quad \underline{m} = m, \quad \underline{\eta} = 1, \quad \forall \underline{\varrho}$
κ-μ shadowed	$\underline{\kappa} = \kappa, \quad \underline{\mu} = \mu, \quad \underline{m} = m, \quad \underline{\eta} = 1, \quad \forall \underline{\varrho}$

Parameters κ, μ and m are analogous to those in the κ-μ shadowed model, and η and ϱ are defined as in the Beckmann distribution in order to account for the power imbalance in NLoS and LoS components, respectively. Thus, the FB distribution provides the unification of a large number of important fading distributions. These connections are summarized in Table 3.1, on which the parameters corresponding to the FB distribution are underlined in order to avoid confusion with the parameters of any of the distributions included as special cases.

First order statistics

A first order characterization of the FB distribution is now provided in terms of its chief probability functions, namely MGF, PDF and CDF. Since fading distributions are usually analyzed in terms of the SNR [18], hereinafter we will consider the random variable

$$\gamma \triangleq \overline{\gamma} \frac{R^2}{\mathbb{E}[R^2]}, \tag{3.36}$$

where $\mathbb{E}[R^2] = \mu(\sigma_x^2 + \sigma_y^2) + \sum_{i=1}^{\mu}(p_i^2 + q_i^2)$ and $\overline{\gamma} \triangleq \mathbb{E}[\gamma]$ is the average SNR, representing the instantaneous SNR at the receiver side. Then, γ follows a FB distribution with parameters κ, μ, m, η and ϱ, and for convenience we denoted it as $\gamma \sim \mathcal{FB}(\overline{\gamma}; \kappa, \mu, m, \eta, \varrho)$.

The MGF of the FB fading model can be obtain by conditioning the MGF of the Beckmann distribution [18, eq. (2.38)] on ξ, after introducing the clustering, and averaging over all the possible values of ξ, as stated in the following lemma.

Lemma 3.8 *Let $\gamma \sim \mathcal{FB}(\overline{\gamma}; \kappa, \mu, m, \eta, \varrho)$. Then, the MGF of γ is given by*

$$M_\gamma(s) = \frac{(-1)^\mu}{s^\mu} \frac{\alpha_2^{m-\mu/2}}{\overline{\gamma}^\mu \alpha_1^m} \left(1 - \frac{\mu(1+\eta)(1+\kappa)}{2\eta\overline{\gamma}s}\right)^{m-\frac{\mu}{2}} \times \left(1 - \frac{\mu(1+\eta)(1+\kappa)}{2\overline{\gamma}s}\right)^{m-\frac{\mu}{2}} \left(1 - \frac{c_1}{\overline{\gamma}s}\right)^{-m} \left(1 - \frac{c_2}{\overline{\gamma}s}\right)^{-m}, \tag{3.37}$$

where $c_{1,2}$ are the roots of $\alpha_1 s^2 + \beta s + 1$ with

$$\alpha_1 = \frac{4\eta}{\mu^2(1+\eta)^2(1+\kappa)^2} + \frac{2\kappa(\varrho^2+\eta)}{m(1+\varrho^2)\mu(1+\eta)(1+\kappa)^2}, \tag{3.38}$$

$$\beta = \frac{-1}{1+\kappa}\left[\frac{2}{\mu} + \frac{\kappa}{m}\right], \tag{3.39}$$

and α_2 is calculated as

$$\alpha_2 = \frac{4\eta}{\mu^2(1+\eta)^2(1+\kappa)^2}. \tag{3.40}$$

Analytic expressions are attainable for the PDF and CDF of γ by performing the inverse Laplace transformation to (3.37), as stated in (3.23), and given below.

Lemma 3.9 *Let $\gamma \sim \mathcal{FB}(\overline{\gamma}; \kappa, \mu, m, \eta, \varrho)$. Then, the PDF and CDF of γ are given by*

$$f_\gamma(\gamma) = \frac{\alpha_2^{m-\mu/2}\gamma^{\mu-1}}{\bar{\gamma}^\mu \Gamma(\mu)\alpha_1^m} \Phi_2^{(4)}\left(\frac{\mu}{2} - m, \frac{\mu}{2} - m, m, m; \mu; \frac{-\gamma}{\bar{\gamma}\sqrt{\eta\alpha_2}}, \frac{-\gamma\sqrt{\eta}}{\bar{\gamma}\sqrt{\alpha_2}}, \frac{-\gamma c_1}{\bar{\gamma}}, \frac{-\gamma c_2}{\bar{\gamma}}\right), \tag{3.41}$$

$$F_\gamma(\gamma) = \frac{\alpha_2^{m-\mu/2}\gamma^{\mu}}{\bar{\gamma}^\mu \Gamma(\mu+1)\alpha_1^m} \Phi_2^{(4)}\left(\frac{\mu}{2} - m, \frac{\mu}{2} - m, m, m; \mu+1; \frac{-\gamma}{\bar{\gamma}\sqrt{\eta\alpha_2}}, \frac{-\gamma\sqrt{\eta}}{\bar{\gamma}\sqrt{\alpha_2}}, \frac{-\gamma c_1}{\bar{\gamma}}, \frac{-\gamma c_2}{\bar{\gamma}}\right), \tag{3.42}$$

where $\Phi_2^{(n)}$ is the confluent form of the generalized Lauricella series defined in [107, p. 34].

As observed, the PDF and CDF of the FB distribution are given in terms of the multivariate $\Phi_2^{(n)}$ function, which also appears in other fading distributions in the literature [29], [31], [108]. Apparently, and because it is defined as an n-fold infinite summation, its numerical evaluation may pose some challenges from a computational point of view. However, the Laplace transform of the $\Phi_2^{(n)}$ function has a comparatively simpler form in terms of a finite product of elementary functions, which becomes evident by inspecting the expression of the MGF in (3.37). Therefore, the $\Phi_2^{(n)}$ function can be evaluated by means of a numerical inverse Laplace transform [109], [110].

Remarkably, as with the κ-μ and η-μ models, the statistics of the FB are also valid for $\mu \in \mathbb{R}^+$, although the underlying model of random variables in (3.34) loses its meaning. Moreover, when $\eta = 1$ the effect of the parameter ϱ vanishes, as can be observed from (3.38); conversely, when setting $\varrho = 1$ the effect of η is still relevant.

Simple and more tractable expressions can be obtained for the PDF and CDF of the FB distribution under certain conditions. Specifically, if m and μ are assumed to be an integer number and an even number, respectively, (3.37) can be expressed in an alternative form thanks to partial fraction expansion, allowing the derivation of PDF and CDF in terms of elementary functions (i.e., exponentials and powers), as stated next.

Corollary 3.10 *Let $\gamma \sim \mathcal{FB}(\bar{\gamma}; \kappa, \mu, m, \eta, \varrho)$ with m being an integer number and μ an even number. Then, the PDF and CDF of γ are given by*

$$f_\gamma(\gamma) = \frac{\alpha_2^{m-\frac{\mu}{2}}}{\alpha_1^m \bar{\gamma}^\mu} \sum_{i=1}^{N(m,\mu)} e^{-\tau_i \gamma/\bar{\gamma}} \sum_{j=1}^{|\omega_i|} \frac{A_{i,j}\gamma^{j-1}}{(j-1)!}, \tag{3.43}$$

$$F_\gamma(\gamma) = 1 + \frac{\alpha_2^{m-\frac{\mu}{2}}}{\alpha_1^m \bar{\gamma}^\mu} \sum_{i=1}^{N(m,\mu)} e^{-\tau_i \gamma/\bar{\gamma}} \sum_{j=1}^{|\omega_i|} \frac{B_{i,j}\gamma^{j-1}}{(j-1)!}, \tag{3.44}$$

where $A_{i,j}$ and $B_{i,j}$ are the residues arising from performing a partial fraction decomposition in (3.37) *after evaluating $M_\gamma(-s)$ and $M_\gamma(-s)/s$, respectively; $N(m,\mu) = 2\left[1 + \mathrm{u}\left(\mu/2 - m\right)\right]$ and ω_i and τ_i are the elements of vectors $\boldsymbol{\omega}$ and $\boldsymbol{\tau}$, defined as*

$$\boldsymbol{\omega} = \left[m, m, \frac{\mu}{2} - m, \frac{\mu}{2} - m\right], \tag{3.45}$$

$$\boldsymbol{\tau} = \left[c_1, c_2, \frac{\mu(1+\eta)(1+\kappa)}{2\eta}, \frac{\mu(1+\eta)(1+\kappa)}{2}\right]. \tag{3.46}$$

Second order statistics

First-order statistics (e.g., PDF and CDF) provide valuable information about the statistical behavior of the amplitude (or, equivalently, power) of the received signal affected by fading. However, they do not incorporate information related to the dynamic behavior of the fading process, which is of paramount relevance in the context of wireless communications because of the relative motion of transmitter, receivers and scatterers due to mobility. In the literature, two metrics are used to capture the dynamics of a general random process: *i)* the level crossing rate (LCR), which measures how often the amplitude of the received signal crosses a given threshold value, and *ii)* the average fade duration (AFD), which measures how long the amplitude of the received signal remains below this threshold.

In the calculation of both statistics (LCR and AFD), we assume that the fluctuations in the diffuse part (i.e., NLoS) occur at a smaller scale compared to those of the LoS component. This is the case, e.g., where such LoS fluctuation (represented by the random variable ξ) is associated to shadowing, which is classically considered to occur at a larger scale than fading.

The LCR of the received signal amplitude R can be computed using Rice's formula [111] as

$$N_R(u) = \int_0^\infty \dot{r} f_{R,\dot{R}}(u, \dot{r})\, d\dot{r}, \tag{3.47}$$

where $\dot{R}$ denotes the time derivative of the signal envelope and $f_{R,\dot{R}}(r, \dot{r})$ is the joint PDF of the received signal amplitude and its time derivative. Although an analytic expression for $N_R(u)$ have been obtained, it is given in terms of a two-fold integral which considerably reduces its usefulness.

It is possible to arrive at a more tractable expression for a simpler yet general case by considering the scenario in which in-phase and quadrature components are independent. Independence between in-phase and quadrature components can be achieved by assuming $q_i = 0$ and $p_i \neq 0$ or vice-versa in (3.34), leading to a simpler underlying model that eases the analysis. Note, however, that such a scenario is still a FB fading model, and does not bear any similarity with other previous models published in the literature. Therefore, assuming the case $q_i = 0 \; \forall \; i$ (a similar expression is obtained for $p_i = 0 \; \forall \; i$), the physical model in (3.34) can be decomposed as

$$R^2 = \sum_{i=1}^{\mu} (\sigma_x X_i + \xi p_i)^2 + \sum_{k=1}^{\mu} \sigma_y^2 Y_i^2, \tag{3.48}$$

facilitating the calculation of the LCR, which is ultimately given by

$$\begin{aligned} N_R(u) = {} & \frac{m^m [\mu(1+\eta)(1+\kappa)]^{\mu-1/2} \sqrt{-\ddot{\rho}(0)}}{2^{\mu-1}\Gamma^2(\mu/2)\eta^{\mu/2}(\frac{\mu\kappa(1+\eta)}{2\eta}+m)^m\sqrt{2\pi}} \cdot u^{(2\mu-1)} \exp\left(-\frac{\mu}{2}(1+\eta)(1+\kappa)u^2\right) \\ & \times \int_0^1 [1+(\eta-1)x]^{\frac{1}{2}} (1-x)^{\mu/2-1} x^{\mu/2-1} \exp\left(-\frac{\mu(1-\eta^2)(1+\kappa)}{2\eta} u^2 x\right) \\ & \times {}_1F_1\left(m, \mu/2; \frac{\frac{\kappa\mu^2(1+\eta)^2(1+\kappa)}{4\eta^2}}{\frac{\mu\kappa(1+\eta)}{2\eta}+m} u^2 x\right) dx \end{aligned} \tag{3.49}$$

where $\Omega = \mathbb{E}[R^2]$ and $\ddot{\rho}(0)$ is the second derivative of the temporal autocorrelation function evaluated at 0.

Note that, although (3.49) is also in integral form, it can be easily computed due to the bounded integral limits and the integrand behavior. Moreover, despite the assumption $q_i = 0$, (3.49) is also valid for $p_i = 0 \; \forall \; i$ and $q_i \neq 0$ by just setting $\eta \to 1/\eta$, since both cases are equivalent as can be observed from (3.34).

Finally, with the knowledge of the LCR, the AFD is straightforwardly calculated as

$$T_R(u) = \frac{F_R(u)}{N_R(u)} \tag{3.50}$$

where $F_R(u)$ is the CDF of the received signal amplitude, which can be derived from (3.42) after a simple change of variables.

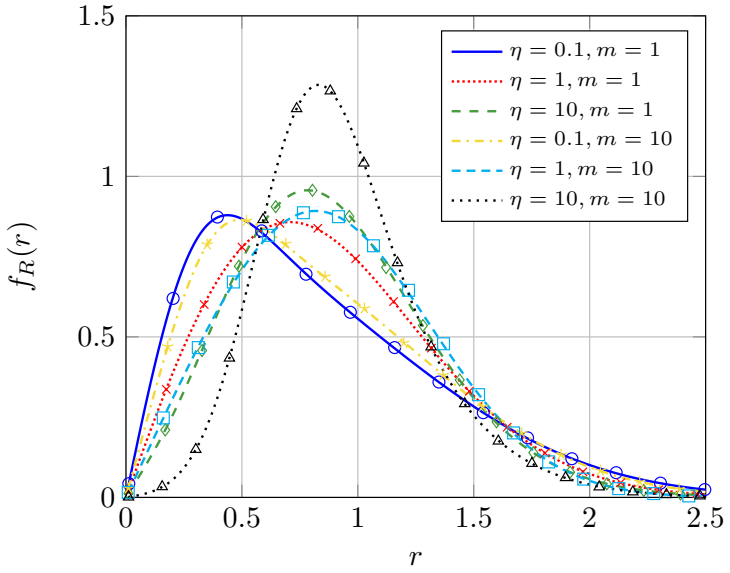

FIGURE 3.10: FB signal envelope distribution for different values of η and m in weak LoS scenario ($\kappa = 1$) with $\varrho = 0.1$, $\mu = 1$ and $\Omega = \mathbb{E}[R^2] = 1$. Solid lines correspond to the exact PDF, while markers correspond to Monte Carlo simulations.

Numerical results and discussion

After attaining a full statistical characterization of the newly proposed distribution, we now exemplify the influence of the distinct parameters of the FB model over the distribution of the received signal amplitude, R, in Figs. 3.10-3.12 and over the second order statistics in Figs. 3.13-3.14. Note that the PDF of R can be directly obtained from (3.41) as $f_R(r) = 2r\frac{\overline{\gamma}}{\Omega} f_\gamma(\overline{\gamma} r^2/\Omega)$. In addition, in order to double-check the validity of the theoretical expressions, Monte Carlo simulations are also provided.

We will focus on understanding the effect of the power imbalance in the LoS and NLoS components (i.e., the effect of ϱ and η), since these are the two parameters that effectively extend the original κ-μ shadowed fading model to a more general case. To that end, Fig. 3.10 represents the PDF of R for different values of η with mild and strong LoS fluctuation ($m = 10$ and $m = 1$, respectively) and $\mu = 1$. The parameter ϱ is set to $\varrho^2 = 0.1$, indicating a moderately large LoS power imbalance. In fact, $\varrho^2 = 0.1$ specifies that the in-phase component of the LoS is 10 times more powerful than the quadrature one.

With this parameters choice, it can be observed from Fig. 3.10 that the effect of increasing η causes the amplitude values to be more concentrated around its mean value. Besides, compared to the case of $\eta = 1$ (i.e., the κ-μ shadowed fading distribution), the effect of having a power imbalance in the NLoS component clearly has an impact on the distribution of the signal envelope. Interestingly, in contrast to the η-μ fading model, the behavior of the distribution with respect to η is no longer symmetrical between $\eta \in [0, 1]$ and $\eta \in [1, \infty)$ for a fixed $\varrho^2 \neq 1$. In fact, one interesting effect comes from the observation of the effect of increasing η: both setting $\eta = 0.1$ or $\eta = 10$ implies that the NLoS

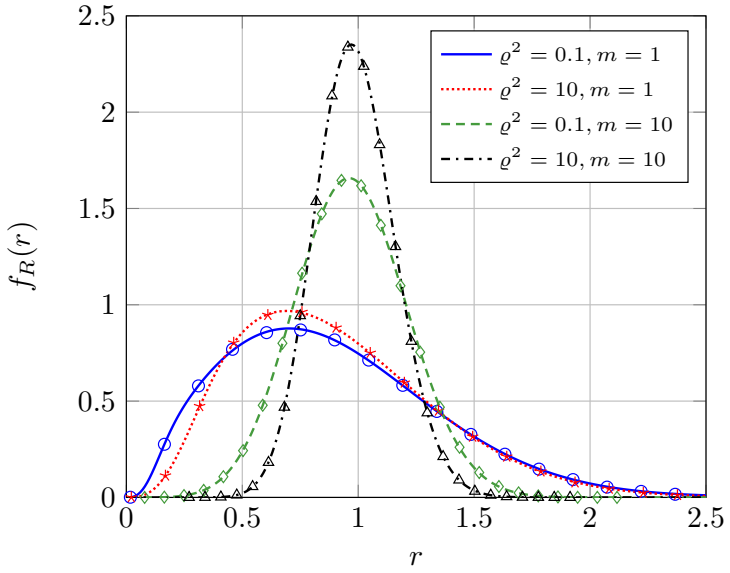

FIGURE 3.11: FB signal envelope distribution for different values of ϱ and m in strong LoS scenario ($\kappa = 10$) with $\eta = 0.1$, $\mu = 2$ and $\Omega = \mathbb{E}[R^2] = 1$. Solid lines correspond to the exact PDF, while markers correspond to Monte Carlo simulations.

power is imbalanced by a factor of 10. However, it is evident that if this NLoS imbalance goes to the component associated with a larger LoS imbalance ($\eta = 0.1$ since $\varrho^2 = 0.1$), this is much more detrimental for the received signal envelope than having the NLoS imbalance in the other component.

Fig. 3.11 focuses now on the impact of the LoS power imbalance, depicting the PDF of the received signal amplitude for different values of ϱ and m with $\kappa = 10$ (i.e., strong LoS scenario), $\mu = 2$ and $\eta = 0.1$. Because the LoS component is now much more relevant, the effect of changing m is more noticeable. It is noticed that low values of ϱ and m cause the amplitude values being more sparse. Also, the same behavior as with η is observed for varying ϱ, i.e., having the LoS imbalance in the opposite component as in the NLoS (in this case, since $\eta = 0.1$, it is obtained for $\varrho^2 = 10$) makes the amplitude values being more concentrated around its mean value than in the case where the imbalance of both LoS and NLoS is in the same component, i.e., $\eta = 0.1$ and $\varrho^2 = 0.1$.

Remarkably, a bimodal behavior is observed as the imbalance is reduced through ϱ or η, as observed in Fig. 3.12. When both ϱ and η decrease, the in-phase components have considerably less power than the quadrature components. Because κ is sufficiently large, the distribution will mostly fluctuate close to the LoS part of the quadrature component due to the low value m, and the first maximum on the PDF in the low-amplitude region appears as the highly imbalanced in-phase component only is able to contribute in this region. We must note that this bimodal behavior does not appear in the original κ-μ shadowed or Beckmann distributions from which the FB distribution originates. Nevertheless, such bimodality indeed appears in other fading models [31], [112].

Finally, the effect of the FB parameters in the second order statistics (LCR and AFD)

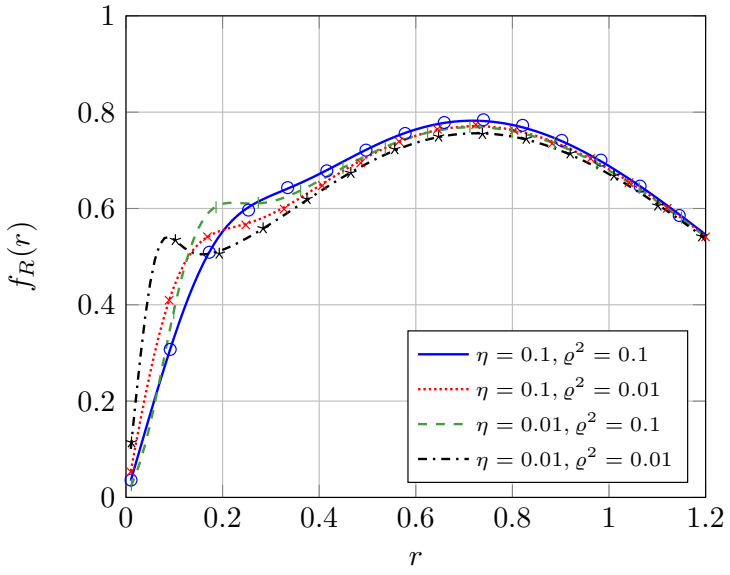

FIGURE 3.12: FB signal envelope distribution for different values of ϱ and η in strong LoS scenario ($\kappa = 10$) with $m = 1$, $\mu = 1$ and $\Omega = \mathbb{E}[R^2] = 1$. Solid lines correspond to the exact PDF, while markers correspond to Monte Carlo simulations.

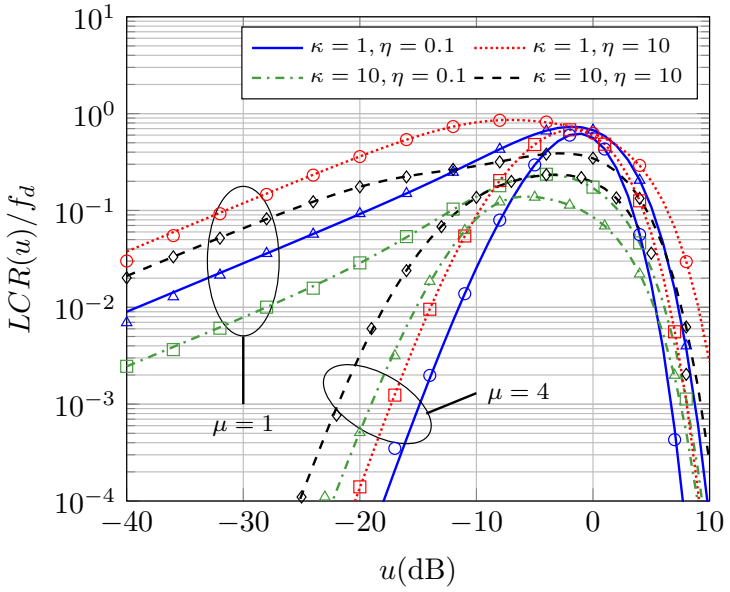

FIGURE 3.13: Normalized LCR vs threshold value u(dB) for different values of κ, η and μ, with $m = 1$, $\varrho \to \infty$ and $\Omega = \mathbb{E}[R^2] = 1$. Solid lines correspond to theoretical calculations, while markers correspond to Monte Carlo simulations.

is investigated in Figs. 3.13-3.14. We assume a time variation of the diffuse component according to Clarke's correlation model [17, sec. 2.1.1] with maximum Doppler shift f_d, implying that $\sqrt{-\ddot{\rho}(0)} = \sqrt{2} f_d \pi$ [113, eq. (34)]. We also consider that $\varrho^2 \to \infty$, so the LCR and AFD are calculated as in (3.49) and (3.50). Also, a sampling period $T_s >> f_d$ is assumed in Monte Carlo simulations in order to avoid missing level crossings at very low threshold values.

Thus, Fig. 3.13 represents the LCR vs the normalized threshold, u, for different values

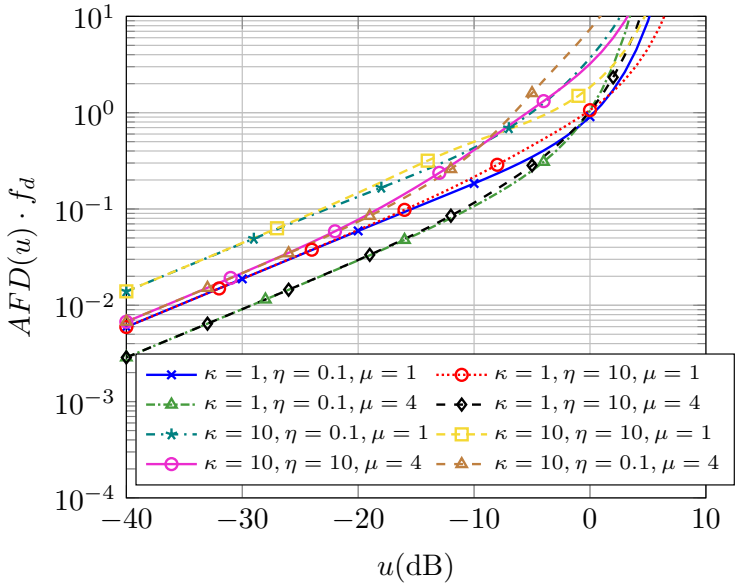

FIGURE 3.14: Normalized AFD vs threshold value u(dB) for different values of κ, η and μ, with $m = 1$, $\varrho \to \infty$ and $\Omega = \mathbb{E}[R^2] = 1$. Solid lines correspond to theoretical calculations, while markers correspond to Monte Carlo simulations.

of the FB model parameters. Interestingly, when increasing μ, the number of crossings at very low threshold values is drastically reduced. Similarly, the number of crossings in this region grows when reducing κ or increasing η. This latter effect is coherent with the fact that $\varrho \to \infty$ in this case, so that having a value of $\eta < 1$ reduces the fading severity.

The beneficial impact of increasing μ is also observed in Fig. 3.14, in which lower values of μ render a larger duration of deep fades. Remarkably, for very low u, the AFD seems to be independent of the values of η.

3.2.2 The κ-μ shadowed fading model with intercluster correlation

This section introduces the second generalization of the κ-μ shadowed fading model proposed in this thesis, showing that this new distribution is closely related to the auxiliary random variables in (3.17) we used to analyze complex GQFs. The physical model of the distribution is given, along with simple closed-form expressions for its first order statistics, namely PDF, CDF and MGF.

The results provided in the following are a summary of those given in

[49] P. Ramírez-Espinosa, J. F. París, J. A. Cortés, and E. Martos-Naya, "The κ-μ shadowed fading model with arbitrary intercluster correlation", in *2018 15th Int. Symp. Wireless Commun. Syst. (ISWCS)*, Aug. 2018, pp. 1–5,

attached in Appendix A.4.

Physical model

The physical model of this new fading distribution arises as a generalization of the physical model of the original κ-μ shadowed distribution in (2.99). Thus, the received signal power is modeled as the sum of the squared modulus of μ Gaussian random variables (clustering structure) whose means randomly fluctuates. The power of each variable is assumed to be the same. However, as opposed to the original model, we here assume that these diffuse waves, i.e., the underlying Gaussian variables, are correlated, introducing an arbitrary correlation factor for the intercluster components. Hence, while the FB model extends the κ-μ shadowed distribution by considering the power imbalance in the LoS and NLoS, this newly proposed model maintains the restriction of equal powers for the in-phase and quadrature components but takes into account the possibility of the distinct contributions of each cluster to be correlated. Therefore, we consider appropriate to name this extension as correlated κ-μ shadowed fading model.

The received signal amplitude under correlated κ-μ shadowed fading can then be written as

$$R = \left(\sum_{i=1}^{\mu} \| Z_i + \xi p_i \|^2 \right)^{1/2}, \tag{3.51}$$

where $\mu \in \mathbb{N}^+$ is the same parameter as in previous models, p_i for $i = 1, \ldots, \mu$ is a complex number representing the LoS contribution and Z_i are complex Gaussian random variables such that $Z_i \sim \mathcal{CN}(0, \sigma^2)$. As in the κ-μ shadowed and the FB distributions, ξ is a random variable, independent of Z_i, such that $\xi^2 \sim \Gamma(m, 1/m)$ with $\mathbb{E}[\xi^2] = 1$, which accounts for the random fluctuations of the LoS component due to shadowing. The novelty is that the distinct Z_i can be correlated with correlation coefficient $\mathrm{corr}(Z_i, Z_j) = \rho_{i,j}$ for $i, j = 1, \ldots, \mu$ with

$$\rho_{i,j} = \frac{\mathbb{E}[Z_i Z_j^\dagger]}{\sigma^2}. \tag{3.52}$$

Note that, if $\rho_{i,j} = 0 \; \forall \; i \neq j$, then (3.51) becomes the original κ-μ shadowed physical model. Equivalently, if we consider the vector $\mathbf{z} \in \mathbb{C}^{\mu \times 1}$ with entries Z_i, then $\mathbf{z} \sim \mathcal{CN}_\mu(\mathbf{0}_{\mu \times 1}, \sigma^2 \mathbf{R})$ with $\mathbf{R}$ the correlation matrix, i.e., $(\mathbf{R})_{i,j} = \rho_{i,j}$.

Regarding (3.51), it can be observed that, when conditioned on ξ, R^2 is a particular case of the complex quadratic form in (2.52) in which $\mathbf{A} = \mathbf{I}_\mu$. Therefore, applying the same procedure as described in Section 2.3.1 for complex GQFs, R is rewritten as

$$R = \left(\sum_{i=1}^{\mu} \left\| \sqrt{\lambda_i} \sigma \widetilde{Z}_i + \xi \sqrt{\lambda_i} \widetilde{p}_i \right\|^2 \right)^{1/2}, \tag{3.53}$$

where $\widetilde{Z}_i \sim \mathcal{CN}(0, 1)$, $\widetilde{p}_i$ are the entries of the vector $\widetilde{\mathbf{p}} = \mathbf{U}^\dagger \mathbf{C}^{-1} \mathbf{p}$ with $\mathbf{p} = (p_1, \ldots, p_\mu)^T$, λ_i are the eigenvalues of $\mathbf{C}^\dagger \mathbf{C}$ (i.e., those of $\mathbf{R}$) and $\mathbf{U}$ is an unitary matrix whose i-th column is the eigenvector of $\mathbf{C}^\dagger \mathbf{C}$ associated with λ_i.

Statistical characterization

As with the FB distribution, we provide the statistical characterization of the correlated κ-μ shadowed fading model based on the instantaneous SNR random variable $\gamma = \overline{\gamma}R^2/\mathbb{E}[R^2]$, with $\overline{\gamma}$ denoting the average SNR at the receiver side and $\mathbb{E}[R^2] = \mu\sigma^2 + \sum_{i=1}^{\mu} \|p_i\|^2$. Therefore, we say that γ follows a correlated κ-μ shadowed distribution with parameters $\kappa = \sum_{i=1}^{\mu} \|p_i\|^2/(\mu\sigma^2)$, μ, m and $\mathbf{R}$, i.e., $\gamma \sim \mathcal{CS}_{\kappa\mu}(\overline{\gamma}; \kappa, \mu, m, \mathbf{R})$. Moreover, aiming to relay the mathematical complexity of the newly proposed fading model, we assume that both m and μ are positive integer numbers, i.e., the proposed model inherits the formulation given in [30].

We will focus first on the MGF of γ. Since, conditioned on ξ, R^2 is a specific complex GQF, the conditioned MGF is straightforwardly obtained from (2.66). Then, the unconditional MGF is derived by averaging over ξ, as given next.

Lemma 3.11 *Let $\gamma \sim \mathcal{CS}_{\kappa\mu}(\overline{\gamma}; \kappa, \mu, m, \mathbf{R})$. Then, its MGF reads as*

$$M_\gamma(s) = \frac{\mu^\mu(\kappa+1)^\mu}{\prod_{i=1}^{\mu}(\mu(\kappa+1) - s\lambda_i\overline{\gamma})} \left(1 - \frac{1}{m}\sum_{j=1}^{\mu} \frac{d_i\lambda_i s\overline{\gamma}}{\mu(\kappa+1) - s\lambda_i\overline{\gamma}}\right)^{-m} \tag{3.54}$$

where $d_i = \|\widetilde{p}_i\|^2/\sigma^2$.

It is easy to prove that, when no correlation is applied ($\mathbf{R} = \mathbf{I}_\mu$), then $\lambda_i = 1$ for $i = 1, \ldots, \mu$, so (3.54) becomes the MGF of the original κ-μ shadowed distribution in [29, eq. (5)].

We observe that (3.54) has a very similar form to the MGF of the auxiliary variables that were used to analyze complex GQFs in (3.18). In fact, (3.54) also admits a formulation in terms of a rational function as

$$M_\gamma(s) = \frac{\mu^\mu(k+1)^\mu}{(-\overline{\gamma})^\mu \left(1 + \sum_{k=1}^{\mu} d_k/m\right)^m \prod_{l=1}^{\mu}\lambda_l} \frac{\prod_{j=1}^{\mu}\left(s - \frac{\mu(\kappa+1)}{\lambda_j\overline{\gamma}}\right)^{m-1}}{\prod_{i=1}^{n_\beta}(s-\beta_i)^{q_i m}}. \tag{3.55}$$

where β_i for $i = 1, \ldots, n_\beta$ are the distinct roots, with multiplicities q_i, of the μ-th order polynomial given by

$$P(s) = m\prod_{i=1}^{\mu} 1 - \frac{\lambda_i\overline{\gamma}}{\mu(\kappa+1)}s - \sum_{j=1}^{\mu}\frac{d_j\lambda_j\overline{\gamma}}{\mu(\kappa+1)}s\prod_{\substack{k=1\\k\neq j}}^{\mu} 1 - \frac{\lambda_k\overline{\gamma}}{\mu(\kappa+1)}s. \tag{3.56}$$

Thus, from (3.55), both the PDF and CDF of γ can be obtained by following the same steps as in previous sections, i.e., performing a partial fraction expansion and using the Laplace transform pairs in (3.23). The results are stated in the following lemma.

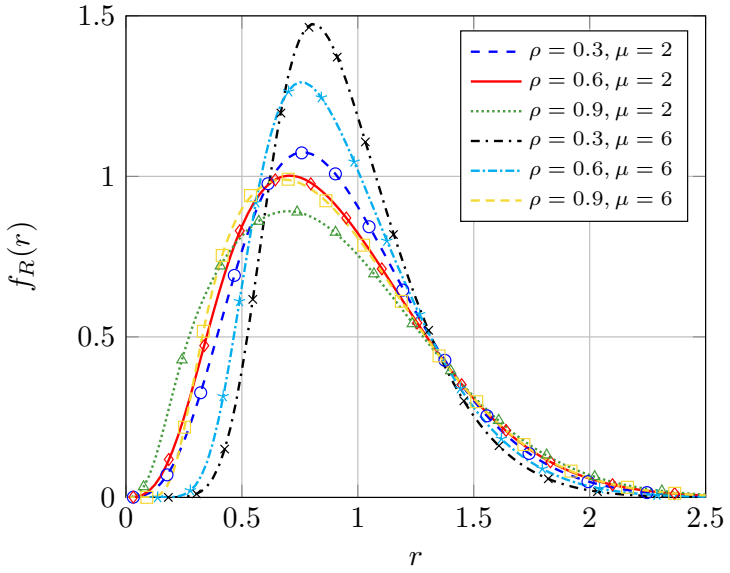

FIGURE 3.15: Signal envelope distribution for different values of μ and ρ with $\kappa = 1$, $m = 1$ and $\mathbb{E}[R^2] = 1$. Solid lines correspond to the exact PDF while markers correspond to Monte Carlo simulations.

Lemma 3.12 *Let $\gamma \sim \mathcal{CS}_{\kappa\mu}(\overline{\gamma}; \kappa, \mu, m, \mathbf{R})$. Then, its PDF and CDF are given by*

$$f_\gamma(\gamma) = \alpha \sum_{i=1}^{n_\beta} \sum_{j=1}^{q_i m} A_{i,j} \gamma^{j-1} e^{-\beta_i \gamma}, \tag{3.57}$$

$$F_\gamma(\gamma) = 1 + \alpha \sum_{i=1}^{n_\beta} \sum_{j=1}^{q_i m} C_{i,j} \gamma^{j-1} e^{-\beta_i \gamma}, \tag{3.58}$$

with

$$\alpha = \frac{\mu^\mu (\kappa+1)^\mu}{\overline{\gamma}^\mu \Gamma(j)} \left(1 + \sum_{j=1}^{\mu} \frac{d_j}{m}\right)^{-m} \prod_{l=1}^{\mu} \lambda_l^{-1} \tag{3.59}$$

and $A_{i,j}$ and $C_{i,j}$ the residues arising from performing a partial fraction expansion in (3.55) *after evaluating $M_\gamma(-s)$ and $M_\gamma(-s)/s$, respectively.*

As can be observed, very simple expressions for the statistics of the newly proposed model are given, being suitable for the further analytic purposes when analyzing systems performance. Remarkably, (3.57) and (3.58) have a similar form to those presented in [30] for the original κ-μ shadowed distribution, and hence the larger generality introduced does not come at the price of an increased mathematical complexity.

Numerical Results

We aim now to exemplify the impact of the intercluster correlation matrix in the distribution of the received signal amplitude since it is the parameter that effectively extends the original κ-μ shadowed model. Note that, as with the FB distribution, the PDF of R is easily obtained from (3.57) by applying a simple change of variables. As usually

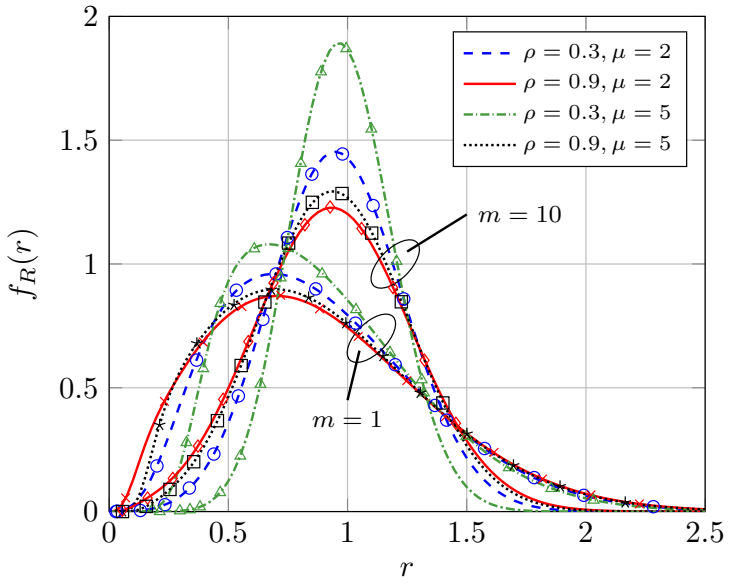

FIGURE 3.16: Signal envelope distribution for different values of μ, ρ and m with $\kappa = 4$ and $\mathbb{E}[R^2] = 1$. Solid lines correspond to the exact PDF while markers correspond to Monte Carlo simulations.

done throughout this thesis, we again assume that the correlation matrix $\mathbf{R}$ is exponential in order to simplify the presentation of the results, i.e., $(\mathbf{R})_{i,j} = \rho^{|i-j|}$ with $0 \leq \|\rho\| < 1$. With this consideration, Figs. 3.15-3.16 depict the distribution of the received signal amplitude for different values of the model parameters.

Thus, Fig. 3.15 shows the PDF of R for distinct values of μ and ρ in a weak LoS scenario ($\kappa = 1$) with heavily fluctuating dominant component ($m = 1$). It is observed that large values of ρ, i.e., more correlation between the components of each cluster, always render more sparse values of the signal amplitude, with independence of the value of μ.

A stronger LoS component is considered in Fig. 3.16, where the impact of m is also taken into account. It can be noticed that the impact of ρ is slightly less relevant in this case, which is a coherent result since the correlation only affects to the scattering according to the physical model in (3.51). Moreover, the impact of ρ in the received signal amplitude distribution seems to be independent of the value of m. However, a severe fluctuation of the dominant component (corresponding to lower values of m) is more detrimental for the signal envelope, as we already saw in the original model [29], [30].

Chapter 4

Conclusions and future work

In this final chapter, the main conclusions that arise from the contributions of this thesis are outlined. Also, some future lines and possible applications of the obtained results are suggested.

4.1 Conclusions

A twofold objective has been achieved in this thesis. On the one hand, it has provided simpler approximated expressions than those given in the literature for the distribution of both real and complex GQFs. To that end, a general method to approximate the PDF and CDF of random variables haven been derived, which has been named *analysis through confluence*.

More specifically, the proposed technique allows us to obtain approximating expressions for the first order statistics of a target variable, X, through the analysis of a suitably defined sequence of variables, $\{X_m\}$. This sequence is obtained from X by perturbing it somehow, i.e., introducing a random fluctuation in the mean or variance of the original variable. The main advantages of this method compared to other solutions available in the literature are: *i)* the resulting expressions *always* represent a valid distribution, and *ii)* any target level of accuracy can be reached with independence of the parametrization of the random variable under analysis.

Before directly apply the analysis through confluence to GQFs, it has been used to provide very general expressions for the PDF and CDF of an arbitrary positive variable in terms of the derivatives of its MGF. Also, it has been shown that these derivatives can be recursively obtained from the derivatives of the CGF. This technique is specially useful when the target MGF is given in terms of the product of easily differentiable functions. In the context of the analysis of GQFs, the following results have been obtained:

- The general expressions for the statistics of positive variables have been particularized to the case of positive definite non-central real GQFs, obtaining simple recursive approximations for the PDF and CDF which outperform the classical solutions.

- Simple closed-form approximants for the statistics of non-central indefinite complex GQFs have been derived, rendering expressions in terms of elementary functions that are suitable for further analytic purposes. Besides, this approximation inherits the properties of the confluence method presented in the thesis.
- To the best of the author's knowledge, very tight approximated expressions for the BER and the outage probability in MRC systems over correlated non-identically distributed Rice fading have been provided for the first time. The results are valid for any number of antennas and for arbitrary correlation between branches.

On the other hand, seeking to unifying the wide variety of existing fading models, two new distributions haven been provided. Both the novel technique to analyze random variables and these two general fading distributions, albeit apparently unconnected, arise in fact from the same underlying methodology. In the context of channel modeling, the contributions are summarized below:

- The versatile Fluctuating Beckmann distribution has been introduced as a generalization of both the κ-μ shadowed and the Beckmann models. It accounts for the clustering of waves and the fluctuation of the LoS component as the κ-μ shadowed model and also for the power imbalance between the in-phase and quadrature components, as the Beckmann distribution does. Expressions of its first and second order statistics have been provided, although its PDF and CDF remains in terms of a generalized hypergeometric function. To circumvent this issue, simple expressions are also provided in terms of elementary functions under certain conditions.
- An alternative extension of the κ-μ shadowed model have been provided, named correlated κ-μ shadowed fading model since it allows the distinct components arising from each cluster to be arbitrary correlated. Exact closed-form expressions of its first order statistics have been derived, proving that the proposed model is as tractable as Nakagami-m distribution, but much more general.

4.2 Future work

As highlighted through this thesis, the proposed method to analyze random variables renders simple and useful approximations when it is suitably applied. Therefore, its usefulness exceeds the analysis of GQFs. In fact, the derived approximants for the statistics of an arbitrary positive random variable could be potentially applied to a considerable number of applications.

Besides, an important future line of work can be the extension of the method to the analysis of more intricate random variables, such as those arising from the sum or product of several variables. In these cases, obtaining expressions for the resulting distribution usually poses a challenge, and the proposed method may simplify the analysis.

Also, due to the fact that most of the involved variables in communications and signal processing are complex, the derived expressions for the PDF and CDF of complex GQFs can be used to analyze multiple systems, e.g. systems with reception diversity, performance analysis of ML estimators or signal detection. The tractability of the proposed expressions can undoubtedly simplify the characterization of these systems, allowing to obtain closed-form expressions for important metrics such as BER and probabilities of detection and false alarm, to mention but a couple of relevant examples.

In the context of diversity systems, a possible future line of work is the extension of the presented analysis to the case of quadratic forms in Gaussian matrices, which naturally arises when multiple antennas are used both at the transmitter and the receiver [105].

Focusing on channel modeling, the analysis through confluence can be applied to the analysis of more general fading models that take into account the multiplicative shadowing, usually referred to as composite models. The analysis of these distributions is usually more difficult, and a general framework to study such a versatile models can simplify the characterization of the joint impact of shadowing and fading. Some preliminary results can already be found in [114].

Finally, the generalized fading models derived in this thesis could lead to sytems performance analyses which are valid in a wide variety of propagation conditions, instead of requiring particular expressions for each scenario. Therefore, the scientific community seems to be interested in these type of general models and some results in this context have already been provided [115], [116].

Appendix A

Publications

A.1 New approximation to distribution of positive random variables applied to Gaussian quadratic forms

[46] P. Ramírez-Espinosa, D. Morales-Jimenez, J. A. Cortés, J. F. París, and E. Martos-Naya, "New approximation to distribution of positive RVs applied to Gaussian quadratic forms", *IEEE Signal Process. Lett.*, vol. 26, no. 6, pp. 923–927, Jun. 2019.

New Approximation to Distribution of Positive RVs Applied to Gaussian Quadratic Forms

Pablo Ramírez-Espinosa, David Morales-Jimenez, José A. Cortés, José F. Paris, and Eduardo Martos-Naya

***Abstract*—This letter introduces a new approach to the problem of approximating the probability density function (PDF) and the cumulative distribution function (CDF) of a positive random variable. The novel approximation strategy is based on the analysis of a suitably defined sequence of auxiliary variables which converges in distribution to the target variable. By leveraging such convergence, simple approximations for both the CDF and PDF of the target variable are given in terms of the derivatives of its moment generating function (MGF). In contrast to classical approximation methods based on truncated series of moments or cumulants, our approximations always represent a valid distribution and the relative error between variables is independent of the variable under analysis. The derived results are then used to approximate the statistics of positive-definite real Gaussian quadratic forms, comparing our proposed approach with other existing approximations in the literature.**

***Index Terms*—Gaussian quadratic forms, random variables, signal detection, statistical distributions.**

I. Introduction

APPROXIMATING the distribution of a random variable (RV) is a classical problem in applied statistics, central to a vast number of applications in signal processing and communication theory, to mention but a couple of relevant fields. In many cases, closed-form expressions for the moment generating function (MGF) of the RV or its moments are known, but the probability density function (PDF) and cumulative distribution function (CDF) remain intractable or given in complicated integral forms. A natural approach is then to approximate the PDF and CDF of a RV from its cumulants or moments, and significant efforts have been made in this direction: Pearson curves [1], saddle point techniques [2], Gram-Charlier and Edgeworth series [3] or orthogonal polynomial series expansions [4] are some well-known examples of these (classical) approximations. These have been extensively used as they are typically simple and provide accurate representations in many cases. Similar techniques have been recently applied in [5], where approximations for the distribution of the sum of independent RVs are investigated.

However, a major drawback of these classical results is that the resulting expressions are not guaranteed to be proper PDFs (in fact, they typically are not); that is, the approximated PDF does not necessarily integrate to one and the probabilities may be negative [4, p. 731][6, sec. 2]. Another important issue is their accuracy, which typically depends on the parametrization of the target RV, leading in some cases to poor approximations.

We here aim to provide an alternative approximation to the distribution of positive RVs which circumvents the aforementioned limitations (of classical approaches). Instead of directly expanding the PDF (or CDF) of the target variable (which typically results in series involving functions of the moments/cumulants), we focus on a sequence of auxiliary RVs, defined so that the chief probability functions (PDF and CDF) converge to those of the target RV under certain conditions. The proposed approach has a double benefit:

- Since the PDF and CDF of the target variable are approximated by those of an auxiliary variable, the resulting expressions always represent a valid distribution.
- The relative error between the target variable and the auxiliary one can be characterized in simple closed form, and it is independent of the variable under analysis.

The derived expressions are then used to approximate the distribution of positive-definite quadratic forms (QFs) in real Gaussian variables, which has been subject of study for decades due to their numerous applications in statistics, signal processing and communications [7]–[15]. Gaussian QFs appear, for instance, in the detection of signals in Gaussian noise [16, sec. 13.5], the spectral detection of normally distributed stationary processes, χ^2 tests [7, sec. 7] and analysis of variance [11]. Complex Gaussian QFs, which can be regarded as a particular case of the real one [17], are also relevant in many signal processing problems such as the performance analysis of adaptive filter algorithms [18], energy detection [19] or performance analysis of maximum likelihood (ML) estimators [20]. Also, in wireless communications, QFs naturally arise when analyzing differential modulation schemes [21] or diversity techniques [15], [22].

II. Approximating the Distribution of Positive RVs

Consider a positive RV X with continuous distribution, and assume that the MGF of X is infinitely differentiable. In order

Manuscript received February 7, 2019; revised March 25, 2019; accepted April 8, 2019. Date of publication April 19, 2019; date of current version May 6, 2019. This work was supported in part by Universidad de Málaga, in part by the Spanish Government, and in part by the European Fund for Regional Development FEDER (project TEC2014-57901-R). The associate editor coordinating the review of this manuscript and approving it for publication was Dr. Ashish Pandharipande. *(Corresponding author: Pablo Ramirez-Espinosa.)*

P. Ramírez-Espinosa, J. A. Cortés, J. F. Paris, and E. Martos-Naya are with the Departmento de Ingeniería de Comunicaciones, Universidad de Malaga - Campus de Excelencia Internacional Andalucía Tech., Malaga 29071, Spain (e-mail: pre@ic.uma.es; jaca@ic.uma.es; paris@ic.uma.es; eduardo@ic.uma.es).

D. Morales-Jimenez is with the ECIT Institute, Queen's University Belfast, BT3 9D3, U.K. (e-mail: d.morales@qub.ac.uk).

Digital Object Identifier 10.1109/LSP.2019.2912295

to approximate its CDF, we define the auxiliary variable

$$X_m = X/\xi_m \tag{1}$$

where ξ_m is a Gamma-distributed RV, independent of X, with PDF:

$$f_{\xi_m}(u) = \frac{(m-1)^m}{\Gamma(m)} u^{m-1} e^{-(m-1)u}. \tag{2}$$

Since the sequence $\{\xi_m : m \in \mathbb{N}^+\}$ converges to one in distribution, it follows from Slutsky's Theorem [23] that the sequence $\{X_m : m \in \mathbb{N}^+\}$ converges to X in distribution. This is stated in the following lemma, where the CDF of X_m is derived, allowing us to approximate the CDF of X by that of X_m, with sufficiently large m.

Lemma 1: Let X be a positive RV with infinitely differentiable MGF given by $M_X(s)$, and X_m as in (1). Then, the CDF of X satisfies

$$\begin{aligned} F_X(x) &= \lim_{m\to\infty} F_{X_m}(x) \\ &= \lim_{m\to\infty} \sum_{k=0}^{m-1} \frac{(m-1)^k}{x^k k!} \frac{d^k}{ds^k} M_X(s)\Big|_{s=(1-m)/x}. \end{aligned} \tag{3}$$

Proof: The CDF of X_m can be calculated as

$$F_{X_m}(x) = \int_0^\infty F_X(ux) f_{\xi_m}(u) du. \tag{4}$$

Performing the change of variables $y = ux$ and integrating by parts we obtain

$$F_{X_m}(x) = 1 - \int_0^\infty f_X(y) F_{\xi_m}(y/x) dy \tag{5}$$

where $f_X(\cdot)$ is the PDF of X and $F_{\xi_m}(\cdot)$ is the CDF of ξ_m, which for integer m is given by

$$F_{\xi_m}(u) = 1 - \sum_{k=0}^{m-1} \frac{(m-1)^k}{k!} u^k e^{-(m-1)u}. \tag{6}$$

Substituting (6) in (5) and rewriting the integral as the expectation in X lead to

$$F_{X_m}(x) = \sum_{k=0}^{m-1} \frac{(m-1)^k}{k! x^k} \mathbb{E}_X \left[X^k e^{-(m-1)X/x} \right], \tag{7}$$

where the expectation can be seen as that of the k-th order derivative of e^{sX} evaluated at $s = (1-m)/x$. By Leibniz's integral rule, we can interchange the derivative and the expectation, yielding (3). ∎

Generally, convergence in distribution does not imply convergence of the PDFs. However, the implication holds under certain conditions. Specifically, if the densities of X and X_m, namely $f_X(x)$ and $f_{X_m}(x)$, are continuous functions and $f_{X_m}(x)$ is bounded and equicontinuous, then the convergence of the CDFs implies the convergence of the density functions [24]. In our case, $f_{X_m}(x)$ is calculated as

$$f_{X_m}(x) = \int_0^\infty u f_X(ux) f_{\xi_m}(u) du \tag{8}$$

Note that, if $f_X(x)$ is uniformly continuous, it can be easily proved that $f_{X_m}(x)$ satisfies the aforementioned conditions, so that $f_{X_m}(x) \to f_X(x)$ as $m \to \infty$. This allows to approximate the PDF of X by that of X_m, as stated next.

Corollary 1: Let X be a positive RV with infinitely differentiable MGF $M_X(s)$ and uniformly continuous PDF, and X_m as in (1). Then, the PDF of X satisfies

$$\begin{aligned} f_X(x) &= \lim_{m\to\infty} f_{X_m}(x) \\ &= \lim_{m\to\infty} \frac{(m-1)^m}{x^{m+1}\Gamma(m)} \frac{d^m}{ds^m} M_X(s)\Big|_{s=(1-m)/x}. \end{aligned} \tag{9}$$

Proof: Similar to the CDF, $f_{X_m}(x)$ is obtained from (8) by substituting $f_{\xi_m}(u)$ and rewriting the resulting integral as the expectation of the k-th order derivative of the exponential function. ∎

Finally, we formulate the relative error between X_m and X:

Lemma 2: Let X be a positive RV, and X_m as in (1). For $m > 2$, the normalized mean square error (NMSE) admits the following compact expression

$$\overline{\epsilon^2} = \mathbb{E}\left[(X - X_m)^2\right] / \mathbb{E}\left[X^2\right] = (m-2)^{-1}. \tag{10}$$

Proof: The result is straightforwardly obtained from the definition of the NMSE by noticing that, since $\xi_m \sim \Gamma(m, 1/(m-1))$, then $1/\xi_m$ is inverse Gamma distributed with $\mathbb{E}[1/\xi_m] = 1$ and $\mathbb{E}\left[(1 - 1/\xi_m)^2\right] = 1/(m-2)$. ∎

Lemma 1 and Corollary 1 provide a general result to approximate the distribution of a positive RV in terms of the derivatives of its MGF. The main benefits of this approach are: (i) we approximate the distribution of a RV X by that of another RV X_m, so that the approximation (for any m) is always a valid distribution, and (ii) the NMSE between X and X_m is under control, and easily characterized. Note however that, although informative on the closeness between X_m and X, the NMSE does not directly translate into the error between the approximated CDF and the true one.

As with classical series expansions, where the moments are required, the calculation of (3) and (9) may be challenging if the derivatives of $M_X(s)$ are difficult to compute or not expressible in closed form. Moreover, the convergence of the proposed series may be slow and a relatively large m may be needed, implying the computation of high-order derivatives of $M_X(s)$, which may be tedious in some cases.

However, there are cases where these derivatives can be readily obtained. That is, for instance, the case of Gaussian QFs, where the moments—equivalently, the derivatives of the MGF—can be easily computed recursively. The approach would further appeal to other cases, e.g., those where the MGF is given as a product of elementary functions [7, eq. (3.2b.3)].

III. Distribution of Real Quadratic Forms

We aim to characterize the random variable

$$Q = (\mathbf{x} + \boldsymbol{\mu})^T \mathbf{A} (\mathbf{x} + \boldsymbol{\mu}) \tag{11}$$

where $\boldsymbol{\mu} \in \mathbb{R}^{n\times 1}$ is a constant vector, $\mathbf{A} \in \mathbb{R}^{n\times n}$ is a symmetric and positive definite matrix and $\mathbf{x} \in \mathbb{R}^{n\times 1}$ is a random vector following a multivariate normal distribution with zero mean and covariance matrix $\boldsymbol{\Sigma}$, i.e. $\mathbf{x} \sim \mathcal{N}_n(\mathbf{0}, \boldsymbol{\Sigma})$.

In this case, the MGF of Q is given by [7, eq. (3.2a.5)]

$$M_Q(s) = \prod_{j=1}^{n} \exp\left(\frac{b_j^2 \lambda_j s}{1 - 2\lambda_j s}\right) (1 - 2\lambda_j s)^{-1/2} \tag{12}$$

where $\lambda_j, j = 1, \ldots, n$, are the eigenvalues of $\mathbf{C} = \boldsymbol{\Sigma}^{1/2}\mathbf{A}\boldsymbol{\Sigma}^{1/2}$ and b_j are the entries of $\mathbf{b} = \mathbf{U}^T\boldsymbol{\Sigma}^{-1/2}\boldsymbol{\mu}$ with $\mathbf{U}$ the unitary matrix resulting from the diagonalization of $\mathbf{C}$.

A. Literature Review

Closed form expressions for the PDF and CDF of real QFs can only be obtained in certain simple cases (e.g., $\mathbf{A} = \boldsymbol{\Sigma} = \mathbf{I}$, the identity matrix), remaining in complicated integral form for the general case, even when the involved Gaussian variables have zero mean. The ubiquitous relevance of Gaussian QFs has motivated a rich body of work over the last few decades, aiming at approximating the chief probability functions of Q. Approximations for both the PDF and CDF are given in terms of infinite series of powers (Maclaurin series) [7]–[9], Laguerre polynomials [7], [8], [10], central χ^2 distributions [7], [8], [11], non-central χ^2 densities [8], [13] and Hermite polynomials [14].

However, these approximations suffer from several drawbacks. The series in [10], [11] are restricted to the central case, and the series coefficients in [9] involve complicated sums, being inefficient for numerical computation. The same happens with the result in [14], where the number of terms to be computed depends on a combinatorial, increasing with the order of the QF. Numerical issues are also relevant in the case of non-central χ^2 expansions [8], [13], where several Marcum-Q functions need to be computed. The approximations based on Maclaurin series and the Laguerre polynomials and central χ^2 expansions in [7], [8] render more useful results, but they fail under a wide range of conditions as we will see later.

Another approximation to the CDF of real QFs was recently given in [15], where the saddle-point technique was applied. Unfortunately, the non-central case was not analyzed.

B. Approximated PDF and CDF

By applying Lemma 1 and Corollary 1 we can approximate the PDF and CDF of Q by a linear combination of derivatives of the MGF of Q, which in this case can be written in closed form in an efficient recursive way [7, pp. 51–53]. The k-th order derivative of $M_Q(s)$ admits

$$\frac{d^k}{ds^k}M_Q(s) = M_Q(s)D_k(s) \tag{13}$$

where $D_0(s) = 1$ and, for $k \geq 1$,

$$D_k(s) = \sum_{j=0}^{k-1}\binom{k-1}{j}g_{k-1-j}(s)D_j(s), \tag{14}$$

$$g_i(s) = 2^i\, i!\sum_{t=1}^{n}\frac{\lambda_t^{i+1}\left[(i+1)b_t^2 + 1 - 2\lambda_t s\right]}{(1-2\lambda_t s)^{i+2}}. \tag{15}$$

Using (13) in (9) and (3) we immediately have the approximated expressions for the PDF and CDF of Q, respectively:

$$f_Q(x) \approx \frac{(m-1)^m}{x^{m+1}\Gamma(m)}M_Q\left(\frac{1-m}{x}\right)D_m\left(\frac{1-m}{x}\right), \tag{16}$$

$$F_Q(x) \approx M_Q\left(\frac{1-m}{x}\right)\sum_{k=0}^{m-1}\frac{(m-1)^k}{x^k k!}D_k\left(\frac{1-m}{x}\right). \tag{17}$$

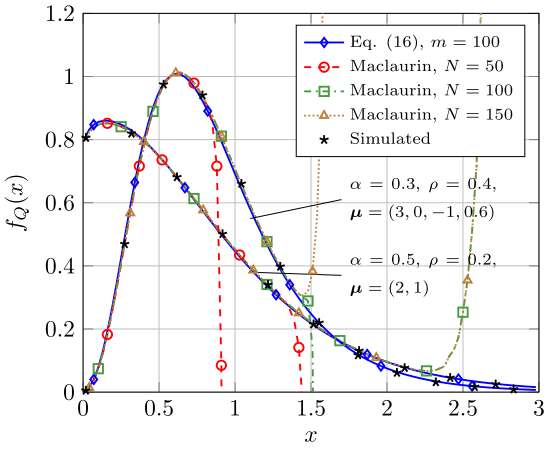

Fig. 1. PDF of Q for different values of α, ρ and $\boldsymbol{\mu}$. The proposed method is compared with the Maclaurin expansion in [7], [8] and with MC simulations.

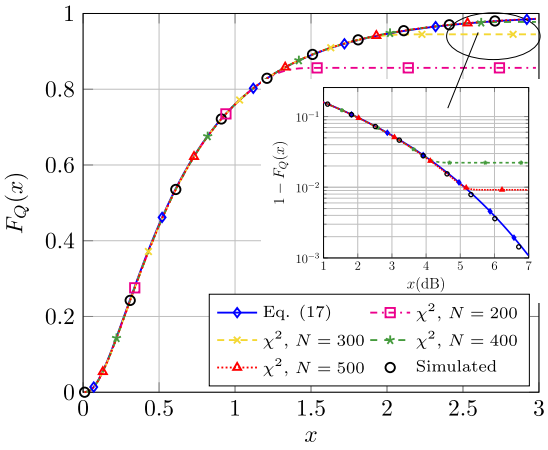

Fig. 2. CDF of Q for $\alpha = 0.7$, $\rho = 0.5$, $\boldsymbol{\mu} = (2, 1, -1, 0.6, -0.9)$. Our proposed method with $m = 100$ is compared with the χ^2 expansion in [7] and with MC simulations.

The recursion in the calculation of $D_k(\cdot)$ and the fact that the derivatives of $M_Q(s)$ are positive—consequently, also $D_k(\cdot)$—allow for an efficient and numerically stable computation of (16) and (17), with independence of the QF parameters. This is in stark contrast to previous (existing) methods, as will be illustrated in the next section.

IV. Numerical Results and Discussion

We now compare the proposed approximation for real QFs in (16) and (17) with the results in terms of Maclaurin series, Laguerre polynomials series and χ^2 densities expansion in [7], [8]. The other classical approaches and the approximation given in [15] are disregarded due to the drawbacks listed in Section III-A. All the calculations haven been done using MATHEMATICA software and validated through Monte Carlo (MC) simulations.

For the sake of simplicity, we consider $(\mathbf{A})_{i,j} = \alpha^{|i-j|}$ and $(\boldsymbol{\Sigma})_{i,j} = \rho^{|i-j|}$, with $0 < \alpha, \rho < 1$, and compare our proposed approximation with previous methods in Figs. 1–4. We use different values of n, α, ρ and $\boldsymbol{\mu}$ in the distinct representations in

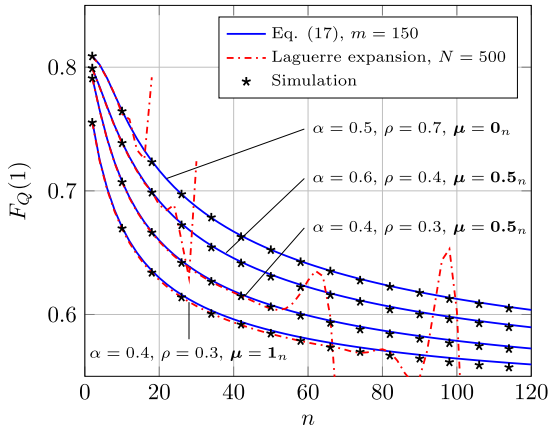

Fig. 3. CDF of Q at $x = 1$ for distinct QF order, n. Our proposed method is compared with the Laplace approximation with $\beta_L = 10$ in [7], [8] and with MC simulations.

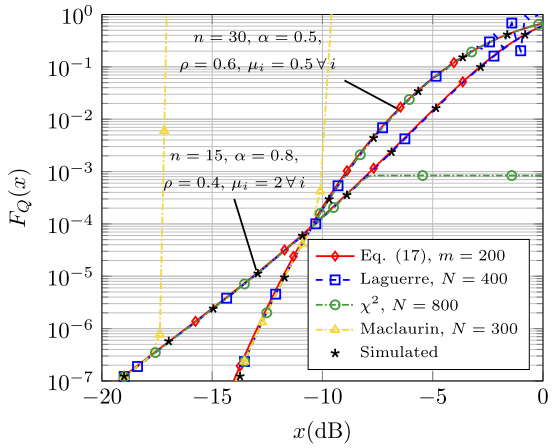

Fig. 4. CDF of Q for different values of n, α, ρ, μ_i. The proposed method is compared with the Maclaurin series, the Laguerre expansion and the χ^2 expansion in [7], [8] and contrasted with MC simulations. $\beta_L = 9$ for $n = 15$ and $\beta_L = 12$ for $n = 30$.

order to show the generality and robustness (in the parameters range) of our proposed approximation.

Fig. 1 focuses on the comparison between our approximation and the Maclaurin series by plotting the approximated PDF of Q. It can be observed that the Maclaurin series renders a valid approximation only up to a certain point in x, remarkably failing thereafter; the value of x from which the series diverges depends on the parameters of the QF. As illustrated, increasing the number of terms in the series from 100 to 150 does not seem to solve the problem. In contrast, our proposed solution shows an excellent agreement with simulations for all parameter choices and all x.

Fig. 2 compares our results with the χ^2 densities expansion by plotting the CDF of Q (similar trends are observed for the PDF). The χ^2 approximation artificially introduces an additional parameter $\beta_\chi < \min_j\{\lambda_j\}$ that controls the series convergence [8]. It has been observed that a high value of β_χ in that range facilitates the convergence, so we fixed $\beta_\chi = 0.9 \min_j\{\lambda_j\}$. We observe that the number of terms required for the χ^2 expansion is much larger than in our method (m) to accurately approximate the distribution of Q. Furthermore, it is important to note that the χ^2 expansion does not yield a valid CDF, as observed in the right-hand tail.

A comparison between (17) and the Laguerre series expansion is shown in Fig. 3. This approximation also introduces a parameter $\beta_L > \max_j\{\lambda_j\}$ that controls the convergence of the series. However, we noticed that the recommended value of β_L in [8] renders considerable numerical errors that prevent the series convergence. Hence, finding the value of β_L that yields the best approximation in each case is a difficult task. For the calculation in Fig. 3, a value of $\beta_L = 10$ has been chosen, which seems to minimize such numerical issues. As shown in Fig. 3 the series diverges when the order of Q increases, with independence of the QF parameters. Note that the considered values of n are not particularly extreme, but rather moderate, particularly in applications such as signal detection where large numbers of samples are typically employed.

The last comparison is shown in Fig. 4, where the CDF of Q is plotted in logarithmic scale in order to analyze the accuracy of the distinct approaches to approximate the left tail of the distribution. As observed, the aforementioned drawbacks of the alternative methods are also relevant when focusing on the left tail of the distribution. In turn, our proposed technique renders again an excellent approximation with independence of the parameters of Q.

The goodness of the approximations in the previous cases has been quantified using the Kolmogorov-Smirnov (K-S) test, showing that the proposed method provides the same (or even better) accuracy than the alternative ones by computing much less terms (m) with independence of the QF parameters. For instance, for data in Fig. 2, our technique achieves a K-S test result of $D = 0.036$ for $m = 100$ while the χ^2 expansion needs $N = 500$ to get $D = 0.035$.

Moreover, the complexity in terms of the computation time has also been investigated, observing that, for a given accuracy, the proposed approximation is faster than the alternative ones (since it needs much less computed terms).

V. Conclusion

This letter addresses the problem of approximating the distribution of positive RVs whose closed-form expression of the MGF is known. A new approach based on a sequence of auxiliary variables that converges in distribution to the target one is proposed, rendering approximations for the PDF and the CDF in terms of the derivatives of the MGF of the RV under analysis. Compared to previous techniques found in the literature, the proposed method offers a twofold benefit: (i) the resulting expressions for the chief probability functions always represent a valid distribution, and (ii) the NMSE between the target variable and the auxiliary one admits a simple formulation which is independent of the considered RV.

The presented approach is then applied to the study of positive-definite real Gaussian quadratic forms, for which we provide novel approximations for the PDF and CDF that can be easily computed and that outperform previous ones given in the literature in a wide range of conditions. The derived expressions provide an accurate approximation using a moderate number of terms even when other approaches fail (e.g., yielding CDF values larger than one).

REFERENCES

[1] H. Solomon and M. A. Stephens, "Approximations to density functions using Pearson curves," *J. Am. Stat. Assoc.*, vol. 73, no. 361, pp. 153–160, 1978.

[2] C. Goutis and G. Casella, "Explaining the saddlepoint approximation," *Am. Stat.*, vol. 53, no. 3, pp. 216–224, 1999.

[3] J. Kolassa, *Series Approximation Methods in Statistics*, ser. Lecture Notes in Statist. New York, NY, USA: Springer-Verlag, 1994.

[4] S. B. Provost, "Moment-based density approximants," *Math. J.*, vol. 9, no. 4, pp. 727–756, 2005.

[5] J. A. Maya, L. R. Vega, and C. G. Galarza, "A closed-form approximation for the CDF of the sum of independent random variables," *IEEE Signal Process. Lett.*, vol. 24, no. 1, pp. 121–125, Jan. 2017.

[6] C. Field and E. Ronchetti, "Small sample asymptotics," *Lect. Notes Monogr. Ser.*, vol. 13, pp. 1–140, 1990.

[7] S. Provost and A. Mathai, *Quadratic Forms in Random Variables: Theory and Applications*, ser. Statistics: Textbooks and monographs. New York, NY, USA: Marcel Dekker, 1992.

[8] S. Kotz, N. L. Johnson, and D. W. Boyd, "Series representations of distributions of quadratic forms in normal variables II. Non-Central case," *Ann. Math. Statist.*, vol. 38, no. 3, pp. 838–848, Jun. 1967.

[9] B. Shah, "Distribution of definite and of indefinite quadratic forms from a non-central normal distribution," *Ann. Math. Statist.*, vol. 34, no. 1, pp. 186–190, 1963.

[10] J. Gurland *et al.*, "Distribution of definite and of indefinite quadratic forms," *Ann. Math. Statist.*, vol. 26, no. 1, pp. 122–127, 1955.

[11] G. E. P. Box, "Some theorems on quadratic forms applied in the study of analysis of variance problems, I. effect of inequality of variance in the one-way classification," *Ann. Math. Statist.*, vol. 25, no. 2, pp. 290–302, 1954.

[12] G. A. Ropokis, A. A. Rontogiannis, and P. T. Mathiopoulos, "Quadratic forms in normal RVs: Theory and applications to OSTBC over Hoyt fading channels," *IEEE Trans. Wireless Commun.*, vol. 7, no. 12, pp. 5009–5019, Dec. 2008.

[13] G. Tziritas, "On the distribution of positive-definite Gaussian quadratic forms," *IEEE Trans. Inf. Theory*, vol. 33, no. 6, pp. 895–906, Nov. 1987.

[14] F. J. Reifler, M. S. Rogers, and K. Malakian, "Distribution of general noncentral positive definite quadratic form in K-dimensions," *IEEE Trans. Aerosp. Electron. Syst.*, vol. 25, no. 3, pp. 411–414, May 1989.

[15] T. Y. Al-Naffouri, M. Moinuddin, N. Ajeeb, B. Hassibi, and A. L. Moustakas, "On the distribution of indefinite quadratic forms in Gaussian random variables," *IEEE Trans. Commun.*, vol. 64, no. 1, pp. 153–165, Jan. 2016.

[16] V. K. Madisetti, *The Digital Signal Processing Handbook*, 2nd ed. Boca Raton, FL, USA: CRC Press, 2009.

[17] D. Raphaeli, "Distribution of noncentral indefinite quadratic forms in complex normal variables," *IEEE Trans. Inf. Theory*, vol. 42, no. 3, pp. 1002–1007, May 1996.

[18] T. Y. Al-Naffouri and M. Moinuddin, "Exact performance analysis of the ϵ-NLMS algorithm for colored circular Gaussian inputs," *IEEE Trans. Signal Process.*, vol. 58, no. 10, pp. 5080–5090, Oct. 2010.

[19] E. H. Gismalla and E. Alsusa, "Performance analysis of the periodogram-based energy detector in fading channels," *IEEE Trans. Signal Process.*, vol. 59, no. 8, pp. 3712–3721, Aug. 2011.

[20] F. Athley, "Threshold region performance of maximum likelihood direction of arrival estimators," *IEEE Trans. Signal Process.*, vol. 53, no. 4, pp. 1359–1373, Apr. 2005.

[21] Q. Zhao and H. Li, "Differential modulation for cooperative wireless systems," *IEEE Trans. Signal Process.*, vol. 55, no. 5, pp. 2273–2283, May 2007.

[22] S. Jin, M. R. McKay, X. Gao, and I. B. Collings, "Asymptotic SER and outage probability of MIMO MRC in correlated fading," *IEEE Signal Process. Lett.*, vol. 14, no. 1, pp. 9–12, Jan. 2007.

[23] A. Goldberger, *Econometric Theory*. Hoboken, NJ, USA: Wiley, 1964.

[24] D. D. Boos, "A converse to Scheffe's theorem," *Ann. Statist.*, vol. 13, no. 1, pp. 423–427, 1985.

A.2 A new approach to the statistical analysis of non-central complex Gaussian quadratic forms with applications

[47] P. Ramírez-Espinosa, L. Moreno-Pozas, J. F. París, J. A. Cortés, and E. Martos-Naya, "A new approach to the statistical analysis of non-central complex Gaussian quadratic forms with applications", *IEEE Trans. Veh. Technol.*, vol. 68, no. 7, pp. 6734–6746, Jul. 2019.

A New Approach to the Statistical Analysis of Non-Central Complex Gaussian Quadratic Forms With Applications

Pablo Ramírez-Espinosa, Laureano Moreno-Pozas, José F. Paris, José A. Cortés, and Eduardo Martos-Naya

***Abstract*—This paper proposes a novel approach to the statistical characterization of non-central complex Gaussian quadratic forms (CGQFs). Its key strategy is the generation of an auxiliary random variable that replaces the original CGQF and converges in distribution to it. This technique is valid for both definite and indefinite CGQFs and yields simple expressions of the probability density function (PDF) and the cumulative distribution function (CDF) that only involve elementary functions. This overcomes a major limitation of previous approaches, where the complexity of the resulting PDF and CDF does not allow for further analytical derivations. Additionally, the mean square error between the original CGQF and the auxiliary one is provided in a simple closed-form formulation. These new results are then leveraged to analyze the outage probability and the average bit error rate of maximal ratio combining systems over correlated Rician channels.**

***Index Terms*—Quadratic forms, Gaussian random vectors, correlation, Rician channels, diversity techniques.**

I. Introduction

COMPLEX Gaussian quadratic forms (CGQFs) play an essential role when analyzing several wireless techniques, including maximal ratio combining (MRC) [1], optimum combining [2], beamforming [3], multibeam strategies [4], orthogonal space time block coding [5], relays [6], non-coherent modulations [7], differential detections [8] and matched-field processing [9].

The analysis of CGQFs has been usually restricted to central CGQFs, i.e. quadratic forms built from zero mean complex Gaussian vectors, which can be given in a very tractable form [10], [11]. However, the analysis of non-central CGQFs remains as an open problem in the literature. Hence, despite its interest in common problems like the study of digital communications over Rician channels, no closed-form expressions are known for chief probability functions like the probability density function (PDF) and the cumulative density function (CDF), for which only approximated solutions have been given.

The statistical analysis of non-central CGQFs can be traced back to the work by Turin [12]. Although their characteristic function was given in closed-form, Turin highlighted the challenge of obtaining the PDF of CGQFs built from non-zero mean Gaussian vectors. Since then, some works made initial progress to pave the way for the complete statistical characterization of non-central CGQFs. To the best of the authors' knowledge, most of the approaches available in the literature are based on the direct inversion of the moment generating function (MGF), or equivalently, the characteristic function, to obtain an approximation of the PDF of CGQFs [13]–[15]. Some works apply different series expansions to the characteristic function to allow such inversion [13], [14], while the work by Biyari and Lindsey considers a specific non-central CGQF and inverts its MGF by solving some convolution integrals [15]. All these works present approximations for the PDF of non-central CGQFs in terms of infinite sums of special functions. In particular, the PDF of positive-definite and indefinite non-central CGQFs is given in terms of a double infinite sum of modified Bessel functions in [13] and [14], and of a double infinite sum of Laguerre polynomials in [15].

Taking into account the limitations of direct inversion methods, since the solutions provided for the PDF and the CDF of non-central CGQFs are difficult to compute and not suitable for any further insightful analysis, very recently, Al-Naffouri *et al.* presented a different approach. They applied a transformation to the inequality that defines the CDF of non-central CGQFs, yielding a problem in which the well-known saddle-point technique allows expressing the CDF as the solution of a differential equation [10].

This paper proposes a completely different approach to the statistical analysis of indefinite non-central CGQFs, which leads to simple expressions that approximate both the PDF and CDF of CGQFs. It is based on appropriately perturbing the non-zero mean components of the Gaussian vectors that build the quadratic form. This yields an auxiliary CGQF, denoted as confluent CGQF, which converges in distribution to the original quadratic form and whose analysis is surprisingly simpler. Specifically, this novel approach offers the following advantages over the recently proposed work in [10] and the other approaches given in the literature [13]–[15]:

Manuscript received September 18, 2018; revised March 15, 2019; accepted May 7, 2019. Date of publication May 15, 2019; date of current version July 16, 2019. This work was supported in part by the Spanish Government and in part by the European Fund for Regional Development FEDER under Project TEC2014-57901-R. The review of this paper was coordinated by Dr. X. Dong. *(Corresponding author: Pablo Ramírez-Espinosa.)*

P. Ramírez-Espinosa, J. F. Paris, J. A. Cortés, and E. Martos-Naya are with the Departmento de Ingeniería de Comunicaciones, Universidad de Malaga - Campus de Excelencia Internacional Andalucía Tech., Malaga 29071, Spain (e-mail: pre@ic.uma.es; paris@ic.uma.es; jaca@ic.uma.es; eduardo@ic.uma.es).

L. Moreno-Pozas is with the Department of Electronic and Computer Engineering, School of Electrical and Computer Engineering, Hong Kong University of Science and Technology, Kowloon, Hong Kong (e-mail: eelaureano@ust.hk).

Digital Object Identifier 10.1109/TVT.2019.2916725

- The probability functions, namely PDF and CDF, are given as a linear combination of elementary functions (exponentials and powers) in a very tractable form, which are useful for further calculations (e.g. expectations over the CGQF).
- Simple closed-form expression for the mean squared error (MSE) between the CGQF and the auxiliary one is provided, allowing the particularization of the auxiliary variable in order to make this error drop below a certain threshold.
- Since the statistics of an auxiliary random variable are used to characterize CGQFs, the approximated solution is always a statistical distribution. This is not the case of the infinite series expressions of the literature, which are no longer strict PDFs when truncated (no-unit area).

Finally, with the aim of exemplifying the tractability of the derived expressions, they are used to further study the performance of MRC systems over non-identically distributed Rician fading channels with arbitrary correlation. Hence, simple expressions for the outage probability and the bit error rate (BER) are provided for different modulation schemes.

The remainder of this paper is structured as follows. The notation and some preliminary results are introduced in Section II. Section III presents the general approach, as well as the statistical characterization of indefinite non-central CGQFs with a very simple and precise approximation which admits a closed-form expression for its associated MSE. In Section IV, an efficient recursive algorithm to compute the derived expressions is introduced. Section V contains a comparison between the proposed approach and some of the aforementioned approximations given in the literature. In Section VI, the new statistical characterization of non-central CGQFs is applied to the performance analysis of MRC systems over correlated Rician channels. Finally, conclusions are drawn in Section VII.

II. Notation and Background

Throughout this paper, the following notation will be used. Vectors and matrices are denoted in bold lowercase and bold uppercase, respectively. $\mathbb{E}[\cdot]$ is the expectation operator, while $\mathcal{L}\{\cdot\}$ and $\mathcal{L}^{-1}\{\cdot\}$ denote the Laplace transform and the inverse Laplace transform operators, respectively. The symbol $\sim$ signifies *statistically distributed as* and $\mathrm{Re}\{\cdot\}$ denotes the real part. The superscript $(\cdot)^\dagger$ indicates matrix complex conjugate transpose and $\mathrm{tr}(\cdot)$ is the matrix trace. The matrices $\mathbf{I}_p$ and $\mathbf{0}_{p\times q}$ denote a $p \times p$ identity and a $p \times q$ all-zero matrix, respectively. When $\mathrm{diag}(\cdot)$ is applied to a matrix, it returns a vector whose entries are the diagonal elements of that matrix. Additionally, $\mathrm{u}(\cdot)$ is the unit step function whose value is 1 if the argument is non-negative and 0 otherwise. $\mathrm{sgn}(\cdot)$ is the sign function whose value is 1 for non-negative arguments and -1 otherwise. Some relevant definitions and preliminary results, which will be used when presenting the main contributions, are now introduced.

A. Basic Distributions

Definition 1 (Gamma distribution): Let X be a real random variable, which follows a Gamma distribution with shape parameter m and scale parameter θ, i.e. $X \sim \Gamma(m, \theta)$. Then, the PDF of X is given by [16, eq. (17.23)]

$$f_X(x) = \frac{1}{\Gamma(m)\theta^m} x^{m-1} e^{-x/\theta} \tag{1}$$

where $\Gamma(\cdot)$ is the gamma function and $m, \theta \in \mathbb{R}^+$.

Definition 2. (Non-central χ^2 distribution with n degrees of freedom):

Consider

$$Y = \sum_{i=1}^{n} X_i^2 \tag{2}$$

where X_i, $i = 1, \ldots, n$, are statistically independent real Gaussian random variables with unit variance and means μ_i, i.e. $X_i \sim \mathcal{N}(\mu_i, 1)$. Then, Y follows a non-central χ^2 distribution with n degrees of freedom and noncentrality parameter $\delta = \sum_{i=1}^{n} \mu_i^2$, i.e. $Y \sim \chi_n^2(\delta)$. The MGF of Y is therefore given by [11, eq. (5.1.23)]

$$M_Y(s) = \frac{1}{(1-2s)^{n/2}} \exp\left(\frac{\delta s}{1-2s}\right) \tag{3}$$

for all $s \in \mathbb{C}$ such that $\mathrm{Re}\{s\} < 1/2$.

B. Complex Gaussian Quadratic Forms

Definition 3 (CGQF): Let $\mathbf{v} \in \mathbb{C}^{n\times 1}$ be a random vector that follows a n-variate Gaussian distribution with mean vector $\overline{\mathbf{v}} \in \mathbb{C}^{n\times 1}$ and non-singular Hermitian covariance matrix $\mathbf{L} \in \mathbb{C}^{n\times n}$, i.e. $\mathbf{v} \sim \mathcal{CN}_n(\overline{\mathbf{v}}, \mathbf{L})$, and let $\mathbf{A} \in \mathbb{C}^{n\times n}$ be a non-singular indefinite Hermitian matrix, i.e. $\mathbf{A}$ can have positive and negative real eigenvalues. Then, the real random variable

$$Q = \mathbf{v}^\dagger \mathbf{A} \mathbf{v} \tag{4}$$

is an indefinite non-central CGQF [12, eq. (3)].

Note that assuming $\mathbf{L}$ is non-singular does not implies any loss of generality. If $\mathrm{rank}(\mathbf{L}) < n$, then some components of $\mathbf{v}$ are linearly related [17, chap. 1] and, consequently, Q can be rewritten in terms of another vector with full-rank covariance matrix. That is equivalent to assuming $\mathbf{L}$ is positive definite.

The expression in (4) has been classically employed in the context of CGQF analysis [12], [14], [18]. However, in this work, an alternative form will be used, which is equivalent to (4) and can be deduced from it by performing some algebraic transformations. This alternative form is formally equivalent to the one in [13, eq. (2)], but it will be derived using a different approach that facilitates the understanding of the subsequent analysis proposed in this paper.

Since the covariance matrix $\mathbf{L}$ is a positive definite Hermitian matrix, a Cholesky factorization is performed such that $\mathbf{L} = \mathbf{C}\mathbf{C}^\dagger$, where $\mathbf{C} \in \mathbb{C}^{n\times n}$ is an invertible lower triangular matrix with non-negative diagonal entries [19]. Then, the vector $\mathbf{v}$ can be expressed as

$$\mathbf{v} = \mathbf{C}\mathbf{z} + \overline{\mathbf{v}} \tag{5}$$

where $\mathbf{z} \sim \mathcal{CN}_n(\mathbf{0}_{n\times 1}, \mathbf{I}_n)$. Substituting (5) in (4) and after some algebraic manipulations, one has

$$Q = \left(\mathbf{z} + \mathbf{C}^{-1}\overline{\mathbf{v}}\right)^\dagger \mathbf{C}^\dagger \mathbf{A} \mathbf{C} \left(\mathbf{z} + \mathbf{C}^{-1}\overline{\mathbf{v}}\right). \tag{6}$$

$\mathbf{C}^\dagger\mathbf{AC}$ is Hermitian, so it can be diagonalized as

$$\mathbf{C}^\dagger\mathbf{AC} = \mathbf{U}\mathbf{\Lambda}\mathbf{U}^\dagger \tag{7}$$

where $\mathbf{U}$ is an unitary matrix and $\mathbf{\Lambda}$ is a diagonal matrix whose entries, λ_i for $i = 1, \ldots, n$, are the eigenvalues of $\mathbf{C}^\dagger\mathbf{AC}$ (or, equivalently, those of $\mathbf{LA}$) [20, chap. 2]. Thus, relabeling $\mathbf{y} = \mathbf{U}^\dagger\mathbf{z}$ and $\overline{\mathbf{h}} = \mathbf{U}^\dagger\mathbf{C}^{-1}\overline{\mathbf{v}}$, one gets

$$Q = \left(\mathbf{y} + \overline{\mathbf{h}}\right)^\dagger \mathbf{\Lambda} \left(\mathbf{y} + \overline{\mathbf{h}}\right). \tag{8}$$

Since $\mathbf{U}$ is unitary, the distribution of $\mathbf{y}$ is the same as that of $\mathbf{z}$, i.e. $\mathbf{y} \sim \mathcal{CN}_n\left(\mathbf{0}_{n\times 1}, \mathbf{I}_n\right)$. Consequently, the quadratic form Q is now expressed in terms of a random vector $\mathbf{y}$ whose elements are independent and the diagonal matrix $\mathbf{\Lambda}$ with the eigenvalues of $\mathbf{LA}$. Depending on whether Q is definite or indefinite, all the eigenvalues have the same sign or not. For positive definite and negative definite CGQFs, $\lambda_i > 0$ and $\lambda_i < 0$ for $i = 1, \ldots, n$, respectively. In turn, when Q is indefinite, the eigenvalues can be either positive or negative. In order to obtain the MGF of Q, (8) is expanded as

$$Q = \sum_{i=1}^{n} \lambda_i \left(y_i + \overline{h}_i\right)^\dagger \left(y_i + \overline{h}_i\right) \tag{9}$$

where y_i and $\overline{h}_i$ for $i = 1, \ldots, n$ represent the entries of $\mathbf{y}$ and $\overline{\mathbf{h}}$, respectively. Additionally, defining $Y_i = 2\left(y_i + \overline{h}_i\right)^\dagger \left(y_i + \overline{h}_i\right)$, the statistical independence of the elements of $\mathbf{y}$ allows expressing Q as

$$Q = \sum_{i=1}^{n} \frac{\lambda_i}{2} Y_i \tag{10}$$

with $Y_i \sim \chi^2_2(2|\overline{h}_i|^2)$. Thus, Q can be expressed in terms of a linear combination of independent non-central χ^2 variables. Hence, its MGF can be straightforwardly obtained as the product of the MGFs of the scaled version of Y_i, which can be deduced from (3), getting the result given in [13, eq. (7)]

$$M_Q(s) = \prod_{i=1}^{n} \frac{\exp\left(\frac{\lambda_i \mu_i s}{1-\lambda_i s}\right)}{1-\lambda_i s} \tag{11}$$

for every $s \in \mathbb{C}$ such that $\lambda_i \mathrm{Re}\{s\} < 1 \; \forall \, i$ where $\mu_i = |\overline{h}_i|^2 = [\mathbf{U}^\dagger\mathbf{C}^{-1}\overline{\mathbf{v}}\overline{\mathbf{v}}^\dagger \left(\mathbf{C}^{-1}\right)^\dagger \mathbf{U}]_{i,i}$. Note that the distinct sign with respect to [13, eq. (7)] is due to a slightly different definition of the MGF, which in (11) is calculated as $M_Q(s) = \mathbb{E}[e^{sQ}]$.

Closed-form expressions for some statistics of Q, e.g., the PDF and CDF, are not known due to the exponential term in (11), which considerably complicates performing an inverse Laplace transformation. This issue is a direct consequence of considering a non-central Gaussian vector $\mathbf{v}$. Actually, this does not occur when $\mathbf{v}$ has zero mean, since the exponential term in (11) vanishes, allowing a straightforward inversion to obtain the distribution of Q. Although the idea behind most previous contributions consists in expanding such exponential function to perform the inverse Laplace transform, the approach here presented will circumvent the need of manipulating this function, which usually leads to complicated statistical expressions that are not suitable for subsequent analyses [13]–[15]. It is based on randomly perturbing the deterministic elements that originate the non-centrality of the quadratic form, such that the exponential term in (11) disappears, thus facilitating the derivation of the distribution of Q. This approach will be referred to as principle of confluence in the next section.

III. Confluent Non-Central Complex Gaussian Quadratic Form

The here proposed approach exploits the fact that the analysis of some statistical problems is notably simplified by introducing a random fluctuation into them. A major innovation of this paper is the determination of an adequate fluctuation to achieve this end in the context of non-central CGQFs. To this aim, an auxiliary CGQF is obtained by perturbing vector $\overline{\mathbf{h}}$ in (8) with a random variable that depends on a shape parameter. When the latter tends to infinity, the auxiliary CGQF converges to the original one. This section firstly formalizes this property, referred to as principle of confluence, and then shows that the statistical analysis of the original CGQF can be derived from that of the auxiliary one.

A. The Principle of Confluence

In the following, the definition of confluent random variable is given, as well as some relevant lemmas that build a general framework that will be used to analyze non-central CGQFs.

Definition 4. (Confluent random variable): Let X_m be a real random variable with a real and positive shape parameter m. Then, the random variable X_m is *confluent* in m to another random variable X if

$$\lim_{m\to\infty} M_{X_m}(s) = M_X(s) \tag{12}$$

for $s = it$ with $i = \sqrt{-1}$ and $t \in \mathbb{R}$, and it is denoted as $X_m \rightsquigarrow X$. Also, X is named the *limit* variable.

Definition 5. (Weak convergence): Let $\{X_n\}$ be a sequence of real random variables. Then, $\{X_n\}$ is said to converge weakly, or converge in distribution, to another random variable X if

$$\lim_{n\to\infty} F_{X_n}(x) = F_X(x) \tag{13}$$

at every continuity point [21], where $F_X(x)$ is the CDF of X.

With the above definitions, the following lemmas are now presented.

Lemma 1: Let X_m and X be two random variables such that $X_m \rightsquigarrow X$. Then, X_m converges weakly to X in m.

Proof: The lemma is a consequence of Lévy's continuity theorem (or Lévy's convergence theorem) [22, chap. 18]. The confluence in m between the random variables X_m and X implies that the MGF of X_m converges pointwise to $M_X(s)$ in the imaginary axis. This is equivalent to the convergence of the characteristic functions, fulfilling Lévy's theorem and ensuring the weak convergence of X_m to X. ■

Lemma 2: Let X_m and X be two random variables such that $X_m \rightsquigarrow X$ in m. If $g : \mathbb{R} \to \mathbb{R}$ is a continuous and bounded function, then

$$\lim_{m\to\infty} \mathbb{E}\left[g(X_m)\right] = \mathbb{E}\left[g(X)\right]. \tag{14}$$

Proof: As $X_m \rightsquigarrow X$, Lemma 1 ensures the weak convergence between X_m and X. According to Helly-Bray theorem, this weak convergence is equivalent to the convergence in expectations if and only if g is a continuous and bounded function [23]. ■

Definition 4 along with Lemma 1 and Lemma 2 constitute the principle of confluence. It allows circumventing the need of manipulating the statistics of X, working with those of X_m instead.

As such, the principle of confluence is a novel approach to characterize complicated random variables, by means of auxiliary variables which are more tractable to analyze.

B. The Principle of Confluence for CGQFs

The principle of confluence is here used to analyze non-central CGQFs. In order to do so, it is necessary to firstly define the auxiliary random variable, which will be referred to as confluent CGQF.

Proposition 1: Let $\xi_{m,i}$ for $i = 1, \ldots, n$ be a set of independent and non-negative random variables such that $\xi^2_{m,i} \sim \Gamma(m, 1/m)\ \forall\ i$. Then, $\xi^2_{m,i} \rightsquigarrow 1$ and $\xi_{m,i} \rightsquigarrow 1$ in $m\ \forall\ i$.

Proof: The confluence of $\xi^2_{m,i}$ is straightforwardly proved since $\lim_{m\to\infty} M_{\xi^2_{m,i}}(s) = e^s$. The confluence of $\xi_{m,i}$ can be proved from the relationship between its CDF and that of $\xi^2_{m,i}$. ■

Proposition 2: Consider Q the non-central CGQF in (8) and let $\mathbf{D}_\xi \in \mathbb{R}^{n\times n}$ be a diagonal matrix with entries $\xi_{m,i}$ such that $\xi^2_{m,i} \sim \Gamma(m, 1/m)$ for $i = 1, \ldots, n$. Then,

$$Q_m = \left(\mathbf{y} + \mathbf{D}_\xi \bar{\mathbf{h}}\right)^\dagger \mathbf{\Lambda} \left(\mathbf{y} + \mathbf{D}_\xi \bar{\mathbf{h}}\right) \tag{15}$$

is a confluent non-central CGQF whose MGF is given by

$$M_{Q_m}(s) = \prod_{i=1}^{n} \frac{\left(1 - \frac{\lambda_i \mu_i s}{m(1-\lambda_i s)}\right)^{-m}}{1 - \lambda_i s} \tag{16}$$

for every $s \in \mathbb{C}$ such that $\mathrm{Re}\{s\}\lambda_i \left(1 + \frac{\mu_i}{m}\right) < 1\ \forall\ i$. Besides, $\lim_{m\to\infty} M_{Q_m}(s) = M_Q(s)$ and, therefore, $Q_m \rightsquigarrow Q$.

Proof: The MGF in (16) is derived in Appendix A and, since

$$\lim_{m\to\infty} \left(1 - \frac{\lambda_i \mu_i s}{m\left(1 - \lambda_i s\right)}\right)^{-m} = \exp\left(\frac{\lambda_i \mu_i s}{1 - \lambda_i s}\right), \tag{17}$$

then $\lim_{m\to\infty} M_{Q_m}(s) = M_Q(s)$, which proves that Q_m is confluent in m to Q. ■

To give an intuitive explanation for Proposition 2, observe (15). Since $\xi_{m,i} \rightsquigarrow 1$ for $i = 1, \ldots, n$, $\mathbf{D}_\xi$ becomes the identity matrix when $m \to \infty$. Consequently, the confluent CQGF in (15) becomes the original one in (8) in the limit. Note also that, in the central case, i.e. $\bar{\mathbf{h}} = \mathbf{0}_{n\times 1}$, $Q_m = Q$ for any value of m. Additionally, the expression in (16) confirms that choosing the perturbing fluctuations to follow Gamma distributions is appropriate since this expression does no longer present the exponential term. In fact, by performing some algebraic manipulations in (16), the MGF of Q_m can be written as

$$M_{Q_m}(s) = \prod_{k=1}^{n} \left[(-\lambda_k)\left(1 + \frac{\mu_k}{m}\right)^m\right]^{-1} \prod_{i=1}^{n} \frac{\left(s - 1/\lambda_i\right)^{m-1}}{\left(s - \beta_i\right)^m} \tag{18}$$

where $M_{Q_m}(s)$ is in terms of a rational polynomial whose zeroes and poles are $1/\lambda_i$ and $\beta_i = \left[\lambda_i\left(1 + \mu_i/m\right)\right]^{-1}$ for $i = 1, \ldots, n$, respectively. Assuming there can be repeated poles and zeroes, and taking into account that, if $\mu_i = 0$ for a certain i, then $\beta_i = 1/\lambda_i$, this rational polynomial can be simplified. Thus, denoting as $\widetilde{\beta}_i$ and $1/\widetilde{\lambda}_j$ for $i = 1, \ldots, n_\beta$ and $j = 1, \ldots, n_\lambda$ the distinct poles and zeroes resulting from simplifying the rational polynomial in (18) with multiplicities p_i and q_i, respectively, the MGF of Q_m is expressed

$$M_{Q_m}(s) = \prod_{k=1}^{n} \left[(-\lambda_k)\left(1 + \frac{\mu_k}{m}\right)^m\right]^{-1} \frac{\prod_{j=1}^{n_\lambda}\left(s - 1/\widetilde{\lambda}_j\right)^{q_j}}{\prod_{i=1}^{n_\beta}\left(s - \widetilde{\beta}_i\right)^{p_i}}. \tag{19}$$

In contrast with the MGF of the original CGQF in (11), the expression of $M_{Q_m}(s)$ in (19) allows a straightforward inversion, i.e. performing an inverse Laplace transformation in order to obtain the PDF and the CDF of Q_m. Moreover, from Proposition 2, since $Q_m \rightsquigarrow Q$, the probability functions of Q can be obtained from those of Q_m by virtue of Lemma 1. Thus, the PDF and CDF of Q_m are calculated in the following propositions, which are easily derived from (19) after expanding the rational polynomial in partial fractions.

Proposition 3: Consider Q_m the confluent CGQF defined in (15). Then, the PDF of Q_m is given by a linear combination of elementary functions as

$$f_{Q_m}(x) = \sum_{i=1}^{n_\beta} \sum_{j=1}^{p_i} \alpha_{i,j} e^{-\widetilde{\beta}_i x} x^{j-1} \mathrm{u}\left(\widetilde{\beta}_i x\right) \mathrm{sgn}(x) \tag{20}$$

where $\alpha_{i,j} = B_j A_{i,j}$ with

$$B_j = \frac{1}{(j-1)!} \prod_{k=1}^{n} \left[(-\lambda_k)\left(1 + \frac{\mu_k}{m}\right)^m\right]^{-1} \tag{21}$$

and $A_{i,j}$ are the residues that arises from performing a partial fraction decomposition in (19) after evaluating $M_{Q_m}(-s)$. A closed-form expression for $A_{i,j}$ is given by

$$A_{i,j} = \sum_{\substack{k_1+\cdots+k_{N-1}=p_i-j \\ k_u \le q_u, u=1,\ldots,n_\lambda}} \prod_{s=1}^{N-1} (k_s!)^{-1} D_i(k_1, \ldots, k_{N-1}) \tag{22}$$

with $D_i(\cdot)$ given in (23), shown at the bottom of the next page, as proved in Appendix B. The sum in (22) is over all possible combinations of $k_1, ..., k_{N-1}$, with $N = n_\lambda + n_\beta$ and $k_u \le q_u$ for $u = 1, \ldots, n_\lambda$, that meet $\sum_{t=1}^{N-1} k_t = p_i - j$.

Proof: The PDF of Q_m is easily obtained from (19) as $f_{Q_m}(x) = \mathcal{L}^{-1}\left\{M_{Q_m}(-s)\right\}$ by performing a partial fraction expansion as detailed in Appendix C. ■

Proposition 4: Consider Q_m the confluent CGQF defined in (15). Then, the CDF of Q_m is given by

$$F_{Q_m}(x) = \mathrm{u}(x) + \sum_{i=1}^{n_\beta} \sum_{j=1}^{p_i} \omega_{i,j} e^{-\widetilde{\beta}_i x} x^{j-1} \mathrm{u}\left(\widetilde{\beta}_i x\right) \mathrm{sgn}(x) \tag{24}$$

where $\omega_{i,j} = B_j C_{i,j}$ with $C_{i,j}$ the partial expansion residues given by

$$C_{i,j} = \sum_{\substack{k_1+\cdots+k_N=p_i-j \\ k_u \leq q_u, u=1,\ldots,n_\lambda}} \prod_{s=1}^{N} \frac{1}{k_s!} \frac{k_N!(-1)^{k_N}}{\left(-\widetilde{\beta}_i\right)^{1+k_N}} D_i(k_1, \ldots, k_{N-1}) \tag{25}$$

as can be deduced from Appendix B.

Proof: Following the same steps as in the previous proof, the CDF of Q_m is straightforwardly calculated from (19) as $F_{Q_m}(x) = \mathcal{L}^{-1}\{M_{Q_m}(-s)/s\}$, as detailed in Appendix D. ■

Propositions 3 and 4 provide simple closed-form expressions for both the PDF and CDF of Q_m in terms of elementary functions, i.e. exponentials and powers. Regarding the argument of the unit step function, it is clear that the domain of $\mathrm{u}(\widetilde{\beta}_i x)$, where the function values are non-negative, will depend on the sign of $\widetilde{\beta}_i$. Thus, if $x < 0$, then the value of $\mathrm{u}(\widetilde{\beta}_i x)$ will be zero for those $\widetilde{\beta}_i > 0$ for $i = 1, \ldots, n_\beta$. In turn, for positive values of x, the value of the step function will be zero for those $\widetilde{\beta}_i < 0$. Moreover, since $\mu_i \geq 0 \; \forall \, i$, the sign of $\widetilde{\beta}_i$ is the same as that of $\widetilde{\lambda}_i$, so the shape of the distribution of Q_m (and, equivalently, that of Q) depends on the positive eigenvalues $\widetilde{\lambda}_i$ for $x \geq 0$, while it depends on the negative eigenvalues for $x < 0$.

From (20) and (24), the PDF and CDF of Q can be approximated by setting m to a sufficiently large value. Note that, although m does not appear explicitly in (20) and (24), both the poles $\widetilde{\beta}_i$ and their multiplicities p_i depends on m, as well as zeroes multiplicities q_j. In the central case, i.e. $\mu_i = 0 \; \forall \, i$, *exact* expressions for both $f_Q(x)$ and $F_Q(x)$ can be obtained from (20) and (24) for any value of m (e.g. $m = 1$). Additionally, in contrast to previous approximations found in the literature, it is possible to quantify the MSE between Q and Q_m in closed-form as given in the following proposition.

Proposition 5: Consider Q the CGQF and Q_m the confluent CGQF given in (8) and (15), respectively. Then, the MSE between Q and Q_m is given by

$$\begin{aligned} \overline{\epsilon^2} &\triangleq \mathbb{E}\left[(Q_m - Q)^2\right] \\ &= \sum_{i=1}^{n} \lambda_i^2 \mu_i \left[4\left(1 - \frac{\Gamma(m+1/2)}{m^{1/2}\Gamma(m)}\right) + \frac{\mu_i}{m}\right]. \end{aligned} \tag{26}$$

Proof: See Appendix E. ■

Observe that, when $\mu_i = |h_i|^2 = 0$ for $i = 1, \ldots, n$ then $\overline{\epsilon^2} = 0$ for any value of m. This is coherent with the fact that setting $\mu_i = 0 \; \forall \, i$ implies having a central CGQF. Additionally, it is easy to prove that the error also goes to zero when $m \to \infty$. By applying the asymptotic formula for the gamma function given in [24, eq. 6.1.39], which allows to write

$$\Gamma(m + \tau) \approx \sqrt{2\pi} e^{-m} m^{m+\tau-1/2} \tag{27}$$

for large m, it is clear that $\lim_{m\to\infty} \overline{\epsilon^2} = 0$. This implies that Q_m converges in mean square to Q, which is a more general type of convergence between random variables. In fact, convergence in mean square also implies convergence in probability and, consequently, weak convergence [25].

When compared to other approximations, the novel approach here presented renders more tractable expressions for the chief probability functions of indefinite non-central CGQFs. The PDF and CDF of Q can be approximated from those of Q_m, which only involves elementary functions in contrast to the more complicated expressions available in the literature [10], [13]–[15]. It is only necessary to set m large enough, such that the MSE between Q_m and Q drops below a certain threshold.

IV. Discussion on the Computation of Partial Fraction Expansion Residues

The expressions of $f_{Q_m}(x)$ and $F_{Q_m}(x)$ have been obtained as the inverse Laplace transformation of $M_{Q_m}(-s)$ and $M_{Q_m}(-s)/s$, respectively. These transformations are performed by expanding the rational polynomial in (19) after evaluating $M_{Q_m}(-s)$, that is

$$R(s) = \frac{\prod_{t=1}^{n_\lambda} \left(s + 1/\widetilde{\lambda}_t\right)^{q_t}}{\prod_{i=1}^{n_\beta} \left(s + \widetilde{\beta}_i\right)^{p_i}}, \tag{28}$$

so the constants $\alpha_{i,j}$ and $\omega_{i,j}$ in (20) and (24) depend on the partial expansion residues of $R(s)$ and $R(s)/s$, namely $A_{i,j}$ and $C_{i,j}$, respectively.

Although closed-form expressions for such constants have been provided in (22) and (25), the computation of these expressions is impractical for very large m. Because the number of terms that needs to be computed for those residues depends on a combinatorial, it grows exponentially with p_i and, consequently, with m. As such, for m sufficiently large, the number of combinations becomes computationally unbearable. This issue is commonly referred to as combinatorial explosion.

Since the partial expansion residues can be defined as derivatives of the rational polynomial [26, eq. (A.36)], an alternative approach to avoid the combinatorial explosion may be the calculation of these derivatives by means of Cauchy's differentiation formula, which allows expressing the derivatives as contour integrals over a closed path [27]. Even though these integrals could

$$D_i(k_1, \ldots, k_{N-1}) = \prod_{t=1}^{n_\lambda} \frac{\left(\widetilde{\lambda}_t^{-1} - \widetilde{\beta}_i\right)^{q_t - k_t}}{(q_t!)^{-1}(q_t - k_t)!} \prod_{r=1}^{i-1} \frac{(-1)^{k_{r+n_\lambda}} (p_r)_{k_{r+n_\lambda}}}{\left(\widetilde{\beta}_r - \widetilde{\beta}_i\right)^{p_r + k_{r+n_\lambda}}} \prod_{l=i+1}^{n_\beta} \frac{(-1)^{k_{l+n_{\lambda^{-1}}}} (p_l)_{k_{l+n_{\lambda^{-1}}}}}{\left(\widetilde{\beta}_l - \widetilde{\beta}_i\right)^{p_r + k_{l+n_{\lambda^{-1}}}}}. \tag{23}$$

be numerically computed, they suffer from significant numerical problems as m increases. These are due to the large amplitude oscillatory behavior (with positive and negative values) of the integrands, which can be tens of orders of magnitude larger than the actual value of the integrals, preventing the integral convergence.

A more suitable approach for the computation of $A_{i,j}$ and $C_{i,j}$ is the algorithm proposed in [28], which provides recursive expressions for the partial fraction residues of both proper and improper rational functions. According to [28, eq. (11a) and (11b)], each residue $A_{i,j}$ for $i = 1, \ldots, n_\beta$ and $j = 1, \ldots, p_i$ is calculated as a linear combination of the previous ones. The recursion starts from A_{i,p_i}, which can be directly computed from the definition in [26, eq. (A.36)] without taking any derivative. From it, this algorithm computes $A_{i,p_i-1}, A_{i,p_i-2}, \ldots, A_{i,1}$ recursively as

$$A_{i,j} = \begin{cases} \frac{1}{p_i - j} \sum_{k=1}^{p_i - j} A_{i,j+k} \rho_A(k, -\widetilde{\beta}_i), & \text{if } 1 \leq j \leq p_i - 1 \\ \frac{\prod_{t=1}^{n_\lambda} (\widetilde{\lambda}_t^{-1} - \widetilde{\beta}_i)^{q_t}}{\prod_{\substack{l=1 \\ l \neq i}}^{n_\beta} (\widetilde{\beta}_l - \widetilde{\beta}_i)^{p_l}}, & \text{if } j = p_i \end{cases} \tag{29}$$

where $\rho_A(k, s)$ is given by

$$\rho_A(k, s) = \sum_{\substack{l=1 \\ l \neq i}}^{n_\beta} \frac{p_l}{\left(-\widetilde{\beta}_l - s\right)^k} - \sum_{t=1}^{n_\lambda} \frac{q_t}{\left(-\widetilde{\lambda}_t^{-1} - s\right)^k}. \tag{30}$$

Analogously, $C_{i,j}$ for $i = 1, \ldots, n_\beta$ and $j = 1, \ldots, p_i$ arises as the partial expansion residues of $R(s)/s$, so following the same steps as with $A_{i,j}$ one has

$$C_{i,j} = \begin{cases} \frac{1}{p_i - j} \sum_{k=1}^{p_i - j} A_{i,j+k} \rho_C(k, -\widetilde{\beta}_i), & \text{if } 1 \leq j \leq p_i - 1 \\ \frac{\prod_{t=1}^{n_\lambda} (\widetilde{\lambda}_t^{-1} - \widetilde{\beta}_i)^{q_t}}{-\widetilde{\beta}_i \prod_{\substack{l=1 \\ l \neq i}}^{n_\beta} (\widetilde{\beta}_l - \widetilde{\beta}_i)^{p_l}}, & \text{if } j = p_i \end{cases} \tag{31}$$

with

$$\rho_C(k, s) = \sum_{\substack{l=1 \\ l \neq i}}^{n_\beta} \frac{p_l}{\left(-\widetilde{\beta}_l - s\right)^k} + \frac{1}{(-s)^k} - \sum_{t=1}^{n_\lambda} \frac{q_t}{\left(-\widetilde{\lambda}_t^{-1} - s\right)^k}. \tag{32}$$

In contrast to (22) and (25), the computational cost of (29) and (31) grows linearly with m instead of exponentially, avoiding the combinatorial explosion. Despite that, numerical errors could still be relevant when computing (29) and (31) due to the limited floating-point precision in calculation software. For very large m, the distinct terms in the summation can still differ in considerable orders of magnitude, which could lead to inaccurate results. However, in contrast to the previous approach that employs Cauchy formula, this computational issue can be solved by working with rational numbers in the software MATHEMATICA. This suite allows the possibility of working with floating-point number with full precision by rationalizing them using the function RATIONALIZE, allowing an error-free computation of $A_{i,j}$ and $C_{i,j}$.

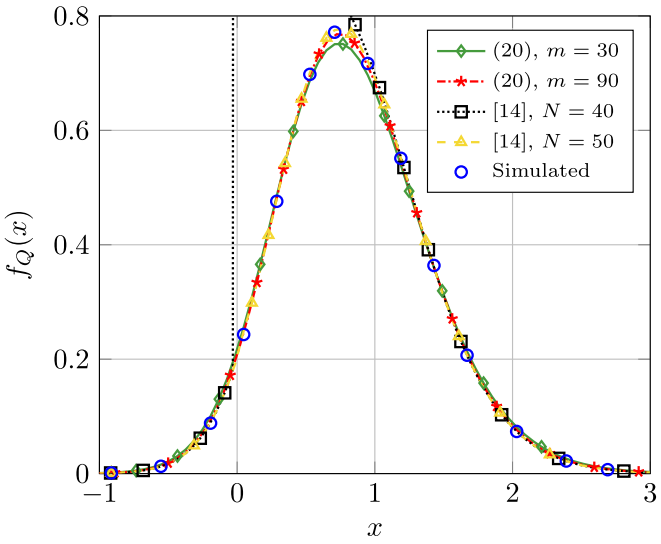

Fig. 1. PDF of Q with $n = 5$, $\boldsymbol{\lambda} = [-3, -1.8, 2, 4, 6]$ and $\boldsymbol{\mu} = [4.3, 2.2, 5.6, 7, 1]$. Exact (simulated) PDF is compared with our approximation in (20) and Raphaeli's approach in [14].

V. COMPARISON WITH OTHER APPROACHES

This section provides a comparison between our proposed approximations in (20) and (24) and other approaches presented in the literature. Concretely, the works in [14] and [10] are considered.

Raphaeli gives two different expressions for the PDF of indefinite non-central CGQFs in terms of infinite series in [14, eqs. (25) and (38)]. Compared to these results, our proposed approximations in (20) and (24) provides a twofold benefit. The first one is that Raphaeli's expressions are not useful for further calculations, e.g. the derivation of error probabilities in communications, due to the recursion that involves the independent variable [14, eq. (25)] or the presence of modified Bessel functions [14, eq. (38)]. In fact, to the best of the authors' knowledge, the CDF cannot be expressed in closed-form by integrating the expressions [14, eq. (25) and (38)] of the PDF. The second benefit is that our approximations always render a valid distribution (for any value of m), in contrast to the truncated series. This is shown in Figs. 1–2, where the PDF and CDF of non-central CGQFs, calculated using both our approach and Raphaeli's one, are depicted. All the calculations have been done using MATHEMATICA software with rational numbers in order to avoid numerical errors, which are also relevant in Raphaeli's series. For simplicity, the vector containing the n eigenvalues λ_i is denoted by $\boldsymbol{\lambda} = [\lambda_1, \ldots, \lambda_n]$. In the same manner, the vector $\boldsymbol{\mu}$ is defined such that $\boldsymbol{\mu} = [\mu_1, \ldots, \mu_n]$. Also, the number of terms employed in Raphaeli's series is denoted by N. The theoretical calculations are also compared with Monte-Carlo simulations of the indefinite non-central CGQF Q.

Thus, the PDF of CGQFs for certain values of the entries of $\boldsymbol{\lambda}$ and $\boldsymbol{\mu}$ is plotted in Fig. 1, observing how the proposed method in [14] produces invalid PDF values for certain x if N is not large enough. Specifically, for $N = 40$ we observe how the resulting PDF produces incorrect values for x between zero

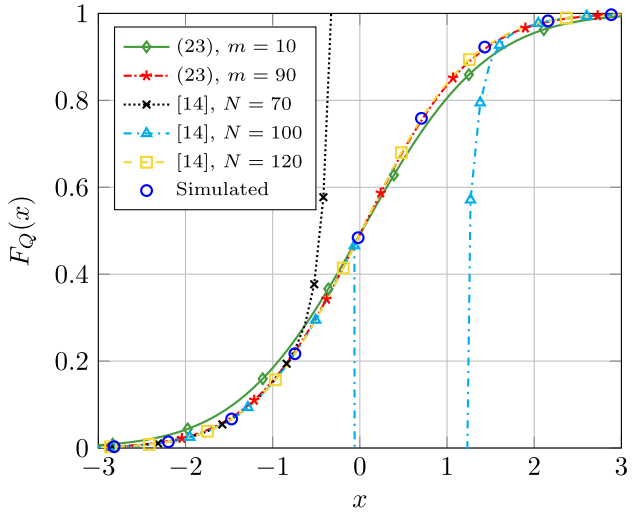

Fig. 2. CDF of Q with $n = 6$, $\boldsymbol{\lambda} = [-3, -1.8, -1, 1, 2.1, 3]$ and $\boldsymbol{\mu} = [8.5, 7.4, 4, 5, 6.8, 7.9]$. Exact (simulated) CDF is compared with our approximation in (23) and Raphaeli's approach in [14].

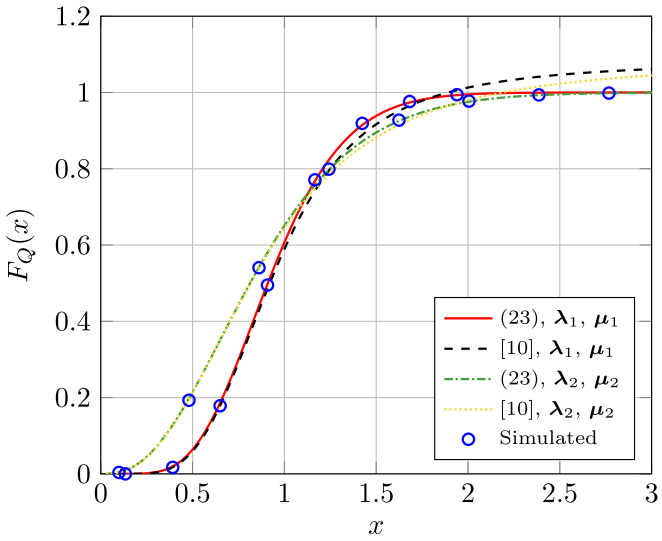

Fig. 3. CDF of Q for different parameters. Exact (simulated) CDF is compared with our proposed approximation in (23) with $m = 50$ and saddle-point approach in [10]. Data: $\boldsymbol{\lambda}_1 = [0.2, 1, 1.4, 3, 5]$, $\boldsymbol{\lambda}_2 = [0.1, 0.6, 1]$, $\boldsymbol{\mu}_1 = [0.6, 7.4, 3, 2.6, 5.5]$ and $\boldsymbol{\mu}_2 = [1, 0.8, 3.4]$.

and one, approximately. Not until a value of $N = 50$ is reached that the PDF converges for all x. In turn, our approach renders a valid distribution with independence of m.

Moreover, the number of terms required in [14] strongly depends on the eigenvalues λ_i. That is, the smaller the difference between the eigenvalues the larger the value of N needed. This can be observed in Fig. 2, where the CDF is depicted. Since the entries of $\boldsymbol{\lambda}$ are less sparse in this case, a larger number of terms are required. Once again, if the required value of $N = 120$ is not reached, we obtain a curve that is not a CDF. Note also that computing Raphaeli's series for such value of N is much slower than computing (24).

Finally, Fig. 3 compares the proposed method with the saddle-point approach in [10]. Although the latter arises as a very efficient approximation, it suffers from the same drawbacks as the previous one. As observed, it gives probabilities greater than one in the right tail. In addition, it is not suitable for further analytic purposes (e.g. expectations over the CGQF).

VI. Practical Example: MRC Systems Over Correlated Rician Fading Channels

The usefulness of the novel results is now exemplified through the performance analysis of MRC systems over correlated Rician channels. To the best of the authors' knowledge, only asymptotic expressions have been given in the literature for the BER and the outage probability (P_{out}) for arbitrary number of branches and correlation between them [29], [30] and infinite series representations when the number of branches is limited to $P = 2$ [31], [32]. In the following, expressions for both the BER and P_{out} are provided using the new approach here presented.

A. System Model

Consider a MRC system with P branches at the receiver side. Then, the received signal can be written as

$$\mathbf{r} = \mathbf{g}z + \mathbf{w} \tag{33}$$

where z is the complex transmitted symbol with $\mathbb{E}[|z|^2] = E_s$, $\mathbf{w} \in \mathbb{C}^{P\times 1}$ is the noise vector, and $\mathbf{g} \in \mathbb{C}^{P\times 1}$ is the normalized channel complex gain vector. The noise at each branch is assumed to be independent and identically distributed with zero-mean and variance N_0. Since the fading at each branch is assumed to be Rician distributed with K_i factor for $i = 1, \ldots, P$, $\mathbf{g}$ is a complex Gaussian vector such that $\mathbf{g} \sim \mathcal{CN}_P(\overline{\mathbf{g}}, \boldsymbol{\Sigma})$, with $\overline{\mathbf{g}} = \mathbb{E}[\mathbf{g}]$ and $\boldsymbol{\Sigma}$ the covariance matrix. The entries of both the mean vector and the covariance matrix can be expressed in terms of the Rician factors as

$$\overline{g}_i = \sqrt{\frac{K_i}{K_i + 1}}, \quad \Sigma_{i,j} = \sqrt{\frac{1}{K_i K_j}} R_{i,j} \tag{34}$$

with $R_{i,j}$ for $i, j = 1, \ldots, P$ the entries of the correlation matrix $\mathbf{R}$ of $\mathbf{g}$. Note that each element of $\mathbf{g}$ has unit power, i.e. $\mathbb{E}[|g_i|^2] = 1$, so the average signal-to-noise ratio (SNR) at each branch is given by $\overline{\gamma} = E_s/N_0$. Considering perfect symbol synchronization and channel estimation, when the MRC principle is applied to the received signal, this yields to a post-processing signal that can be expressed as

$$r_{\text{out}} = \sum_{k=1}^{P} r_k \frac{g_k^\dagger}{\mathbf{g}^\dagger \mathbf{g}} = z + \sum_{k=1}^{P} \frac{g_k^\dagger w_k}{\mathbf{g}^\dagger \mathbf{g}}. \tag{35}$$

Thus, the post-processing SNR is given by

$$\gamma = \overline{\gamma}\, \mathbf{g}^\dagger \mathbf{g}. \tag{36}$$

Since (36) is the non-central CGQF given in (4) with $\mathbf{A} = \mathbf{I}$, the theoretical results derived in this paper can be used to analyze the performance analysis of such system. To that end, it is necessary to define an auxiliary variable γ_m as in (15) such as

$$\gamma_m = \overline{\gamma} \left(\mathbf{y} + \mathbf{D}_\xi \overline{\mathbf{h}}\right)^\dagger \boldsymbol{\Lambda} \left(\mathbf{y} + \mathbf{D}_\xi \overline{\mathbf{h}}\right), \tag{37}$$

where $\mathbf{y} \sim \mathcal{CN}_P(\mathbf{0}_{P\times 1}, \mathbf{I}_P)$, $\overline{\mathbf{h}} = \mathbf{U}^\dagger \mathbf{C}^{-1}\overline{\mathbf{g}}$ with $\mathbf{U}$ and $\mathbf{\Lambda}$ being the unitary matrix and the diagonal matrix built with the eigenvalues of $\mathbf{C}^\dagger\mathbf{C}$, respectively, with $\mathbf{\Sigma} = \mathbf{C}\mathbf{C}^\dagger$. When defining $\mathbf{D}_\xi$ as in Section III-B, γ_m is confluent to γ by virtue of Proposition 2. Therefore, the performance analysis of the system will be based on the characterization of γ_m when m takes appropriate large values.

B. Outage Probability

Defining $\gamma_{\rm th}$ as the minimum SNR required for a reliable communication, the outage probability is given by [33, eq. (6.46)]

$$\begin{aligned} P_{\rm out}(\gamma_{\rm th}) &= P(\gamma < \gamma_{\rm th}) \approx P(\gamma_m < \gamma_{\rm th}) \\ &= \int_0^{\gamma_{\rm th}} f_{\gamma_m}(\gamma_m)\, d\gamma_m, \end{aligned} \tag{38}$$

which corresponds to the CDF of γ_m. Moreover, since $\mathbf{\Lambda}$ is positive definite, then $\widetilde{\beta}_i > 0 \;\forall\; i$, such that the outage probability is written as

$$P_{\rm out}(\gamma_{\rm th}) \approx 1 + \sum_{i=1}^{n_\beta}\sum_{j=1}^{p_i} \omega_{i,j} e^{-\widetilde{\beta}_i \gamma_{th}/\overline{\gamma}} \left(\frac{\overline{\gamma}}{\gamma_{\rm th}}\right)^{-j+1} \tag{39}$$

where $\omega_{i,j}$, $\widetilde{\beta}_k$, n_β and p_i can be given by identification with expressions in Section III, e.g. $n = P$.

C. BER for M-QAM

Since the BER is a continuous and bounded function, by virtue of Lemma 2 it is possible to approximate the BER over the SNR variable γ through the analysis of the confluent variable γ_m. Therefore, assuming a Gray coded constellation, the exact BER expression conditioned to a certain γ_m for arbitrary M-ary square QAM is given by [34]

$$P_b(\gamma_m) = L\sum_{i=1}^{L-1} \omega(i)\, Q\left((2i-1)\sqrt{\frac{3\gamma_m}{M-1}}\right) \tag{40}$$

where $\omega(i)$ are constants defined in [34, eq. (6), (14) and (21)], $L = \sqrt{M}$ and $Q(\cdot)$ is the Gaussian Q-function [35, eq. (4.1)]. In order to obtain the BER for the system model described in the previous section over correlated Rician channels, (40) is averaged over the distribution of γ_m, such as

$$P_b(\overline{\gamma}) \approx \int_0^\infty P_b(\gamma_m)\, f_{\gamma_m}(\gamma_m)\, d\gamma_m. \tag{41}$$

From (40) and (41), and using the relation between the Gaussian Q-function and the error function $\mathrm{erf}(\cdot)$ given in [36, eq. (8.250 1)], the average BER is calculated by applying [36, eq. (3.381 4)] and [37, eq. (4.3.8)], obtaining

$$\begin{aligned} P_b(\overline{\gamma}) \approx\; & L\sum_{i=1}^{n_\beta}\sum_{j=1}^{p_i}\sum_{k=1}^{L-1} \omega(k)\alpha_{i,j}\left[\frac{\Gamma(j)}{2\widetilde{\beta}_i^{\,j}} - \frac{\delta_k \Gamma\left(j+\frac{1}{2}\right)}{\widetilde{\beta}_i^{\,j+1/2}}\right. \\ & \left. \times \sqrt{\frac{\overline{\gamma}}{2\pi}}\, {}_2F_1\left(\frac{1}{2}, j+\frac{1}{2}; \frac{3}{2}; \frac{-\delta_k^2}{2\widetilde{\beta}_i}\overline{\gamma}\right)\right] \end{aligned} \tag{42}$$

where $\delta_k = (2k-1)\sqrt{3/(M-1)}$ and ${}_2F_1(\cdot)$ is the Gauss hypergeometric function [24, eq. (15.1.1)].

D. Numerical Results

In the following, the influence of the channel parameters and the number of branches of the receiver in the outage probability and the BER is assessed using (39) and (42) and contrasted through Monte-Carlo simulations. Although the theoretical expressions in (39) and (42) were derived using the confluent SNR γ_m in (37), the original variable γ in (36) is used in the simulations in order to validate the accuracy of the approximation. For the sake of simplicity, the vector containing the P Rician K factors is denoted as $\mathbf{k} = [K_1, \ldots, K_P]$. Also, the correlation matrix $\mathbf{R}$ is assumed to be exponential, i.e. $(\mathbf{R})_{i,j} = \rho^{|i-j|}$ with $|\rho| < 1$ [38]–[40]. A thorough study has been performed by considering multiple combinations of ρ, $\mathbf{k}$ and the number of branches, P, which are varied over a large range of SNR. While a detailed analysis of the results, depicted in Figs. 4–9, is given below, it is important to notice that there is a perfect match between the analytical and the simulated values in all cases.

Firstly, the impact of the correlation matrix and the Rician K factors in the outage probability is studied both in the low-SNR and high-SNR regime. Since $P_{\rm out}$ exhibits complementary behaviors in both regimes, a different representation is employed in each case. Fig. 4 depicts the complementary outage probability $(1 - P_{\rm out})$ when the SNR takes low values compared to the threshold, whereas Fig. 5 show the values of $P_{\rm out}$ in the high-SNR regime. In both cases the number of branches at the receiver is fixed to $P = 2$. Note that the correlation between branches and the strength of the line of sight (LoS) have opposite effects in the low and high SNR regimes. Hence, while in the latter a strong LoS achieves a better performance than a weak one, in the low SNR range a weak direct component seems to be beneficial. This behavior can be justified as follows. A strong LoS component implies less random fluctuation in the received signal, i.e. the scattering is less relevant. In the high SNR regime, where the mean of the instantaneous SNR is large enough, this fluctuation represented by the scattering may occasionally lead to deep fading that makes the instantaneous SNR drops below the threshold. Therefore, increasing the K factor (the power of the LoS) when the mean SNR takes large values is beneficial since it reduces such probability. In turn, in the low SNR regime, the fluctuation in the received signal may have the opposite effect, punctually rendering values for the instantaneous SNR much larger than the mean value. In that case, increasing the K factor will reduce the probability of getting SNR values that are greater than the threshold.

Similarly, while a high correlation factor gives better performance than a low one when $\overline{\gamma}$ is large, the opposite behavior is observed for low values of $\overline{\gamma}$. Although similar conclusions are given in [31], [32] for $P_{\rm out}$ in the high SNR regime, no attention have been paid in the literature to the behavior of the outage probability when the SNR takes very low values compared to the threshold.

The analysis of the outage probability now focuses on the high-SNR regime. The number of branches is extended to $P = 4$ to enrich the system. Fig. 6 assesses the influence of the correlation factor in strong and weak LoS scenarios. It can be observed that the impact of ρ depends on the strength of the LoS. Hence,

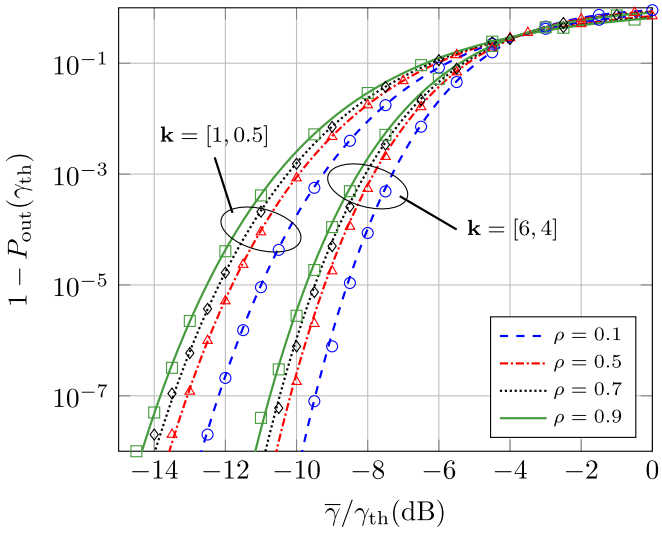

Fig. 4. Complementary P_{out} vs. $\overline{\gamma}/\gamma_{\text{th}}$ for $P=2$, different values of ρ and different values of K at each path. Solid lines correspond to theoretical calculation with $m=40$ for $\mathbf{k}=[1,0.5]$ and $m=100$ for $\mathbf{k}=[6,4]$, while markers correspond to Monte Carlo simulations.

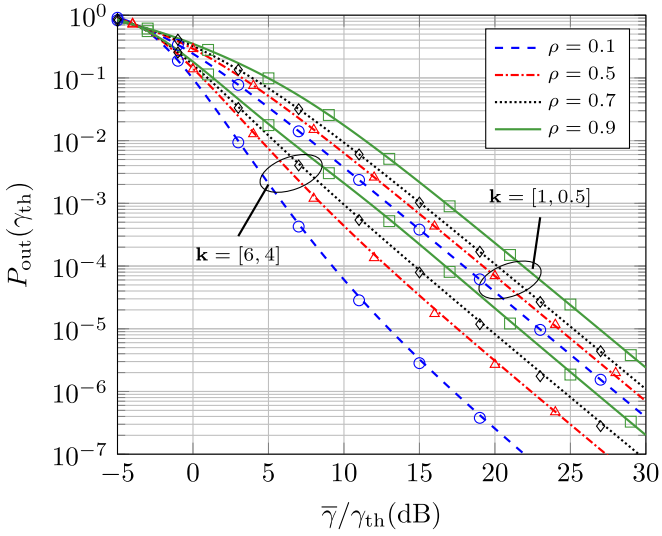

Fig. 5. P_{out} vs. $\overline{\gamma}/\gamma_{\text{th}}$ for $P=2$, different values of ρ and different values of K at each path. Solid lines correspond to theoretical calculation with $m=50$ for $\mathbf{k}=[1,0.5]$ and $m=150$ for $\mathbf{k}=[6,4]$, while markers correspond to Monte Carlo simulations.

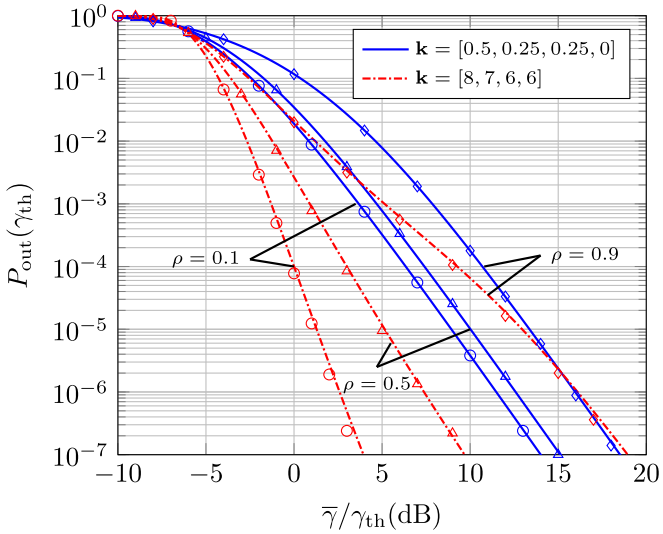

Fig. 6. P_{out} vs. $\overline{\gamma}/\gamma_{\text{th}}$ for $P=4$, different values of ρ and different values of K at each path. Solid lines correspond to theoretical P_{out} while markers correspond to Monte Carlo simulations. For theoretical calculation, $m=40$ for $\mathbf{k}=[0.5,0.25,0.25,0]$ and $m=200$ for $\mathbf{k}=[8,7,6,6]$.

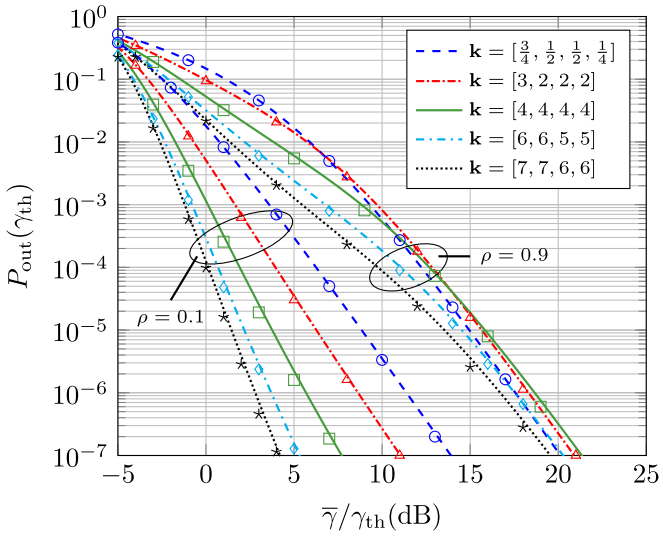

Fig. 7. P_{out} vs. $\overline{\gamma}/\gamma_{\text{th}}$ for $P=4$ and different values of $\mathbf{k}$ with a strong correlation factor ($\rho=0.9$) and a weak correlation factor ($\rho=0.1$). Solid lines correspond to theoretical P_{out} while markers correspond to Monte Carlo simulations. For theoretical calculation, $m\in[40,200]$.

increasing the correlation between branches implies a considerable degradation of the system performance when the LoS is strong (large K_i factors). In fact, when $\rho=0.9$, the outage probability is asymptotically higher in a strong LoS scenario than in a weak one. This effect is analyzed in more detail in Fig. 7, where P_{out} is plotted for different vales of $\mathbf{k}$ when $\rho=0.1$ (low correlation between branches) and $\rho=0.9$ (branches highly correlated). As seen, the system behaves as expected when $\rho=0.1$, since P_{out} decreases as the entries of $\mathbf{k}$ increases. However, when $\rho=0.9$, the system performance does not monotonically improves with the strength of the LoS. Only when the distinct K_i factors reach a certain value, P_{out} decreases as the K_i factors increase. The value of this turning point seems to depend on the number of branches and the correlation between them. This behavior was deeply analyzed in [41], where a multiple-input multiple-output maximum-ratio combining (MIMO-MRC) system is considered, providing expressions for this threshold when assuming identically distributed Rician channels. Despite this assumption, it is difficult to determine how an arbitrary correlation matrix between branches would impact in the turning value of K, as stated in [41, sec. IV-B].

Here, we consider an even more general case, where we have an arbitrary correlation matrix and non-identically distributed fading in each branch. We believe that a similar behavior to that of [41] is observed. However, deriving such threshold in our

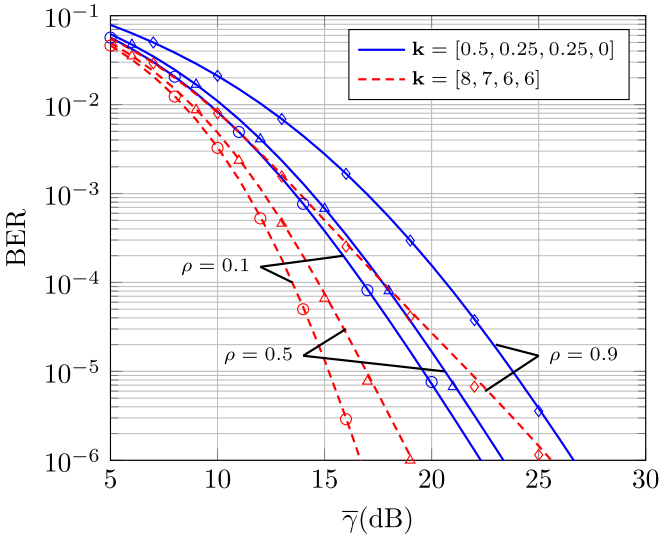

Fig. 8. BER vs. $\overline{\gamma}$ for 16-QAM, $P = 4$ and different values of ρ and $\mathbf{k}$. Solid lines correspond to theoretical BER with $m = 40$ for $\mathbf{k} = [0.5, 0.25, 0.25, 0]$ and $m = 150$ for $\mathbf{k} = [8, 7, 6, 6]$, while markers correspond to Monte Carlo simulations.

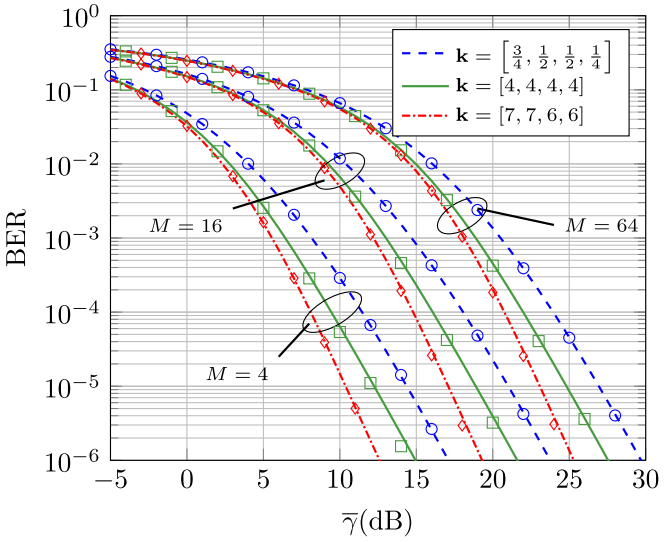

Fig. 9. BER vs. $\overline{\gamma}$ for different modulation schemes and different values of $\mathbf{k}$ with $P = 4$ and $\rho = 0.5$. Solid lines correspond to theoretical BER while markers correspond to Monte Carlo simulations. For theoretical calculation, $m \in [50, 150]$.

general case is a very challenging task, which is left for future works.

Regarding the BER, the impact of the correlation factor and of the strength of the LoS is firstly evaluated. Fig. 8 depicts the BER for 16-QAM with different values of ρ in strong and weak LoS scenarios. The influence of the modulation scheme is appraised in Fig. 9, where the BER for various QAM constellations and different values of $\mathbf{k}$ are represented for a fixed correlation factor. It is interesting to observe that the BER suffers the same relative degradation in all modulation schemes when the K_i factors decrease. Similar conclusions were drawn in [42], [43] when

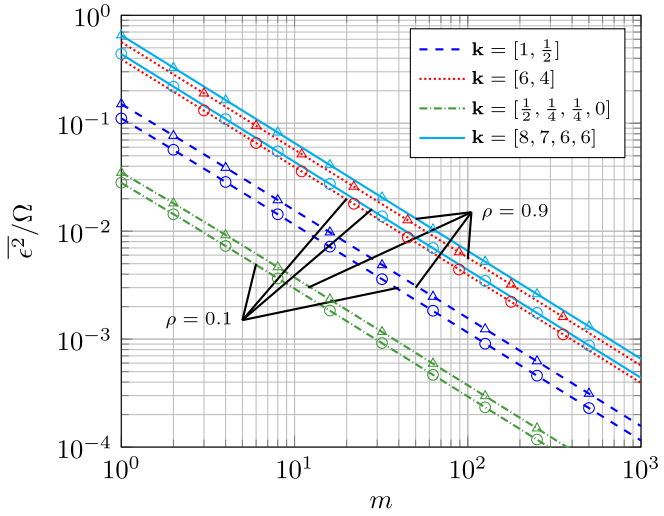

Fig. 10. Normalized MSE vs. m for different values of P, ρ and $\mathbf{k}$. Solid lines correspond to theoretical MSE while markers correspond to Monte Carlo simulations.

different reception techniques are applied over correlated Rician channels.

Results displayed in Figs. 4–9 have been obtained with different values of the shape parameter m. As the latter increases, the MSE between the confluent CGQF and the original one decreases, rendering a better accuracy in the approximation. However, the value of m required to achieve a given MSE depends on the characteristics of the CGQF. Fig. 10 shows the MSE given in (26), normalized by $\Omega = \mathbb{E}\left[\gamma^2\right]$. The MSE is always below 10^{-2} for the values of m used in the theoretical calculations, which justifies the good match with the simulations. Note also that larger K_i factors and higher correlation between branches require larger values of m to reach a certain MSE. Interestingly, the slope of the MSE does not depend on the channel parameters, being the same for all the cases. Based on our result, a practical criterion could be choosing a value of m such that the normalized MSE between the target variable and the auxiliary one drops below 10^{-2}.

VII. Conclusion

This paper has presented a novel approach to the statistical characterization of indefinite non-central CGQFs. Its key idea is to perturb the non-central vector of the CGQF with a random variable that depends on a shape parameter. The resulting auxiliary CGQF, which converges to the original one when this parameter tends to infinity, has simpler PDF and CDF expressions. In contrast to previous approaches available in the literature, results derived herein permits further insightful analyses, since the resulting probability functions are expressed in terms of elementary functions (exponential and powers) that can be used in subsequent calculations. Also, the MSE between the auxiliary CGQF and the original one is given in closed-form, allowing the particularization of the auxiliary CGQF in order to make this error drop below a certain threshold.

The usefulness of the proposed method has been exemplified by the analysis of MRC systems over non-identically distributed

Rician fading channels with arbitrary correlation, whose outage probability and BER expressions are given and validated through Monte-Carlo simulations, showing a perfect match between the theoretical calculations and the simulations.

Appendix A
Proof of Proposition 2

Consider the confluent CGQF Q_m defined in (15). When conditioned on $\mathbf{D}_\xi$, its MGF is obtained from (11) as

$$M_{Q_m|\mathbf{D}_\xi}(s) = \prod_{i=1}^{n} \frac{\exp\left(\frac{\xi_{m,i}^2 \lambda_i \mu_i s}{1-\lambda_i s}\right)}{1-\lambda_i s}, \tag{43}$$

The unconditional MGF is obtained by integrating over each variable $\xi_{m,i}^2$ as

$$M_{Q_m}(s) = \int_0^\infty \cdots \int_0^\infty M_{Q_m|\mathbf{D}_\xi}(s) \times f_{\xi_{m,1}^2,\ldots\xi_{m,n}^2}(u_1,\ldots,u_n)\, du_1 \ldots du_n. \tag{44}$$

with $f_{\xi_{m,1}^2,\ldots,\xi_{m,n}^2}(\cdot)$ the joint probability density function of $\xi_{m,1}^2,\ldots,\xi_{m,n}^2$. Since $\xi_{m,i}^2$ for $i=1,\ldots,n$ are independent random variables, their joint density function can be calculated as

$$f_{\xi_{m,1}^2,\ldots\xi_{m,n}^2}(u_1,\ldots,u_n) = \prod_{i=1}^{n} f_{\xi_{m,i}^2}(u_i), \tag{45}$$

where $f_{\xi_{m,i}^2}(u_i)$ for $i=1,\ldots,n$ is the PDF of the Gamma distribution with shape parameter m and scale parameter $1/m$, given in (1). By substituting in (44), the MGF of the confluent CGQF is rewritten as follows

$$M_{Q_m}(s) = \prod_{i=1}^{n} \frac{m^m}{\Gamma(m)(1-\lambda_i s)} \int_0^\infty \cdots \int_0^\infty \prod_{k=1}^{n} u_k^{m-1} \times \exp\left(-u_k\left[m - \frac{\lambda_k \mu_k s}{1-\lambda_k s}\right]\right) du_1 \ldots du_n. \tag{46}$$

The above integral can be calculated for every $s \in \mathbb{C}$ such that $\mathrm{Re}\{s\}\lambda_i\left(1+\frac{\mu_i}{m}\right) < 1 \;\forall\; i$. Due to the independence between variables, each individual integral in (46) can be solved separately using [36, eq. 3.381 4], which yields to (16) after some algebraic manipulations.

Appendix B
Derivation of $A_{i,j}$ and $C_{i,j}$

$A_{i,j}$ for $i=1,\ldots,n_\beta$ and $j=1,\ldots,p_i$ arise as the partial expansion residues of the rational polynomial in (19) after evaluating $M_{Q_m}(-s)$, whose general expression is given in terms of derivatives of the rational polynomial as [26, eq. (A. 36)]

$$A_{i,j} = \frac{1}{(p_i-j)!}\frac{d^{p_i-j}}{ds^{p_i-j}}\left(\frac{\prod_{t=1}^{n_\lambda}\left(s+1/\widetilde{\lambda}_t\right)^{q_t}}{\prod_{\substack{l=1\\ l\neq i}}^{n_\beta}\left(s+\widetilde{\beta}_l\right)^{p_l}}\right)\Bigg|_{s=-\widetilde{\beta}_i}. \tag{47}$$

By using the generalization of Leibniz's rule, the rational polynomial derivatives can be rewritten in term of the derivatives of the individual binomials as

$$A_{i,j} = \sum_{k_1+\cdots+k_{N-1}=p_i-j}\left(\frac{1}{\prod_{s=1}^{N}k_s}\prod_{t=1}^{n_\lambda}\left[\left(s+\widetilde{\lambda}^{-1}\right)^{q_t}\right]^{(k_t)} \times \prod_{r=1}^{i-1}\left[\left(s+\widetilde{\beta}_r\right)^{-p_r}\right]^{(k_{r+n})} \times \prod_{l=i+1}^{n_\beta}\left[\left(s+\widetilde{\beta}_l\right)^{-p_l}\right]^{(k_{l+n-1})}\right)\Bigg|_{s=-\widetilde{\beta}_i} \tag{48}$$

where the sum is over all possible combinations of $k_1, ..., k_{N-1}$, with $N = n_\lambda + n_\beta$, that meet $\sum_{t=1}^{N-1} k_t = p_i - j$. Thus, $A_{i,j}$ for $i=1,\ldots,n_\beta$ and $j=1,\ldots,p_i$ are expressed as a finite sum of the q-th derivative of binomials with positive and negative exponents, which can be written in closed-form by using

$$\frac{d^q}{dx^q}(x+a)^\nu = \begin{cases} \frac{(-1)^q(-\nu)_q}{(x+a)^{-\nu+q}}, & \text{if } \nu<0 \\ \frac{\nu!}{(\nu-q)!}(x+a)^{\nu-q}, & \text{if } \nu>0 \end{cases}. \tag{49}$$

Then, the final expression for $A_{i,j}$ is given in (22), which has been obtained from (48) and (49) after evaluating at $s=-\widetilde{\beta}_i$. Note that, if $\nu>0$, (49) is only valid for $q\le\nu$ since the derivative is zero otherwise. Therefore, the restriction $k_u \le q_u, u = 1,\ldots,n_\lambda$ is imposed in (22).

Analogously, $C_{i,j}$ are the partial expansion residues of $R(s)/s$, so following the same steps as with $A_{i,j}$ one gets (25).

Appendix C
Proof of Proposition 3

The PDF of Q_m is obtained by performing an inverse Laplace transformation to the MGF such as

$$f_{Q_m}(x) = \mathcal{L}^{-1}\left\{M_{Q_m}(-s)\right\}. \tag{50}$$

Thus, evaluating (19) at $-s$ and performing a partial fraction decomposition, one has

$$M_{Q_m}(-s) = \prod_{k=1}^{n}\left[\lambda_k\left(1+\frac{\mu_k}{m}\right)^m\right]^{-1}\sum_{i=1}^{n_\beta}\sum_{j=1}^{p_i}\frac{A_{i,j}}{\left(s+\widetilde{\beta}_i\right)^j} \tag{51}$$

with $A_{i,j}$ the partial fraction decomposition residues given in (22), which are deduced in Appendix B. The expression of the PDF is easily derived from above equation just applying the Laplace transform pair [26, p. 692]

$$\mathcal{L}^{-1}\left\{\frac{1}{(s+\alpha)^\nu}\right\} = \begin{cases} \frac{t^{\nu-1}}{(\nu-1)!}e^{-\alpha t}\mathrm{u}(t), & \text{if } \alpha\ge 0 \\ \frac{-t^{\nu-1}}{(\nu-1)!}e^{-\alpha t}\mathrm{u}(-t), & \text{if } \alpha<0 \end{cases}, \tag{52}$$

which are valid for $\mathrm{Re}\{s\} > -\alpha$ and $\mathrm{Re}\{s\} < -\alpha$ respectively, yielding to (20) after further algebraic manipulations.

APPENDIX D
PROOF OF PROPOSITION 4

The CDF of Q_m is obtained from the MGF as

$$F_{Q_m}(t) = \mathcal{L}^{-1}\left\{\frac{1}{s}M_{Q_m}(-s)\right\}. \tag{53}$$

Similarly as in Appendix C, after performing a partial fraction expansion one has

$$\frac{1}{s}M_{Q_m}(-s) = \frac{1}{s} + \prod_{k=1}^{n}\left[\lambda_k\left(1+\frac{\mu_k}{m}\right)^m\right]^{-1} \times \sum_{i=1}^{n_\beta}\sum_{j=1}^{p_i}\frac{C_{i,j}}{\left(s+\widetilde{\beta}_j\right)^j}. \tag{54}$$

where $C_{i,j}$ are the partial expansion residues given in (25), whose proof can be deduced from that of $A_{i,j}$ in Appendix B. The final expression for the CDF in (24) is straightforwardly obtained from (54) by applying the Laplace transform pair shown in (52).

APPENDIX E
CALCULATION OF MSE

The MSE between Q_m and Q is given by

$$\overline{\epsilon^2} = \mathbb{E}\left[(Q_m - Q)^2\right] = \mathbb{E}_{\mathbf{y},\mathbf{D}_\xi}\left[\left(\left(\mathbf{y}+\mathbf{D}_\xi\bar{\mathbf{h}}\right)^\dagger\mathbf{\Lambda}\left(\mathbf{y}+\mathbf{D}_\xi\bar{\mathbf{h}}\right) - \left(\mathbf{y}+\bar{\mathbf{h}}\right)^\dagger\mathbf{\Lambda}\left(\mathbf{y}+\bar{\mathbf{h}}\right)\right)^2\right]. \tag{55}$$

A simple way of performing the above expectation is considering first the MSE conditioned to $\mathbf{D}_\xi$ (or equivalently, to $\xi_{m,i}$ for $i = 1,\ldots,n$). Expanding the square in (55), considering the expectation of a CGQF given in [11, eq. (3.2b.2)] and taking into account the fact that the entries of $\mathbf{y}$ are mutually independent zero-mean complex Gaussian random variables whose real and imaginary parts are also independent and identically distributed, the conditioned MSE is expressed as

$$\begin{aligned}\overline{\epsilon^2}\Big|_{\mathbf{D}_\xi} &= \operatorname{tr}\left(\mathbf{\Lambda}\left(\mathbf{D}_\xi-\mathbf{I}\right)\overline{\mathbf{h}\mathbf{h}}^\dagger\left(\mathbf{D}_\xi-\mathbf{I}\right)\mathbf{\Lambda}\right)\\ &\quad+\overline{\mathbf{h}}^\dagger\left(\mathbf{D}_\xi-\mathbf{I}\right)\mathbf{\Lambda}^{\mathbf{2}}\left(\mathbf{D}_\xi-\mathbf{I}\right)\overline{\mathbf{h}}\\ &\quad+\overline{\mathbf{h}}^\dagger\left(\mathbf{D}_\xi^2-\mathbf{I}\right)\mathbf{\Lambda}\overline{\mathbf{h}\mathbf{h}}^\dagger\left(\mathbf{D}_\xi^2-\mathbf{I}\right)\mathbf{\Lambda}\overline{\mathbf{h}}.\end{aligned} \tag{56}$$

The unconditional MSE is obtained by averaging (56) as

$$\overline{\epsilon^2} = \mathbb{E}_{\mathbf{D}_\xi}\left[\epsilon^2\big|_{\mathbf{D}_\xi}\right]. \tag{57}$$

Considering that both $\mathbf{D}_\xi$ and $\mathbf{\Lambda}$ are diagonal matrices and $\mathbb{E}[\mathbf{D}_\xi^2] = \mathbf{I}_n$,

$$\overline{\epsilon^2} = 4\left(1-\overline{\xi}\right)\sum_{i=1}^{n}\lambda_i^2\left|h_i\right|^2 + \operatorname{tr}\left(\mathbf{\Lambda}\overline{\mathbf{h}\mathbf{h}}^\dagger\mathbf{\Sigma}\right) \tag{58}$$

where $\overline{\xi} = \mathbb{E}\left[\xi_{m,i}\right]$ for $i = 1,\ldots,n$ is the expectation of a Nakagami-m random variable which is given by

$$\overline{\xi} = \frac{\Gamma(m+1/2)}{m^{1/2}\Gamma(m)} \tag{59}$$

and $\mathbf{\Sigma}$ is the covariance matrix of $\mathbf{x} = \mathbf{D}_\xi^{\mathbf{2}}\overline{\mathbf{h}}$. Due to the statistical independence of the elements of $\mathbf{x}$, x_i for $i = 1,\ldots,n$, $\mathbf{\Sigma}$ is a diagonal matrix whose entries are the variances of the entries of $\mathbf{x}$. Since $\xi_{m,i}^2 \sim \Gamma\left(m, 1/m\right)\ \forall\, i$, then $\operatorname{Var}[x_i] = \left|h_i\right|^2/m$, where h_i for $i = 1,\ldots,n$ are the entries of $\overline{\mathbf{h}}$. The final expression for the MSE in (26) is obtained by substituting the value of $\mathbf{\Sigma}$ in (58) and performing some algebraic manipulations.

REFERENCES

[1] B. D. Rao, M. Wengler, and B. Judson, "Performance analysis and comparison of MRC and optimal combining in antenna array systems," in *Proc. IEEE Int. Conf. Acoust., Speech, Signal Process. (Cat. No.01CH37221)*, 2001, vol. 5, pp. 2949–2952.

[2] D. Lao and A. M. Haimovich, "Exact closed-form performance analysis of optimum combining with multiple cochannel interferers and Rayleigh fading," *IEEE Trans. Commun.*, vol. 51, no. 6, pp. 995–1003, Jun. 2003.

[3] C. Kim, S. Lee, and J. Lee, "SINR and throughput analysis for random beamforming systems with adaptive modulation," *IEEE Trans. Wireless Commun.*, vol. 12, no. 4, pp. 1460–1471, Apr. 2013.

[4] C. Schlegel, "Error probability calculation for multibeam Rayleigh channels," *IEEE Trans. Commun.*, vol. 44, no. 3, pp. 290–293, Mar. 1996.

[5] G. A. Ropokis, A. A. Rontogiannis, and P. T. Mathiopoulos, "Quadratic forms in normal RVs: Theory and applications to OSTBC over Hoyt fading channels," *IEEE Trans. Wireless Commun.*, vol. 7, no. 12, pp. 5009–5019, Dec. 2008.

[6] V. Havary-Nassab, S. Shahbazpanahi, and A. Grami, "Optimal distributed beamforming for two-way relay networks," *IEEE Trans. Signal Process.*, vol. 58, no. 3, pp. 1238–1250, Mar. 2010.

[7] D. Raphaeli, "Noncoherent coded modulation," *IEEE Trans. Commun.*, vol. 44, no. 2, pp. 172–183, Feb. 1996.

[8] V. Pauli, R. Schober, and L. Lampe, "A unified performance analysis framework for differential detection in MIMO Rayleigh fading channels," *IEEE Trans. Commun.*, vol. 56, no. 11, pp. 1972–1981, Nov. 2008.

[9] Y. L. Gall, F. X. Socheleau, and J. Bonnel, "Matched-field processing performance under the stochastic and deterministic signal models," *IEEE Trans. Signal Process.*, vol. 62, no. 22, pp. 5825–5838, Nov. 2014.

[10] T. Y. Al-Naffouri, M. Moinuddin, N. Ajeeb, B. Hassibi, and A. L. Moustakas, "On the distribution of indefinite quadratic forms in Gaussian random variables," *IEEE Trans. Commun.*, vol. 64, no. 1, pp. 153–165, Jan. 2016.

[11] S. Provost and A. Mathai, *Quadratic Forms in Random Variables: Theory and Applications* (Statistics : Textbooks and Monographs). New York, NY, USA: Marcel Dekker, 1992.

[12] G. L. Turin, "The characteristic function of Hermitian quadratic forms in complex normal variables," *Biometrika*, vol. 47, no. 1/2, pp. 199–201, 1960.

[13] G. Tziritas, "On the distribution of positive-definite Gaussian quadratic forms," *IEEE Trans. Inf. Theory*, vol. IT-33, no. 6, pp. 895–906, Nov. 1987.

[14] D. Raphaeli, "Distribution of noncentral indefinite quadratic forms in complex normal variables," *IEEE Trans. Inf. Theory*, vol. 42, no. 3, pp. 1002–1007, May 1996.

[15] K. H. Biyari and W. C. Lindsey, "Statistical distributions of Hermitian quadratic forms in complex Gaussian variables," *IEEE Trans. Inf. Theory*, vol. 39, no. 3, pp. 1076–1082, May 1993.

[16] N. Johnson, S. Kotz, and N. Balakrishnan, *Continuous Univariate Distributions* (Wiley Series in Probability and Statistics), vol. 1, 2nd ed. Hoboken, NJ, USA: Wiley, 1994.

[17] R. J. Muirhead, *Aspects of Multivariate Statistical Theory*. Hoboken, NJ, USA: Wiley, 1982.

[18] M. P. Slichenko, "Characteristic function of a quadratic form formed by correlated complex Gaussian variables," *J. Commun. Technol. Electron.*, vol. 59, no. 5, pp. 433–440, 2014.

[19] R. Horn and C. Johnson, *Matrix Analysis*. Cambridge, U.K.: Cambridge Univ. Press, 1990.

[20] L. L. Scharf, *Statistical Signal Processing*, vol. 98. Reading, MA, USA: Addison-Wesley, 1991.
[21] P. Billingsley, *Probability and Measure* (Wiley Series in Probability and Statistics). Hoboken, NJ, USA: Wiley, 2012.
[22] D. Williams, *Probability with Martingales* (Cambridge Mathematical Textbooks). Cambridge, U.K.: Cambridge Univ. Press, 1991.
[23] E. B. Manoukian, *Mathematical Nonparametric Statistics*. Boca Raton, FL, USA: CRC Press, 1986.
[24] M. Abramowitz *et al.*, *Handbook of Mathematical Functions With Formulas, Graphs, and Mathematical Tables*, vol. 9. New York, NY, USA: Dover, 1972.
[25] S. Resnick, *A Probability Path*. Boston, MA, USA: Birkhaüser, 1998.
[26] A. V. Oppenheim, A. S. Willsky, and S. H. Nawab, *Signals & Systems*, 2nd ed. Englewood Cliffs, NJ, USA: Prentice-Hall, 1996.
[27] L. Ahlfors, *Complex Analysis*. New York, NY, USA: McGraw-Hill, 1966.
[28] Y. Ma, J. Yu, and Y. Wang, "Efficient recursive methods for partial fraction expansion of general rational functions," *J. Appl. Math.*, vol. 2014, 2014, Art. no. 895036.
[29] R. K. Mallik and N. C. Sagias, "Distribution of inner product of complex Gaussian random vectors and its applications," *IEEE Trans. Commun.*, vol. 59, no. 12, pp. 3353–3362, Dec. 2011.
[30] Y. Ma, "Impact of correlated diversity branches in Rician fading channels," in *Proc. IEEE Int. Conf. Commun.*, May 2005, vol. 1, pp. 473–477.
[31] P. S. Bithas, N. C. Sagias, and P. T. Mathiopoulos, "Dual diversity over correlated Ricean fading channels," *J. Commun. Netw.*, vol. 9, no. 1, pp. 67–74, Mar. 2007.
[32] M. Ilic-Delibasic and M. Pejanovic-Djurisic, "MRC dual-diversity system over correlated and non-identical Ricean fading channels," *IEEE Commun. Lett.*, vol. 17, no. 12, pp. 2280–2283, Dec. 2013.
[33] A. Goldsmith, *Wireless Communications*. Cambridge, U.K.: Cambridge Univ. Press, 2005.
[34] F. J. Lopez-Martinez, E. Martos-Naya, J. F. Paris, and U. Fernandez-Plazaola, "Generalized BER analysis of QAM and its application to MRC under imperfect CSI and interference in Ricean fading channels," *IEEE Trans. Veh. Technol*, vol. 59, no. 5, pp. 2598–2604, Jun. 2010.
[35] M. K. Simon and M.-S. Alouini, *Digital Communication Over Fading Channels*, vol. 95. Hoboken, NJ, USA: Wiley, 2005.
[36] I. S. Gradshteyn and I. M. Ryzhik, *Table of Integrals, Series, and Products*. New York, NY, USA: Academic, 2007.
[37] E. W. Ng and M. Geller, "A table of integrals of the error functions," *J. Res. Nat. Bur. Stand. B*, vol. 73, no. 1, pp. 1–20, 1969.
[38] G. K. Karagiannidis, D. A. Zogas, and S. A. Kotsopoulos, "On the multivariate Nakagami-m distribution with exponential correlation," *IEEE Trans. Commun.*, vol. 51, no. 8, pp. 1240–1244, Aug. 2003.
[39] R. Subadar and R. Mudoi, "Performance of multiuser TAS/MRC-MIMO systems over Rayleigh fading channels with exponential correlation," in *Proc. Int. Conf. Electron. Design, Comput. Netw. Automated Verification*, Jan. 2015, pp. 165–168.
[40] S. L. Loyka, "Channel capacity of MIMO architecture using the exponential correlation matrix," *IEEE Commun. Lett.*, vol. 5, no. 9, pp. 369–371, Sep. 2001.
[41] Y. Wu, R. H. Y. Louie, and M. R. McKay, "Asymptotic outage probability of MIMO-MRC systems in double-correlated Rician environments," *IEEE Trans. Wireless Commun.*, vol. 15, no. 1, pp. 367–376, Jan. 2016.
[42] S. Haghani and N. C. Beaulieu, "Performance of two dual-branch post-detection switch-and-stay combining schemes in correlated Rayleigh and Rician fading," *IEEE Trans. Commun.*, vol. 55, no. 5, pp. 1007–1019, May 2007.
[43] S. Haghani and N. C. Beaulieu, "Performance of s + n selection diversity receivers in correlated Rician and Rayleigh fading," *IEEE Trans. Wireless Commun.*, vol. 7, no. 1, pp. 146–154, Jan. 2008.

Pablo Ramírez-Espinosa received the M.Sc. degree in telecommunication engineering in 2017 from the University of Málaga, Málaga, Spain, where he has been working toward the Ph.D. degree in communication theory. Since 2017, he has been with the Communication Engineering Department, University of Málaga, as an Associate Researcher. His main research interests include wireless communications, channel modeling, and signal processing for communications.

Laureano Moreno-Pozas received the M.Sc. degree in electrical engineering in 2011 and the Ph.D. degree in electrical engineering in 2017 from the University of Málaga, Málaga, Spain. He has been involved in different fields of research. In 2009, he worked on optics with the Instituto de Astrofísica de Canarias. From 2010 to 2013, his main research activities were in microwave circuit design. Since 2014, he has been working on communication theory and random matrix theory to obtain the Ph.D. degree. Since January 2018, he has been a Postdoctoral Fellow with the Electronic and Computer Engineering Department, Hong Kong University of Science and Technology, working on random matrix theory.

He was selected as one of the six Best Student Paper finalists in the National Symposium URSI, Madrid, Spain, 2016. He was an Exemplary Reviewer of the IEEE TRANSACTIONS ON COMMUNICATIONS in 2017. In addition, he has been reviewer of several international journals, illustrating international recognition in communication theory and random matrices, including IEEE TRANSACTIONS ON INFORMATION THEORY, IEEE TRANSACTIONS ON WIRELESS COMMUNICATIONS, IEEE COMMUNICATION LETTER, and *Random Matrices: Theory and Applications* He is also a member of the IEEE Society.

José F. Paris received the M.Sc. and Ph.D. degrees in telecommunication engineering from the Universidad de Málaga, Málaga, Spain, in 1996 and 2004, respectively. From 1994 to 1996, he was with Alcatel, mainly in the development of wireless telephones. In 1997, he joined the Universidad de Málaga, where he is currently a Professor with the Communication Engineering Department. His teaching activities include several courses on digital communications, signal processing, and acoustic engineering. His research interests include wireless communications, especially channel modeling and performance analysis. In 2005, he spent five months as a Visiting Associate Professor with Stanford University, with Prof. A. J. Goldsmith. Since 2017, he has been a Full Professor with the Communication Engineering Department. He received the 2016 Neil Shepherd Memorial Best Propagation Paper Award by the IEEE Vehicular Technology Society. He is an Associate Editor of the IEEE COMMUNICATIONS LETTERS and IEEE TRANSACTIONS ON VEHICULAR TECHNOLOGY.

José A. Cortés received the M.S. and Ph.D. degrees in telecommunication engineering from the Universidad de Málaga, Málaga, Spain, in 1998 and 2007, respectively. In 1999, he was with Alcatel España R&D. In 1999, he joined the Communication Engineering Department, Universidad de Málaga, where he became an Associate Professor in 2010. From 2000 to 2002, he was with the Nokia System Competence Team, Málaga. From 2014 to 2016, he was on a leave of absence, working as a Consultant. As such, he collaborated on the development of Atmels power line communications (PLC) solutions. His research interests include signal processing for communications, channel characterization, and modeling and transmission techniques. He was the co-author of the Best Paper Award at the IEEE International Symposium on Power Line Communications (ISPLC) 2012. He was the TPC Co-Chair of the IEEE ISPLC in 2014 and 2019.

Eduardo Martos-Naya received the M.Sc. and Ph.D. degrees in telecommunication engineering from the University of Málaga, Málaga, Spain, in 1996 and 2005, respectively. In 1997, he joined the Department of Communication Engineering, University of Málaga, where he is currently an Associate Professor. His research interests include digital signal processing for communications, synchronization and channel estimation, and performance analysis of wireless systems. He is currently the Leader of a project supported by the Andalusian regional Government on cooperative and adaptive wireless communications systems.

A.3 An extension of the κ-μ shadowed fading model: statistical characterization and applications

[48] P. Ramírez-Espinosa, F. J. López-Martínez, J. F. París, M. D. Yacoub, and E. Martos-Naya, "An extension of the κ-μ shadowed fading model: Statistical characterization and applications", *IEEE Trans. Veh. Technol.*, vol. 67, no. 5, pp. 3826–3837, May 2018.

An Extension of the κ-μ Shadowed Fading Model: Statistical Characterization and Applications

Pablo Ramirez-Espinosa, F. Javier Lopez-Martinez, *Senior Member, IEEE*, Jose Francisco Paris, Michel Daoud Yacoub, and Eduardo Martos-Naya

***Abstract*—We here introduce an extension and natural generalization of both the κ-μ shadowed and the classical Beckmann fading models: the Fluctuating Beckmann (FB) fading model. This new model considers the clustering of multipath waves on which the line-of-sight (LoS) components randomly fluctuate, together with the effect of in-phase/quadrature power imbalance in the LoS and non-LoS components. Thus, it unifies a variety of important fading distributions as the one-sided Gaussian, Rayleigh, Nakagami-m, Rician, κ-μ, η-μ, η-κ, Beckmann, Rician shadowed, and the κ-μ shadowed distribution. The chief probability functions of the FB fading model, namely probability density function, cumulative distribution function, and moment generating function are derived. The second-order statistics such as the level crossing rate and the average fade duration are also analyzed. These results can be used to derive some performance metrics of interest of wireless communication systems operating over FB fading channels.**

***Index Terms*—Fading channels, Beckmann, Rayleigh, Nakagami -m, Rician, κ-μ, Rician shadowed, κ-μ shadowed.**

I. Introduction

In WIRELESS environments, the radio signal is affected by a number of random phenomena including reflection (both specular and diffuse), diffraction, and scattering as they travel from transmitter to receiver, giving rise to the so-called multipath propagation. At the receiver, the resulting signal appears as a linear combination of the multipath waves, each of which with their own amplitudes and phases. When the number of paths is sufficiently large, the complex baseband signal can be regarded as Gaussian because of the Central Limit Theorem (CLT). Depending on the choice of the parameters characterizing this complex Gaussian random variable, namely the mean and variance of the in-phase and quadrature components, different fading models emerge: Rayleigh (zero-mean and equal variances), Hoyt (zero-mean and unequal variances) and Rice (non-zero mean, equal variances), which are perhaps the most popular fading models arising from the CLT assumption [1], [2].

The most general case (i.e., unequal means and variances for the in-phase and quadrature components) was considered by Beckmann [3], [4] when characterizing the scattering from rough surfaces. However, its greater flexibility comes at the price of an increased mathematical complexity; in fact, its chief probability functions, Probability Density Function (PDF) and Cumulative Distribution Function (CDF) are known to be given in infinite-series form expression [5], as opposed to Rayleigh, Hoyt and Rician models. Other models characterizing the joint effects of imbalances in the mean and variance between in-phase and quadrature components whose PDF and CDF are given in infinite-series form are the so-called η-κ [6], [7] and the very recently proposed α-η-κ-μ [8].

In order to provide a better statistical characterization of the received radio signal in multipath environments, some alternative models have been proposed as generalizations of classical Rayleigh, Hoyt and Rician. By means of considering the effect of clustering of multipath waves, two new fading models arise [9]: the η-μ fading model as a generalization of Hoyt model, well-suited for non line-of-sight (NLoS) propagation environments, and the κ-μ fading model as a generalization of Rice model in line-of-sight[1] (LoS) scenarios. These models have become of widespread use in the recent years because of their flexibility and relatively simple mathematical tractability, as their chief probability functions; PDF, CDF and Moment Generating Function (MGF), are given in closed-form [9]–[11]. Besides, both models also include the versatile and popular Nakagami-m model as particular case [12].

A further generalization of these models was introduced in [13] and [14] under the name of κ-μ shadowed fading distribution. This new distribution provides an additional degree of freedom compared to the κ-μ distribution by allowing the LoS component to randomly fluctuate. Notably, the κ-μ shadowed fading model includes both the κ-μ and η-μ models [15] as special cases, as well as the Rician shadowed fading model [16]. Thus, most popular fading models in the literature for LoS and NLoS conditions are unified under the umbrella of the κ-μ shadowed fading channel model. This greater flexibility does not come at the price of an increased mathematical complexity; in fact, in some cases its PDF and CDF admit a representation

Manuscript received June 28, 2017; revised November 3, 2017; accepted December 20, 2017. Date of publication December 25, 2017; date of current version May 14, 2018. This work was supported in part by the Consejería de Economía, Innovación, Ciencia y Empleo of the Junta de Andalucía, in part by the Spanish Government, and in part by the European Fund for Regional Development FEDER (Projects P2011-TIC-7109, P2011-TIC-8238, and TEC2014-57901-R). The review of this paper was coordinated by Prof. T. Kuerner. *(Corresponding author: Pablo Ramirez-Espinosa.)*

P. Ramirez-Espinosa, F. J. Lopez-Martinez, J. F. Paris, and E. Martos-Naya are with the Departmento de Ingeniería de Comunicaciones, Universidad de Malaga—Campus de Excelencia Internacional Andalucía Tech., Málaga 29071, Spain (e-mail: pre@ic.uma.es; fjlopezm@ic.uma.es; paris@ic.uma.es; eduardo@ic.uma.es).

M. D. Yacoub is with the Wireless Technology Laboratory, School of Electrical and Computer Engineering, University of Campinas, Campinas 13083-970, Brazil (e-mail: michel@decom.fee.unicamp.br).

Color versions of one or more of the figures in this paper are available online at http://ieeexplore.ieee.org.

Digital Object Identifier 10.1109/TVT.2017.2787204

[1] Line-of-sight is used here to mean the more precise phenomenon concerning the presence of dominant components.

in terms of a finite number of powers and exponentials, thus becoming even as tractable as the Nakagami-m distribution [17].

Even though the κ-μ shadowed fading model succeeds on capturing different propagation phenomena such as clustering and LoS fluctuation, it fails when it comes to accounting for the effect of power imbalance in the LoS and NLoS components as originally considered by Beckmann [3], [4]. Motivated by this issue, in this paper we introduce an extended κ-μ shadowed fading model which effectively captures such propagation conditions. This new model can be regarded as a generalization of the original fading model in [13], but also as a generalization of Beckmann fading model by also including the effects of clustering and LoS fluctuation. For this reason, and for the sake of notational brevity, we deem appropriate to name it as the Fluctuating Beckmann (FB) fading model (or equivalently, fading distribution).

The FB model includes as special cases an important set of fading distributions as the one-sided Gaussian, Rayleigh, Nakagami-m, Rician, κ-μ, η-μ, η-κ, Beckmann, Rician shadowed and the κ-μ shadowed distributions.

Interestingly, the CDF and PDF of the FB fading model are given in terms of a well-known function in the context of communication theory, having a functional form similar to the original κ-μ shadowed fading model. The randomization of the LoS component allows for including an additional degree of freedom when compared to the Beckmann model. We provide a full statistical characterization of the FB fading model in terms of its first-order statistics (PDF, CDF and MGF) and second-order statistics (level crossing rate and average fade duration), and then exemplify its applicability to wireless performance analysis.

The remainder of this paper is structured as follows: the physical model of the FB fading distribution is described in Section II. In Section III the PDF, CDF and MGF of this distribution are derived. Then, in Section IV the level crossing rate (LCR) and average fade duration (AFD) are computed. These statistical results are then used to derive some performance metrics of interest in Section V. Finally, the main conclusions are outlined in Section VI.

II. Physical Model

The physical model of the FB distribution arises as a generalization of the physical model of the κ-μ shadowed distribution [13], [18]. The received radio signal is built out of a superposition of radio waves grouped into a number of clusters of waves, and the received signal power W can be expressed in terms of the in-phase and quadrature components of the received signal affected by fading as follows

$$W = \sum_{i=1}^{\mu} \left(X_i + p_i\xi\right)^2 + \left(Y_i + q_i\xi\right)^2, \tag{1}$$

where μ is a natural number indicating the number of clusters, X_i and Y_i are mutually independent Gaussian random processes with $E[X_i] = E[Y_i] = 0$, $E[X_i^2] = \sigma_x^2$, $E[Y_i^2] = \sigma_y^2$, p_i and q_i are real numbers and ξ is[2] a Nakagami-m distributed random variable with shape parameter m and $E[\xi^2] = 1$ which accounts for the fluctuation of the LoS component.

[2]or equivalently, ξ^2 is a Gamma random variable with $E[\xi^2] = 1$, shape parameter m and scale parameter $1/m$.

As opposed to the κ-μ shadowed fading model, we here consider that X_i and Y_i can have different variances. Thus, the effect of power imbalance in the diffuse components associated to non-LoS propagation is considered. Similarly, we also assume that the power of the LoS components can be imbalanced, i.e., $p^2 \triangleq \sum_{i=1}^{\mu} p_i^2 \neq q^2 \triangleq \sum_{i=1}^{\mu} q_i^2$. Hence, the physical model in (1) can be regarded as a generalization of the Beckmann fading model through the consideration of clustering and LoS fluctuation.

III. First Order Statistics

We will now provide a first-order characterization of the FB distribution in terms of its chief probability functions; as we will later see, tractable analytical expressions are attainable for its MGF, PDF and CDF. Hereinafter, we will consider the random variable $\gamma \triangleq \bar{\gamma} W/\overline{W}$, where $\overline{W} = E[W]$, representing the instantaneous SNR at the receiver side.

A. Initial Definitions

Definition 1: Let γ be a random variable characterizing the instantaneous SNR for the physical model in (1). Then, γ is said to follow a Fluctuating Beckmann (FB) distribution with mean $\bar{\gamma} = \mathbb{E}[\gamma]$ and non-negative real shape parameters κ, μ, m, η and ϱ, i.e., $\gamma \sim \mathcal{FB}(\bar{\gamma}; \kappa, \mu, m, \eta, \varrho)$, with

$$\kappa = \frac{p^2 + q^2}{\mu\left(\sigma_x^2 + \sigma_y^2\right)},\ \varrho^2 = \frac{p^2}{q^2},\ \eta = \frac{\sigma_x^2}{\sigma_y^2}, \tag{2}$$

μ representing the number of clusters and m accounts for the fluctuation of the LoS component.

B. First Order Statistics for the General Case

With the above definition, we now calculate the MGF of γ in the following lemma.

Lemma 1: Let $\gamma \sim \mathcal{FB}(\bar{\gamma}; \kappa, \mu, m, \eta, \varrho)$. Then, the MGF of γ is given at the bottom of the next page in (4).

Proof: See Appendix A. ■

Lemma 1 provides a simple closed-form expression for the MGF of the FB fading distribution. From (4), we will now show that the PDF and CDF of the FB fading distribution have a similar functional form as the κ-μ shadowed fading distribution [13].

Lemma 2: Let $\gamma \sim \mathcal{FB}(\bar{\gamma}; \kappa, \mu, m, \eta, \varrho)$. Then, the PDF of γ is given by (5) at the bottom of the next page, where c_x and α_x, with $x = \{1, 2\}$ depend on the parameters of the FB distribution as described in the sequel, and $\Phi_2^{(n)}$ is the confluent form of the generalized Lauricella series defined in [19, eq. (7.2), pp. 446].

Proof: Manipulating (4) it is possible to write the MGF expression as follows

$$M_\gamma(s) = \frac{(-1)^\mu}{s^\mu} \frac{\alpha_2^{m-\mu/2}}{\bar{\gamma}^\mu \alpha_1^m} \left(1 - \frac{\frac{\mu(1+\eta)(1+\kappa)}{2\eta\bar{\gamma}}}{s}\right)^{m-\frac{\mu}{2}} \times \left(1 - \frac{\frac{\mu(1+\eta)(1+\kappa)}{2\bar{\gamma}}}{s}\right)^{m-\frac{\mu}{2}} \left(1 - \frac{c_1}{\bar{\gamma}s}\right)^{-m} \left(1 - \frac{c_2}{\bar{\gamma}s}\right)^{-m}, \tag{3}$$

where $c_{1,2}$ are the roots of $\alpha_1 s^2 + \beta s + 1$ with

$$\alpha_1 = \frac{4\eta}{\mu^2(1+\eta)^2(1+\kappa)^2} + \frac{2\kappa(\varrho^2+\eta)}{m(1+\varrho^2)\mu(1+\eta)(1+\kappa)^2}, \tag{7}$$

$$\beta = \frac{-1}{1+\kappa}\left[\frac{2}{\mu} + \frac{\kappa}{m}\right], \tag{8}$$

and α_2 is given by

$$\alpha_2 = \frac{4\eta}{\mu^2(1+\eta)^2(1+\kappa)^2}. \tag{9}$$

The expression for the PDF can be derived from (3) as $f_\gamma(\gamma) = \mathcal{L}^{-1}\{M_\gamma(-s)\}$ using [20, eq. (9.55)], yielding (5). ■

Lemma 3: Let $\gamma \sim \mathcal{FB}(\bar{\gamma}; \kappa, \mu, m, \eta, \varrho)$. Then, the CDF of γ is given by (6) at the bottom of this page.

Proof: Following the same steps as in the previous proof, the CDF expression is given by $F_\gamma(\gamma) = \mathcal{L}^{-1}\{\frac{M_\gamma(-s)}{s}\}$, yielding (6) directly from [20, eq. (9.55)]. ■

Note that the CDF and PDF of the received signal envelope can be directly derived from (5) and (6) straightforwardly through a change of variables. Thus, we get $f_R(R) = 2Rf_\gamma(R^2)$ and $F_R(R) = F_\gamma(R^2)$, with $\bar{\gamma}$ being replaced by $\Omega = E\{R^2\}$.

The PDF and CDF of the FB distribution are given in terms of the multivariate Φ_2 function, which also appears in other fading distributions in the literature [10], [13], [21]. Apparently, and because it is defined as an n-fold infinite summation, its numerical evaluation may pose some challenges from a computational point of view. However, the Laplace transform of the Φ_2 function has a comparatively simpler form in terms of a finite product of elementary functions, which becomes evident by inspecting the expression of the MGF in (4). Therefore, the Φ_2 function can be evaluated by means of a numerical inverse Laplace transform [22], [23].

As previously mentioned, the FB distribution provides the unification of a large number of important fading distributions. These connections are summarized in Table I, on which the parameters corresponding to the FB distribution are underlined in order to avoid confusion with the parameters of any of the distributions included as special cases. Notably, the Beckmann distribution arises as a special case of the more general FB distribution for $\mu = 1$ and sufficiently large m. Thus, the additional degrees of freedom of the FB distribution also facilitates the anaytical characterization of the Beckmann distribution.

TABLE I
CONNECTIONS BETWEEN THE FLUCTUATING BECKMANN FADING MODEL AND OTHER MODELS IN THE LITERATURE

Channels	Fluctuating Beckmann Fading Parameters
One-sided Gaussian	$\underline{\kappa} = 0,\ \underline{\mu} = 1,\ \underline{\eta} = 0$
Rayleigh	$\underline{\kappa} = 0,\ \underline{\mu} = 1,\ \underline{\eta} = 1$
Nakagami-m	$\underline{\kappa} = 0,\ \underline{\mu} = m,\ \underline{\eta} = 1$
Hoyt	$\underline{\kappa} = 0,\ \underline{\mu} = 1,\ \underline{\eta} = q$
η-μ	$\underline{\kappa} = 0,\ \underline{\mu} = \mu,\ \underline{\eta} = \eta$
Rice	$\underline{\kappa} = K,\ \underline{\mu} = 1,\ \underline{m} \to \infty,\ \underline{\eta} = 1\ ,\forall\varrho$
Symmetrical η-κ	$\underline{\kappa} = \kappa,\ \underline{\mu} = 1,\ \underline{m} \to \infty,\ \underline{\eta} = \eta,\ \underline{\varrho} = \eta$
Asymmetrical η-κ	$\underline{\kappa} = \kappa,\ \underline{\mu} = 1,\ \underline{m} \to \infty,\ \underline{\eta} = \eta,\ \underline{\varrho} = 0$
Beckmann	$\underline{\kappa} = K,\ \underline{\mu} = 1,\ \underline{m} \to \infty,\ \underline{\eta} = q,\ \underline{\varrho} = r$
κ-μ	$\underline{\kappa} = \kappa,\ \underline{\mu} = \mu,\ \underline{m} \to \infty,\ \underline{\eta} = 1,\ \forall\varrho$
Rician Shadowed	$\underline{\kappa} = \kappa,\ \underline{\mu} = 1,\ \underline{m} = m,\ \underline{\eta} = 1,\ \forall\varrho$
κ-μ shadowed	$\underline{\kappa} = \kappa,\ \underline{\mu} = \mu,\ \underline{m} = m,\ \underline{\eta} = 1,\ \forall\varrho$

Note that setting $\kappa = 0$ implies that m and ϱ vanish.

Interestingly, when $\eta = 1$ the effect of the parameter ϱ vanishes; conversely, when setting $\varrho = 1$ the effect of η is still relevant. This is in coherence with the behavior of the Beckmann distribution as observed in [24].

Under certain conditions, the PDF and CDF expressions shown in (5) and (6) can be rewritten in a much simpler way. Specifically, if the m parameter is assumed to be an integer number and the μ parameter to be an even number, (3) can be expressed in an alternative form thanks to partial fraction expansion, allowing the derivation of PDF and CDF in terms of elementary functions (i.e., exponentials and powers). This particular case is detailed in the following subsection.

C. First Order Statistics for the Special Cases

As introduced before, considering the special case in which m parameter is an integer number and μ parameter is an even number, the PDF and the CDF of the FB fading distribution can be expressed in an alternative way which can be useful in that it simplifies further analytical purposes. Under such assumption, more tractable expressions for PDF and CDF in terms of elementary functions are calculated in the following corollaries.

Corollary 1: Let $\gamma \sim \mathcal{FB}(\bar{\gamma}; \kappa, \mu, m, \eta, \varrho)$ with m being an integer number and μ an even number. Then, the PDF of γ is

$$M_\gamma(s) = \frac{1}{\left(1 - \frac{2\eta}{\mu(1+\eta)(1+\kappa)}\bar{\gamma}s\right)^{\mu/2}\left(1 - \frac{2}{\mu(1+\eta)(1+\kappa)}\bar{\gamma}s\right)^{\mu/2}} \times \left[1 - \frac{1}{m}\left(\frac{\mu\kappa\left(\frac{\varrho^2}{1+\varrho^2}\right)(1+\eta)\bar{\gamma}s}{(1+\eta)(1+\kappa)\mu - 2\eta\bar{\gamma}s} + \frac{\mu\kappa\left(\frac{1}{1+\varrho^2}\right)(1+\eta)\bar{\gamma}s}{(1+\eta)(1+\kappa)\mu - 2\bar{\gamma}s}\right)\right]^{-m}. \tag{4}$$

$$f_\gamma(\gamma) = \frac{\alpha_2^{m-\mu/2}\gamma^{\mu-1}}{\bar{\gamma}^\mu\Gamma(\mu)\alpha_1^m}\Phi_2^{(4)}\left(-m+\frac{\mu}{2}, -m+\frac{\mu}{2}, m, m; \mu; \frac{-\gamma}{\bar{\gamma}\sqrt{\eta\alpha_2}}, \frac{-\gamma\sqrt{\eta}}{\bar{\gamma}\sqrt{\alpha_2}}, \frac{-\gamma c_1}{\bar{\gamma}}, \frac{-\gamma c_2}{\bar{\gamma}}\right). \tag{5}$$

$$F_\gamma(\gamma) = \frac{\alpha_2^{m-\mu/2}\gamma^{\mu}}{\bar{\gamma}^\mu\Gamma(\mu+1)\alpha_1^m}\Phi_2^{(4)}\left(-m+\frac{\mu}{2}, -m+\frac{\mu}{2}, m, m; \mu+1; \frac{-\gamma}{\bar{\gamma}\sqrt{\eta\alpha_2}}, \frac{-\gamma\sqrt{\eta}}{\bar{\gamma}\sqrt{\alpha_2}}, \frac{-\gamma c_1}{\bar{\gamma}}, \frac{-\gamma c_2}{\bar{\gamma}}\right). \tag{6}$$

given by

$$f_\gamma(\gamma) = \frac{\alpha_2^{m-\frac{\mu}{2}}}{\alpha_1^m \bar{\gamma}^\mu} \sum_{i=1}^{N(m,\mu)} e^{-\tau_i \gamma/\bar{\gamma}} \sum_{j=1}^{|\omega_i|} \frac{A_{ij}\gamma^{j-1}}{(j-1)!}, \quad (10)$$

where A_{ij} are the residues of partial fraction decomposition given by (51), constants ω_i and τ_i are the elements of vector $\boldsymbol{\omega}$ and $\boldsymbol{\tau}$, defined as

$$\boldsymbol{\omega} = \left[m, m, \frac{\mu}{2} - m, \frac{\mu}{2} - m\right], \quad (11)$$

$$\boldsymbol{\tau} = \left[c_1, c_2, \frac{\mu(1+\eta)(1+\kappa)}{2\eta}, \frac{\mu(1+\eta)(1+\kappa)}{2}\right], \quad (12)$$

and $N(m,\mu)$ is defined as

$$N(m,\mu) = 2\left[1 + \mathrm{u}\left(\frac{\mu}{2} - m\right)\right], \quad (13)$$

where $\mathrm{u}(\cdot)$ is the unit step function whose value is 1 if the argument is non-negative and 0 otherwise.

Proof: See Appendix B. ■

Corollary 2: Let $\gamma \sim \mathcal{FB}(\bar{\gamma}; \kappa, \mu, m, \eta, \varrho)$ with m being an integer number and μ an even number. Then, the CDF of γ is given by

$$F_\gamma(\gamma) = 1 + \frac{\alpha_2^{m-\frac{\mu}{2}}}{\alpha_1^m \bar{\gamma}^\mu} \sum_{i=1}^{N(m,\mu)} e^{-\tau_i \gamma/\bar{\gamma}} \sum_{j=1}^{|\omega_i|} \frac{B_{ij}\gamma^{j-1}}{(j-1)!}. \quad (14)$$

Proof: See Appendix C. ■

We here provide more tractable expressions for both PDF and CDF of FB distribution in terms of a finite sum of elementary functions, avoiding the use of multivariate Φ_2 function. However, this simplification comes at the price of a mild loss of generality in that both m and μ parameters are restricted to be an integer and even number, respectively.

IV. Second Order Statistics

First-order statistics such as the PDF, CDF or MGF provide valuable information about the statistical behavior of the amplitude (or equivalently power) of the received signal affected by fading. However, they do not incorporate information related to the dynamic behavior of the fading process, which is of paramount relevance in the context of wireless communications because of the relative motion of transmitter, receivers and scatterers due to mobility. In the literature, two metrics are used to capture the dynamics of a general random process: the level crossing rate (LCR), which measures how often the amplitude of the received signal crosses a given threshold value, and the average fade duration (AFD), which measures how long the amplitude of the received signal remains below this threshold [1].

A. Level Crossing Rate

The LCR of the received signal amplitude R can be computed using Rice's formula [1] as

$$N_R(u) = \int_0^\infty \dot{r} f_{R,\dot{R}}(u, \dot{r})\, d\dot{r}, \quad (15)$$

where $\dot{R}$ denotes the time derivative of the signal envelope and $f_{R,\dot{R}}(r, \dot{r})$ is the joint PDF of the received signal amplitude and its time derivative. Thus, in order to characterize the LCR of R, we must calculate the joint distribution of R and $\dot{R}$. In our derivations, we will assume that the fluctuations in the diffuse part (i.e., NLoS) occur at a smaller scale compared to those of the LoS component in the fluctuating Beckmann fading model. This is the case, for instance, on which such LoS fluctuation can be associated to shadowing.

Let us express the squared signal envelope as

$$R^2 = R_1^2 + R_2^2. \quad (16)$$

where R_1 and R_2 are defined as

$$R_1^2 = \sum_{k=1}^{\mu}(X_k + \xi p_k)^2, \quad R_2^2 = \sum_{k=1}^{\mu}(Y_k + \xi q_k)^2, \quad (17)$$

Note that both variables, when conditioned to ξ, are independent. After normalizing by $\Omega = E[R^2]$, we have that R_1 and R_2 are distributed as a κ-μ random variables, with PDF given by

$$f_{R_k}(r_k) = \frac{\Omega^{\mu/4+1/2}}{\sigma_k^2(\xi d_k)^{\mu/2-1}}\, r_k^{\mu/2}\, e^{-\frac{\Omega r_k^2}{2\sigma_k^2} - \frac{\xi^2 d_k^2}{2\sigma_k^2}}\, I_{\mu/2-1}\left(\frac{\Omega^{1/2} r_k \xi d_k}{\sigma_k^2}\right), \quad (18)$$

where $d_1^2 = p^2 = \sum_{k=1}^{\mu} p_k^2$, $d_2^2 = q^2 = \sum_{k=1}^{\mu} q_k^2$, $\mathrm{I}_\nu(\cdot)$ is the modified Bessel function of the first kind and ξ is a Nakagami-m distributed random variable with PDF given by

$$f_\xi(\xi) = \frac{2m^m}{\Gamma(m)} \xi^{2m-1} \exp(-m\xi^2). \quad (19)$$

The derivative of R with respect to time, $\dot{R}$, can be expressed as

$$\dot{R} = \frac{\dot{R}_1 R_1 + \dot{R}_2 R_2}{R}. \quad (20)$$

Conditioned to R_1, R_2 and R, the derivative of R is a zero-mean Gaussian variable with variance

$$\sigma_{\dot{R}}^2 = \frac{\sigma_{\dot{R}_1}^2 R_1^2 + \sigma_{\dot{R}_2}^2 R_2^2}{R^2} = \frac{\sigma_{\dot{R}_1}^2 R_1^2 + \sigma_{\dot{R}_2}^2 R_2^2}{R_1^2 + R_2^2}. \quad (21)$$

Hence, the distribution of $\dot{R}$ conditioned to R_1 and R_2 is

$$f_{\dot{R}|R_1,R_2}(\dot{r}, r_1, r_2) = \frac{1}{\sqrt{2\pi\left(\frac{\sigma_{\dot{r}_1}^2 r_1^2 + \sigma_{\dot{r}_2}^2 r_2^2}{r_1^2 + r_2^2}\right)}} \cdot e^{-\frac{(r_1^2+r_2^2)\dot{r}^2}{2(\sigma_{\dot{r}_1}^2 r_1^2 + \sigma_{\dot{r}_2}^2 r_2^2)}}, \quad (22)$$

The LCR can be obtained as

$$\begin{aligned} N_R(u) &= \int_0^\infty \dot{r} f_{R,\dot{R}}(u,\dot{r}) d\dot{r} \\ &= \int_0^\infty \dot{r} \left(\int_0^u f_{\dot{R}|R,R1}(\dot{r},u,r_1) f_{R,R1}(u,r_1) dr_1 \right) d\dot{r} \\ &= \int_0^u f_{R,R_1}(u,r_1) \left(\int_0^\infty \dot{r} f_{\dot{R}|R,R_1}(\dot{r},u,r_1) d\dot{r} \right) dr_1. \end{aligned}$$

Using the PDF of $\dot{R}$ conditioned to R and R_1 in (22),

$$\int_0^\infty \dot{r} f_{\dot{R}|R,R_1}(\dot{r},u,r_1) d\dot{r} = \sqrt{\frac{\sigma_{\dot{R}}^2}{2\pi}}. \tag{23}$$

The joint distribution of R_1 and R_2 can be obtained as

$$\begin{aligned} f_{R_1,R_2}(r_1,r_2) &= \int_0^\infty f_{R_1|\xi}(r_1,\xi) f_{R_2|\xi}(r_2,\xi) f_\Xi(\xi) d\xi \\ &= \frac{2m^m \Omega^{\mu/2+1}}{\Gamma(m)\sigma_1^2\sigma_2^2 (pq)^{\mu/2-1}} r_1^{\mu/2} r_2^{\mu/2} \exp\left(-r_1^2 \frac{\Omega}{2\sigma_1^2} - r_2^2 \frac{\Omega}{2\sigma_2^2} \right) \\ &\quad \times \int_0^\infty \left\{ \xi^{2m-\mu+1} \exp\left(-\xi^2 \left(\frac{p^2}{2\sigma_1^2} + \frac{q^2}{2\sigma_2^2} + m \right) \right) \right. \\ &\quad \left. \times \mathrm{I}_{\mu/2-1}\left(\frac{\Omega^{1/2} r_1 \xi p}{\sigma_1^2} \right) \mathrm{I}_{\mu/2-1}\left(\frac{\Omega^{1/2} r_2 \xi q}{\sigma_2^2} \right) d\xi \right\}. \end{aligned} \tag{24}$$

In the general case, the last integral cannot be solved analytically in closed-form, to the best of the authors' knowledge.

B. Level Crossing Rate for Independent In-Phase and Quadrature Components

As can be seen, the LCR obtained in the previous section involves the calculation of two integrals. It is possible to arrive at a more tractable expression for a simpler yet general case by considering the scenario in which in-phase and quadrature components are independent. We note, however, that such a scenario is still a FB fading model, and does not bear any similarity with any other previous model published in the literature. Independence between in-phase and quadrature components can be achieved by assuming $q_i = 0$ and $p_i \neq 0$ or vice-versa in (1).

Assuming the special case of $q_i = 0$ (the case of $p_i = 0$ can be solved similarly) in which R_1 and R_2 are independent, the distribution of $f_{R,R_1}(r,r_1)$ can be obtained as

$$\begin{aligned} f_{R,R_1}(u,r_1) &= |J_{r_1,r_2}(u,r_1)| f_{R_1,R_2}\left(r_1, \sqrt{u^2 - r_1^2} \right) \\ &= |J_{r_1,r_2}(u,r_1)| f_{R_1}(r_1) f_{R_2}\left(\sqrt{u^2 - r_1^2} \right) \\ &= \frac{m^m \Omega^\mu u \cdot r_1^{\mu-1} \cdot (u^2 - r_1^2)^{\mu/2-1}}{2^{\mu-2}\Gamma^2(\mu/2)\sigma_1^\mu \sigma_2^\mu (\frac{p^2}{2\sigma_1^2} + m)^m} \\ &\quad \times e^{-\frac{\Omega(u^2-r_1^2)}{2\sigma_2^2} - \frac{\Omega r_1^2}{2\sigma_1^2}} \cdot {}_1F_1\left(m, \mu/2; \frac{\Omega \frac{p^2}{4\sigma_1^4}}{\frac{p^2}{2\sigma_1^2} + m} r_1^2 \right), \end{aligned} \tag{25}$$

for $0 \leq r_1 \leq r$, where $|J_{r_1,r_2}(\cdot,\cdot)|$ denotes the Jacobian of the transformation of random variables and ${}_1F_1(\cdot)$ is the confluent hypergeometric function [25]. In this particular case, the LCR of the normalized envelope R can be expressed as

$$\begin{aligned} N_R(u) &= \frac{m^m \Omega^\mu u}{2^{\mu-2}\Gamma^2(\mu/2)\sigma_1^\mu \sigma_2^\mu (\frac{p^2}{2\sigma_1^2} + m)^m \sqrt{2\pi}} \\ &\quad \times \int_0^u \left(\sigma_{\dot{R}_1}^2 r_1^2/u^2 + \sigma_{\dot{R}_2}^2 (1 - r_1^2/u^2) \right)^{\frac{1}{2}} (u^2 - r_1^2)^{\mu/2-1} \\ &\quad \times r_1^{\mu-1} e^{-\frac{\Omega(u^2-r_1^2)}{2\sigma_2^2} - \frac{\Omega r_1^2}{2\sigma_1^2}} {}_1F_1\left(m, \frac{\mu}{2}; \frac{\Omega \frac{p^2}{4\sigma_1^4}}{\frac{p^2}{2\sigma_1^2} + m} r_1^2 \right) dr_1, \end{aligned} \tag{26}$$

and after a change of variables we have

$$\begin{aligned} N_R(u) &= \frac{m^m \Omega^\mu u^{(2\mu-1)}}{2^{\mu-1}\Gamma^2(\mu/2)\sigma_1^\mu \sigma_2^\mu (\frac{p^2}{2\sigma_1^2} + m)^m \sqrt{2\pi}} \cdot e^{-\frac{\Omega u^2}{2\sigma_2^2}} \\ &\quad \times \int_0^1 [\sigma_{\dot{R}_2}^2 + (\sigma_{\dot{R}_1}^2 - \sigma_{\dot{R}_2}^2)x]^{\frac{1}{2}} (1-x)^{(\mu/2-1)} x^{(\mu/2-1)} \\ &\quad \times e^{-\frac{\Omega(\sigma_2^2 - \sigma_1^2)u^2 x}{2\sigma_1^2\sigma_2^2}} {}_1F_1\left(m, \frac{\mu}{2}; \frac{\Omega \frac{p^2}{4\sigma_1^4}}{\frac{p^2}{2\sigma_1^2} + m} u^2 x \right) dx, \end{aligned} \tag{27}$$

where $\sigma_{\dot{R}_1}^2 = \frac{-\ddot{\rho}(0)\sigma_1^2}{\Omega}$ and $\sigma_{\dot{R}_2}^2 = \frac{-\ddot{\rho}(0)\sigma_2^2}{\Omega}$ from (21), and $\ddot{\rho}(0)$ is the second derivative of the autocorrelation function evaluated at 0.

Finally, (26) can be expressed in terms of the parameters of the FB distribution[3], yielding

$$\begin{aligned} N_R(u) &= \frac{m^m [\mu(1+\eta)(1+\kappa)]^{\mu-1/2} \sqrt{-\ddot{\rho}(0)}}{2^{\mu-1}\Gamma^2(\mu/2)\eta^{\mu/2} (\frac{\mu\kappa(1+\eta)}{2\eta} + m)^m \sqrt{2\pi}} \cdot u^{(2\mu-1)} \\ &\quad \times e^{-\mu/2(1+\eta)(1+\kappa)u^2} \int_0^1 [1+(\eta-1)x]^{\frac{1}{2}} (1-x)^{(\mu/2-1)} x^{(\mu/2-1)} \\ &\quad \times e^{-\frac{\mu(1-\eta^2)(1+\kappa)}{2\eta} u^2 x} {}_1F_1\left(m, \mu/2; \frac{\frac{\kappa\mu^2(1+\eta)^2(1+\kappa)}{4\eta^2}}{\frac{\mu\kappa(1+\eta)}{2\eta} + m} u^2 x \right) dx. \end{aligned} \tag{28}$$

Note that, although above result for the LCR has been derived for the special case $q_i = 0$, it is fully equivalent to the case with $p_i = 0$ just setting $\eta \to 1/\eta$, since both cases are actually the same, as can be seen in (1).

C. Average Fade Duration

With the knowledge of the LCR and the CDF of the FB distribution, the AFD can be directly obtained as

$$T_R(u) = \frac{F_R(u)}{N_R(u)}, \tag{29}$$

where $F_R(u)$ is the CDF of the fading amplitude envelope derived in (6), after a proper change of variables.

V. Numerical Results and Applications

A. First Order Statistics

After attaining a full statistical characterization of the newly proposed Fluctuating Beckmann fading distribution, we aim to

[3]Note that, because of the assumption of $q_k = 0$, this implies that the parameter $\varrho \to \infty$.

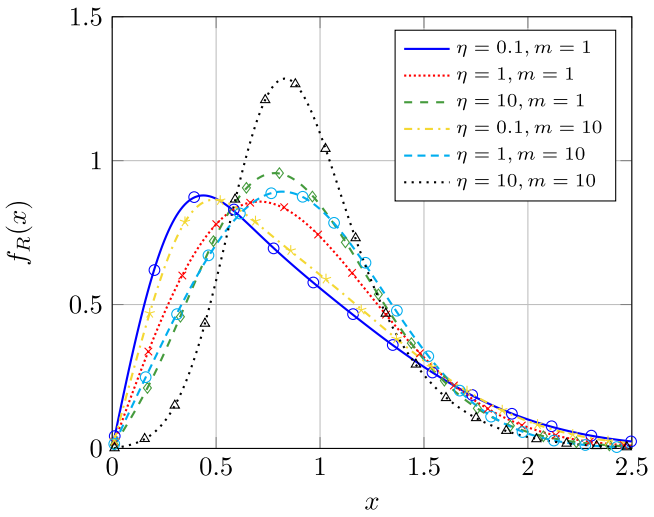

Fig. 1. FB signal envelope distribution for different values of η and m in weak LoS scenario ($\kappa = 1$) with $\varrho^2 = 0.1$, $\mu = 1$ and $\Omega = E\{R^2\} = 1$. Solid lines correspond to the exact PDF, markers correspond Monte Carlo simulations.

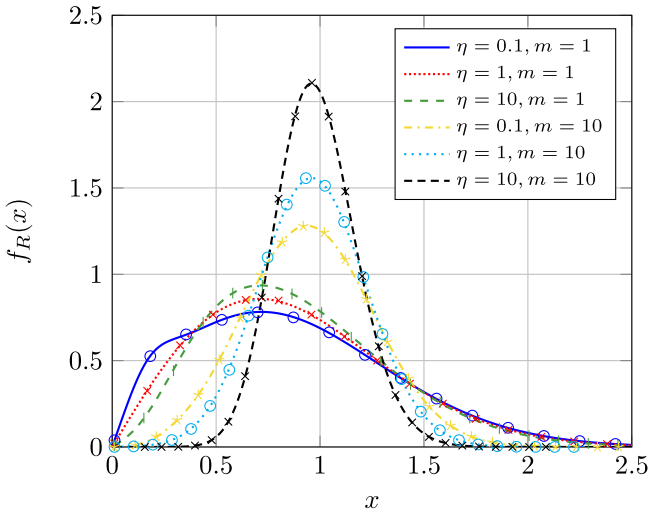

Fig. 2. FB signal envelope distribution for different values of η and m in strong LoS scenario ($\kappa = 10$) with $\varrho^2 = 0.1$, $\mu = 1$ and $\Omega = E\{R^2\} = 1$. Solid lines correspond to the exact PDF, markers correspond Monte Carlo simulations.

exemplify the influence of the parameters of this fading model over the distribution of the received amplitude. We will first focus on understanding the effect of the power imbalance in the LoS and NLoS components (i.e., the effect of ϱ and η), since these are the two parameters that effectively extend the original κ-μ shadowed fading model to a more general case. Monte Carlo simulations are provided in order to double-check the validity of the derived expressions.

In Figs. 1 and 2, the PDF of the received signal amplitude is represented for different values of NLoS power imbalance η and LoS fluctuation severity m. The values $m = 1$ and $m = 10$ correspond to the cases of heavy and mild fluctuation of the LoS component, respectively. The parameter ϱ is set to $\varrho^2 = 0.1$, indicating a moderately large LoS power imbalance, and $\mu = 1$. Let us first focus on Fig. 1, where we set $\kappa = 1$ to indicate

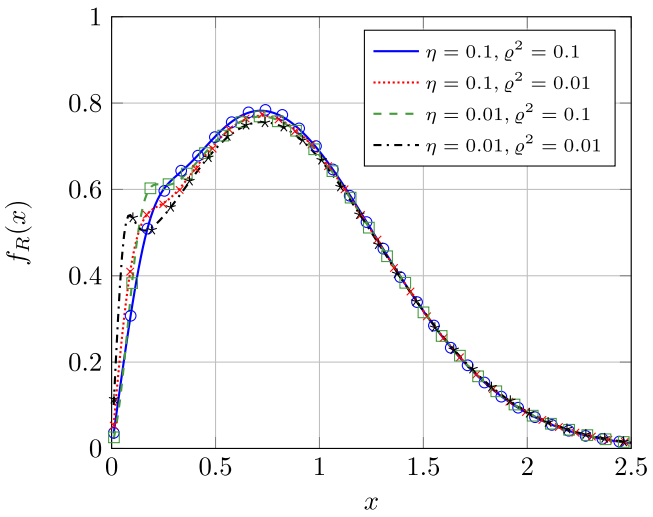

Fig. 3. FB signal envelope distribution for different values of η and ϱ in strong LoS scenario ($\kappa = 10$) with $m = 1$, $\mu = 1$ and $\Omega = E\{R^2\} = 1$. Solid lines correspond to the exact PDF, markers correspond Monte Carlo simulations.

a weak LoS scenario on which the LoS and NLoS power is the same. We observe that the effect of increasing η causes the amplitude values to be more concentrated around its mean value. Besides, compared to the case of $\eta = 1$ (i.e., the κ-μ shadowed fading distribution), the effect of having a power imbalance in the NLoS component clearly has an impact on the distribution of the signal envelope. Differently from the η-μ fading model, the behavior of the distribution with respect to η is no longer symmetrical between $\eta \in [0, 1]$ and $\eta \in [1, \infty)$ for a fixed $\varrho \neq 1$. One interesting effect comes from the observation of the effect of increasing η: both setting $\eta = 0.1$ or $\eta = 10$ implies that the NLoS power is imbalanced by a factor of 10. However, it is evident that if this NLoS imbalance goes to the component associated with a larger LoS imbalance ($\eta = 0.1$ since we have $\varrho^2 = 0.1$), this is way more detrimental for the received signal envelope than having the NLoS imbalance in the other component.

Fig. 2 now considers a strong LoS scenario on which $\kappa = 10$. The rest of the parameters are the same ones as in the previous figure. Because the LoS component is now much more relevant, the effect of changing m is more noticeable. We observe that for $m = 10$, which corresponds to a mild fluctuation on the LoS component, the shape of the PDF is only slightly altered when changing η. Conversely, the shape of the PDF is more affected by η for low values of amplitude when $m = 1$. This is further exemplified in Fig. 3, on which a bimodal behavior is observed as the imbalance is reduced through ϱ or η. When both $\{\varrho, \eta\}$ decrease, the in-phase components have considerably less power than the quadrature components. Because κ is sufficiently large, the distribution will mostly fluctuate close to the LoS part of the quadrature component due to m, and the first maximum on the PDF in the low-amplitude region appears as the highly imbalanced in-phase component only is able to contribute in this region. We must note that this bimodal behavior does not appear in the original κ-μ shadowed or Beckmann distributions from which the FB distribution originates. Nevertheless, such bimodality indeed shows in other fading models such as the α-

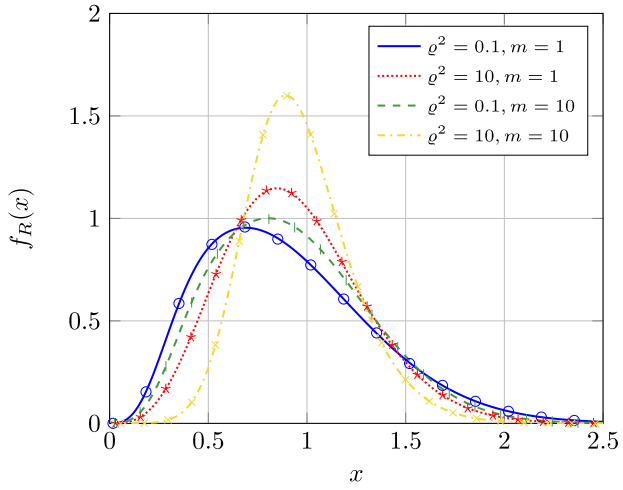

Fig. 4. FB signal envelope distribution for different values of ϱ and m in weak LoS scenario ($\kappa = 1$) with $\eta = 0.1$, $\mu = 2$ and $\Omega = E\{R^2\} = 1$. Solid lines correspond to the exact PDF derived, markers correspond Monte Carlo simulations.

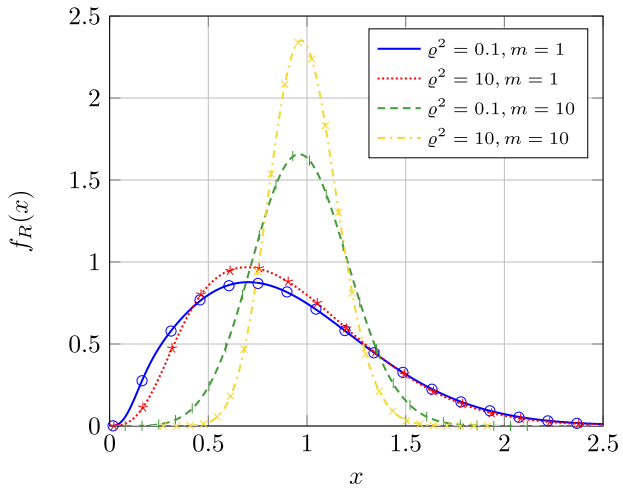

Fig. 5. FB signal envelope distribution for different values of ϱ and m in strong LoS scenario($\kappa = 10$) with $\eta = 0.1$, $\mu = 2$ and $\Omega = E\{R^2\} = 1$. Solid lines correspond to the exact PDF, markers correspond Monte Carlo simulations.

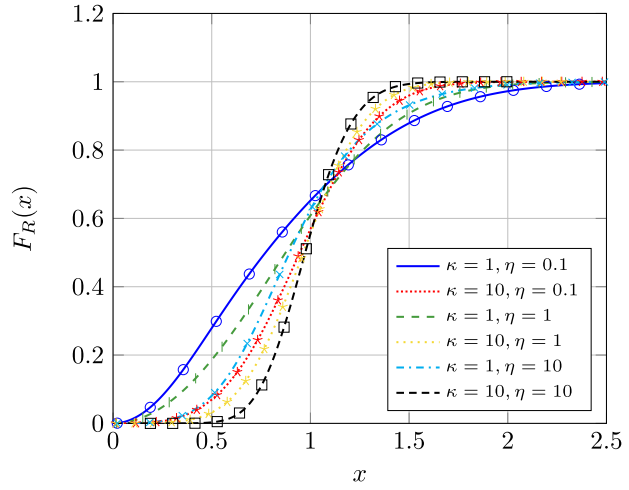

Fig. 6. FB signal envelope CDF for different values of κ and η with $\varrho^2 = 0.1$, $\mu = 1, m = 10$ and $\Omega = E\{R^2\} = 1$. Solid lines correspond to the exact CDF, markers correspond Monte Carlo simulations.

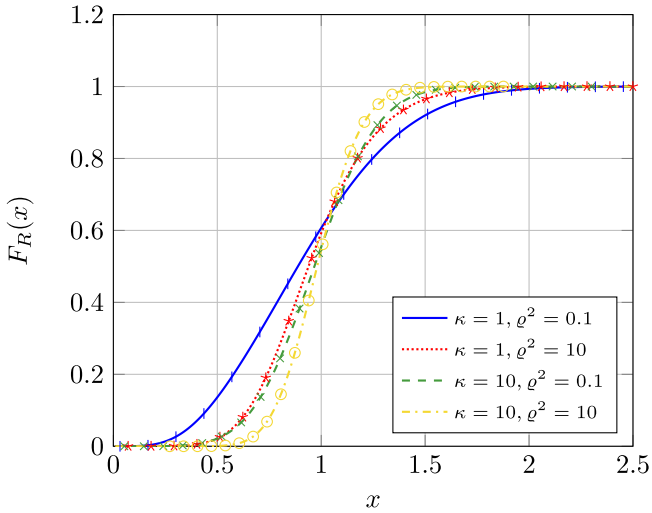

Fig. 7. FB signal envelope CDF for different values of κ and ϱ with $\eta = 0.1$, $\mu = 2, m = 10$ and $\Omega = E\{R^2\} = 1$. Solid lines correspond to the exact CDF, markers correspond Monte Carlo simulations.

η-κ-μ [8], the two-wave with diffuse power [26], the fluctuating two-ray [21] and some others [18], [27].

We represent in Figs. 4 and 5 the PDF of the received signal amplitude for different values of LoS power imbalance ϱ and LoS fluctuation severity m. We first consider the weak LoS scenario with $\kappa = 1$, and setting $\mu = 2$ and $\eta = 0.1$. We observe that low values of ϱ and m cause the amplitude values being more sparse. When the LoS component is stronger, i.e., $\kappa = 10$ in Fig. 5 the effect of increasing m (i.e., eliminating the LoS fluctuation) or ϱ is more relevant.

Figs. 6 and 7 are useful to understanding the effect of the parameters ϱ and η over the CDF. Spefically, in Fig. 6 we compare the shape of the CDF in weak and strong LoS scenarios as η varies. The LoS fluctuation parameter is set to $m = 10$ in order to eliminate its influence, whereas $\varrho^2 = 0.1$ and $\mu = 1$. We observe that increasing either η or κ makes the slope of the CDF rise close to $x = 1$. A similar observation can be made when inspecting Fig. 7. We see that having the LoS and NLoS imbalances in the same component ($\varrho^2 = \eta = 0.1$) is more detrimental for the signal envelope, and the probability of having very low values of signal level is higher.

B. Second Order Statistics

We will now investigate the effect of the FB fading parameters on the second-order statistics of the distribution. We assume that a time variation of the diffuse component according to Clarke's correlation model [28] with maximum Doppler shift f_d; this implies that $\sqrt{-\ddot{\rho}} = \sqrt{2} f_d \pi$ [29]. As argued in Section IV, we consider that $\varrho \to \infty$ and hence the LCR and AFD are given by (28) and (29). Monte Carlo simulations are also included, by generating a sampled fluctuating Beckmann random process with sampling period $T_s >> f_d$ in order to avoid missing level crossings at very low threshold values [30].

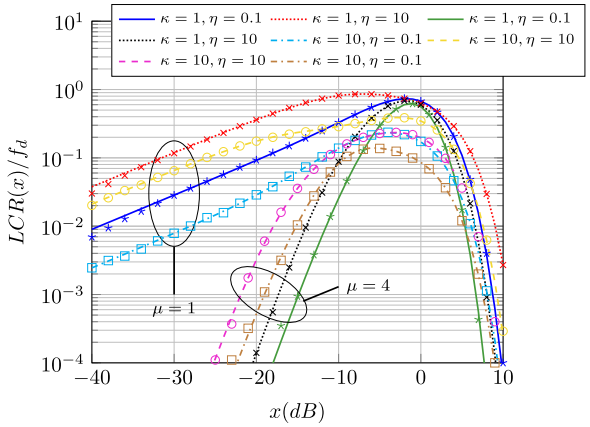

Fig. 8. Normalized LCR vs threshold value x (dB) normalized to Ω for different values of κ, η and μ, with $m = 1$ and $\varrho \to \infty$. Solid lines correspond to the exact LCR, markers correspond Monte Carlo simulations.

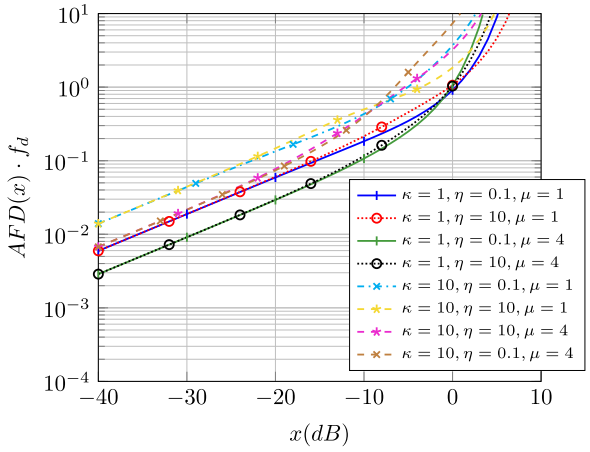

Fig. 9. Normalized AFD vs threshold value x (dB) normalized to Ω for different values of κ, η and μ, with $m = 1$ and $\varrho \to \infty$. Solid lines correspond to the exact AFD, markers correspond Monte Carlo simulations.

Fig. 8 represents the LCR vs the normalized threshold for different sets of fading parameter values. When increasing μ, i.e., the number of multipath clusters, the number of crossings at very low threshold values is drastically reduced. Similarly, the number of crossings in this region grows when reducing κ or increasing η. This latter effect is coherent with the fact that $\varrho \to \infty$ in this case, so that having a value of $\eta < 1$ is beneficial in terms of fading severity. Thus, the maximum number of crossings for low threshold values in the investigated scenarios is attained for low μ and κ, and large η.

Fig. 9 represents the AFD vs the normalized threshold for the same set of fading parameter values as in Fig. 8. Interestingly, we see that the duration of deep fades is not affected by η. We also observe that a larger AFD is associated with a lower value of μ and a larger value of κ; this is in coherence with the observations in [31] for the particular case of the κ-μ fading model.

C. Error Probability Analysis

We now exemplify how the performance analysis of wireless communication systems operating under FB fading can be carried out. For the sake of simplicity, we here focus on the symbol error probability (SEP) analysis for a number of well-known modulation schemes.

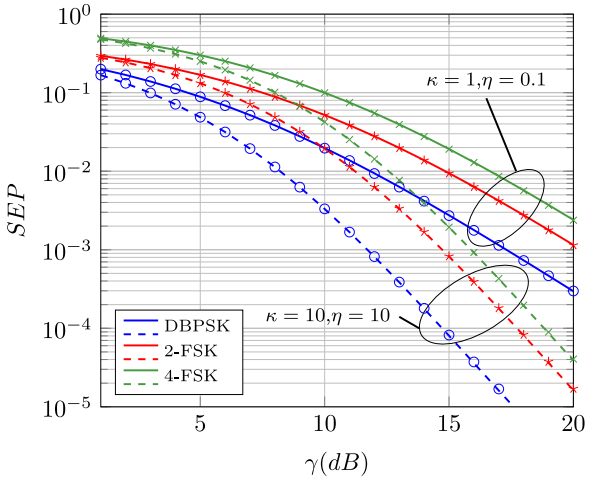

Fig. 10. SEP vs. γ for different values of κ and η and different modulation schemes. Parameter values are $m = 4$, $\mu = 2$ and $\varrho^2 = 0.2$. Solid lines correspond to the exact SEP, markers correspond Monte Carlo simulations.

The SEP in the presence of fading is known to be given by

$$P_s(\bar{\gamma}) = \int_0^\infty P_{AWGN}(\gamma) f_\gamma(\gamma) d\gamma, \tag{30}$$

where $P_{AWGN}(\gamma)$ is the symbol error probability in the AWGN case, which is given by [5, eq. (8.85)] when using coherent DBPSK (Differential Binary Phase-Shift Keying) modulation. Since the SEP of DBPSK modulation has exponential form, introducing this in the above equation yields

$$P_s(\bar{\gamma}) = \frac{1}{2} \int_0^\infty e^{-\gamma} f_\gamma(\gamma) d\gamma, \tag{31}$$

which is fully equivalent to

$$P_s(\bar{\gamma}) = \frac{1}{2} M_\gamma(s)|_{s=-1}. \tag{32}$$

Thus, the SEP of DPBSK when assuming the FB fading model is given in (34) at the top of the next page.

In the case of assuming orthogonal M-ary FSK (Frequency-Shift Keying) signals and non-coherent demodulation, the symbol error probability over AWGN channels is given in [5, eq. (8.67] as

$$P_s(\bar{\gamma}) = \sum_{n=1}^{M-1} (-1)^{n+1} \binom{M-1}{n} \frac{1}{n+1} M_\gamma(s)\Big|_{s=\frac{-n}{n+1}}, \tag{33}$$

yielding the expression given in (35) at the top of the next page when assuming the FB fading model.

The SEP is evaluated in Fig. 10, assuming coherent DBPSK, and non-coherent 2-FSK and 4-FSK. We observe that the SEP performance of DBPSK is much better than the non-coherent schemes, especially when the fading severity is reduced (i.e., large κ and η, for $\varrho < 1$).

VI. Conclusion

We presented an extension of the κ-μ shadowed fading distribution, by including the effects of power imbalance between

$$P_s(\bar{\gamma}) = \frac{1}{2\left(1+\frac{2\eta}{\mu(1+\eta)(1+\kappa)}\bar{\gamma}\right)^{\mu/2}\left(1+\frac{2}{\mu(1+\eta)(1+\kappa)}\bar{\gamma}\right)^{\mu/2}} \times\left[1+\frac{1}{m}\left(\frac{\mu\kappa\left(\frac{\varrho^2}{1+\varrho^2}\right)(1+\eta)\bar{\gamma}}{(1+\eta)(1+\kappa)\mu+2\eta\bar{\gamma}}+\frac{\mu\kappa\left(\frac{1}{1+\varrho^2}\right)(1+\eta)\bar{\gamma}}{(1+\eta)(1+\kappa)\mu+2\bar{\gamma}}\right)\right]^{-m}. \tag{34}$$

$$P_s(\bar{\gamma}) = \sum_{n=1}^{M-1}(-1)^{n+1}\binom{M-1}{n}\frac{1}{n+1}\times\frac{1}{\left(1+\frac{2n\eta}{(n+1)\mu(1+\eta)(1+\kappa)}\bar{\gamma}\right)^{\mu/2}}\times\frac{1}{\left(1+\frac{2n}{(n+1)\mu(1+\eta)(1+\kappa)}\bar{\gamma}\right)^{\mu/2}} \times\left[1+\frac{1}{m}\left(\frac{\mu\kappa\left(\frac{\varrho^2}{1+\varrho^2}\right)(1+\eta)\bar{\gamma}\left(\frac{n}{n+1}\right)}{(1+\eta)(1+\kappa)\mu+2\eta\bar{\gamma}\left(\frac{n}{n+1}\right)}+\frac{\mu\kappa\left(\frac{1}{1+\varrho^2}\right)(1+\eta)\bar{\gamma}\left(\frac{n}{n+1}\right)}{(1+\eta)(1+\kappa)\mu+2\bar{\gamma}\left(\frac{n}{n+1}\right)}\right)\right]^{-m}. \tag{35}$$

the LoS and NLoS components through two additional parameters, ϱ and η, respectively. This generalization also includes the classical and notoriously unwieldy Beckmann fading distribution as special case, with the advantage of admitting a relatively simple analytical characterization when compared to state-of-the-art fading models. Thus, we are able to unify a wide set of fading models in the literature under the umbrella of a more general model, for which we suggest the name of Fluctuating Beckmann fading model.

We observed that when the LoS and NLoS imbalances are both large for the same component (i.e., $\varrho < 1$ and $\eta < 1$ for the in-phase component, or $\varrho > 1$ and $\eta > 1$ for the quadrature component), the fading severity is increased. Conversely, when the LoS imbalance is larger in one component (e.g., $\varrho < 1$) it is beneficial that its NLoS part has less power (i.e., $\eta > 1$ in this case) in order to reduce fading severity. Strikingly and somehow counterintuitively, the FB distribution exhibits a bimodal behavior in some specific scenarios, unlike the distributions from which it originates.

Appendix A
Proof of Lemma I

Let us consider the physical model in (1). Specializing for $\mu = 1$, the conditional MGF of the signal power W given ξ follows a Beckmann distribution with MGF given by [5, eq. (2.38)]

$$M_W(s|\xi) = \frac{1}{(1-2\sigma_x^2 s)^{1/2}(1-2\sigma_y^2 s)^{1/2}} \times\exp\left(\frac{p_1^2\xi s}{1-2\sigma_x^2 s}+\frac{q_1^2\xi s}{1-2\sigma_y^2 s}\right). \tag{36}$$

Since the Gaussian processes within (1) are mutually independent, then the conditional moment-generating function of the FB distribution can be obtained by multiplying the μ terms of the sum. Thus, the conditional MGF of the signal power W is given by

$$M_W(s|\xi) = \frac{1}{(1-2\sigma_x^2 s)^{\mu/2}(1-2\sigma_y^2 s)^{\mu/2}} \times\exp\left(\frac{p^2\xi s}{1-2\sigma_x^2 s}+\frac{q^2\xi s}{1-2\sigma_y^2 s}\right), \tag{37}$$

where $p^2 = \sum_{i=1}^{\mu} p_i^2$ and $q^2 = \sum_{i=1}^{\mu} q_i^2$.

With the definitions in (2), the conditional MGF in (37) can be rewritten as:

$$M_\gamma(s|\xi) = \frac{1}{\left(1-\frac{2\eta}{\mu(1+\eta)(1+\kappa)}\bar{\gamma}s\right)^{\mu/2}\left(1-\frac{2}{\mu(1+\eta)(1+\kappa)}\bar{\gamma}s\right)^{\mu/2}} \times\exp\left(\frac{\mu\kappa\left(\frac{\varrho^2}{1+\varrho^2}\right)(1+\eta)\xi\bar{\gamma}s}{(1+\eta)(1+\kappa)\mu-2\eta\bar{\gamma}s}+\frac{\mu\kappa\left(\frac{1}{1+\varrho^2}\right)(1+\eta)\xi\bar{\gamma}s}{(1+\eta)(1+\kappa)\mu-2\bar{\gamma}s}\right). \tag{38}$$

Finally, the unconditional MGF for the FB fading model can be obtained by averaging (38) as

$$M_\gamma(s) = \int_0^\infty M_\gamma(s|\xi)\, f_\xi(\xi)\, d\xi, \tag{39}$$

where $f_\xi(\xi)$ is the Nakagami-m PDF, yielding (4).

Appendix B
Proof of Corollary I

The expression for the PDF can be derived as $f_\gamma(\gamma) = \mathcal{L}^{-1}\{M_\gamma(-s)\}$ as in the general case. Manipulating (3) and evaluating it at $s = -s$ it is possible to write

$$M_\gamma(-s) = \frac{\alpha_2^{m-\frac{\mu}{2}}}{\alpha_1^m\bar{\gamma}^\mu}\left(s+\frac{\mu(1+\eta)(1+\kappa)}{2\eta\bar{\gamma}}\right)^{m-\frac{\mu}{2}} \times\left(s+\frac{\mu(1+\eta)(1+\kappa)}{2\bar{\gamma}}\right)^{m-\frac{\mu}{2}}\left(s+\frac{c_1}{\bar{\gamma}}\right)^{-m}\left(s+\frac{c_2}{\bar{\gamma}}\right)^{-m}, \tag{40}$$

where, taking partial fraction expansion the expression for $M_\gamma(-s)$ yields

$$M_\gamma(-s) = \frac{\alpha_2^{m-\frac{\mu}{2}}}{\alpha_1^m\bar{\gamma}^\mu}\sum_{i=1}^{N(m,\mu)}\sum_{j=1}^{|\omega_i|}\frac{A_{ij}}{(s+\tau_i/\bar{\gamma})^j}, \tag{41}$$

with ω_i and τ_i the elements of vectors $\boldsymbol{\omega}$ and $\boldsymbol{\tau}$ given by (11) and (12), N a constant defined in (13) and $A_{i,j}$ the partial fraction decomposition residues given by (51), whose calculation is detailed in D.

$$A_{ij} = \begin{cases} \sum_{\substack{k_1+\ldots k_3=m-j \\ k_1,k_2\leq m-\mu/2}} \left[\frac{1}{\prod_{t=1}^{3} k_t!} \prod_{l=1}^{2} \frac{(m-\frac{\mu}{2})!}{(m-\frac{\mu}{2}-k_l)!} \left(\frac{\tau_l}{\bar{\gamma}} - \frac{\tau_i}{\bar{\gamma}}\right)^{m-\frac{\mu}{2}-k_l} \prod_{\substack{z=3 \\ z\neq i}}^{4} (-1)^{k_3}(m)_{k_3} \left(\frac{\tau_z}{\bar{\gamma}} - \frac{\tau_i}{\bar{\gamma}}\right)^{-m-k_3} \right] & \text{if } m \geq \frac{\mu}{2} \\ \sum_{k_1+\ldots k_3=\omega_i-j} \left[\frac{1}{\prod_{t=1}^{3} k_t!} \prod_{z=1}^{i-1} \frac{(-1)^{k_z}(\omega_z)_{k_z}}{\left(\frac{\tau_z}{\bar{\gamma}} - \frac{\tau_i}{\bar{\gamma}}\right)^{\omega_z+k_z}} \prod_{l=i+1}^{4} \frac{(-1)^{k_{l-1}}(\omega_l)_{k_{l-1}}}{\left(\frac{\tau_l}{\bar{\gamma}} - \frac{\tau_i}{\bar{\gamma}}\right)^{\omega_l+k_{l-1}}} \right] & \text{if } m < \frac{\mu}{2} \end{cases} \tag{51}$$

Thanks to this new expression for the MGF, the PDF can be obtained directly using the Laplace transform pair [32]

$$\mathcal{L}^{-1}\left\{\frac{1}{(s+\nu)^n}\right\} = \frac{t^{n-1}}{(n-1)!}e^{-\nu t}, \tag{42}$$

yielding the expression for the PDF shown in (10).

Appendix C
Proof of Corollary II

Proceeding analogously to the PDF case, the CDF expression is given by $F_\gamma(\gamma) = \mathcal{L}^{-1}\left\{\frac{M_\gamma(-s)}{s}\right\}$. From MGF expression shown in (3), it is possible to write

$$\frac{M_\gamma(-s)}{s} = \frac{\alpha_2^{m-\frac{\mu}{2}}}{\alpha_1^m \bar{\gamma}^\mu} \frac{1}{s} \left(s + \frac{\mu(1+\eta)(1+\kappa)}{2\eta\bar{\gamma}}\right)^{m-\frac{\mu}{2}} \times \left(s + \frac{\mu(1+\eta)(1+\kappa)}{2\bar{\gamma}}\right)^{m-\frac{\mu}{2}} \left(s + \frac{c_1}{\bar{\gamma}}\right)^{-m} \left(s + \frac{c_2}{\bar{\gamma}}\right)^{-m}, \tag{43}$$

where partial expansion leads us to

$$\frac{M_\gamma(-s)}{s} = \frac{\alpha_2^{m-\frac{\mu}{2}}}{\alpha_1^m \bar{\gamma}^\mu} \left(\frac{B_s}{s} + \sum_{i=1}^{N(m,\mu)} \sum_{j=1}^{|\omega_i|} \frac{B_{ij}}{(s+\tau_i/\bar{\gamma})^j} \right), \tag{44}$$

where constants ω_i, τ_i and N are the same as in PDF case, which are defined in (11)–(13), respectively. As before, B_s and $B_{i,j}$ are the partial fraction decomposition residues given by (50) and (52), whose derivation is detailed in Appendix D. Applying the Laplace transform pair listed in (42), and after some algebraic manipulations, we arrive to the CDF expression given in (14).

Appendix D
Derivation of Partial Fraction Expansion Residues

The general expression for partial expansion residues is given in [32, eq. (A.36)], which allows us to write A_{ij} and B_{ij} as

$$A_{ij} = \frac{1}{(|\omega_i|-j)!} \frac{d^{|\omega_i|-j}}{ds^{|\omega_i|-j}} \left[\prod_{\substack{k=1 \\ k\neq i}}^{4} \left(s + \frac{\tau_k}{\bar{\gamma}}\right)^{-\omega_k} \right] \Bigg|_{s=\frac{-\tau_i}{\bar{\gamma}}}, \tag{45}$$

$$B_{ij} = \frac{1}{(|\omega_i|-j)!} \frac{d^{|\omega_i|-j}}{ds^{|\omega_i|-j}} \left[\frac{1}{s} \prod_{\substack{k=1 \\ k\neq i}}^{4} \left(s + \frac{\tau_k}{\bar{\gamma}}\right)^{-\omega_k} \right] \Bigg|_{s=\frac{-\tau_i}{\bar{\gamma}}}, \tag{46}$$

where each one is obtained as a $|\omega_i| - j$-th order derivative, which can be tedious of computing. In the following, a closed-form expression for the residues is presented.

Focusing on A_{ij} residues, (45) can be rewritten using the general Leibniz rule, which gives

$$A_{ij} = \frac{1}{(|\omega_i|-j)!} \left(\sum_{k_1+\ldots k_3=|\omega_i|-j} \binom{|\omega_i|-j}{k_1 \ldots k_3} \times \prod_{\substack{z=1 \\ z\neq i}}^{4} \left[(s+\tau_z/\bar{\gamma})^{-\omega_z}\right]^{(k_z)} \right) \Bigg|_{s=-\tau_i/\bar{\gamma}}, \tag{47}$$

where $\binom{|\omega_i|-j}{k_1\ldots k_3} = \frac{(|\omega_i|-j)!}{k_1!k_2!k_3!}$. The sum condition $k_1 + \ldots k_3 = |\omega_i| - j$ represents that there are as many terms as combinations of k_1, k_2 and k_3 exist that fulfil $\sum_{t=1}^{3} k_t = |\omega_i| - j$.

General Leibniz rule has allowed us to express derivatives of the rational polynomial as the product of the binomials derivatives. Moreover, closed-form expressions for binomial derivatives are given below

$$\frac{d^q}{ds^q}(s+\alpha)^\nu = \begin{cases} \frac{(\nu)!}{(\nu-q)!}(s+\alpha)^{\nu-q} & \text{if } \nu \geq 0 \\ (-1)^q(-\nu)_q(s+\alpha)^{\nu-q} & \text{if } \nu < 0 \end{cases}. \tag{48}$$

We see that the number of poles the MGF (and consequently the closed-form expression for each binomial derivative) is a function of m and μ parameters. Thus, it is necessary to distinguish between the cases where $m \geq \mu/2$, and $m < \mu/2$, respectively. Taking this into consideration, and introducing the above equation in (47), the final expression for the residues A_{ij} is given in (51) at the top of this page.

Following the same steps as with A_{ij} residues, the final result for B_{ij} constants after applying the general Leibniz rule and introducing the closed-form derivatives expressions is also shown in (52) at the top of the next page, where the same cases has been considered.

Finally, the residue B_s is given by

$$B_s = \left(\prod_{k=1}^{4} (s+\tau_k/\bar{\gamma})^{-\omega_k} \right) \Bigg|_{s=0}, \tag{49}$$

which immediately leads to

$$B_s = \prod_{k=1}^{4} (\tau_k/\bar{\gamma})^{-\omega_k}. \tag{50}$$

$$B_{ij} = \begin{cases} \sum_{\substack{k_1+\ldots k_4=m-j \\ k_1,k_2\leq m-\mu/2}} \left[\frac{(1)_{k_4}}{\prod_{t=1}^{4} k_t!} \left(\frac{-\tau_i}{\bar{\gamma}}\right)^{-(k_4+1)} \prod_{l=1}^{2} \frac{(m-\frac{\mu}{2})!}{(m-\frac{\mu}{2}-k_l)!} \left(\frac{\tau_l}{\bar{\gamma}} - \frac{\tau_i}{\bar{\gamma}}\right)^{m-\frac{\mu}{2}-k_l} \prod_{\substack{z=3 \\ z\neq i}}^{4} \frac{(-1)^{k_3}(m)_{k_3}}{\left(\frac{\tau_z}{\bar{\gamma}} - \frac{\tau_i}{\bar{\gamma}}\right)^{m+k_3}} \right] & \text{if } m \geq \frac{\mu}{2} \\ \sum_{k_1+\ldots k_4=\omega_i-j} \left[\frac{(1)_{k_4}}{\prod_{t=1}^{4} k_t!} \left(\frac{-\tau_i}{\bar{\gamma}}\right)^{-(k_4+1)} \prod_{z=1}^{i-1} \frac{(-1)^{k_z}(\omega_z)_{k_z}}{\left(\frac{\tau_z}{\bar{\gamma}} - \frac{\tau_i}{\bar{\gamma}}\right)^{\omega_z+k_z}} \prod_{l=i+1}^{4} \frac{(-1)^{k_{l-1}}(\omega_l)_{k_{l-1}}}{\left(\frac{\tau_l}{\bar{\gamma}} - \frac{\tau_i}{\bar{\gamma}}\right)^{\omega_l+k_{l-1}}} \right] & \text{if } m < \frac{\mu}{2} \end{cases} \quad (52)$$

REFERENCES

[1] S. O. Rice, "Mathematical analysis of random noise," *Bell Syst. Tech. J.*, vol. 23, no. 3, pp. 282–332, Jul. 1944.

[2] R. S. Hoyt, "Probability functions for the modulus and angle of the normal complex variate," *Bell Syst. Tech. J.*, vol. 26, no. 4, pp. 318–359, Apr. 1947.

[3] P. Beckmann, "Statistical distribution of the amplitude and phase of a multiply scattered field," *J. Res. Nat. Bureau Standards D Radio Propag.*, vol. 66D, no. 3, pp. 231–240, 1962.

[4] P. Beckmann, "Rayleigh distribution and its generalizations," *Radio Sci. J. Res. NBS/USNC-URSI*, vol. 68D, no. 9, pp. 927–932, Sep. 1964.

[5] M. K. Simon and M.-S. Alouini, *Digital Communication Over Fading Channels*. Hoboken, NJ, USA: Wiley, 2005. [Online]. Available: http://www.worldcat.org/isbn/0471649538

[6] M. D. Yacoub, G. Fraidenraich, H. B. Tercius, and F. C. Martins, "The symmetrical η-κ distribution: a general fading distribution," *IEEE Trans. Broadcast.*, vol. 51, no. 4, pp. 504–511, Dec. 2005.

[7] M. D. Yacoub, G. Fraidenraich, H. B. Tercius, and F. C. Martins, "The asymmetrical η-κ distribution," *J. Commun. Inf. Syst.*, vol. 20, no. 3, pp. 182–187, 2005.

[8] M. D. Yacoub, "The α-η-κ-μ fading model," *IEEE Trans. Antennas Propag.*, vol. 64, no. 8, pp. 3597–3610, Aug. 2016.

[9] M. Yacoub, "The κ-μ distribution and the eta-μ distribution," *IEEE Antennas Propag. Mag.*, vol. 49, no. 1, pp. 68–81, Feb. 2007.

[10] D. Morales-Jimenez and J. F. Paris, "Outage probability analysis for η-μ fading channels," *IEEE Commun. Lett.*, vol. 14, no. 6, pp. 521–523, Jun. 2010.

[11] N. Ermolova, "Moment generating functions of the generalized η-μ and κ-μ distributions and their applications to performance evaluations of communication systems," *IEEE Commun. Lett.*, vol. 12, no. 7, pp. 502–504, Jul. 2008.

[12] M. Nakagami, "The m-distribution—A general formula of intensity distribution of rapid fading," in *Statistical Method of Radio Propagation*. New York, NY, USA: Pergamon Press, 1960, pp. 3–36.

[13] J. F. Paris, "Statistical Characterization of κ-μ Shadowed Fading," *IEEE Trans. Veh. Technol.*, vol. 63, no. 2, pp. 518–526, Feb. 2014.

[14] S. L. Cotton, "Human body shadowing in cellular device-to-device communications: Channel modeling using the shadowed κ-μ fading model," *IEEE J. Sel. Areas Commun.*, vol. 33, no. 1, pp. 111–119, Jan. 2015.

[15] L. Moreno-Pozas, F. J. Lopez-Martinez, J. F. Paris, and E. Martos-Naya, "The κ-μ shadowed fading model: Unifying the κ-μ and η-μ distributions," *IEEE Trans. Veh. Technol.*, vol. 65, no. 12, pp. 9630–9641, Dec. 2016.

[16] A. Abdi, W. Lau, M.-S. Alouini, and M. Kaveh, "A new simple model for land mobile satellite channels: First- and second-order statistics," *IEEE Trans. Wireless Commun.*, vol. 2, no. 3, pp. 519–528, May 2003.

[17] F. J. Lopez-Martinez, J. F. Paris, and J. M. Romero-Jerez, "The κ-μ shadowed fading model with integer fading parameters," *IEEE Trans. Veh. Technol.*, vol. 66, no. 9, pp. 7653–7662, Sep. 2017.

[18] L. Moreno-Pozas, F. J. Lopez-Martinez, S. L. Cotton, J. F. Paris, and E. Martos-Naya, "Comments on human body shadowing in cellular device-to-device communications: Channel modeling using the shadowed κ-μ fading model," *IEEE J. Sel. Areas Commun.*, vol. 35, no. 2, pp. 517–520, Feb. 2017.

[19] A. Erdélyi, *Beitrag zur theorie der konfluenten hypergeometrischen funktionen von mehreren veränderlichen*. Hölder-Pichler-Tempsky in Komm., 1937.

[20] H. M. Srivastava and P. W. Karlsson, *Multiple Gaussian Hypergeometric Series*. Hoboken, NJ, USA: Wiley, 1985.

[21] J. M. Romero-Jerez, F. J. Lopez-Martinez, J. F. Paris, and A. J. Goldsmith, "The fluctuating two-ray fading model: Statistical characterization and performance analysis," *IEEE Trans. Wireless Commun.*, vol. 16, no. 7, pp. 4420–4432, Jul. 2017.

[22] E. Martos-Naya, J. M. Romero-Jerez, F. J. Lopez-Martinez, and J. F. Paris, "A MATLAB program for the computation of the confluent hypergeometric function Φ 2," Repositorio Institucional Universidad de Málaga, Málaga, Spain, Tech. Rep. 10630/12068, 2016.

[23] J. Abate and W. Whitt, "Numerical inversion of Laplace transforms of probability distributions," *ORSA J. Comput.*, vol. 7, no. 1, pp. 36–43, 1995.

[24] J. P. Pena-Martin, J. M. Romero-Jerez, and F. J. Lopez-Martinez, "Generalized MGF of Beckmann fading with applications to wireless communications performance analysis," *IEEE Trans. Commun.*, vol. 65, no. 9, pp. 3933–3943, Sep. 2017.

[25] I. S. Gradshteyn and I. M. Ryzhik, *Table of Integrals, Series and Products*, 7th ed. New York, NY, USA: Academic, 2007. [Online]. Available: http://www.worldcat.org/isbn/012294755X

[26] G. D. Durgin, T. S. Rappaport, and D. A. de Wolf, "New analytical models and probability density functions for fading in wireless communications," *IEEE Trans. Commun.*, vol. 50, no. 6, pp. 1005–1015, Jun. 2002.

[27] N. C. Beaulieu and S. A. Saberali, "A generalized diffuse scatter plus line-of-sight fading channel model," in *Proc. 2014 IEEE Int. Conf. Commun.*, Jun. 2014, pp. 5849–5853.

[28] G. L. Stüber, *Principles of Mobile Communication*. New York, NY, USA: Springer, 2011.

[29] F. Ramos-Alarcon, V. Kontorovich, and M. Lara, "On the level crossing duration distributions of Nakagami processes," *IEEE Trans. Commun.*, vol. 57, no. 2, pp. 542–552, Feb. 2009.

[30] F. J. López-Martínez, E. Martos-Naya, J. F. Paris, and U. Fernández-Plazaola, "Higher order statistics of sampled fading channels with applications," *IEEE Trans. Veh. Technol.*, vol. 61, no. 7, pp. 3342–3346, Sep. 2012.

[31] S. L. Cotton and W. G. Scanlon, "Higher-order statistics for κ-μ distribution," *Electron. Lett.*, vol. 43, no. 22, pp. 1215–1217, Oct. 2007.

[32] A. V. Oppenheim, A. S. Willsky, and S. H. Nawab, *Signals & Systems (2nd Ed.)*. Englewood Cliffs, NJ, USA: Prentice-Hall, 1996.

Pablo Ramirez-Espinosa received the M.Sc. degree in electrical engineering from the University of Málaga, Málaga, Spain, in 2017, where he is currently working toward the Ph.D. degree in communication theory. Since 2017, he has been an Associate Researcher with the Communication Engineering Department, University of Málaga. His research interest include wireless communications, particularly channel modeling.

F. Javier Lopez-Martinez (SM'17) received the M.Sc. and Ph.D. degrees in telecommunication engineering from the Universidad de Málaga, Málaga, Spain, in 2005 and 2010, respectively. He joined the Communication Engineering Department, Universidad de Málaga, in 2005, as an Associate Researcher. In 2010, he stayed for three months as a Visitor Researcher with the University College London. He was a Marie Curie Postdoctoral Fellow with the Wireless Systems Lab, Stanford University, from 2012 to 2014, and with the Universidad de Málaga, from 2014 to 2015. Since 2015, he has been an Assistant Professor with the Communication Engineering Department, Universidad de Málaga. His research interests include a diverse set of topics in the wide areas of communication theory and wireless communications: stochastic processes, wireless channel modeling, random matrix theory, physical layer security, massive MIMO, and mmWave for 5G. He is an Editor of the IEEE TRANSACTIONS ON COMMUNICATIONS, in the area of Wireless Communications. He has received several research awards, including the Best Paper Award in the Communication Theory Symposium at IEEE Globecom 2013, the IEEE Communications Letters Exemplary Reviewer certificate in 2014, and the IEEE Transactions on Communications Exemplary Reviewer certificate in 2015 and 2017.

José Francisco Paris received the M.Sc. and Ph.D. degrees in telecommunication engineering from the Universidad de Málaga, Málaga, Spain, in 1996 and 2004, respectively. From 1994 to 1996, he was with Alcatel, mainly in the development of wireless telephones. In 1997, he joined the Universidad de Málaga, where is currently a Professor with the Communication Engineering Department. In 2005, he spent five months as a Visiting Associate Professor with Stanford University, with Professor A. J. Goldsmith. From 2017, he has been a Full Professor with the Communication Engineering Department. His teaching activities include several courses on digital communications, signal processing, and acoustic engineering. His research interests include wireless communications, especially channel modeling, and performance analysis. He serves as an Associate Editor for the IEEE COMMUNICATIONS LETTERS, and the IEEE TRANSACTIONS ON VEHICULAR TECHNOLOGY. He received the 2016 Neil Shepherd Memorial Best Propagation Paper Award by the IEEE Vehicular Technology Society.

Michel Daoud Yacoub was born in Brazil in 1955. He received the B.S.E.E. and M.Sc. degrees from the School of Electrical and Computer Engineering, State University of Campinas, UNICAMP, Campinas, Brazil, in 1978 and 1983, respectively, and the Ph.D. degree from University of Essex, Colchester, U.K., in 1988. From 1978 to 1985, he was a Research Specialist in the development of the Tropico digital exchange family with the Research and Development Center of Telebrs, Brazil. In 1989, he joined the School of Electrical and Computer Engineering, UNICAMP, where he is currently a Full Professor. He consults for several operating companies and industries in the wireless communications area. He is the author of *Foundations of Mobile Radio Engineering* (CRC, 1993), *Wireless Technology: Protocols, Standards, and Techniques* (CRC, 2001), and the coauthor of *Telecommunications: Principles and Trends* (Erica, 1997, in Portuguese). He holds two patents. His research interests include wireless communications.

Eduardo Martos-Naya received the M.Sc. and Ph.D. degrees in telecommunication engineering from the University of Málaga, Málaga, Spain, in 1996 and 2005, respectively. In 1997, he joined the Department of Communication Engineering, University of Málaga, where he is currently an Associate Professor. His research interests include digital signal processing for communications, synchronization and channel estimation, and performance analysis of wireless systems. He is currently the Leader of a project supported by the Andalusian regional Government on cooperative and adaptive wireless communications systems.

A.4 The κ-μ shadowed fading model with arbitrary intercluster correlation

[49] P. Ramírez-Espinosa, J. F. París, J. A. Cortés, and E. Martos-Naya, "The κ-μ shadowed fading model with arbitrary intercluster correlation", in *2018 15th Int. Symp. Wireless Commun. Syst. (ISWCS)*, Aug. 2018, pp. 1–5.

The κ-μ Shadowed Fading Model with Arbitrary Intercluster Correlation

Pablo Ramírez-Espinosa, José F. Paris, José A. Cortés and Eduardo Martos-Naya

Dpto. de Ingeniería de Comunicaciones, ETSI Telecomunicacion, Universidad de Málaga, Málaga, E-29071, Spain
email: {pre, paris, jaca, eduardo}@ic.uma.es

***Abstract*—In this paper, we propose a generalization of the well-known κ-μ shadowed fading model. Based on the clustering of multipath waves as the baseline model, the novelty of this new distribution is the addition of an arbitrary correlation for the scattered components within each cluster. It also inherits the random fluctuation of the dominant component, which is assumed to be the same for all clusters. Thus, it unifies a wide variety of models: Rayleigh, Rician, Rician shadowed, Nakagami-m, κ-μ and κ-μ shadowed as well as multivariate Rayleigh, Rician and Rician shadowed. The main statistics of the newly proposed model, i.e. moment generating function, probability density function and cumulative density function, are given in terms of exponentials and powers, and some numerical results are provided in order to analyze the impact of the arbitrary intercluster correlation.**

I. Introduction

The statistical characterization of the received radio signal is a classical problem in wireless communications, where the transmitted radio waves are affected by several random phenomena. As a result, the received signal can be seen as a linear combination of multipath waves with random amplitudes and phases. By applying the central limit theorem, the baseband signal is modeled using complex Gaussian processes, rendering the widely-used fading models, namely Rayleigh, Rice, Hoyt and Nakagami-m [1].

In order to provide a better statistical characterization in intricate multipath environments, several distributions have been proposed in the literature as generalizations of the classical ones. In [2], Yacoub introduces two new models based on the effect of clustering of multipath waves: the η-μ fading model as a generalization of the Hoyt model and the κ-μ fading model, which arises as a generalization of the Rician model. Due to the small number of parameters along with the comparatively simple mathematical tractability, a lot of attention has been paid to the κ-μ model in the last years [3–5]. Although a more general model was introduced in [6], its larger flexibility comes at the price of an increased mathematical complexity, ultimately affecting its practical applicability.

A further generalization of the κ-μ distribution was presented in [7] where the line of sight (LoS) component is affected by a random fluctuation representing the shadowing, rendering the well-known κ-μ shadowed model. This fading distribution has applications in mobile satellite (LMS) communications and underwater acoustic communications (UAC), including a wide variety of models as special cases: Rayleigh, Rice, Rician shadowed [8], Nakagami-m, κ-μ and Hoyt.

However, all of the aforementioned fading models assume the statistical independence between the radio signal components of all clusters. Attempting to consider the effect of the correlation, Bhatnagar characterizes in [9] the sum of κ-μ shadowed variables with correlated LoS fluctuation, providing the PDF in terms of infinite series. Nonetheless, the scattered components are still mutually uncorrelated.

In order to account for the impact of such intercluster cross correlation, we here introduce a novel extension of the κ-μ shadowed fading model which considers an arbitrary correlation between the scattered components. Thus, we consider appropriate to name this new distribution as correlated κ-μ shadowed distribution. Aiming to relay the mathematical complexity of the newly proposed fading model, we take the formulation of the κ-μ shadowed model with integer parameters as starting point [10]. Interestingly, despite being more general than the original κ-μ shadowed distribution, this new model inherits its simple mathematical tractability. Hence, the main statistics of the proposed model: Moment Generating Function (MGF), Probability Density Function (PDF) and Cumulative Distribution Function (CDF) are given in simple closed-form involving only elementary functions (exponentials and powers). Notably, in contrast to the original one, the correlated κ-μ shadowed fading model also includes as particular cases the multivariate Rayleigh, Rician and Rician shadowed distributions [11–14].

Throughout this paper, we will use the following notation. The symbol $\sim$ means *statistically distributed as*. Matrices and vectors are represented with upper-case boldface and lower-case boldface, respectively. The superscript $(\cdot)^\dagger$ denotes matrix complex conjugate transpose. Additionally, $\mathbf{I}_n$ represents the $n \times n$ identity matrix and $\mathbf{0}_{n\times p}$ a $n \times p$ all-zero matrix. Finally, $(a)_b$ is the Pochhammer symbol and $\mathbb{E}[\cdot]$ is the expectation operator.

This paper is structured as follows. In Section II, we describe the physical model of the proposed fading distribution. Then, the first order statistics (MGF, PDF and CDF) are derived in Section III, while we provide some numerical results in Section IV to exemplify the impact of the distribution

This work has been funded by the Spanish Government and the European Fund for Regional Development FEDER (project TEC2014-57901-R) and also by the Campus de Excelencia Internacional Andalucía TECH, Universidad de Málaga.

978-1-5386-5005-9/18/$31.00 ©2018 IEEE

parameters. Finally, main conclusions are given in Section V.

II. Physical Model

The physical model of the correlated κ-μ shadowed fading distribution arises as a generalization of the original one in [7]. The received radio signal is modeled as the superposition of radio waves structured in clusters of waves, where we consider that the scattered component has the same power within each cluster. The same applies to the dominant components, which are assumed to have equal power for all clusters. As opposed to the κ-μ shadowed distribution, we here introduce an arbitrary correlation factor for the intercluster scattered components. Thus, the received signal power W can be formulated using complex random variables as

$$W = \sum_{i=1}^{\mu} |Z_i + \xi p|^2 \tag{1}$$

where μ is a natural number indicating the number of clusters and Z_i for $i = 1, \ldots, \mu$ are complex Gaussian random variables such that $Z_i \sim \mathcal{CN}(0, \sigma^2)$. Additionally, p is a complex number and ξ is a real random variable such that ξ^2 is Gamma distributed with shape parameter m and scale parameter $1/m$, i.e. $\xi^2 \sim \Gamma(m, 1/m)$ with $\mathbb{E}\left[\xi^2\right] = 1$. As with the original κ-μ shadowed model, ξ represents the random fluctuation of the dominant component of all clusters of waves. The distinct variables Z_i in (1) are assumed to be correlated with correlation factor given by $\mathrm{corr}\left(Z_i, Z_j\right) = \rho_{i,j}$ for $i, j = 1, \ldots, \mu$ with

$$\rho_{i,j} = \frac{\mathbb{E}\left[Z_i Z_j^*\right]}{\sigma^2}. \tag{2}$$

Therefore, the novelty of the model here introduced is the addition of such arbitrary intercluster correlation factor. Note that, if we impose $\rho_{i,j} = 0 \ \forall \ i \neq j$, then (1) becomes the κ-μ shadowed physical model in [7, eq. (1)]. Since this correlation implies a considerable difficulty in the statistical characterization of the physical model in (1), we will reformulate W in terms of statistically independent random variables as follows.

The summation in (1) can be written in matrix form as a non-central complex Gaussian quadratic form as

$$W = \left(\mathbf{z} + \xi \mathbf{p}\right)^{\dagger} \left(\mathbf{z} + \xi \mathbf{p}\right) \tag{3}$$

where $\mathbf{z} \in \mathbb{C}^{\mu \times 1}$ and $\mathbf{p} \in \mathbb{C}^{\mu \times 1}$ are column vectors whose entries are Z_i and p for $i = 1, \ldots, \mu$, respectively. As such, $\mathbf{z}$ follows a complex multivariate normal distribution with zero mean and correlation matrix $\mathbf{\Sigma}$ with entries $[\mathbf{\Sigma}]_{i,j} = \rho_{i,j}$, i.e. $\mathbf{z} \sim \mathcal{CN}_{\mu}\left(\mathbf{0}_{\mu \times 1}, \sigma^2 \mathbf{\Sigma}\right)$. The correlation matrix $\mathbf{\Sigma}$ is Hermitian, so it can be decomposed as $\mathbf{\Sigma} = \mathbf{C}\mathbf{C}^{\dagger}$ where $\mathbf{C} \in \mathbb{C}^{\mu \times \mu}$ is a lower triangular matrix with non-negative diagonal entries (Cholesky decomposition)[15].

Then, $\mathbf{z}$ can be expressed as $\mathbf{z} = \sigma \mathbf{C} \widetilde{\mathbf{z}}$, with $\widetilde{\mathbf{z}}$ a standard complex multivariate Gaussian vector, i.e. $\widetilde{\mathbf{z}} \sim \mathcal{CN}_{\mu}\left(\mathbf{0}_{\mu \times 1}, \mathbf{I}_{\mu}\right)$. By doing so, (3) is rewritten as

$$W = \left(\sigma \widetilde{\mathbf{z}} + \xi \mathbf{C}^{-1} \mathbf{p}\right)^{\dagger} \mathbf{C}^{\dagger} \mathbf{C} \left(\sigma \widetilde{\mathbf{z}} + \xi \mathbf{C}^{-1} \mathbf{p}\right). \tag{4}$$

Since $\mathbf{C}^{\dagger}\mathbf{C}$ is clearly Hermitian, it can be diagonalized as $\mathbf{C}^{\dagger}\mathbf{C} = \mathbf{U}\mathbf{\Lambda}\mathbf{U}^{\dagger}$, where $\mathbf{\Lambda}$ is a diagonal matrix whose entries, λ_i, are the eigenvalues of $\mathbf{C}^{\dagger}\mathbf{C}$ (or, equivalently, those of $\mathbf{\Sigma}$) and $\mathbf{U}$ is an unitary matrix whose i-th column is the eigenvector associated with λ_i. Therefore, (4) is finally expressed in a similar way to (1) as

$$W = \sum_{i=1}^{\mu} \left| \sqrt{\lambda_i} \sigma \widetilde{Z}_i + \xi \sqrt{\lambda_i} \widetilde{p}_i \right|^2 \tag{5}$$

where Z_i are statistically independent complex Gaussian random processes with zero mean and unit variance, i.e. $Z_i \sim \mathcal{CN}(0, 1)$, and $\widetilde{p}_i$ are the entries of the vector $\widetilde{\mathbf{p}} = \mathbf{U}^{\dagger}\mathbf{C}^{-1}\mathbf{p}$ for $i = 1, \ldots, \mu$.

Thus, we have proved that the physical model in (1) is equivalent to another one where all the involved random variables are independent. Consequently, the power of each Gaussian variable Z_i in (5) is rescaled by the eigenvalues of $\mathbf{\Sigma}$ and, in contrast with (1), the power of the dominant component is not the same for all clusters. This new representation of the physical model in terms of independent random variables will lead us to simple expressions of the main statistics (MGF, PDF and CDF) of the here proposed model.

III. Statistical Characterization

We will now provide the first-order statistics of the correlated κ-μ shadowed distribution where its MGF, PDF and CDF will be given in closed-form in terms of elementary functions. Hence, as usually done in the related literature, hereinafter we will consider the random variable $\gamma \triangleq \overline{\gamma} W / \overline{W}$ representing the instantaneous SNR at the receiver side, where $\overline{\gamma} \triangleq \mathbb{E}[\gamma]$ and $\overline{W} = \mathbb{E}[W] = \mu\left(|p|^2 + \sigma^2\right)$.

Therefore, let γ be a random variable characterizing the instantaneous SNR for the physical model in (1) or, equivalently, that in (5). Then, γ follows a correlated κ-μ shadowed distribution with parameters μ, m, κ and $\mathbf{\Sigma}$, i.e. $\gamma \sim \mathcal{CS}_{\kappa\mu}(\overline{\gamma}; \kappa, \mu, m, \mathbf{\Sigma})$ with $\kappa = |p|^2 / \sigma^2$.

Lemma 1: Let $\gamma \sim \mathcal{CS}_{\kappa\mu}(\overline{\gamma}; \kappa, \mu, m, \mathbf{\Sigma})$. Then, its MGF is given by

$$M_{\gamma}(s) = \frac{\mu^{\mu}(\kappa+1)^{\mu}}{\prod_{i=1}^{\mu} \mu(\kappa+1) - s\lambda_i\overline{\gamma}} \times \left(1 - \frac{1}{m} \sum_{j=1}^{\mu} \frac{d_i \lambda_i s \overline{\gamma}}{\mu(\kappa+1) - s\lambda_i\overline{\gamma}}\right)^{-m} \tag{9}$$

where $d_i = |\widetilde{p}_i|^2 / \sigma^2 = \left[\mathbf{U}^{\dagger}\mathbf{C}^{-1}\mathbf{K}\left(\mathbf{C}^{-1}\right)^{\dagger}\mathbf{U}\right]_{i,i}$ with $\mathbf{K} \in \mathbb{R}^{\mu \times \mu}$ a constant matrix whose entries are given by $[\mathbf{K}]_{i,j} = \kappa$ for $i, j = 1, \ldots, \mu$.

Proof: See Appendix A. ∎

Lemma 1 provides a closed-form expression for the MGF of γ. It is easy to prove that, when no correlation is applied, then $\lambda_i = 1$ and $d_i = \kappa$ for $i = 1, \ldots, \mu$. If so, then (9) becomes the MGF of the κ-μ shadowed distribution given in [7, eq. (5)].

$$D_i(k_1,\ldots,k_{N-1}) = \prod_{t=1}^{\mu} \frac{\left(\frac{\mu(k+1)}{\lambda_t\overline{\gamma}} - \beta_i\right)^{m-k_t-1}}{\Gamma(m)^{-1}\Gamma(m-k_t)} \prod_{r=1}^{i-1} \frac{(-1)^{k_{r+\mu}}(q_r m)_{k_{r+\mu}}}{(\beta_r-\beta_i)^{q_r m+k_{r+\mu}}} \prod_{l=i+1}^{n} \frac{(-1)^{k_{l+\mu-1}}(q_l m)_{k_{l+\mu-1}}}{(\beta_l-\beta_i)^{q_l m+k_{l+\mu-1}}}. \quad (8)$$

From $M_\gamma(s)$, we now calculate the PDF and the CDF of γ. In order to do so, it is necessary to perform some algebraic manipulations in (9). Hence, $M_\gamma(s)$ is rewritten in terms of a rational polynomial as follows:

$$M_\gamma(s) = \frac{1}{\prod_{i=1}^{\mu} 1 - \frac{\lambda_i\overline{\gamma}}{\mu(\kappa+1)}s} \left(\frac{\prod_{j=1}^{\mu} 1 - \frac{\lambda_j\overline{\gamma}}{\mu(\kappa+1)}s}{P(s)} \right)^m \quad (10)$$

where $P(s)$ is the μ-th order polynomial given by

$$P(s) = m\prod_{i=1}^{\mu} 1 - \frac{\lambda_i\overline{\gamma}}{\mu(\kappa+1)}s - \sum_{j=1}^{\mu} \frac{d_j\lambda_j\overline{\gamma}}{\mu(\kappa+1)}s \prod_{\substack{k=1\\k\neq j}}^{\mu} 1 - \frac{\lambda_k\overline{\gamma}}{\mu(\kappa+1)}s. \quad (11)$$

Therefore, denoting as β_i for $i = 1,\ldots,n$ the distinct roots of $P(s)$ with multiplicity q_i, the rational function in (10) is expressed as

$$M_\gamma(s) = \frac{(-\overline{\gamma})^{-\mu}\mu^\mu(k+1)^\mu}{\left(1+\sum_{k=1}^{\mu}\frac{d_k}{m}\right)^m \prod_{l=1}^{\mu}\lambda_l} \frac{\prod_{j=1}^{\mu}\left(s-\frac{\mu(\kappa+1)}{\lambda_j\overline{\gamma}}\right)^{m-1}}{\prod_{i=1}^{n}(s-\beta_i)^{q_i m}}. \quad (12)$$

From (12), the PDF and CDF of γ are provided in the following lemmas.

Lemma 2: Let $\gamma \sim \mathcal{CS}_{\kappa\mu}(\overline{\gamma};\kappa,\mu,m,\mathbf{\Sigma})$. Then, its PDF is given by

$$f_\gamma(\gamma) = \alpha\sum_{i=1}^{n}\sum_{j=1}^{q_i m} A_{i,j}\gamma^{j-1}e^{-\beta_i\gamma} \quad (10)$$

with

$$\alpha = \frac{\mu^\mu(\kappa+1)^\mu}{\overline{\gamma}^\mu\Gamma(j)}\left(1+\sum_{j=1}^{\mu}\frac{d_j}{m}\right)^{-m}\prod_{l=1}^{\mu}\lambda_l^{-1}, \quad (11)$$

$$A_{i,j} = \sum_{\substack{k_1+\ldots+k_{N-1}=q_i m-j\\k_1,\ldots,k_\mu\leq m-1}} \frac{1}{\prod_{p=1}^{N-1}k_p!} D_i(k_1,\ldots,k_{N-1}) \quad (12)$$

where $N = n+\mu$ and $D_i(k_1,\ldots,k_N)$ is given in (8) at the top of this page. The sum in (12) is over all combinations of $k_1,\ldots,k_{N-1}$ that satisfy $\sum_{p=1}^{N-1}k_p = q_i m - j$ and $k_1,\ldots,k_\mu \leq m-1$.

Proof: The PDF of γ is obtained by means of an inverse Laplace transform as $f_\gamma(\gamma) = \mathcal{L}^{-1}\{M_\gamma(-s)\}$. By performing a partial fraction expansion of the rational polynomial in (12), $M_\gamma(-s)$ is rewritten as

$$M_\gamma(-s) = \alpha\sum_{i=1}^{n}\sum_{j=1}^{q_i m}\frac{A_{i,j}}{(s+\beta_i)^j} \quad (13)$$

where $A_{i,j}$ are the partial fraction expansion residues given in (12) as proved in Appendix B. Finally, (10) is obtained by applying the Laplace transform pair given in [16, eq. (5.4.1)]. ■

Lemma 3: Let $\gamma \sim \mathcal{CS}_{\kappa\mu}(\overline{\gamma};\kappa,\mu,m,\mathbf{\Sigma})$. Then, its CDF is given by

$$F_\gamma(\gamma) = 1 + \alpha\sum_{i=1}^{n}\sum_{j=1}^{q_i m} C_{i,j}\gamma^{j-1}e^{-\beta_i\gamma}, \quad (12)$$

with

$$C_{i,j} = \sum_{\substack{k_1+\ldots+k_N=q_i m-j\\k_1,\ldots,k_\mu\leq m-1}} \frac{D_i(k_1,\ldots,k_{N-1})k_N!(-1)^{k_N}}{\prod_{p=1}^{N}k_p!\,(-\beta_i)^{1+k_N}}. \quad (13)$$

Proof: Following the same steps as in the previous proof, the CDF of γ is derived from (12) as $F_\gamma(\gamma) = \mathcal{L}^{-1}\left\{\frac{1}{s}M_\gamma(s)\right\}$ by performing a partial fraction decomposition and applying [16, eq. (5.4.1)] with $C_{i,j}$ the residues given in (13) as deduced from the proof of $A_{i,j}$ in Appendix B. ■

Lemmas 2 and 3 provide simple closed-form expressions for the PDF and CDF of γ in terms of a finite number of elementary functions, i.e. exponentials and powers. In fact, these expressions have a similar form to those presented in [10] for the PDF and the CDF of the original κ-μ shadowed distribution with integer parameters. This is an important result, since the larger generality introduced in this paper does not come at the price of an increased analytical complexity.

As introduced before, the correlated κ-μ shadowed distribution arises as a generalization of a wide variety of fading models, thus unifying the statistical characterization of all these underlying models. The tractability of the here derived expressions make them useful for further analytical purposes, specially in the case of multivariate distributions (Rayleigh, Rician and Rician shadowed) for which the results are generally scarce due to their mathematical complexity.

Note that, although we here give expressions for the main statistics of the instantaneous SNR, the PDF and the CDF of the signal envelope R are straightforwardly obtained from (10) and (12) as $f_R(r) = 2rf_\gamma(r^2)$ and $F_R(r) = F_\gamma(r^2)$, respectively, with $\overline{\gamma}$ being replaced by $\mathbb{E}[R^2]$.

IV. Numerical Results

We will now provide some numerical results with the aim of exemplifying the influence of the parameters of the newly proposed model over the distribution of the received signal amplitude R. Since the novelty of this model is the addition of a correlation between clusters, we will here focus on the analysis of the impact of such correlation matrix $\mathbf{\Sigma}$. For the sake of simplicity, we consider an exponential correlation

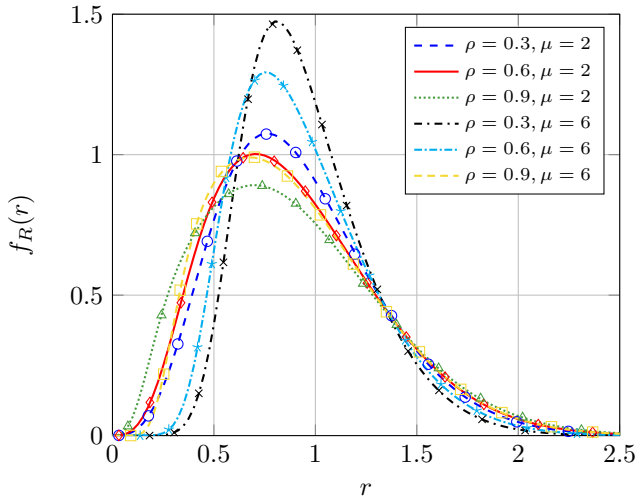

Fig. 1. Signal envelope distribution for different values of μ and ρ with $\kappa = 1$, $m = 1$ and $\mathbb{E}[R^2] = 1$. Solid lines correspond to the exact PDF while markers correspond to Monte Carlo simulations.

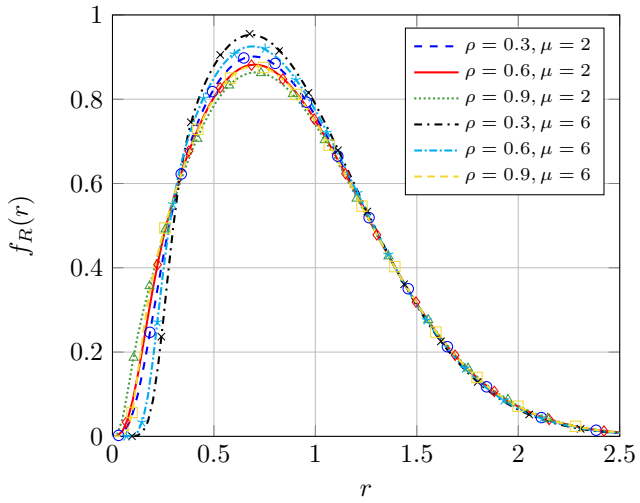

Fig. 2. Signal envelope distribution for different values of μ and ρ with $\kappa = 10$, $m = 1$ and $\mathbb{E}[R^2] = 1$. Solid lines correspond to the exact PDF while markers correspond to Monte Carlo simulations.

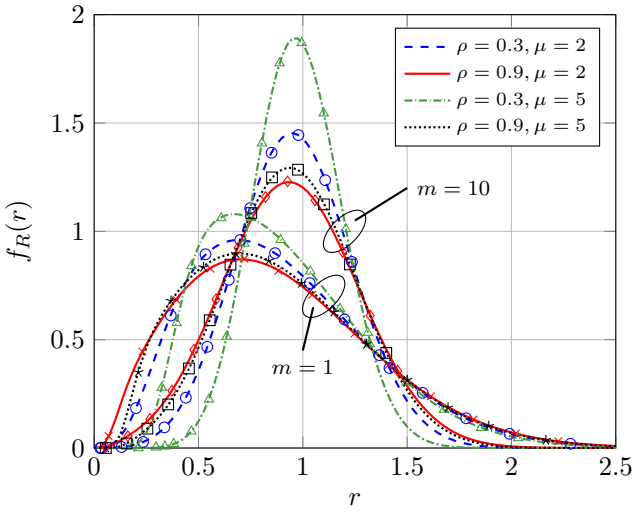

Fig. 3. Signal envelope distribution for different values of μ, ρ and m with $\kappa = 4$ and $\mathbb{E}[R^2] = 1$. Solid lines correspond to the exact PDF while markers correspond to Monte Carlo simulations.

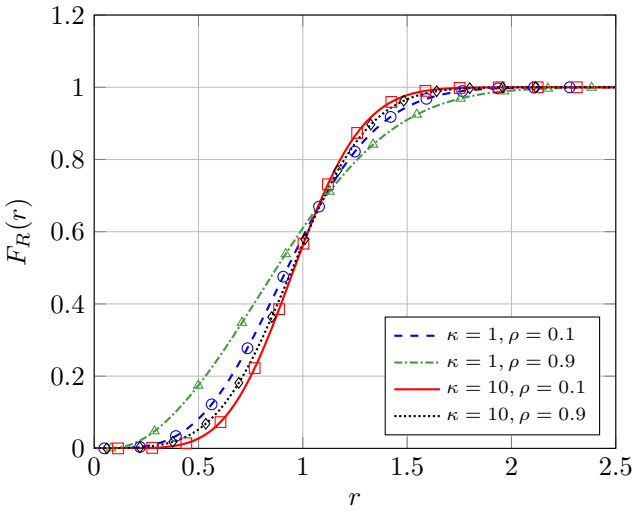

Fig. 4. CDF of the signal envelope for different values of κ and ρ with $\mu = 2$, $m = 5$ and $\mathbb{E}[R^2] = 1$. Solid lines correspond to the exact PDF while markers correspond to Monte Carlo simulations.

matrix whose entries are given by $[\mathbf{\Sigma}]_{i,j} = \rho^{|i-j|}$ with $0 \leq |\rho| < 1$, where a value of $\rho = 0$ implies uncorrelated scattered components.

Thus, we show in Figs. 1 and 2 the PDF of the received signal envelope for different values of ρ and μ in a weak ($\kappa = 1$) and a strong ($\kappa = 10$) LoS scenario, respectively. The value of m is fixed to $m = 1$, corresponding to the case of heavy random fluctuation of the dominant component of each cluster. Regarding both figures, it is easy to notice that the influence of ρ is less relevant for large κ. This is a coherent result, since the correlation factor only affects to the scattered component (NLoS) according to the physical model in (1). We also observe in Fig. 1 that low values of ρ render more sparse values of the signal amplitude. Besides, the effect of that correlation has a larger impact as μ grows, which seems to be logical since we are increasing the number of clusters.

Fig. 3 depicts the PDF of the received signal amplitude for different values of ρ, μ and m for a fixed LoS power. We compare the effect of m in the cases of low correlation ($\rho = 0.3$) and high correlation ($\rho = 0.9$). Nonetheless, the impact of the correlation factor seems to be independent of the value of m. However, a severe fluctuation of the dominant component ($m = 1$) is more detrimental for the signal envelope, as we already saw in the original model [7, 10]. Finally, we represent in Fig. 4 the shape of the CDF of R in a weak ($\kappa = 1$) and a strong ($\kappa = 10$) for low and high intercluster correlation. We fix $\mu = 2$ and $m = 5$ in order to minimize the influence of the

LoS fluctuation, observing that low values of κ and ρ makes the slope of the CDF rise slowly, as expected from the results of the previous figures.

V. Conclusions

We here presented the correlated κ-μ shadowed fading model, which arises as a generalization of the original κ-μ shadowed distribution. This new model considers an arbitrary correlation between the scattered components of each cluster, represented by the matrix parameter $\mathbf{\Sigma}$. The MGF, PDF and CDF of the proposed model are given in closed-form in terms of elementary functions, being appropriated for further theoretical calculations and providing a simple framework for the analysis of the underlying fading models. The correlated κ-μ shadowed statistics are also useful for characterizing the multivariate Rayleigh, Rician and Rician shadowed distributions, which are particular cases of the here proposed model.

The influence of the arbitrary correlation is of relevant interest specially in weak LoS scenarios, rendering more sparse values of the fading amplitude as the correlation factor increases. This effects remains even vanishing the fluctuation of the dominant component.

Appendix A
Proof of Lemma 1

Let us consider the physical model in (5). When conditioned on ξ, the received signal power can be seen as the summation of μ independent and non-identically distributed Rician random variables whose MGFs are given in [1, eq. (2.17)] by setting $n^2 = \xi^2 \left|\widetilde{p}_i\right|^2 / \sigma^2$ and $\overline{\gamma} = \lambda_i \left(\xi^2 \left|\widetilde{p}_i\right|^2 + \sigma^2\right)$ for $i = 1, \ldots, \mu$. As such, the conditional MGF of W is obtained as the product of the MGFs of each Rician variable in (5). By performing some algebraic manipulations, the conditional MGF of the the instantaneous SNR γ is given as

$$M_{\gamma|_\xi}(s) = \mu^\mu \left(\kappa+1\right)^\mu \prod_{i=1}^{\mu} \frac{\exp\left(\frac{\xi^2 d_i \lambda_i \overline{\gamma} s}{\mu(\kappa+1)-\lambda_i \overline{\gamma} s}\right)}{\mu(\kappa+1)-\lambda_i \overline{\gamma} s}. \tag{14}$$

Finally, the unconditional MGF of γ is obtained by averaging (14) as

$$M_\gamma(s) = \int_0^\infty M_{\gamma|_\xi}(s) f_{\xi^2}(x)\, dx \tag{15}$$

with $f_{\xi^2}(x)$ the PDF of the Gamma distribution, yielding (9).

Appendix B
Derivation of Partial Fraction Expansion Residues

Residues $A_{i,j}$ arise from performing a partial fraction expansion in (12) after evaluating $M_\gamma(-s)$. Then, $A_{i,j}$ for $i = 1, \ldots, n$ and $j = 1, \ldots, q_i m$ are defined as

$$A_{i,j} = \frac{1}{(\widetilde{q}_{i,j})!} \frac{d^{\widetilde{q}_{i,j}}}{ds^{\widetilde{q}_{i,j}}} \left(\frac{\prod_{l=1}^{\mu} \left(s + \frac{\mu(\kappa+1)}{\lambda_l \overline{\gamma}}\right)^{m-1}}{\prod_{k=1, k\neq i}^{n} \left(s+\beta_k\right)^{q_k m}} \right) \Bigg|_{s=-\beta_i} \tag{16}$$

with $\widetilde{q}_{i,j} = q_i m - j$. By applying the generalization of Léibniz's rule, the derivatives in (16) can be expressed as a linear combination of the derivatives of the distinct binomials. Therefore, since the k-th derivative of a binomial is a well-known expression which is given by

$$\frac{d^q}{dx^q}(x+a)^\nu = \begin{cases} \dfrac{(-1)^q(-\nu)_q}{(x+a)^{-\nu+q}} & \text{if } \nu < 0 \\ \dfrac{\nu!}{(\nu-q)!}(x+a)^{\nu-q} & \text{if } \nu > 0 \end{cases}, \tag{17}$$

the final expression for $A_{i,j}$ is obtained by applying (17) in (16), yielding (12). By following the same steps as with $A_{i,j}$, we obtain (13) as the residues resulting from performing a partial fraction expansion of $M_\gamma(-s)/s$.

References

[1] M. K. Simon and M.-S. Alouini, *Digital Communication over Fading Channels*. John Wiley & Sons, 2005, vol. 95.

[2] M. D. Yacoub, "The $\kappa-\mu$ distribution and the $\eta-\mu$ distribution," *IEEE Antennas and Propag. Mag.*, vol. 49, no. 1, pp. 68–81, Feb. 2007.

[3] P. C. Sofotasios, E. Rebeiz, L. Zhang, T. A. Tsiftsis, D. Cabric, and S. Freear, "Energy detection based spectrum sensing over $\kappa-\mu$ and $\kappa-\mu$ extreme fading channels," *IEEE Trans. Veh. Technol.*, vol. 62, no. 3, pp. 1031–1040, Mar. 2013.

[4] S. L. Cotton, W. G. Scanlon, and J. Guy, "The $\kappa-\mu$ distribution applied to the analysis of fading in body to body communication channels for fire and rescue personnel," *IEEE Antennas Wireless Propag. Lett.*, vol. 7, pp. 66–69, 2008.

[5] J. Zhang, Z. Tan, H. Wang, Q. Huang, and L. Hanzo, "The effective throughput of MISO systems over $\kappa-\mu$ fading channels," *IEEE Trans. Veh. Technol.*, vol. 63, no. 2, pp. 943–947, Feb. 2014.

[6] M. D. Yacoub, "The α - η - κ - μ fading model," *IEEE Transactions on Antennas and Propagation*, vol. 64, no. 8, pp. 3597–3610, Aug. 2016.

[7] J. F. Paris, "Statistical characterization of $\kappa-\mu$ shadowed fading," *IEEE Trans. Veh. Technol.*, vol. 63, no. 2, pp. 518–526, Feb. 2014.

[8] A. Abdi, W. C. Lau, M. S. Alouini, and M. Kaveh, "A new simple model for land mobile satellite channels: first- and second-order statistics," *IEEE Transactions on Wireless Communications*, vol. 2, no. 3, pp. 519–528, May 2003.

[9] M. R. Bhatnagar, "On the sum of correlated squared $\kappa - \mu$ shadowed random variables and its application to performance analysis of MRC," *IEEE Trans. on Veh. Technol.*, vol. 64, no. 6, pp. 2678–2684, June 2015.

[10] F. J. Lopez-Martinez, J. F. Paris, and J. M. Romero-Jerez, "The κ- μ shadowed fading model with integer fading parameters," *IEEE Trans. Veh. Technol.*, vol. 66, no. 9, pp. 7653–7662, Sept. 2017.

[11] J. R. Mendes and M. D. Yacoub, "A general bivariate Ricean model and its statistics," *IEEE Transactions on Vehicular Technology*, vol. 56, no. 2, pp. 404–415, Mar. 2007.

[12] N. C. Beaulieu and K. T. Hemachandra, "Novel simple representations for Gaussian class multivariate distributions with generalized correlation," *IEEE Transactions on Information Theory*, vol. 57, no. 12, pp. 8072–8083, Dec. 2011.

[13] Y. Chen and C. Tellambura, "Infinite series representations of the trivariate and quadrivariate Rayleigh distribution and their applications," *IEEE Transactions on Communications*, vol. 53, no. 12, pp. 2092–2101, Dec 2005.

[14] J. Lopez-Fernandez, J. F. Paris, and E. Martos-Naya, "Bivariate Rician shadowed fading model," *IEEE Transactions on Vehicular Technology*, vol. 67, no. 1, pp. 378–384, Jan 2018.

[15] R. Horn and C. Johnson, *Matrix Analysis*. Cambridge University Press, 1990.

[16] A. Erdelyi, W. Magnus, F. Oberhettinger, and F. G. Tricomi, *Tables of Integral Transforms: Vol.: 1*. McGraw-Hill Book Company, Incorporated, 1954.

Appendix B

Resumen en Castellano

Según el reglamento de doctorado de la Universidad de Málaga, si la memoria de tesis se redacta al completo en inglés, se requiere incluir un breve resumen en castellano donde se reflejen las principales contribuciones de la misma. Nótese, sin embargo, que este anexo no es el propio manuscrito de la tesis sino un sólo resumen para mostrar los resultados más relevantes.

B.1 Introducción y motivación

El análisis de FCG, o combinaciones lineales de variables gaussianas al cuadrado, es de gran interés en el ámbito de las comunicaciones y el procesado de señal debido al incontable número de aplicaciones de este tipo de variables no sólo en dichos campos sino en estadística en general. Por ejemplo, las FCG aparecen en problemas de detección [2], [3], pruebas χ^2 [4], análisis de filtros adaptativos [6] y problemas de estimación [8].

Las FCG también juegan un papel fundamental en comunicaciones, surgiendo de manera natural en el estudio de distintos esquemas de modulación [9], [10] así como en el análisis de sistemas con diversidad [11]–[14], debido a que la relación señal a ruido (SNR, *signal-to-noise ratio*) a la salida de estos sistemas viene dada por una FCG cuando se asumen ganancias gaussianas en los distintos canales. De hecho, la mayoría de modelos de canal empleados actualmente pueden verse como casos particulares de una forma cuadrática más general, incluyendo tanto los modelos clásicos que surgen de la aplicación del teorema central del límite [17]–[19] como nuevas distribuciones presentadas en los últimos años con el fin de otorgar mayor flexibilidad y un mejor ajuste en escenarios emergentes [28]–[31]. Por tanto, el análisis de las FCG aparece como una solución para el estudio unificado de la mayoría de modelos de canal existentes.

Desafortunadamente, a pesar de su gran número de aplicaciones, no se conocen expresiones cerradas para la distribución de las FCG en el caso general. Es por ello que a lo largo de los años se han ido desarrollando distintas aproximaciones para la función densidad de probabilidad (PDF, *probability density function*) y la función de distribución (CDF, *cumulative distribution function*) de este tipo de variables [4], [5], [11], [69]–[79]. Sin

embargo, todas estas aproximaciones tienen la misma desventaja presente en la mayoría de técnicas clásicas para aproximar la distribución de variables aleatorias: las funciones resultantes no representan una *distribución válida*, i.e., la PDF aproximada puede no tener área unidad y se pueden obtener probabilidades mayores a uno e incluso negativas.

En este contexto, esta tesis tiene un doble objetivo. En primer lugar, se pretende obtener un nuevo método para el análisis de FCG, con el propósito de derivar aproximaciones simples y cerradas para sus estadísticos de primer orden que no presenten el principal inconveniente de los métodos clásicos anteriormente citados. Igualmente, sacando partido de la relación entre los distintos modelos de desvanecimiento y este tipo de variables, se buscan nuevos modelos de canal que generalicen y unifiquen la gran variedad de distribuciones presentes en la literatura.

B.2 Análisis de variables aleatorias por confluencia

En esta sección se presenta el nuevo método para análisis de variables aleatorias y su aplicación a las variables de interés en esta tesis: las FCG tanto reales como complejas.

B.2.1 Método propuesto

La mayoría de métodos clásicos para aproximar la distribución de variables aleatorias, entre los que se incluyen la técnica del *saddle-point* [32]–[35], las series de Edgeworth [35]–[38] o las expansiones en términos de polinomios ortogonales [39], presentan el problema anteriormente comentado: no se garantiza que las expresiones obtenidas representen distribuciones válidas. Otras técnicas, como las aproximaciones basadas en mixturas [40]–[45] solventan ese inconveniente, pero la falta de un método general y la complejidad de su aplicación limitan su utilidad.

La técnica aquí propuesta busca, en vez de aproximar los estadísticos de la variable en cuestión por expansiones en series, analizar una secuencia de variables auxiliares que converjan a la variable objetivo en el límite. De esta forma, se garantiza que las funciones obtenidas para cualquier grado de precisión representen distribuciones válidas. Específicamente, dada una variable X, se busca una secuencia $\{X_m : m \in \mathbb{N}^+\}$ tal que $\{X_m\} \Rightarrow X$, donde X_m se obtiene introduciendo alguna perturbación aleatoria en X de modo que se simplifique su análisis.

Como primer ejemplo, se aplicará el método propuesto a la caracterización estadística de variables positivas. Considérese por tanto una variable aleatoria $X \in \mathbb{R}^+$ con distribución continua y función generadora de momentos (MGF, *moment generating function*) $M_X(s)$. Con el fin de aproximar su CDF, se define la secuencia $\{X_m : m \in \mathbb{N}^+\}$ tal que

$$X_m \triangleq X/\xi_m, \tag{B.1}$$

donde ξ_m es una variable aleatoria independiente de X siguiendo una distribución gamma con parámetros m y $1/(m-1)$, i.e. $\xi_m \sim \Gamma(m, 1/(m-1))$. Es sencillo comprobar que $\{\xi_m : m \in \mathbb{N}^+\} \Rightarrow 1$ y por tanto, aplicando el teorema de Slutsky [93, sec. 3.6][55, sec. 1.2], se tiene que $\{X_m\} \Rightarrow X$. Es decir, es posible aproximar la CDF de X por la de X_m

$$F_X(x) = \lim_{m\to\infty} F_{X_m}(x) = \lim_{m\to\infty} \sum_{k=0}^{m-1} \frac{(m-1)^k}{x^k k!} \frac{d^k}{ds^k} M_X(s)\bigg|_{s=(1-m)/x}. \tag{B.2}$$

En general, la convergencia en CDF no implica el mismo comportamiento para la PDF. Sin embargo, bajo ciertas condiciones [53], la convergencia en distribución también garantiza que las funciones de densidad converjan. En el caso bajo consideración, puede comprobarse como dichas condiciones son válidas, pudiendo por tanto extender el método para aproximar también la PDF de X como

$$f_X(x) = \lim_{m\to\infty} f_{X_m}(x) = \lim_{m\to\infty} \frac{(m-1)^m}{x^{m+1}\Gamma(m)} \frac{d^m}{ds^m} M_X(s)\bigg|_{s=(1-m)/x}. \tag{B.3}$$

Finalmente, el error cuadrático medio (MSE, *mean squared error*) normalizado entre X y la variable auxiliar viene dado por

$$\overline{\epsilon^2} = \mathbb{E}\left[(X - X_m)^2\right] / \mathbb{E}\left[X^2\right] = (m-2)^{-1}, \tag{B.4}$$

viéndose claro que $\lim_{m\to\infty} \overline{\epsilon^2} = 0$. Nótese, sin embargo, que el MSE no equivale directamente a una medida del error cometido al aproximar la CDF o la PDF, aunque no obstante da información de la similitud entre la variable objetivo y la auxiliar. Por ende, una reducción en el MSE también conlleva una disminución del error cometido al aproximar los estadísticos de X.

Este método general de análisis de variables basado en secuencias auxiliares obtenidas introduciendo un perturbación en la variable original ha sido denominado como *análisis por confluencia*, ya que se lleva al límite la secuencia auxiliar de variables (nombradas *confluentes*) para converger o *confluir* a la variable original.

La principal dificultad para aplicar esta nueva técnica vendría dada por la complejidad en el cálculo de las derivadas de la MGF. Sin embargo, hay situaciones donde estas derivadas pueden obtenerse de manera sencilla, como es el caso donde $M_X(s)$ venga dada por el producto de funciones elementales. Bajo estas condiciones, las derivadas de la MGF pueden calcularse recursivamente a partir de las derivadas de su logaritmo como

$$\frac{d^k}{ds^k} M_X(s) = M_X(s) D_k(s) \tag{B.5}$$

con $D_0(s) = 1$ y

$$D_k(s) = \sum_{j=0}^{k-1} \frac{(k-1)!}{j!(k-j-1)!} g_{k-1-j}(s) D_j(s), \quad k > 1, \tag{B.6}$$

$$g_k(s) = \frac{d^k}{ds^k} g(s) = \frac{d^{k+1}}{ds^{k+1}} \ln M_X(s). \tag{B.7}$$

B.2.2 Aplicación a FCG reales no centrales

Una vez presentando el método de análisis por confluencia, se va a proceder a su aplicación para el estudio de las FCG, comenzando por el caso de formas reales definidas positivas. Es decir, se buscan expresiones aproximadas para la PDF y CDF de la forma cuadrática

$$Q_R = (\mathbf{x} + \overline{\mathbf{x}})^T \mathbf{A} (\mathbf{x} + \overline{\mathbf{x}}) \tag{B.8}$$

donde $\overline{\mathbf{x}} \in \mathbb{R}^{n \times 1}$ es un vector constante, $\mathbf{A} \in \mathbb{R}^{n \times n}$ es una matriz simétrica y *definida positiva* y $\mathbf{x} \sim \mathcal{N}_n(\mathbf{0}_{n \times 1}, \mathbf{\Sigma})$.

Dado que Q_R es definida positiva, es posible aplicar directamente (B.2) y (B.3) para aproximar sus estadísticos, obteniéndose

$$f_{Q_R}(x) \approx \frac{(m-1)^m}{x^{m+1}\Gamma(m)} M_{Q_R}\left(\frac{1-m}{x}\right) D_m\left(\frac{1-m}{x}\right), \tag{B.9}$$

$$F_{Q_R}(x) \approx M_{Q_R}\left(\frac{1-m}{x}\right) \sum_{k=0}^{m-1} \frac{(m-1)^k}{x^k k!} D_k\left(\frac{1-m}{x}\right), \tag{B.10}$$

donde

$$M_{Q_R}(s) = \prod_{i=1}^{n} \exp\left(\frac{b_i^2 \lambda_i s}{1 - 2\lambda_i s}\right) (1 - 2\lambda_i s)^{-1/2}, \quad \lambda_i \mathrm{Re}\{s\} < 1/2 \; \forall \, i, \tag{B.11}$$

$$g_k(s) = \frac{d^{k+1}}{ds^{k+1}} \ln M_{Q_R}(s) = 2^k \, k! \sum_{j=1}^{n} \frac{\lambda_j^{k+1} \left[(k+1) b_j^2 + 1 - 2\lambda_j s\right]}{(1 - 2\lambda_j s)^{k+2}}. \tag{B.12}$$

con λ_i para $i = 1, \ldots, n$ los autovalores de la matrix $\widetilde{\mathbf{A}} = \mathbf{C}^T \mathbf{A} \mathbf{C}$ y b_i los elementos del vector $\mathbf{b} = \mathbf{U}^T \mathbf{C}^{-1} \overline{\mathbf{x}}$, donde $\mathbf{U}$ es la matriz ortogonal resultante de la diagonalización de $\widetilde{\mathbf{A}}$.

Con el fin de resaltar las ventajas de las aproximaciones propuestas en (B.9) y (B.10), éstas se van a comparar con otros métodos disponibles en la literatura. En concreto, se consideran las aproximaciones en términos de series infinitas de potencias, de polinomios de Laguerre y de funciones de densidad χ^2 [4], [70], [71]. Por simplicidad en la presentación de los resultados, se asume que tanto $\mathbf{A}$ como $\mathbf{\Sigma}$ son matrices exponenciales, i.e., $(\mathbf{A})_{i,j} = \alpha^{|i-j|}$ y $(\mathbf{\Sigma})_{i,j} = \rho^{|i-j|}$ con $0 < \alpha, \rho < 1$.

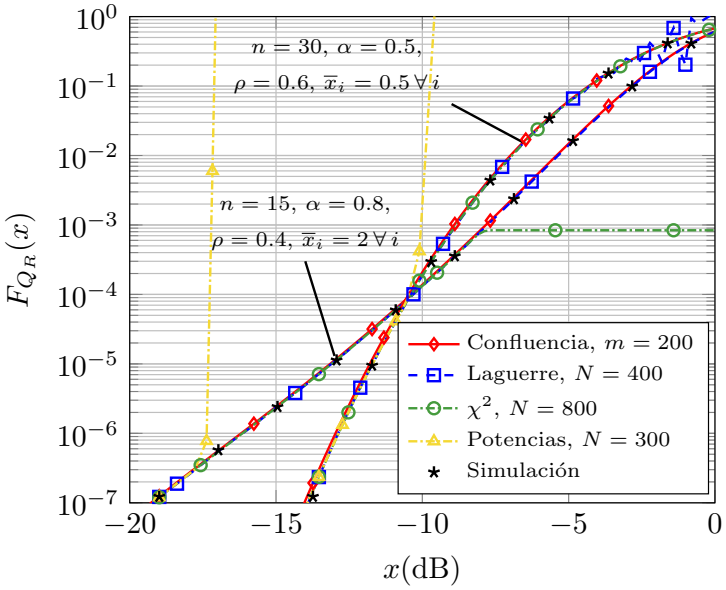

FIGURA B.1: PDF de Q_R para distintos valores de α, ρ y $\overline{\mathbf{x}}$. El método propuesto se compara con distintas técnicas alternativas y con simulaciones de Monte Carlo. N denota el número de términos computados en cada una de las aproximaciones.

Como se observa en la Fig. B.1, las aproximaciones clásicas divergen a partir de determinados valores de x, obteniendo resultados que claramente no son una CDF válida. Específicamente, las series de potencias tienden a infinito a partir de cierto valor, mientras que la expansión en χ^2 satura en un determinado valor de probabilidad distinto de uno y la serie en polinomios de Laguerre presenta un carácter oscilatorio para valores de probabilidad cercanos a la unidad. En cambio, la aproximación propuesta en esta tesis se muestra suficientemente precisa con independencia de los valores de los parámetros de la forma cuadrática y del punto donde evaluemos su CDF.

Los comportamientos anteriormente descritos para las aproximaciones clásicas siguen siendo visibles aún aumentando el número de términos de las series, y mostrando una fuerte dependencia con la parametrización de la variable bajo análisis. A ello, se suma la presencia de ciertos parámetros artificiales en las expansiones en términos de χ^2 y Laguerre que son introducidos para controlar la convergencia de las series, y cuyo valor óptimo se ha comprobado difícil de elegir y dependiente una vez más de los parámetros de la forma cuadrática.

En conclusión, la técnica aquí propuesta se muestra como una opción más robusta que los distintos métodos disponibles en la literatura, permitiendo aproximaciones precisas y garantizando que los resultados obtenidos representan distribuciones válidas.

B.2.3 Aplicación a FCG complejas no centrales

En esta sección, nuestro método va a aplicarse al análisis de FCG complejas indefinidas y no centrales, i.e. se buscan expresiones para la PDF y CDF de

$$Q_C = (\mathbf{v} + \overline{\mathbf{v}})^\dagger \mathbf{A} (\mathbf{v} + \overline{\mathbf{v}}) \tag{B.13}$$

donde $\overline{\mathbf{v}} \in \mathbb{C}^{n\times 1}$ es un vector constante, $\mathbf{A} \in \mathbb{C}^{n\times n}$ es una matriz hermítica y $\mathbf{v} \sim \mathcal{CN}_n(\mathbf{0}_{n\times 1}, \mathbf{\Sigma})$.

Distribución de Q_C

Sacando partido de las particularidades del caso de formas complejas frente a las reales, se va a aplicar el método de análisis por confluencia de una forma ligeramente distinta, de modo que las expresiones resultantes no sean recursivas y sean válidas más allá del caso definido positivo, a diferencia de (B.9) y (B.10).

Con este fin, se adopta una formulación distinta de Q_C, la cual se obtiene aplicando transformaciones algebraicas a (B.13), resultando

$$Q_C = (\mathbf{s} + \overline{\mathbf{h}})^\dagger \mathbf{\Lambda} (\mathbf{s} + \overline{\mathbf{h}}), \tag{B.14}$$

donde $\mathbf{s} \sim \mathcal{CN}_n(\mathbf{0}_{n\times 1}, \mathbf{I}_n)$, $\overline{\mathbf{h}} = \mathbf{U}^\dagger \mathbf{C}^{-1} \overline{\mathbf{v}}$ con $\mathbf{C}\mathbf{C}^\dagger = \mathbf{\Sigma}$ y $\mathbf{U}$, $\mathbf{\Lambda}$ son las matrices resultantes de la diagonalización de $\mathbf{C}^\dagger \mathbf{A} \mathbf{C}$.

A partir de (B.14), se define la secuencia de variables auxiliares (confluentes) introduciendo la perturbación aleatoria en la media de las gaussianas subyacentes, en lugar de introducirlas en la varianza como en el caso de las formas cuadráticas reales. Así pues, se define $\{Q_m : m \in \mathbb{N}^+\}$ con

$$Q_m = (\mathbf{s} + \mathbf{D}_\xi \overline{\mathbf{h}})^\dagger \mathbf{\Lambda} (\mathbf{s} + \mathbf{D}_\xi \overline{\mathbf{h}}), \tag{B.15}$$

donde $\mathbf{D}_\xi \in \mathbb{R}^{n\times n}$ es una matriz diagonal cuyos elementos, $\xi_{m,i}$ para $i = 1, \ldots, n$, son variables aleatorias independientes e idénticamente distribuidas tal que $\xi_{m,i}^2 \sim \Gamma(m, 1/m)$.

A partir de la MGF de Q_m, es posible demostrar que $\{Q_m\} \Rightarrow Q_C$, pudiendo aproximar nuevamente los estadísticos de Q_C por los de sus variables confluentes, con la ventaja adicional de que Q_m admite expresiones cerradas para su PDF y CDF. Con el fin de derivar dichas expresiones, la MGF de Q_m necesita ser formulada en términos de una función racional, obteniendo

$$M_{Q_m}(s) = B \prod_{i=1}^{n} \frac{(s - 1/\lambda_i)^{m-1}}{(s - \beta_i)^m} \tag{B.16}$$

con $\beta_i = [\lambda_i(1+\mu_i/m)]^{-1}$ y

$$B = \prod_{k=1}^{n} \left[-\lambda_k \left(1 + \frac{\mu_k}{m} \right)^m \right]^{-1}, \tag{B.17}$$

donde λ_i para $i = 1, \ldots, n$ son los elementos de $\mathbf{\Lambda}$ y $\mu_i = \|\overline{h}_i\|^2$.

Simplificando la función racional de (B.16) y denotando por $\widetilde{\beta}_i$ y $1/\widetilde{\lambda}_j$ para $i = 1, \ldots, n_\beta$ y $j = 1, \ldots, n_\lambda$ a los distintos polos y ceros resultantes de dicha simplificación, la PDF y la CDF de Q_m se obtienen directamente aplicando la transformada inversa de Laplace a $M_{Q_m}(-s)$ y $M_{Q_m}(-s)/s$, respectivamente, llegando a

$$f_{Q_C}(x) \approx f_{Q_m}(x) = \sum_{i=1}^{n_\beta} \sum_{j=1}^{p_i} \alpha_{i,j} e^{-\widetilde{\beta}_i x} x^{j-1} \mathrm{u}\left(\widetilde{\beta}_i x\right) \mathrm{sgn}(x), \tag{B.18}$$

$$F_{Q_C}(x) \approx F_{Q_m}(x) = \mathrm{u}(x) + \sum_{i=1}^{n_\beta} \sum_{j=1}^{p_i} \omega_{i,j} e^{-\widetilde{\beta}_i x} x^{j-1} \mathrm{u}\left(\widetilde{\beta}_i x\right) \mathrm{sgn}(x). \tag{B.19}$$

En dichas expresiones, $\mathrm{u}(\cdot)$ representa la función escalón unitario, $\mathrm{sgn}(\cdot)$ denota la función signo y

$$\alpha_{i,j} = \frac{(-1)^n}{(j-1)!} B A_{i,j}, \qquad \omega_{i,j} = \frac{(-1)^n}{(j-1)!} B C_{i,j}, \tag{B.20}$$

con $A_{i,j}$ y $C_{i,j}$ los residuos resultantes de descomponer en fracciones simples la función racional en (B.16), una vez evaluada la MGF en los puntos anteriormente indicados.

Para finalizar la caracterización estadística de las FCG complejas no centrales, al igual que se hizo en el caso de variables reales, se proporciona una métrica para el error cometido en la aproximación. En este caso, dado la dificultad de extraer expresiones y cotas útiles para el error cometido entre la CDF real y la aproximada, se proporciona nuevamente el MSE normalizado como medida de la similitud entre la variable original y las confluentes, el cual viene dado por

$$\overline{\epsilon^2} \triangleq \frac{\mathbb{E}\left[(Q_m - Q)^2\right]}{\mathbb{E}\left[Q^2\right]} = \frac{\sum_{i=1}^{n} \lambda_i^2 \mu_i \left[4\left(1 - \frac{\Gamma(m+1/2)}{m^{1/2}\Gamma(m)}\right) + \frac{\mu_i}{m} \right]}{\sum_{j=1}^{n} \left(\lambda_j^2(1+2\mu_j)\right) + \left(\sum_{j=1}^{n} \lambda_i(1+\mu_i)\right)^2}. \tag{B.21}$$

Aplicación a sistemas MRC sobre canales Rice correlados

La utilidad de los resultados derivados en la sección anterior se va a ejemplificar a través de su aplicación para el análisis de sistemas MRC (*maximal ratio combining*) sobre canales Rice correlados, obteniendo precisas aproximaciones para la probabilidad de *outage* y la probabilidad de error (BER, *bit error rate*). Bajo estas condiciones, sólo se conocen

resultados asintóticos [97], [98] o resultados parciales limitados a un número de antenas $P = 2$ [99], [100].

Asumiendo que tanto la sincronización como la estimación del canal son ideales, la SNR a la salida del receptor tras aplicar MRC viene dada por

$$\gamma = \overline{\gamma}\, \mathbf{g}^{\dagger}\mathbf{g}, \tag{B.22}$$

donde $\overline{\gamma}$ es la SNR media en cada rama y $\mathbf{g} \in \mathbb{C}^{P\times 1}$ es el vector de ganancias del canal. Dado que los desvanecimientos en cada rama siguen una distribución Rice con parámetro K_i para $i = 1, \ldots, P$, entonces $\mathbf{g} \sim \mathcal{CN}_P(\overline{\mathbf{g}}, \mathbf{\Sigma})$. Los elementos del vector de medias y de la matriz de covarianzas pueden obtenerse a partir de las relaciones

$$\overline{g}_i = \sqrt{\frac{K_i}{K_i+1}}, \quad (\mathbf{\Sigma})_{i,j} = \sqrt{\frac{1}{(1+K_i)(1+K_j)}}(\mathbf{R})_{i,j} \tag{B.23}$$

con $\mathbf{R}$ la matriz de coeficientes de correlación entre las distintas antenas. Nótese que se están considerando canales normalizados, i.e. $\mathbb{E}[\|g_i\|^2] = 1$.

Como puede observarse, (B.22) es un caso particular de la forma cuadrática en (B.13), y por tanto podemos aplicar los resultados anteriormente derivados para caracterizar γ. Por consiguiente, definiendo γ_{th} como la SNR mínima requerida para una comunicación fiable, la probabilidad de *outage* puede aproximarse por

$$P_{\mathrm{out}}(\gamma_{\mathrm{th}}) \approx 1 + \sum_{i=1}^{n_\beta}\sum_{j=1}^{p_i} \omega_{i,j} e^{-\widetilde{\beta}_i \gamma_{th}/\overline{\gamma}} \left(\frac{\overline{\gamma}}{\gamma_{\mathrm{th}}}\right)^{-j+1} \tag{B.24}$$

donde $\omega_{i,j}$, $\widetilde{\beta}_k$, n_β y p_i se obtienen por identificación con (B.19).

Igualmente, dado que la BER es una función continua y acotada, se puede explotar la convergencia en distribución entre γ y la variable confluente empleada para su análisis y obtener una expresión para la BER gracias al teorema de Helly-Bray [55, sec. 1.3], la cual viene dada por

$$\begin{aligned} P_b\left(\overline{\gamma}\right) \approx \sqrt{M}\sum_{i=1}^{n_\beta}\sum_{j=1}^{p_i}\sum_{k=1}^{\sqrt{M}-1} \omega(k)\alpha_{i,j} \Bigg[& \frac{\Gamma(j)}{2\widetilde{\beta}_i^{j}} - \frac{\delta_k \Gamma\left(j+\frac{1}{2}\right)}{\widetilde{\beta}_i^{j+1/2}} \\ & \times \sqrt{\frac{\overline{\gamma}}{2\pi}}\, {}_2F_1\left(\frac{1}{2}, j+\frac{1}{2}; \frac{3}{2}; \frac{-\delta_k^2}{2\widetilde{\beta}_i}\overline{\gamma}\right)\Bigg], \end{aligned} \tag{B.25}$$

donde $\delta_k = (2k-1)\sqrt{3/(M-1)}$, las constantes $\omega(k)$ vienen dadas en [102, eqs. (6), (14) and (21)] y ${}_2F_1(\cdot)$ es la función hipergeométrica de Gauss [50, eq. (15.1.1)].

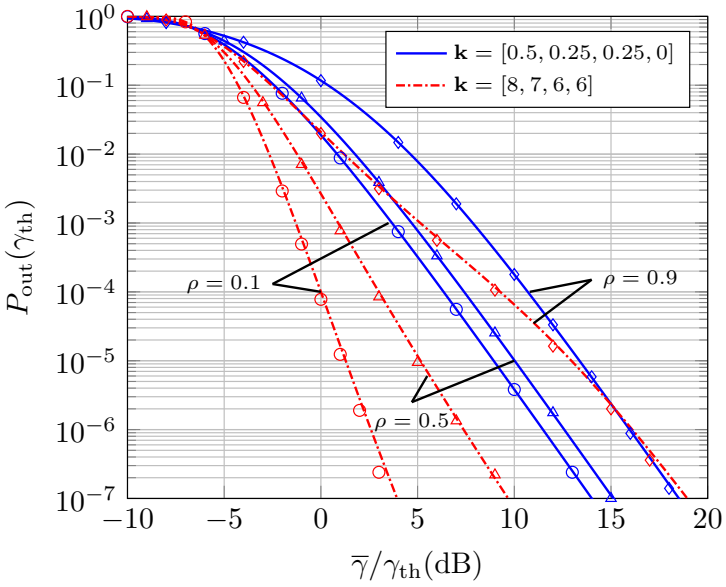

FIGURA B.2: P_{out} en función de $\overline{\gamma}/\gamma_{\text{th}}$ para $P = 4$ y distintos valores de ρ y K_i. Las líneas sólidas corresponden con los resultados teóricos mientras que los marcadores representan los resultados simulados. Para los cálculos teóricos se ha empleado un valor de $m = 40$ para $\mathbf{k} = (0.5, 0.25, 0.25, 0)$ y de $m = 200$ para $\mathbf{k} = (8, 7, 6, 6)$.

Resultados numéricos

A continuación, se va a estudiar el impacto del parámetro Rice en cada rama y de la matriz de coeficientes de correlación en ambas métricas (probabilidad de *outage* y BER). Para comprobar la precisión de los resultados teóricos, éstos se comparan nuevamente con el resultado de las simulaciones. Por simplicidad, se denota como $\mathbf{k} = (K_1, \ldots, K_P)$ al vector que contiene los P parámetros Rice, K, e igualmente se asume que la matriz de coeficientes de correlación $\mathbf{R}$ es exponencial, i.e. $(\mathbf{R})_{i,j} = \rho^{|i-j|}$ con $|\rho| < 1$ [103], [104].

En primer lugar, en la Fig. B.2 se estudia el efecto de los parámetros del canal en la probabilidad de *outage*. Fijándonos en primer lugar en el efecto de los parámetros K (equivalentemente, la potencia de la componente directa), se observa cómo generalmente un incremento en estos parámetros conlleva una mejora de prestaciones del sistema. Sin embargo, para valores muy elevados de ρ (correlación muy alta entre antenas), vemos que el comportamiento del sistema es opuesto; un aumento de la potencia de la línea de visión directa conlleva a una mayor probabilidad de *outage* para valores altos de $\overline{\gamma}$. Este mismo efecto es analizado con más detalle en [105].

Finalmente, en la Fig. B.3 se evalúa el impacto de la correlación y la potencia de la componente directa en la BER, extrayéndose las mismas conclusiones que para la probabilidad de *outage*: efecto negativo de la correlación y mejor rendimiento en general para valores de K elevados.

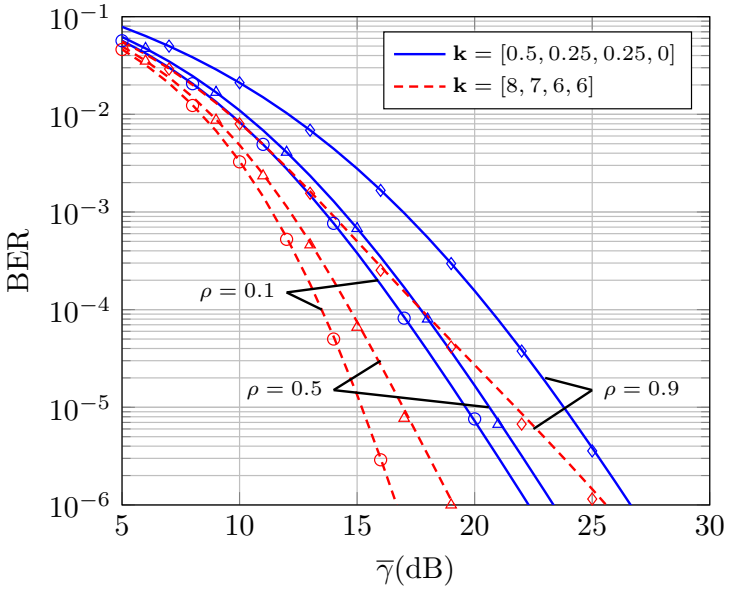

FIGURA B.3: BER para una constelación 16-QAM para $P = 4$ y distintos valores de ρ y K_i. Las líneas sólidas corresponden con los resultados teóricos mientras que los marcadores representan los resultados simulados. Para los cálculos teóricos se ha empleado un valor de $m = 40$ para $\mathbf{k} = (0.5, 0.25, 0.25, 0)$ y de $m = 150$ para $\mathbf{k} = (8, 7, 6, 6)$.

B.3 Generalizaciones del modelo de desvanecimientos κ-μ *shadowed*

Las variables aleatorias confluentes definidas en secciones anteriores han sido usadas simplemente como herramientas matemáticas para estudiar otras variables cuyo análisis es complejo. Es decir, el interés recaía únicamente en el comportamiento límite de su distribución.

Sin embargo, estas variables pueden tener utilidad por sí mismas. Un ejemplo de ello es el caso del modelado de canal, donde la introducción de una fluctuación aleatoria en la variable original puede usarse para caracterizar el *shadowing*. De hecho, esta es la misma idea de la que surgen distintos modelos de canal generalizados, tales como el Rician *shadowed* [86], [87] y el κ-μ *shadowed* [29].

Aunque estas distribuciones son generalizaciones de los modelos clásicos, desde el punto de vista del análisis por confluencia una variable Rician *shadowed* puede verse como la versión confluente de una variable Rice, y la misma relación puede establecerse entre los modelos κ-μ [28], [88] y κ-μ *shadowed*.

Con esta idea, y sacando partido del análisis de las FCG, en esta tesis se presentan dos nuevos modelos de canal, los cuales buscan unificar a la mayoría de distribuciones de desvanecimientos existentes en la literatura.

B.3.1 El modelo Beckmann fluctuante

El primero modelo aquí presentado es el Beckmann fluctuante (BF), el cual es una generalización tanto de la distribución Beckmann [85] como de la κ-μ *shadowed*. En el contexto del análisis por confluencias, el modelo BF puede verse como la variable auxiliar para analizar la distribución Beckmann. Si se compara con el κ-μ *shadowed*, el modelo BF es su extensión natural considerando el efecto del desequilibrio de potencia entre las componentes en fase y cuadratura.

Modelo físico

De acuerdo con el modelo BF, la amplitud de la señal recibida se expresa como

$$R = \left(\sum_{i=1}^{\mu} |\sigma_x X_i + j\sigma_y Y_i + \xi(p_i + jq_i)|^2 \right)^{1/2} \tag{B.26}$$

donde $\mu \in \mathbb{N}^+$, $\sigma_x, \sigma_y \in \mathbb{R}^+$ y $p_i, q_i \in \mathbb{R}$ son constantes; X_i, Y_i para todo i son variables gaussianas estándar independientes e idénticamente distribuidas, i.e. $X_i, Y_i \sim \mathcal{N}(0,1)$, y ξ es una variable aleatoria, independiente de X_i y Y_i, tal que $\xi^2 \sim \Gamma(m, 1/m)$.

Este nuevo modelo queda totalmente caracterizado por los parámetros m, μ y

$$\kappa = \frac{\sum_{i=1}^{\mu} p_i^2 + q_i^2}{\mu(\sigma_x^2 + \sigma_y^2)}, \qquad \eta = \frac{\sigma_x^2}{\sigma_y^2}, \qquad \varrho^2 = \frac{\sum_{i=1}^{\mu} p_i^2}{\sum_{i=1}^{\mu} q_i^2}. \tag{B.27}$$

Debido a su generalidad y flexibilidad, la mayoría de distribuciones de desvanecimientos presentes en la literatura quedan recogidas como casos particulares del modelo BF, tal y como se indica en la Tabla B.1.

Caracterización estadística

Una vez presentado el modelo físico de la nueva distribución, se procede a la caracterización estadística de primer orden, i.e. la obtención de expresiones para su PDF, CDF y MGF. Dado que es habitual analizar los modelos de desvanecimientos en términos de la SNR [18], de aquí en adelante se considera la variable aleatoria

$$\gamma \triangleq \overline{\gamma} \frac{R^2}{\mathbb{E}[R^2]}, \tag{B.28}$$

donde $\mathbb{E}[R^2] = \mu(\sigma_x^2 + \sigma_y^2) + \sum_{i=1}^{\mu}(p_i^2 + q_i^2)$ y $\overline{\gamma} \triangleq \mathbb{E}[\gamma]$ es la SNR media. Por tanto, γ representa la SNR instantánea en el receptor, la cual sigue una distribución BF, i.e. $\gamma \sim \mathcal{FB}(\overline{\gamma}; \kappa, \mu, m, \eta, \varrho)$.

TABLE B.1: Relación entre el modelo BF y distintas distribuciones de desvanecimientos dadas en la literatura. Para evitar confusión, los parámetros del BF están subrayados. Nótese que $\kappa = 0$ implica que m y ϱ desaparecen.

Modelo de canal	Parámetros del modelo Beckmann fluctuante
Rayleigh	$\underline{\kappa} = 0, \quad \underline{\mu} = 1, \quad \underline{\eta} = 1$
Rice	$\underline{\kappa} = K, \quad \underline{\mu} = 1, \quad \underline{m} \to \infty, \quad \underline{\eta} = 1 \quad , \forall \varrho$
Nakagami-m	$\underline{\kappa} = 0, \quad \underline{\mu} = m, \quad \underline{\eta} = 1$
Hoyt	$\underline{\kappa} = 0, \quad \underline{\mu} = 1, \quad \underline{\eta} = \eta$
η-μ	$\underline{\kappa} = 0, \quad \underline{\mu} = \mu, \quad \underline{\eta} = \eta$
Beckmann	$\underline{\kappa} = K, \quad \underline{\mu} = 1, \quad \underline{m} \to \infty, \quad \underline{\eta} = \eta, \quad \underline{\varrho} = \varrho$
κ-μ	$\underline{\kappa} = \kappa, \quad \underline{\mu} = \mu, \quad \underline{m} \to \infty, \quad \underline{\eta} = 1, \quad \forall \varrho$
Rician Shadowed	$\underline{\kappa} = \kappa, \quad \underline{\mu} = 1, \quad \underline{m} = m, \quad \underline{\eta} = 1, \quad \forall \varrho$
κ-μ shadowed	$\underline{\kappa} = \kappa, \quad \underline{\mu} = \mu, \quad \underline{m} = m, \quad \underline{\eta} = 1, \quad \forall \varrho$

La MGF del modelo propuesto puede obtenerse condicionando a ξ la MGF de la distribución Beckmann [18, eq. (2.38)] y posteriormente promediando sobre todos sus posibles valores, llegando a

$$M_\gamma(s) = \frac{(-1)^\mu}{s^\mu} \frac{\alpha_2^{m-\mu/2}}{\overline{\gamma}^\mu \alpha_1^m} \left(1 - \frac{\mu(1+\eta)(1+\kappa)}{2\eta\overline{\gamma}s}\right)^{m-\frac{\mu}{2}} \times \left(1 - \frac{\mu(1+\eta)(1+\kappa)}{2\overline{\gamma}s}\right)^{m-\frac{\mu}{2}} \left(1 - \frac{c_1}{\overline{\gamma}s}\right)^{-m} \left(1 - \frac{c_2}{\overline{\gamma}s}\right)^{-m}, \tag{B.29}$$

donde $c_{1,2}$ y $\alpha_{1,2}$ son constantes que dependen de los parámetros de la distribución.

La PDF y la CDF de γ se obtienen aplicando la transformada inversa de Laplace a (B.29), de forma análoga a como se hizo en el análisis de las FCGs complejas, resultando

$$f_\gamma(\gamma) = \frac{\alpha_2^{m-\mu/2}\gamma^{\mu-1}}{\bar{\gamma}^\mu \Gamma(\mu)\alpha_1^m} \Phi_2^{(4)}\left(\frac{\mu}{2} - m, \frac{\mu}{2} - m, m, m; \mu; \frac{-\gamma}{\bar{\gamma}\sqrt{\eta\alpha_2}}, \frac{-\gamma\sqrt{\eta}}{\bar{\gamma}\sqrt{\alpha_2}}, \frac{-\gamma c_1}{\bar{\gamma}}, \frac{-\gamma c_2}{\bar{\gamma}}\right), \tag{B.30}$$

$$F_\gamma(\gamma) = \frac{\alpha_2^{m-\mu/2}\gamma^{\mu}}{\bar{\gamma}^\mu \Gamma(\mu+1)\alpha_1^m} \Phi_2^{(4)}\left(\frac{\mu}{2} - m, \frac{\mu}{2} - m, m, m; \mu+1; \frac{-\gamma}{\bar{\gamma}\sqrt{\eta\alpha_2}}, \frac{-\gamma\sqrt{\eta}}{\bar{\gamma}\sqrt{\alpha_2}}, \frac{-\gamma c_1}{\bar{\gamma}}, \frac{-\gamma c_2}{\bar{\gamma}}\right), \tag{B.31}$$

donde $\Phi_2^{(n)}$ es la serie confluente de Lauricella [107, p. 34], la cual aparece también en otros modelos presentes en la literatura [29], [31], [108] y puede calcularse fácilmente de forma numérica a través de una transformada inversa de Laplace [109], [110].

Bajo ciertas condiciones, la PDF y la CDF del modelo FB se simplifican, obteniéndose expresiones más sencillas y matemáticamente tratables. Específicamente, si m toma valores enteros y μ es par, entonces (B.29) permite una descomposición en fracciones

simples, y (B.30) y (B.31) pueden expresarse en términos de funciones elementales (exponenciales y potencias).

Dado que la PDF y la CDF de una distribución, no reflejan el comportamiento dinámico de la misma, se proporcionan dos métricas adicionales para reflejar este comportamiento: *i)* el *level crossing rate* (LCR), que mide la frecuencia con que la amplitud recibida cruza un determinado umbral, y *ii)* el *average fade duration* (AFD), que caracteriza cuánto tiempo permanece dicha amplitud bajo el umbral.

El LCR de la señal recibida según el modelo BF puede calcularse mediante la fórmula de Rice [111]. No obstante, a pesar de que se ha obtenido una expresión analítica para $N_R(u)$, ésta viene dada en términos de una integral doble que limita su practicidad. Sin embargo, bajo la suposición de $q_i = 0$ y $p_i \neq 0$ o viceversa en (B.26), es posible llegar a una expresión más sencilla. Así pues, asumiendo $q_i = 0 \; \forall \; i$ (la expresión resultante es válida para $p_i = 0 \, \forall \, i$ simplemente realizando el cambio $\eta \to 1/\eta$), el LCR viene dado por

$$\begin{aligned} N_R(u) = & \frac{m^m[\mu(1+\eta)(1+\kappa)]^{\mu-1/2}\sqrt{-\ddot{\rho}(0)}}{2^{\mu-1}\Gamma^2(\mu/2)\eta^{\mu/2}(\frac{\mu\kappa(1+\eta)}{2\eta}+m)^m\sqrt{2\pi}} \cdot u^{(2\mu-1)} \exp\left(-\frac{\mu}{2}(1+\eta)(1+\kappa)u^2\right) \\ & \times \int_0^1 [1+(\eta-1)x]^{\frac{1}{2}}(1-x)^{\mu/2-1}x^{\mu/2-1} \exp\left(-\frac{\mu(1-\eta^2)(1+\kappa)}{2\eta}u^2x\right) \\ & \times {}_1F_1\left(m, \mu/2; \frac{\frac{\kappa\mu^2(1+\eta)^2(1+\kappa)}{4\eta^2}}{\frac{\mu\kappa(1+\eta)}{2\eta}+m}u^2x\right) dx \end{aligned} \tag{B.32}$$

donde $\Omega = \mathbb{E}[R^2]$ y $\ddot{\rho}(0)$ es la derivada segunda de la función de autocorrelación evaluada en 0.

Finalmente, el AFD se calcula de forma inmediata como

$$T_R(u) = \frac{F_R(u)}{N_R(u)}. \tag{B.33}$$

Resultados numéricos

Una vez caracterizado el nuevo modelo, se va a ejemplificar la influencia de sus parámetros en la distribución de la amplitud de señal recibida, la cual puede obtenerse a partir de (B.29) mediante el cambio de variables $f_R(r) = 2r\frac{\overline{\gamma}}{\Omega}f_\gamma(\overline{\gamma}r^2/\Omega)$.

Dado que el desequilibrio en potencia caracterizado por los parámetros η y ϱ^2 representa la generalización del modelo propuesto respecto al κ-μ *shadowed*, nos vamos a centrar en el estudio del impacto producido por la variación de dichos parámetros. Para ello, en la Fig. B.4 se representa la PDF de R para distintos valores de η en un escenario con fluctuaciones medias y severas para la componente directa ($m = 10$ y $m = 1$, respectivamente). En este caso, ϱ^2 se fija a $\varrho^2 = 0.1$, i.e. la componente en fase de la línea de visión directa tiene diez veces más potencia que la componente en cuadratura. Con estos parámetros, se observa cómo, a diferencia del modelo η-μ *shadowed*, la distribución BF no

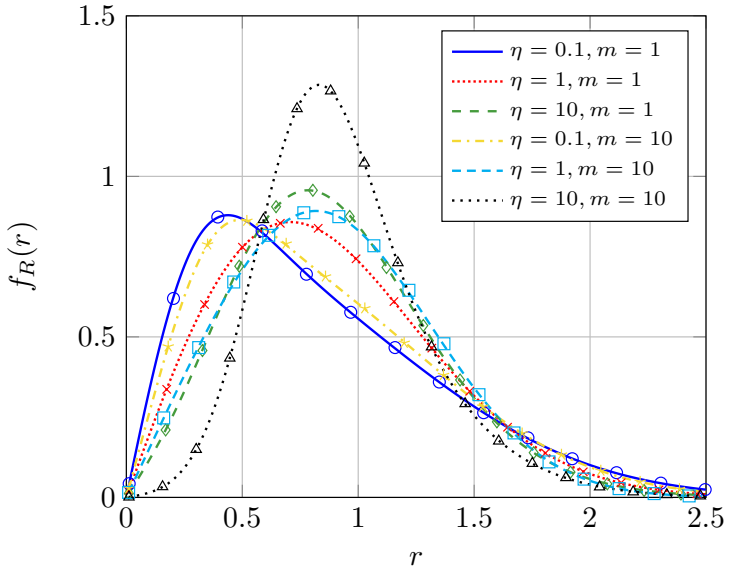

FIGURA B.4: Amplitud recibida según modelo BF para distintos valores de η y m con $\kappa = 1$, $\varrho = 0.1$, $\mu = 1$ y $\Omega = 1$. Las líneas continuas corresponden con los valores teóricos, mientras que los marcadores corresponden a los resultados de la simulación.

es simétrica respecto a $\eta \in [0, 1]$ y $\eta \in [1, \infty)$ para un determinado $\rho^2 \neq 1$. De hecho, si el desequilibrio en potencia de la parte difusa se produce en favor de la misma componente que en la línea de visión de directa, el efecto es mucho más perjudicial que si se produjese hacia la componente contraria. Un comportamiento similar se reproduce para distintos valores de ϱ^2 dado un η fijo.

Por último, se va a analizar el efecto de los parámetros de la distribución en el LCR. Para ello, se asume una variación de la componente difusa acorde al modelo de correlación de Clarke [17, sec. 2.1.1] con una frecuencia Doppler máxima f_d. Por tanto, $\sqrt{-\ddot{\rho}(0)} = \sqrt{2} f_d \pi$ [113, eq. (34)]. Igualmente, se asume $\varrho^2 \to \infty$ de modo que el LCR pueda calcularse como en (B.32).

Con dichas consideraciones, en la Fig. B.5 se representa el LCR en función del umbral, u, para distintos valores de los parámetros de la distribución BF. Curiosamente, al aumentar μ, el número de cruces para umbrales bajos se reduce drásticamente, mientras que éstos aumentan al reducir κ o aumentar η.

B.3.2 El modelo κ-μ *shadowed* con correlación

Modelo físico

La segunda extensión del modelo κ-μ *shadowed* presentada en esta tesis recibe el nombre de κ-μ *shadowed* correlado. Según este nuevo modelo, la amplitud de señal recibida

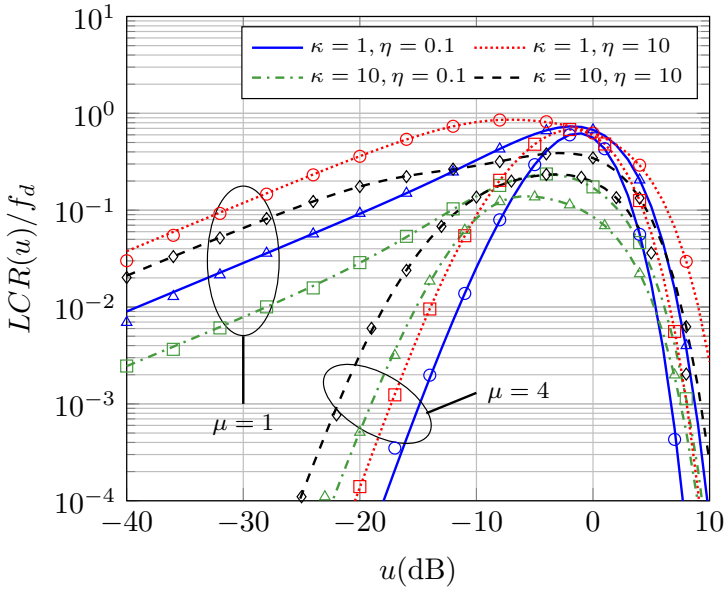

FIGURA B.5: LCR normalizado para distintos valores de κ, η y μ con $m = 1$, $\varrho \to \infty$ y $\Omega = 1$. Las líneas continuas corresponden con los valores teóricos, mientras que los marcadores corresponden a los resultados de la simulación.

viene dada por

$$R = \left(\sum_{i=1}^{\mu} |Z_i + \xi p_i|^2 \right)^{1/2}, \tag{B.34}$$

donde $\mu \in \mathbb{N}^+$, p_i para $i = 1, \ldots, \mu$ son números complejos representando la contribución de la componente directa y $Z_i \sim \mathcal{CN}(0, \sigma^2)$. La variable ξ representa las fluctuaciones debido al *shadowing*, al igual que en el modelo BF. La novedad aquí respecto al modelo original es que las variables Z_i pueden estar correladas con coeficiente de correlación $\text{corr}(Z_i, Z_j) = \rho_{i,j}$ para $i, j = 1, \ldots, \mu$, con

$$\rho_{i,j} = \frac{\mathbb{E}[Z_i Z_j^\dagger]}{\sigma^2}. \tag{B.35}$$

Obsérvese que, condicionado a ξ, R^2 en (B.34) es un caso particular de la FCG compleja en (B.13), donde $\mathbf{A} = \mathbf{I}_\mu$. Por tanto, aplicando las mismas manipulaciones que para Q_C, R puede escribirse como

$$R = \left(\sum_{i=1}^{\mu} \left| \sqrt{\lambda_i} \sigma \widetilde{Z}_i + \xi \sqrt{\lambda_i} \widetilde{p}_i \right|^2 \right)^{1/2}, \tag{B.36}$$

donde $\widetilde{Z}_i \sim \mathcal{CN}(0, 1)$, $\widetilde{p}_i$ son los elementos del vector $\widetilde{\mathbf{p}} = \mathbf{U}^\dagger \mathbf{C}^{-1} \mathbf{p}$ con $\mathbf{p} = (p_1, \ldots, p_\mu)^T$, λ_i son los autovalores de $\mathbf{C}^\dagger \mathbf{C}$ y $\mathbf{U}$ es una matriz unitaria cuya columna i-ésima es el autovector de $\mathbf{C}^\dagger \mathbf{C}$ asociado con λ_i.

Caracterización estadística

Al igual que en la distribución BF, nos basaremos en el análisis estadístico de la SNR instantánea, definida como $\gamma = \overline{\gamma}R^2/\mathbb{E}[R^2]$, donde $\overline{\gamma}$ denota la SNR media y $\mathbb{E}[R^2] = \mu\sigma^2 + \sum_{i=1}^{\mu} \|p_i^2\|$.

La MGF de γ viene dada por

$$M_\gamma(s) = \frac{\mu^\mu(\kappa+1)^\mu}{\prod_{i=1}^{\mu}(\mu(\kappa+1) - s\lambda_i\overline{\gamma})} \left(1 - \frac{1}{m}\sum_{j=1}^{\mu} \frac{d_i\lambda_i s\overline{\gamma}}{\mu(\kappa+1) - s\lambda_i\overline{\gamma}}\right)^{-m}, \tag{B.37}$$

con $d_i = |\widetilde{p}_i|^2/\sigma^2$.

A partir de (B.37), la PDF y la CDF de γ pueden obtenerse realizando una descomposición en fracciones simples y aplicando la transformada inversa de Laplace, resultando

$$f_\gamma(\gamma) = \alpha \sum_{i=1}^{n_\beta} \sum_{j=1}^{q_i m} A_{i,j}\gamma^{j-1}e^{-\beta_i\gamma}, \tag{B.38}$$

$$F_\gamma(\gamma) = 1 + \alpha \sum_{i=1}^{n_\beta} \sum_{j=1}^{q_i m} C_{i,j}\gamma^{j-1}e^{-\beta_i\gamma}, \tag{B.39}$$

donde α, $A_{i,j}$ y $C_{i,j}$ son constantes que dependen de los parámetros de la distribución.

Resultados numéricos

Finalmente, se va a ejemplificar la influencia de la correlación en la distribución de la amplitud de señal recibida. Por simplicidad, asumimos que la correlación sigue un perfil exponencial, i.e., $\mathrm{corr}(Z_i, Z_j) = \rho_{i,j} = \rho^{|i-j|}$ con $0 \leq \rho < 1$. Bajo esta suposición, en la Fig. B.6 se representa la PDF de la amplitud recibida para distintos valores de ρ, μ y m con $\kappa = 4$. Se observa que, independientemente del resto de parámetros, una correlación alta (valores de ρ próximos a la unidad) siempre producen valores de la señal más distribuidos, siendo prácticamente independiente de los valores de m empleados. Sin embargo, al aumentar μ, este efecto de la correlación es aún más notorio.

B.4 Conclusiones y líneas futuras

Conclusiones

En esta tesis se ha conseguido un doble objtivo. Por un lado, se ha presentado un nuevo método de aproximar la distribución de variables aleatorias basado en el análisis de una secuencia de variables aleatorias auxiliares definidas a partir de la variable

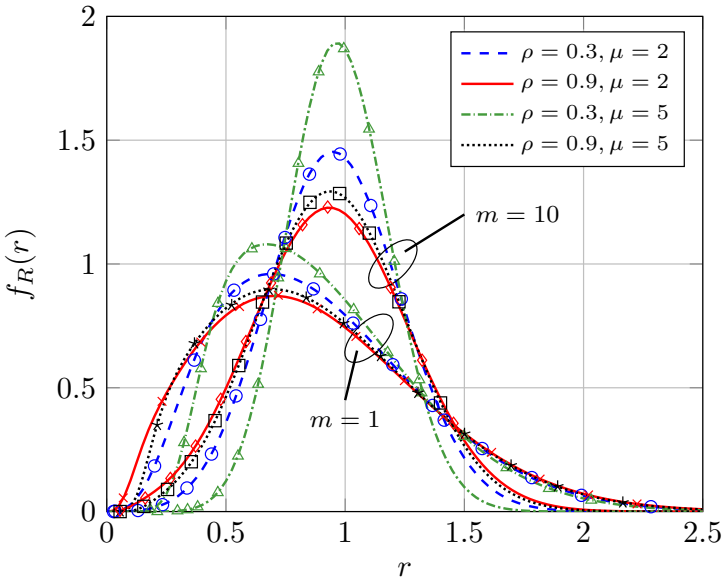

FIGURA B.6: Distribución de la amplitud recibida para distintos valores de μ, ρ y m para $\kappa = 4$ y $\mathbb{E}[R] = 1$. Las líneas continuas corresponden a los cálculos teóricos mientras que los marcadores representan el valor de las simulaciones.

objetivo. La ventaja de este método respecto a otras soluciones disponibles en la literatura son: *i)* las expresiones obtenidas *siempre* representan una distribución válida y *ii)* puede obtenerse cualquier grado de precisión con independencia de los parámetros de la variable en cuestión.

Esta técnica de análisis se ha aplicado en el contexto de las FCG, dando lugar a las siguientes contribuciones:

- Se han proporcionado expresiones para la PDF y CDF de las FCG reales y definidas positivas que pueden computarse fácilmente de forma recursiva.
- Se han obtenido aproximaciones tratables matemáticamente en términos de funciones elementales para las FCG complejas.
- Se dan, por primera vez en la literatura, expresiones generales para la probabilidad de error y la probabilidad de *outage* en sistemas MRC sobre canales Rice correlados.

Por otro lado, la aplicación del método propuesto en el contexto de modelado de canal ha dado lugar a la presentación de dos modelos de canal generalizados que unifican a la mayoría de distribuciones de desvanecimientos más usadas. Específicamente, las contribuciones son:

- Presentación y análisis del modelo Beckmann fluctuante como generalización tanto de la distribución κ-μ *shadowed* como de la Beckmann, proporcionando expresiones para sus estadísticos de primer y segundo orden.
- Introducción del modelo κ-μ *shadowed* correlado, extendiendo la distribución original.

Líneas futuras

En el contexto del análisis de variables aleatorias, una posible línea futura de investigación sería la aplicación del método general aquí propuesto a otros tipos de variables cuyo estudio es en general sumamente complejo, tales como aquellas variables que surgen de la suma o producto de otras.

Además, debido al número de aplicaciones de las FCG en procesado de señal y comunicaciones, y dada la relativa tratabilidad de las aproximaciones dadas en esta tesis, las expresiones aquí aportadas pueden ser útiles para el análisis de múltiples sistemas, e.g., sistemas con diversidad, detección de señales o análisis de prestaciones de estimadores.

Por otro lado, en lo referente a modelado de canal, el propio método aquí propuesto es interesante para el análisis de modelos *composite*, i.e., aquellos que contemplan a la vez el efecto de los desvanecimientos y un *shadowing* multiplicativo. En esta línea, algunos resultados preliminares pueden encontrarse ya en [114]. Finalmente, los dos modelos generalizados que se han introducido pueden ser de utilidad para el análisis de prestaciones de sistemas sobre una gran variedad de condiciones de propagación. Ejemplos del interés de la comunidad científica en estas distribuciones pueden encontrarse en [115], [116].

Bibliography

[1] P. Billingsley, *Probability and Measure*, ser. Wiley Series in Probability and Statistics. Wiley, 2012.

[2] H. Van Trees, K. Bell, and Z. Tian, *Detection Estimation and Modulation Theory, Part I: Detection, Estimation, and Filtering Theory*, ser. Detection Estimation and Modulation Theory. Wiley, 2013.

[3] V. K. Madisetti, *The Digital Signal Processing Handbook*, 2nd. CRC Press, 2009.

[4] S. Provost and A. Mathai, *Quadratic Forms in Random Variables: Theory and Applications*, ser. Statistics : textbooks and monographs. Marcel Dek ker, 1992.

[5] G. E. P. Box, "Some theorems on quadratic forms applied in the study of analysis of variance problems, i. effect of inequality of variance in the one-way classification", *Ann. Math. Statist.*, vol. 25, no. 2, pp. 290–302, 1954.

[6] T. Y. Al-Naffouri and M. Moinuddin, "Exact performance analysis of the ϵ-NLMS algorithm for colored circular Gaussian inputs", *IEEE Trans. Signal Process.*, vol. 58, no. 10, pp. 5080–5090, 2010.

[7] E. H. Gismalla and E. Alsusa, "Performance analysis of the periodogram-based energy detector in fading channels", *IEEE Trans. Signal Process.*, vol. 59, no. 8, pp. 3712–3721, 2011.

[8] F. Athley, "Threshold region performance of maximum likelihood direction of arrival estimators", *IEEE Trans. Signal Process.*, vol. 53, no. 4, pp. 1359–1373, 2005.

[9] Q. Zhao and H. Li, "Differential modulation for cooperative wireless systems", *IEEE Trans. Signal Process.*, vol. 55, no. 5, pp. 2273–2283, 2007.

[10] D. Raphaeli, "Noncoherent coded modulation", *IEEE Trans. Commun.*, vol. 44, no. 2, pp. 172–183, Feb. 1996.

[11] T. Y. Al-Naffouri, M. Moinuddin, N. Ajeeb, B. Hassibi, and A. L. Moustakas, "On the distribution of indefinite quadratic forms in Gaussian random variables", *IEEE Trans. Commun.*, vol. 64, no. 1, pp. 153–165, 2016.

[12] B. D. Rao, M. Wengler, and B. Judson, "Performance analysis and comparison of MRC and optimal combining in antenna array systems", in *IEEE Int. Conf. Acoust. Speech Signal Process. Proceedings (Cat. No.01CH37221)*, vol. 5, 2001, pp. 2949–2952.

[13] D. Lao and A. M. Haimovich, "Exact closed-form performance analysis of optimum combining with multiple cochannel interferers and Rayleigh fading", *IEEE Trans. Commun.*, vol. 51, no. 6, pp. 995–1003, Jun. 2003.

[14] C. Kim, S. Lee, and J. Lee, "SINR and throughput analysis for random beamforming systems with adaptive modulation", *IEEE Trans. Wireless Commun.*, vol. 12, no. 4, pp. 1460–1471, Apr. 2013.

[15] G. A. Ropokis, A. A. Rontogiannis, and P. T. Mathiopoulos, "Quadratic forms in normal RVs: Theory and applications to OSTBC over Hoyt fading channels", *IEEE Trans. Wireless Commun.*, vol. 7, no. 12, pp. 5009–5019, 2008.

[16] V. Havary-Nassab, S. Shahbazpanahi, and A. Grami, "Optimal distributed beamforming for two-way relay networks", *IEEE Trans. Signal Process.*, vol. 58, no. 3, pp. 1238–1250, Mar. 2010.

[17] G. L. Stuber, *"Principles of Mobile Communication"*, 2nd. Kluwer Academic Publishers, 2002.

[18] M. K. Simon and M.-S. Alouini, *Digital communication over fading channels*. John Wiley & Sons, 2005, vol. 95.

[19] J. Proakis and M Salehi, "Digital communications", *McGraw-Hill Education*, vol. 31, 2007.

[20] M. Nakagami, "The m-distribution — a general formula of intensity distribution of rapid fading", in *Statistical Methods in Radio Wave Propagation*, W. Hoffman, Ed., Pergamon, 1960, pp. 3 –36.

[21] M. R. Akdeniz, Y. Liu, M. K. Samimi, S. Sun, S. Rangan, T. S. Rappaport, and E. Erkip, "Millimeter wave channel modeling and cellular capacity evaluation", *IEEE J. Sel. Areas Commun.*, vol. 32, no. 6, pp. 1164–1179, Jun. 2014.

[22] T. S. Rappaport, G. R. MacCartney, M. K. Samimi, and S. Sun, "Wideband millimeter-wave propagation measurements and channel models for future wireless communication system design", *IEEE Trans. Commun.*, vol. 63, no. 9, pp. 3029–3056, Sep. 2015.

[23] J. Medbo, K. Börner, K. Haneda, V. Hovinen, T. Imai, J. Järvelainen, T. Jämsä, A. Karttunen, K. Kusume, J. Kyröläinen, P. Kyösti, J. Meinilä, V. Nurmela, L. Raschkowski, A. Roivainen, and J. Ylitalo, "Channel modelling for the fifth generation mobile communications", in *Proc. 8th Eur. Conf. Antennas Propag. (EuCAP)*, Apr. 2014, pp. 219–223.

[24] S. Hur, S. Baek, B. Kim, Y. Chang, A. F. Molisch, T. S. Rappaport, K. Haneda, and J. Park, "Proposal on millimeter-wave channel modeling for 5G cellular system", *IEEE J. Sel. Topics Signal Process.*, vol. 10, no. 3, pp. 454–469, Apr. 2016.

[25] Q.-U.-A. Nadeem, A. Kammoun, A. Chaaban, M. Debbah, and M.-S. Alouini, "Large intelligent surface assisted MIMO communications", *arXiv preprint arXiv:1903.08127*, 2019.

[26] A. Taha, M. Alrabeiah, and A. Alkhateeb, "Enabling large intelligent surfaces with compressive sensing and deep learning", *arXiv preprint arXiv:1904.10136*, 2019.

[27] M. Stojanovic and J. Preisig, "Underwater acoustic communication channels: Propagation models and statistical characterization", *IEEE Commun. Mag.*, vol. 47, no. 1, pp. 84–89, Jan. 2009.

[28] M. D. Yacoub, "The κ-μ distribution and the η-μ distribution", *IEEE Antennas Propag. Mag.*, vol. 49, no. 1, pp. 68–81, Feb. 2007.

[29] J. F. Paris, "Statistical characterization of κ-μ shadowed fading", *IEEE Trans. Veh. Technol.*, vol. 63, no. 2, pp. 518–526, Feb. 2014.

[30] F. J. Lopez-Martinez, J. F. Paris, and J. M. Romero-Jerez, "The κ- μ shadowed fading model with integer fading parameters", *IEEE Trans. Veh. Technol.*, vol. 66, no. 9, pp. 7653–7662, Sep. 2017.

[31] J. M. Romero-Jerez, F. J. Lopez-Martinez, J. F. Paris, and A. J. Goldsmith, "The fluctuating two-ray fading model: Statistical characterization and performance analysis", *IEEE Tran. Wireless Commun.*, vol. 16, no. 7, pp. 4420–4432, Jul. 2017.

[32] C. Goutis and G. Casella, "Explaining the saddlepoint approximation", *Am. Stat.*, vol. 53, no. 3, pp. 216–224, 1999.

[33] R. W. Butler and A. T. A. Wood, *Ann. Statist.*, vol. 32, no. 6, pp. 2712–2730, Dec. 2004.

[34] H. E. Daniels, "Saddlepoint approximations in statistics", *Ann. Math. Statist.*, vol. 25, no. 4, pp. 631–650, Dec. 1954.

[35] J. E. Kolassa, *Series approximation methods in statistics*. Springer Science & Business Media, 2006, vol. 88.

[36] P. McCullagh, *Tensor Methods in Statistics*, ser. Monographs on statistics and applied probability. Kluwer Academic Publishers, 1987.

[37] D. L. Wallace, "Asymptotic approximations to distributions", *Ann. Math. Statist.*, vol. 29, no. 3, pp. 635–654, Sep. 1958.

[38] C. Field and E. Ronchetti, *Small Sample Asymptotics*, ser. Lecture notes-monograph. Institute of Mathematical Statistics, 1990, vol. 13.

[39] S. B. Provost, "Moment-based density approximants", *Math. J.*, vol. 9, no. 4, pp. 727–756, 2005.

[40] H. Sorenson and D. Alspach, "Recursive bayesian estimation using gaussian sums", *Automatica*, vol. 7, no. 4, pp. 465 –479, 1971.

[41] B. Everitt and D. Hand, *Finite mixture distributions*, ser. Monographs on applied probability and statistics. Chapman and Hall, 1981.

[42] M. Wiper, D. Rios, and F. Ruggeri, "Mixtures of gamma distributions with applications", *J. Comput. Graph. Stat.*, vol. 10, pp. 440–454, Sep. 2001.

[43] A. Bacharoglou, "Approximation of probability distributions by convex mixtures of Gaussian measures", *Proc. Amer. Math. Soc.*, vol. 138, pp. 2619–2619, Jul. 2010.

[44] "Universal series induced by approximate identities and some relevant applications", *J. Approx. Theory*, vol. 163, no. 12, pp. 1783 –1797, 2011.

[45] D. Alspach and H. Sorenson, "Nonlinear bayesian estimation using gaussian sum approximations", *IEEE Trans. Autom. Control*, vol. 17, no. 4, pp. 439–448, Aug. 1972.

[46] P. Ramírez-Espinosa, D. Morales-Jimenez, J. A. Cortés, J. F. París, and E. Martos-Naya, "New approximation to distribution of positive RVs applied to Gaussian quadratic forms", *IEEE Signal Process. Lett.*, vol. 26, no. 6, pp. 923–927, Jun. 2019.

[47] P. Ramírez-Espinosa, L. Moreno-Pozas, J. F. París, J. A. Cortés, and E. Martos-Naya, "A new approach to the statistical analysis of non-central complex Gaussian quadratic forms with applications", *IEEE Trans. Veh. Technol.*, vol. 68, no. 7, pp. 6734–6746, Jul. 2019.

[48] P. Ramírez-Espinosa, F. J. López-Martínez, J. F. París, M. D. Yacoub, and E. Martos-Naya, "An extension of the κ-μ shadowed fading model: Statistical characterization and applications", *IEEE Trans. Veh. Technol.*, vol. 67, no. 5, pp. 3826–3837, May 2018.

[49] P. Ramírez-Espinosa, J. F. París, J. A. Cortés, and E. Martos-Naya, "The κ-μ shadowed fading model with arbitrary intercluster correlation", in *2018 15th Int. Symp. Wireless Commun. Syst. (ISWCS)*, Aug. 2018, pp. 1–5.

[50] M. Abramowitz, I. A. Stegun, *et al.*, *Handbook of Mathematical Functions with Formulas, Graphs, and Mathematical Tables*. Dover, New York, 1972, vol. 9.

[51] I. S. Gradshteyn and I. M. Ryzhik, *Table of Integrals, Series, and Products*. Academic Press, 2007.

[52] D. Williams, *Probability with Martingales*, ser. Cambridge mathematical textbooks. Cambridge University Press, 1991.

[53] D. D. Boos, "A converse to Scheffe's theorem", *Ann. Statist.*, vol. 13, no. 1, pp. 423–427, 1985.

[54] H. Scheffe, "A useful convergence theorem for probability distributions", *Ann. Math. Statist.*, vol. 18, no. 3, pp. 434–438, Sep. 1947.

[55] E. B. Manoukian, *Mathematical Nonparametric Statistics*. CRC Press, 1986.

[56] S. Resnick, *A Probability Path*, ser. A Probability Path. Birkhäuser Boston, 2003.

[57] B. Sklar, *Digital communications: fundamentals and applications*, 2nd, ser. Prentice Hall Communications Engineering and Emerging Technologies Series. Prentice-Hall PTR, 2001.

[58] R. Hankin, "The complex multivariate Gaussian distribution", *R Journal*, vol. 7, pp. 73–80, Jun. 2015.

[59] N. R. Goodman, "Statistical analysis based on a certain multivariate complex gaussian distribution (an introduction)", *Ann. Math. Statist.*, vol. 34, no. 1, pp. 152–177, Mar. 1963.

[60] H. Cramér, *Mathematical Methods of Statistics*, ser. Princeton landmarks in mathematics and physics. Princeton University Press, 1999.

[61] G. Bolch, S. Greiner, H. de Meer, and K. Trivedi, *Queueing Networks and Markov Chains: Modeling and Performance Evaluation with Computer Science Applications*. Wiley, 2006.

[62] C. Ming Tan, N. Raghavan, and A. Roy, "Application of gamma distribution in electromigration for submicron interconnects", *J. Appl. Phys.*, vol. 102, no. 10, p. 103 703, 2007.

[63] N. Johnson, S. Kotz, and N. Balakrishnan, *Continuous Univariate Distributions*, 2nd, ser. Wiley Series in Probability and Statistics. Wiley, 1994, vol. 1.

[64] V. Sundarapandian, *Probability, statistics and queuing theory*. PHI Learning Pvt. Ltd., 2009.

[65] P. J. Smith, "A recursive formulation of the old problem of obtaining moments from cumulants and vice versa", *Am. Stat.*, vol. 49, no. 2, pp. 217–218, 1995.

[66] A. Mathai and H. Haubold, *Special Functions for Applied Scientists*. Springer New York, 2008.

[67] L. L. Scharf, *Statistical Signal Processing*. Addison-Wesley Reading, MA, 1991, vol. 98.

[68] R. Horn and C. Johnson, *Matrix Analysis*. Cambridge University Press, 1990.

[69] H. Robbins and E. J. G. Pitman, "Application of the method of mixtures to quadratic forms in normal variates", *Ann. Math. Statist.*, vol. 20, no. 4, pp. 552–560, Dec. 1949.

[70] S. Kotz, N. L. Johnson, and D. W. Boyd, "Series representations of distributions of quadratic forms in normal variables. i. central case", *Ann. Math. Statist.*, vol. 38, no. 3, pp. 823–837, Jun. 1967.

[71] ——, "Series representations of distributions of quadratic forms in normal variables II. Non-Central case", *Ann. Math. Statist.*, vol. 38, no. 3, pp. 838–848, Jun. 1967.

[72] B. Shah, "Distribution of definite and of indefinite quadratic forms from a non-central normal distribution", *Ann. Math. Statist.*, vol. 34, no. 1, pp. 186–190, 1963.

[73] J. P. Imhof, "Computing the distribution of quadratic forms in normal variables", *Biometrika*, vol. 48, no. 3/4, pp. 419–426, 1961.

[74] J. Gurland *et al.*, "Distribution of definite and of indefinite quadratic forms", *Ann. Math. Statist.*, vol. 26, no. 1, pp. 122–127, 1955.

[75] F. J. Reifler, M. S. Rogers, and K. Malakian, "Distribution of general noncentral positive definite quadratic form in K-dimensions", *IEEE Trans. Aerosp. Electron. Syst.*, vol. 25, no. 3, pp. 411–414, 1989.

[76] G. L. Turin, "The characteristic function of Hermitian quadratic forms in complex normal variables", *Biometrika*, vol. 47, no. 1/2, pp. 199–201, 1960.

[77] K. H. Biyari and W. C. Lindsey, "Statistical distributions of Hermitian quadratic forms in complex Gaussian variables", *IEEE Trans. Inf. Theory*, vol. 39, no. 3, pp. 1076–1082, May 1993.

[78] D. Raphaeli, "Distribution of noncentral indefinite quadratic forms in complex normal variables", *IEEE Trans. Inf. Theory*, vol. 42, no. 3, pp. 1002–1007, May 1996.

[79] G. Tziritas, "On the distribution of positive-definite Gaussian quadratic forms", *IEEE Trans. Inf. Theory*, vol. 33, no. 6, pp. 895–906, 1987.

[80] H. Ruben, "A new result on the distribution of quadratic forms", *Ann. Math. Statist.*, vol. 34, no. 4, pp. 1582–1584, 1963.

[81] G. D. Durgin, T. S. Rappaport, and D. A. de Wolf, "New analytical models and probability density functions for fading in wireless communications", *IEEE Trans. Commun.*, vol. 50, no. 6, pp. 1005–1015, Jun. 2002.

[82] S. O. Rice, "Statistical properties of a sine wave plus random noise", *Bell Syst.Tech. J.*, vol. 27, no. 1, pp. 109–157, Jan. 1948.

[83] R. Hoyt, "Probability functions for the modulus and angle of the normal complex variate", *Bell Syst. Tech. J.*, vol. 26, no. 2, pp. 318–359, Apr. 1947.

[84] K. Bischoff and B. Chytil, "A note on scintillation indices", *Planet. Space Sci.*, vol. 17, no. 5, pp. 1059 –1066, 1969.

[85] P. Beckmann and A. Spizzichino, *The scattering of electromagnetic waves from rough surfaces*, ser. International series of monographs on electromagnetic waves. Pergamon Press, 1963.

[86] Chun Loo, "A statistical model for a land mobile satellite link", *IEEE Trans. Veh. Technol.*, vol. 34, no. 3, pp. 122–127, Aug. 1985.

[87] A. Abdi, W. C. Lau, M. Alouini, and M. Kaveh, "A new simple model for land mobile satellite channels: First- and second-order statistics", *IEEE Trans. Wireless Commun.*, vol. 2, no. 3, pp. 519–528, May 2003.

[88] U. S. Dias and M. D. Yacoub, "The κ-μ phase-envelope joint distribution", *IEEE Trans. Commun.*, vol. 58, no. 1, pp. 40–45, Jan. 2010.

[89] S. L. Cotton, "Human body shadowing in cellular device-to-device communications: Channel modeling using the shadowed κ-μ fading model", *IEEE J. Sel. Areas Commun.*, vol. 33, no. 1, pp. 111–119, Jan. 2015.

[90] L. Moreno-Pozas, F. J. Lopez-Martinez, S. L. Cotton, J. F. Paris, and E. Martos-Naya, "Comments on "human body shadowing in cellular device-to-device communications: Channel modeling using the shadowed κ-μ fading model"", *IEEE J. Sel. Areas Commun.*, vol. 35, no. 2, pp. 517–520, Feb. 2017.

[91] L. Moreno-Pozas, F. J. Lopez-Martinez, J. F. Paris, and E. Martos-Naya, "The κ-μ shadowed fading model: Unifying the κ-μ and η-μ distributions", *IEEE Trans. Veh. Technol.*, vol. 65, no. 12, pp. 9630–9641, Dec. 2016.

[92] F. J. Cañete, J. López-Fernández, C. García-Corrales, A. Sánchez, E. Robles, F. J. Rodrigo, and J. F. Paris, "Measurement and modeling of narrowband channels for ultrasonic underwater communications", *Sensors*, vol. 16, no. 2, 2016.

[93] A. Goldberger, *Econometric theory*. J. Wiley, 1964.

[94] F. Bornemann, "Accuracy and stability of computing high-order derivatives of analytic functions by Cauchy integrals", *Found. Comput. Math.*, vol. 11, no. 1, pp. 1–63, 2011.

[95] Y. Ma, J. Yu, and Y. Wang, "Efficient recursive methods for partial fraction expansion of general rational functions", *J. Appl. Math.*, vol. 2014, 2014.

[96] A. V. Oppenheim, A. S. Willsky, and S. H. Nawab, *Signals & Systems (2Nd Ed.)* Upper Saddle River, NJ, USA: Prentice-Hall, Inc., 1996.

[97] R. K. Mallik and N. C. Sagias, "Distribution of inner product of complex Gaussian random vectors and its applications", *IEEE Trans. Commun.*, vol. 59, no. 12, pp. 3353–3362, Dec. 2011.

[98] Yao Ma, "Impact of correlated diversity branches in Rician fading channels", in *IEEE Int. Conf. Commun. ICC 2005*, vol. 1, May 2005, 473–477 Vol. 1.

[99] P. Bithas, N. C. Sagias, and P. T. Mathiopoulos, "Dual diversity over correlated Ricean fading channels", *J. Commun. Netw.*, vol. 9, pp. 67–74, Mar. 2007.

[100] M. Ilic-Delibasic and M. Pejanovic-Djurisic, "MRC dual-diversity system over correlated and non-identical Ricean fading channels", *IEEE Commun. Lett.*, vol. 17, no. 12, pp. 2280–2283, Dec. 2013.

[101] A. Goldsmith, *Wireless Communications*. Cambridge university press, 2005.

[102] F. J. Lopez-Martinez, E. Martos-Naya, J. F. Paris, and U. Fernandez-Plazaola, "Generalized BER analysis of QAM and its application to MRC under imperfect CSI and interference in Ricean fading channels", *IEEE Trans. Veh. Technol.*, vol. 59, no. 5, pp. 2598–2604, Jun. 2010.

[103] G. K. Karagiannidis, D. A. Zogas, and S. A. Kotsopoulos, "On the multivariate Nakagami-m distribution with exponential correlation", *IEEE Transactions on Communications*, vol. 51, no. 8, pp. 1240–1244, Aug. 2003.

[104] S. L. Loyka, "Channel capacity of MIMO architecture using the exponential correlation matrix", *IEEE Commun. Lett.*, vol. 5, no. 9, pp. 369–371, Sep. 2001.

[105] Y. Wu, R. H. Y. Louie, and M. R. McKay, "Asymptotic outage probability of MIMO-MRC systems in double-correlated Rician environments", *IEEE Trans. Wireless Commun.*, vol. 15, no. 1, pp. 367–376, Jun. 2016.

[106] A. Abdi and M. Kaveh, "On the utility of gamma PDF in modeling shadow fading (slow fading)", in *IEEE 49th Veh. Technol. Conf.*, vol. 3, May 1999, pp. 2308–2312.

[107] P. W. K. H. M. Srivastava, *Multiple Gaussian Hypergeometric Series*. John Wiley & Sons, 1985.

[108] D. Morales-Jimenez and J. F. Paris, "Outage probability analysis for η-μ fading channels", *IEEE Commun. Lett.*, vol. 14, no. 6, pp. 521–523, Jun. 2010.

[109] E. Martos-Naya, J. M. Romero-Jerez, F. J. Lopez-Martinez, and J. F. Paris, "A MATLAB program for the computation of the confluent hypergeometric function $\Phi 2$", Repositorio Institucional Universidad de Malaga RIUMA., Tech. Rep., 2016.

[110] J. Abate and W. Whitt, "Numerical inversion of Laplace transforms of probability distributions", *ORSA J. Comput.*, vol. 7, no. 1, pp. 36–43, 1995.

[111] S. O. Rice, "Mathematical analysis of random noise", *Bell Syst. Tech. J.*, vol. 23, no. 3, pp. 282–332, 1944.

[112] N. C. Beaulieu and S. A. Saberali, "A generalized diffuse scatter plus line-of-sight fading channel model", in *Proc. 2014 IEEE Int. Conf. Commun.*, Jun. 2014, pp. 5849–5853.

[113] F. Ramos-Alarcon, V. Kontorovich, and M. Lara, "On the level crossing duration distributions of Nakagami processes", *IEEE Trans. Commun.*, vol. 57, no. 2, pp. 542–552, Feb. 2009.

[114] P. Ramírez-Espinosa and F. J. López-Martinez, "On the utility of the inverse gamma distribution in modeling composite fading channels", *arXiv preprint arXiv:1905.00069*, 2019.

[115] H. Al-Hmood and H. S. Al-Raweshidy, "Performance analysis of physical layer security over fluctuating Beckmann fading channels", *arXiv preprint arXiv:1904.08230*, 2019.

[116] J. Chen and C. Yuan, "Coverage and rate analysis in downlink L-tier hetnets with fluctuating Beckmann fading", *IEEE Wireless Commun. Lett.*, 2019.